

UNIVERSITÉ DU QUÉBEC À MONTRÉAL

THÈSE PRÉSENTÉE À
L'UNIVERSITÉ DU QUÉBEC À CHICOUTIMI
COMME EXIGENCE PARTIELLE
DU DOCTORAT EN RESSOURCES MINÉRALES
OFFERT À
L'UNIVERSITÉ DU QUÉBEC À MONTRÉAL
EN VERTU D'UNE ENTENTE AVEC
L'UNIVERSITÉ DU QUÉBEC À CHICOUTIMI

PAR

MUZUKA ALFRED NZIBAVUGA NYARUBAKULA

*TAUX D'ENFOUISSEMENT ET ALTÉRATIONS DIAGÉNÉTIQUES DE MATIÈRE
ORGANIQUE AZOTÉE DANS LE NORD-OUEST ATLANTIQUE SUBARCTIQUE*

(BURIAL RATE AND DIAGENETIC CHANGES OF NITROGEN BEARING ORGANIC
MATTER IN THE SUBARCTIC NORTHWEST ATLANTIC)

SEPTEMBRE 1995



Mise en garde/Advice

Afin de rendre accessible au plus grand nombre le résultat des travaux de recherche menés par ses étudiants gradués et dans l'esprit des règles qui régissent le dépôt et la diffusion des mémoires et thèses produits dans cette Institution, **l'Université du Québec à Chicoutimi (UQAC)** est fière de rendre accessible une version complète et gratuite de cette œuvre.

Motivated by a desire to make the results of its graduate students' research accessible to all, and in accordance with the rules governing the acceptance and diffusion of dissertations and theses in this Institution, the **Université du Québec à Chicoutimi (UQAC)** is proud to make a complete version of this work available at no cost to the reader.

L'auteur conserve néanmoins la propriété du droit d'auteur qui protège ce mémoire ou cette thèse. Ni le mémoire ou la thèse ni des extraits substantiels de ceux-ci ne peuvent être imprimés ou autrement reproduits sans son autorisation.

The author retains ownership of the copyright of this dissertation or thesis. Neither the dissertation or thesis, nor substantial extracts from it, may be printed or otherwise reproduced without the author's permission.

RÉSUMÉ

La mer du Labrador et le golfe du Saint-Laurent sont situés à proximité des centres de formation et de déclin des calottes laurentidienne et groenlandaise. En comparaison avec l'Holocène, des conditions froides et des apports élevés de l'eau de fonte dans ces régions, lors des périodes de glaciation-déglaciation, ont eu des impacts importants sur la productivité primaire, les taux d'enfouissement du carbone organique/inorganique, ainsi que sur les apports de matière organique (MO) allochtone. Cette étude fut entreprise afin de déterminer les différences spatiales et temporelles (depuis le dernier maximum glaciaire) de la productivité primaire, des taux d'enfouissement de l'azote et du carbone, des sources de la MO ainsi que des taux de pertes diagénétiques de la MO azotée. Les compositions des isotopes stables du carbone organique et de l'azote, les concentrations en carbone organique, azote et CaCO_3 , et les acides aminés totalement hydrolisables (AATH) de la MO sédimentaire du golfe du Saint-Laurent et de la mer du Labrador ont été analysés pour répondre à ces objectifs. Les échantillons provenant du talus continental de Nouvelle Ecosse et du golfe du Saint-Laurent ont été recueillis lors des missions CSS-Hudson 90-028 et 90-031, tandis que ceux provenant de la mer du Labrador ont été recueillis lors des missions HU-90-013 et HU-90-045.

Au large du golfe du Saint-Laurent, les compositions des isotopes stables du carbone organique et de l'azote et les rapports C/N indiquent que la MO récente est principalement d'origine marine. Des rapports C/N légèrement supérieurs à 10 suggèrent toutefois une évolution diagénétique avec une perte préférentielle des composés azotés par rapport aux hydrates de carbone.

Dans la mer du Labrador, entre 1130 et 3000m de profondeur, les sédiments holocènes sont représentés par une mince couche résultant d'une sédimentation minimale et/ou du vannage dû au puissant sous-courant côtier de l'ouest (Western Boundary Undercurrent; WUBC)". À ces profondeurs, les compositions des isotopes stables du carbone organique et de l'azote ainsi que les rapports C/N indiquent que la MO d'origine marine est restreinte aux 5 à 10 cm de sédiment de surface, c'est à dire à la partie holocène du sédiment. Au dessous, les sédiments du Pléistocène supérieur sont caractérisés par des valeurs $\delta^{15}\text{N}$ et $\delta^{13}\text{C}$ très faibles et des rapports C/N élevés. La diminution des teneurs en isotopes lourds dans les carottes sédimentaires pourrait refléter (i) des effets diagénétiques, (ii) des différences de productivité primaire entre le Pléistocène supérieur et l'Holocène, ou (iii) des changements dans la proportion relative de MO terrestre vs marine. Des apports relatifs relativement élevés de MO terrestre au cours du Pléistocène supérieur semblent constituer le mécanisme principal. Le transport de matériel allochtone des courants de turbidité, des décharge d'iceberg et des panaches d'eau de fonte sont les processus majeurs impliqués.

Dans les sédiments du dernier glaciaire de la mer du Labrador, les épisodes de délestage sédimentaire intense par les icebergs ("Heinrich events": H0, H1, H2 et H3) sont caractérisés par de faibles valeurs δ et de faibles concentrations en carbone organique et en azote, indiquant des apports relatifs élevés de MO terrestre et une productivité primaire réduite pendant ces intervalles. Aux environs de 8.5-7.5 ^{14}C ka, un phénomène similaire est observé, probablement en réponse à une étape finale de désintégration de la calotte laurentidienne.

Un contenu minimal assez uniforme (~0.2 à 0.4 %) de MO hautement réfractaire est observé dans la majorité des carottes et représente probablement du matériel remanié provenant de dépôts marins plus anciens et/ou d'origine terrestre. Les vitesses de sédimentation sensiblement plus élevées des périodes glaciaires-tardiglaciaire s'accompagnent de taux plus élevés d'enfouissement de la MO par comparaison avec l'Holocène. Toutefois, dans l'ensemble, les taux d'enfouissement de la MO sont plus élevés sur le talus de Nouvelle Ecosse que dans la mer du Labrador. Ceci suggère que les marges continentales constituent des dépôts-centres majeurs de MO. Les taux d'enfouissement estimés diminuent avec la profondeur dans le golfe du Saint-Laurent et au large. Dans la mer du Labrador, la "focalisation" des sédiments est responsable de flux de MO plus élevés dans la partie centrale du bassin que sur les talus environnants.

Dans le golfe du Saint-Laurent, la glycine, l'acide aspartique et l'acide glutamique constituent au minimum 50% des AATH. Dans quelques sites, des diminutions en AATH, dues à l'altération diagénétique de la MO, sont observées dans les carottes. Dans d'autres sites, des variations dans l'apport de MO pourraient conduire à d'apparentes augmentations en AATH, mais un ratio AATH/TN (pourcentage d'azote représenté par les acides aminés par rapport à l'azote total) de moins de 38% indique tout de même une certaine altération diagénétique de la MO.

ABSTRACT

The Labrador Sea and Gulf of St. Lawrence were in close proximity to the centers of formation and decay of the Laurentide and Greenland ice sheets. Compared to the Holocene, cold conditions and high input of meltwater to these areas during glacial-deglacial periods had great impact on the primary productivity, burial rate of organic/inorganic carbon, and input of allochthonous organic matter (OM). This study was undertaken to document spatial and temporal (since last glacial maximum) differences in primary productivity, burial rates of nitrogen and carbon, sources of OM as well as rate of diagenetic loss of nitrogen bearing OM. The stable isotopic compositions of organic carbon (OC) and nitrogen, contents of OC, nitrogen and CaCO_3 , and total hydrolyzable amino acids (THAA) of sedimentary OM from the Gulf of St. Lawrence and Labrador Sea were used to achieve these objectives. Samples from the Gulf of St. Lawrence-Scotia slope were collected during CSS-Hudson cruises 90-028 and 90-031, while those from the Labrador sea were collected during cruises HU-90-013 and HU-90-045.

In the Gulf of St. Lawrence-Scotia slope, the stable isotopic compositions of OC and nitrogen and the C/N ratios indicate that recent OM is primarily of marine origin. C/N ratios slightly higher than 10 suggest diagenetic evolution with preferential loss of nitrogen-bearing compounds over that of carbon hydrates.

In the Labrador Sea, at sites between 1300 and 3000 m deep, Holocene sediments are represented by a thin layer due to minimum deposition and/or winnowing by the strong western boundary undercurrent (WBUC). At these sites, stable isotopic compositions of OC and nitrogen as well as C/N ratios indicate that marine OM is confined in the upper 5-10 cm of sediment, i.e. to the Holocene part of the sediment. Below, the Late Pleistocene sediment is characterized by very low $\delta^{15}\text{N}$ and $\delta^{13}\text{C}$ values and high C/N ratios. The downcore decrease in the isotopic compositions may respond to (i) diagenetic effects, (ii) differences in primary productivity between the late Pleistocene and the Holocene, and (iii) to changes in the relative proportion of terrestrial/marine OM. Elevated relative inputs of terrestrial OM during the late Pleistocene seem to constitute the main mechanism. Transportation of allochthonous material by turbidity currents, iceberg deposition, meltwater plumes are the major processes involved.

In the last glacial sediments from the Labrador Sea, episodes of intense ice rafted deposition (Heinrich events: H0, H1, H2, and H3) are characterized by low δ -values, low OC and nitrogen content, indicating that high relative inputs of terrestrial OM and reduced primary productivity prevailed during these intervals. At approximately 8.5-7.5 ka, a similar feature is recorded, likely in response to a final stage of disintegration of the Laurentide ice sheet.

A fairly uniform background content (~ 0.2 to 0.4 %) of highly refractory OM is found in most cores and likely represents material reworked from older marine deposits and/or of terrestrial origin. Due to much higher sedimentation rates during glacial and deglacial periods, higher burial rates of OM are often estimated for such intervals compared to the Holocene.

However, overall burial rates of OM are higher in the Gulf of St. Lawrence-Scotia slope than in the Labrador Sea. This suggests that continental margins constitute major depocenters of OM. The estimated burial rates decrease with increasing water depths in the Gulf of St. Lawrence-Scotia slope. Within the Labrador Sea, sediment focusing, is responsible for higher OM fluxes in the central part of the basin, than on surrounding slopes.

In the Gulf of St. Lawrence, glycine, aspartic acid and glutamic acid constitute at least 50% of the THAA. At a few sites, downcore decreases in THAA are observed owing to diagenetic alteration of OM. At other sites, variations in the input of OM may result in apparent increases in THAA, but THAA-N/TN (percentage of nitrogen represented by the amino acids relative to total nitrogen) of less than 38% still indicate some diagenetic alteration of OM.

ACKNOWLEDGMENT

I have been privileged to receive financial and moral support from many individuals and institutions that made my dreams come true. Due to space limitation, I am unable to mention all of them, but for those whose names are not mentioned, I highly appreciated their contribution. I deeply appreciate the cooperation, as well as fruitful discussions and critical comments from my supervisor Dr. Claude Hillaire-Marcel, and from Dr. Stephen A. Macko that led to better presentation of this thesis. I appreciate the Chaire de Recherche en Environnement and Centre de Recherche en Géochimie Isotopique et en Géochronologie (GEOTOP) for the financial support, and the Bureau de la Coopération Internationale de l'Université du Québec à Montréal for providing exemption funds for my deferential tuition fees.

I am grateful to Dr. Clement Galiépy, Céline Hallé-Polèse, Alice Chassagne, and Isabelle Jacob for their patience and readiness to answer all my financial and social questions all the time. I appreciate Louise Cournoyer, Patricia Wickham, Monique Labelle, Dr. Guy Bilodeau, and Maryse Henry for help in the laboratory work. I acknowledge the crew members of four cruise missions (HU-90-013, HU-90-028, HU-90-031 and HU-91-045) for the sample collection, and Lisa Kellman, and Dr. Atiur Rahman for editorial comments.

Last but not least, I am greatly indebted to my parents for their hard work and sacrifices they made to fulfill their ambition '*we will fight by all means for a child who is thirst for education*'. I further appreciate the support from my wife and children, brothers and sister as well as the University of Dar es Salaam.

TABLE OF CONTENTS

	PAGE
RÉSUMÉ.....	ii
ABSTRACT	iv
ACKNOWLEDGEMENT	vi
CHAPTER 1	1
1.0.0. INTRODUCTION	1
1.1.0. Introductory Remarks	1
1.1.1. Definition and Objectives of Research Project	5
1.1.2. Importance of the Sub Arctic Environment	7
1.1.3. Parameters used in Achieving Objectives	9
1.2.0. THEORETICAL BACKGROUND OF APPLICATION OF STABLE ISOTOPES, ORGANIC CARBON, NITROGEN, C/N RATIOS AND AMINO ACIDS	9
1.2.1. Organic Carbon Stable Isotopes	10
1.2.2. Nitrogen Stable Isotopes	18
1.2.3. Content of Organic Carbon and Nitrogen	24
1.2.4. C/N Ratios	25
1.2.5. Hydrolyzable Amino Acids	26
CHAPTER 2	30
2.0.0. STUDY AREA DESCRIPTION AND PREVIOUS WORK DONE	30
2.1.0. GULF OF ST. LAWRENCE	30
2.1.1. Location and Physiography	30
2.1.2. Physical and Geological Setting	30

2.1.3. Paleoproductivity and Burial Rates	34
2.1.4. Sources of Organic Matter	34
2.1.5. Diagenetic Changes	36
2.2.0. LABRADOR SEA	36
2.2.1. Physical and Geological Setting	36
2.2.2. Paleoproductivity and Burial Rates	39
2.2.3. Sources of Organic Matter	40
2.2.4. Diagenetic Changes	41
2.3.0. WHAT REMAINS TO BE DONE	41
CHAPTER 3	43
3.0.0. MATERIAL AND METHODS	43
3.1.0. MATERIAL.....	43
3.1.1. Core Description: Labrador Continental Margin	43
3.1.2. Core Description: Greenland Continental Margin	47
3.1.3. Core Description: Gulf of St. Lawrence	49
3.2.0. METHODOLOGY	52
3.2.1. Geochemical Analysis	52
3.2.2. Estimation of Burial Rates and Paleoproductivity	54
3.2.3. Diagenetic Model	56
CHAPTER 4	60
4.0.0. LATERAL VARIATION IN SOURCES OF ORGANIC CARBON AND NITROGEN IN THE LABRADOR SEA AND GULF OF ST. LAWRENCE	60
4.1.0. GEOCHEMICAL RESULTS FOR SHORT CORES FROM THE LABRADOR SEA	60
4.1.1. Organic Carbon Stable Isotopes	60

4.1.2. Nitrogen Stable Isotopes	64
4.1.2. Organic Carbon Content	72
4.1.4. Nitrogen Content	72
4.1.5. CaCO ₃ Content	73
4.1.6. C/N Ratios	73
4.2.0. GEOCHEMICAL RESULTS FOR SHORT CORES FROM THE GULF OF ST. LAWRENCE	74
4.2.1. Organic carbon stable isotopes	74
4.2.2. Nitrogen Stable Isotopes	83
4.2.3. Organic Carbon Content	83
4.2.4. Nitrogen Content	85
4.2.5. CaCO ₃ Content	86
4.2.6. C/N ratios	86
4.3.0. LATERAL VARIATIONS	87
4.3.1. Labrador Sea	87
4.3.2. Gulf of St. Lawrence	89
4.4.0. DISCUSSION	91
4.4.1. Labrador Sea	91
4.4.2. Gulf of st. Lawrence	102
4.5.0. CONCLUSION	114
4.5.1. Labrador Sea	114
4.5.2. Gulf of St. Lawrence	115
CHAPTER 5	116

5.0.0. GLACIAL-INTERGLACIAL VARIATIONS IN SOURCES OF ORGANIC MATTER, PALEOPRODUCTIVITY AND BURIAL RATES OF NITROGEN AND CARBON.BURIAL RATES AND PRIMARY PRODUCTIVITY	116
5.1.0. GEOCHEMICAL RESULTS	117
5.1.1. HU-91-045-94 PC	117
5.1.2. HU-91-013-13 PC	121
5.1.3. HU-91-031-44 PC	124
5.2.0. VARIATION IN ACCUMULATION RATES AND PRIMARY PRODUCTIVITY	126
5.2.1. Lateral Variation in Accumulation Rates	126
5.2.2. Glacial-Interglacial Variations in Burial Rate	128
5.3.0. DISCUSSION	139
5.3.1. HU-91-045-94 PC	139
5.3.2. HU-91-013-13 PC	145
5.3.3. HU-91-031-44 PC	150
5.4.0. CONCLUSION	155
CHAPTER 6	157
6.0.0. DIAGENETIC CHANGES	157
6.1.0. GEOCHEMICAL RESULTS OF THE AMINO ACIDS DISTRIBUTION IN SEDIMENTS	157
6.1.1. HU-90-031-43 PC	157
6.1.2. HU-90-031-29 BC	160
6.1.3. HU-90-031-45 BC	163
6.1.4. HU-90-031-17 BC	166
6.2.0. RESULTS OF DIAGENETIC MODEL	176

6.2.1. Organic Carbon and Nitrogen	176
6.2.2. Amino Acids	173
6.3.0. DISCUSSION	173
6.3.1. HU-90-031-43 PC and HU-90-031-17 BC	173
6.3.2. HU-90-031-29 BC and HU-90-031-45 BC	175
6.4.0. CONCLUSION	177
CHAPTER 7	179
7.0.0. GENERAL CONCLUSIONS	179
7.1.0. METHODOLOGICAL ASPECT	179
7.2.0. REGIONAL TRENDS IN ORGANIC MATTER FLUXES	180
7.2.1. Labrador Sea	180
7.2.2. Gulf of St. Lawrence	181
7.2.3. Lateral Trends	182
7.3.0. GLACIAL/INTERGLACIAL	183
7.4.0. AMINO ACIDS: AN INSIGHT INTO DIAGENETIC EFFECTS?	184
7.5.0. PROBLEMS OF INTERPRETATION	185
7.6.0. SCIENTIFIC CONTRIBUTIONS	186
8.0.0. REFERENCES	188
9.0.0. APPENDIX	212

	PAGE
LIST OF FIGURES	
Fig. 1.1. Simplified conceptual model of the role of oceans in global carbon cycle (Source: JGOFS-Canada, 1989)	2
Fig. 1.2. Schematic representation of trends in pore-water profiles, showing the sequence of redox reactions involved in oxidative degradation of organic matter (modified after Van der Weijden, 1992)	4
Fig. 1.3. Schematic of major sedimentary or chemical carbon components and their $\delta^{13}\text{C}$ values or ranges (modified after Anderson and Arthur, 1983)	11
Fig. 1.4. General distribution of $\delta^{15}\text{N}$ for various natural substances (Modified after Kaplan, 1983)	12
Fig. 1.5. Major carbon pathways in marine, estuarine and freshwater environments (source: Tan, 1989)	13
Fig. 1.6. Variations in $\delta^{13}\text{C}$ composition of photosynthetically fixed carbon . A: Terrestrial plants; B: known C_3 and C_4 plants; C: known CAM plants; D: Algae; E: Aquatic plants; F: Marine plants exclusive of plankton; H: Marine plankton. (Source: Deines, 1980)	14
Fig. 1.7. $\delta^{13}\text{C}$ compositions of plankton samples versus water temperature (Source: Sackett, 1989)	16
Fig. 1.8. Relationship between $[\text{CO}_2(\text{aq})]$ and stable carbon isotope abundance in the bulk organic fraction of plankton (modified after Rau et al., 1991a)	17
Fig. 1.9. $\delta^{13}\text{C}$ in various biochemical constituents isolated from marine plankton. The $\delta^{13}\text{C}$ for Recent and ancient sediments are included for comparison. Diamond shaped figures represent 1-sigma ranges (Enlarged after Degens, 1969)	19
Fig. 1.10. The abundance of ^{15}N in terrestrial materials (Source: L��tolle, 1980).....	21
Fig. 1.11. (a) Variation in $\delta^{13}\text{C}$ and %C with depth in a sedimentary core from the Baffin Bay, Texas, algal mat laminations. (b) Variation in $\delta^{15}\text{N}$ and %N with depth in a sedimentary core from a Laguna Madre, Texas, seagrass bed. (Source: Macko et al., 1993)	24
Fig. 1.12. Means and ranges for mole % protein amino acid compositions of different groups of source organisms (Cowie and Hedges, 1992)	29
Fig. 2.1. Physiographic elements of the Gulf of St. Lawrence (Source: Loring, 1975)	31
Fig. 2.2. Typical summer-surface circulation pattern in the Gulf of St. Lawrence (After Sundby, 1974)	34
Fig. 2.3. Average $\delta^{13}\text{C}$ (��) of the particulate organic carbon in the top centimetre of the sediments from the lower estuarine of St. Lawrence (Modified after Lucotte et al., 1991)	35

Fig. 2.4. A map showing bathymetry and the present-day surface water circulation of the northwest Atlantic Ocean (Source: Lucotte and Hillaire-Marcel, 1994).	37
Fig. 3.1. A map showing sampling sites in the the Gulf of St. Lawrence-Scotian slope	45
Fig. 3.2. A map showing sampling sites in the Labrador Sea	46
Fig. 3.3. Onsite redox potential (Eh in mV) for short cores collected from the Labrador Sea	48
Fig. 3.4. Onsite redox potential (mV) for short cores collected from the Gulf of St. Lawrence	51
Fig. 3.5. Curve fitting results for ^{14}C and calender ages (left), and downcore variations in the estimated sedimentation rates based on ^{14}C and calender ages (right) at site HU-90-031-44 PC	57
Fig. 4.1. Downcore variation in $\delta^{13}\text{C}$, $\delta^{15}\text{N}$, CaCO_3 , organic carbon, nitrogen and C/N ratios for core HU-91-045-05 BC	61
Fig. 4.2. Downcore variation in $\delta^{13}\text{C}$, $\delta^{15}\text{N}$, CaCO_3 , organic carbon, nitrogen and C/N ratios for core HU-91-045-93 BC	62
Fig. 4.3. Downcore variation in $\delta^{13}\text{C}$, $\delta^{15}\text{N}$, CaCO_3 , organic carbon, nitrogen and C/N ratios for core HU-91-045-14 BC	63
Fig. 4.4. Downcore variation in $\delta^{13}\text{C}$, $\delta^{15}\text{N}$, CaCO_3 , organic carbon, nitrogen and C/N ratios for core HU-91-045-16 BC	65
Fig. 4.5. Downcore variation in $\delta^{13}\text{C}$, $\delta^{15}\text{N}$, CaCO_3 , organic carbon, nitrogen and C/N ratios for core HU-91-045-18 BC	66
Fig. 4.6. Downcore variation in $\delta^{13}\text{C}$, $\delta^{15}\text{N}$, CaCO_3 , organic carbon, nitrogen and C/N ratios for core HU-91-045-23 BC	67
Fig. 4.7. Downcore variation in $\delta^{13}\text{C}$, $\delta^{15}\text{N}$, CaCO_3 , organic carbon, nitrogen and C/N ratios for core HU-91-045-38 TWC	68
Fig. 4.8. Downcore variation in $\delta^{13}\text{C}$, $\delta^{15}\text{N}$, CaCO_3 , organic carbon, nitrogen and C/N ratios for core HU-91-045-40 LHC	69
Fig. 4.9. Downcore variation in $\delta^{13}\text{C}$, $\delta^{15}\text{N}$, CaCO_3 , organic carbon, nitrogen and C/N ratios for core HU-91-045-28 BC	70
Fig. 4.10. Downcore variation in $\delta^{13}\text{C}$, $\delta^{15}\text{N}$, CaCO_3 , organic carbon, nitrogen and C/N ratios for core HU-90-013-11 BC	71
Fig. 4.11. Downcore variation in $\delta^{13}\text{C}$, $\delta^{15}\text{N}$, CaCO_3 , organic carbon, nitrogen and C/N ratios for core HU-90-031-45 BC	75
Fig. 4.12. Downcore variation in $\delta^{13}\text{C}$, $\delta^{15}\text{N}$, CaCO_3 , organic carbon, nitrogen and C/N ratios for core HU-90-031-29 BC	76

Fig. 4.13. Downcore variation in $\delta^{13}\text{C}$, $\delta^{15}\text{N}$, CaCO_3 , organic carbon, nitrogen and C/N ratios for core HU-90-031-34 BC	77
Fig. 4.14. Downcore variation in $\delta^{13}\text{C}$, $\delta^{15}\text{N}$, CaCO_3 , organic carbon, nitrogen and C/N ratios for core HU-90-031-41 BC	78
Fig. 4.15. Downcore variation in $\delta^{13}\text{C}$, $\delta^{15}\text{N}$, CaCO_3 , organic carbon, nitrogen and C/N ratios for core HU-90-031-59 BC	79
Fig. 4.16. Downcore variation in $\delta^{13}\text{C}$, $\delta^{15}\text{N}$, CaCO_3 , organic carbon, nitrogen and C/N ratios for core HU-90-031-17 BC	80
Fig. 4.17. Downcore variation in $\delta^{13}\text{C}$, $\delta^{15}\text{N}$, CaCO_3 , organic carbon, nitrogen and C/N ratios for core HU-90-031-43 PC	81
Fig. 4.18. Downcore variation in $\delta^{13}\text{C}$, $\delta^{15}\text{N}$, CaCO_3 , organic carbon, nitrogen and C/N ratios for core HU-90-031-13 BC	82
Fig. 4.19. Downcore variation in $\delta^{13}\text{C}$, $\delta^{15}\text{N}$, CaCO_3 , organic carbon, nitrogen and C/N ratios for core HU-90-028-06 BC	84
Fig. 4.20. Lateral variation in $\delta^{13}\text{C}$, $\delta^{15}\text{N}$, CaCO_3 , organic carbon, nitrogen and C/N ratios in the Labrador Sea	88
Fig. 4.21. Lateral variation in $\delta^{13}\text{C}$, $\delta^{15}\text{N}$, CaCO_3 , organic carbon, nitrogen and C/N ratios in the Gulf of St. Lawrence-Scotia slope	90
Fig. 4.22. Scatter plots for cores HU-91-045-14 BC (solid circle), and HU-90-013-11 BC (solid rectangle)	92
Fig. 4.23. Scatter plots for cores HU-91-045-23 BC (open circle), and HU-91-045-28 BC (solid circle)	93
Fig. 4.24. Scatter plots for cores HU-91-045-16 BC (solid circle), and HU-91-045-18 BC (solid rectangle)	94
Fig. 4.25. Scatter plots for cores HU-90-031 34 BC (solid circle), All Gulf data (crossed rectangle) and HU-90-031-29 BC (solid rectangle)	105
Fig. 4.26. Scatter plots for cores HU-90-031-13 BC (solid rectangle), HU-90-031-45 BC (crossed rectangle), HU-90-031-41 BC (solid circle), HU-90-031-17 BC (open circle) and HU-90-031-06 BC (open rectangle)	109
Fig. 4.27. Scatter plots for cores HU-90-031-43 PC (solid diamond), and HU-90-031-59 BC (solid circle)	111
Fig. 5.1. Downcore variation of various geochemical parameters for core HU-91-045-94 PC	118
Fig. 5.2. Profiles of reworked palynomorphs, marine and terrestrial OM, dinocysts and organic lining of benthic foraminifera for core HU-91-045-94 PC	119
Fig. 5.3. Downcore variation of various geochemical parameters for core HU-90-013-13 PC	122

Fig. 5.4. Downcore variation of various geochemical parameters and ^{14}C ages for core HU-90-031-44 PC	125
Fig. 5.5. Lateral variation in burial rate, paleoproductivity and paleoflux in the Labrador Sea and Gulf of St. Lawrence-Scotia slope	127
Fig. 5.6. Downcore variation in burial rate, paleoproductivity and paleoflux at site HU-90-013-11 BC	130
Fig. 5.7. Downcore variation in various primary productivity indicators at Site HU-90-013-11 BC	131
Fig. 5.8. Downcore variation in burial rate, paleoproductivity and paleoflux at Site HU-91-045-94 PC	133
Fig. 5.9. Downcore variation in burial rate, paleoproductivity and paleoflux at Site HU-90-013-13 PC	135
Fig. 5.10. Downcore variation in burial rate, paleoproductivity and paleoflux at Site HU-90-031-44 PC	136
Fig. 5.11. Downcore variation in reworked palynomorph and various primary productivity indicators at Site HU-90-013-13 PC	137
Fig. 5.12. Downcore variation in spores, pollen and dinocyst at Site HU-90-031-44 PC	152
Fig. 6.1. Downcore variations of individual amino acids for core HU-90-031-43 PC	158
Fig. 6.2. Downcore variations of THAA (%), THAA-C (%), THAA-N (%), THAA-N/TN (%) and THAA-C/OC for core HU-90-031-43 PC	159
Fig. 6.3. Downcore variations of individual amino acids for core HU-90-031-29 BC	161
Fig. 6.4. Downcore variations of THAA (%), THAA-C (%), THAA-N (%), THAA-N/TN (%) and THAA-C/OC for core HU-90-031-29 BC	162
Fig. 6.5. Downcore variations of THAA (%), THAA-C (%), THAA-N (%), THAA-N/TN (%) and THAA-C/OC for core HU-90-031-45 BC	164
Fig. 6.6. Downcore variations of individual amino acids for core HU-90-031-45 BC	165
Fig. 6.7. Downcore variations of individual amino acids for core HU-90-031-17 BC	167
Fig. 6.8. Downcore variations of THAA (%), THAA-C (%), THAA-N (%), THAA-N/TN (%) and THAA-C/OC for core HU-90-031-17 BC	168
Fig. 6.9. Plots showing curve fitting results of organic carbon and/or total nitrogen for cores HU-90-031-44 PC, HU-90-031-17 BC, HU-90-031-29 BC and HU-90-031-41 BC	170

Fig. 6.10. Plots showing curve fitting results of organic carbon and/or total nitrogen for cores HU-90-031-45 BC and HU-90-031-43 PC, total hydrolysable amino acids (THAA), total hydrolysable amino acids carbon (THAA-C) and total hydrolysable amino acids nitrogen (THAA-N) for core HU-90-031-43 PC 171

LIST OF TABLES

TABLE	PAGE
Table 1.1. Nitrogen Isotope Fractionation in Various Biochemical Processes	21
Table 3.1. Cores used in this study	47
Table 3.2. Colour, sediment types and number of samples analyzed for various cores used in this study	213
Table 3.3. Various constants used to express relationships between fluxes of OM and primary productivity	216
Table 4.1. Geochemical results for cores:	
HU-91-045-05 BC	218
HU-91-045-14 BC	219
HU-91-045-16 BC	220
HU-91-045-18 BC	221
HU-91-045-23 BC	222
HU-91-045-28 BC	223
HU-91-045-93 BC	224
HU-91-045-38 TWC	225
HU-91-045-40 LHC	225
HU-90-013-11 BC	226
Table 4.2. Geochemical Results for Cores:	
HU-90-031-13 BC	227
HU-90-031-17 BC	228
HU-90-031-29 BC	229
HU-90-031-34 BC	230
HU-90-031-41 BC	231
HU-90-031-43 PC	232
HU-90-028-06 BC	233
HU-90-031-45 BC	234
HU-90-031-59 BC	235
Table 5.1. Geochemical Results for core HU-91-045-94 PC	237
Table 5.2. Geochemical Results for core HU-90-013-13 PC	239

Table 5.3. Geochemical Results for core HU-90-031-44 PC	241
Table 5.4. Estimated accumulation rate of OC (AR_{OC} , gC/m ² /yr), and nitrogen (AR_N gN/m ² /yr), new paleoproductivity (PP_N , gC/m ² /yr), total paleoproductivity (PP_T , gC/m ² /yr), and fluxes (gC/m ² /yr) of OC at various sites	244
Table 5.5. Estimated accumulation rate of total OC (AR_{OC} , mgC/m ² /yr), nitrogen (AR_N , mgN/m ² /yr) and marine OC (AR_{MOC} , mgC/m ² /yr), new paleoproductivity (PP_N gC/m ² /yr), total paleoproductivity (PP_T , gC/m ² /yr), and fluxes (gC/m ² /yr) of OC for core HU-90-013-11 BC	245
Table 5.6. Estimated accumulation rate of total OC (AR_{OC} , mgC/m ² /yr), nitrogen (AR_N mgN/m ² /yr) and marine OC (AR_{MOC} mgC/m ² /yr), new paleoproductivity (PP_N , gC/m ² /yr), total paleoproductivity (PP_T , gC/m ² /yr), and fluxes (gC/m ² /yr) of OC for core HU-91-045-94 PC	246
Table 5.7. Estimated accumulation rate of total OC (AR_{OC} , mgC/m ² /yr), nitrogen (AR_N , mgN/m ² /yr) and marine OC (AR_{MOC} , mg/m ² /yr), new paleoproductivity (PP_N , gC/m ² /yr), total paleoproductivity (PP_T gC/m ² /yr), and fluxes (gC/m ² /yr) of OC for core HU-90-013-13 PC	248
Table 5.8. Estimated accumulation rate of total OC (AR_{OC} , gC/m ² /yr), nitrogen (AR_N gN/m ² /yr) and marine OC (AR_{MOC} gC/m ² /yr), new paleoproductivity (PP_N , gC/m ² /yr), total paleoproductivity (PP_T , gC/m ² /yr), and fluxes (gC/m ² /yr) of OC for core HU-90-031-44 PC	250
Table 6.1. Geochemical results of total hydrolyzable amino acids (THAA) for core HU-90-031-43 PC	255
Table 6.2. Geochemical results of total hydrolyzable amino acids (THAA) for core HU-90-031-29 BC	257
Table 6.3. Geochemical results of total amino acids (THAA) for core HU-90-031- 45 BC	259
Table 6.4. Geochemical results of total hydrolyzable amino acids (THAA) for core HU-90-031-17 BC	261
Table 6.5. Results of curve fitting (model)	175

CHAPTER 1

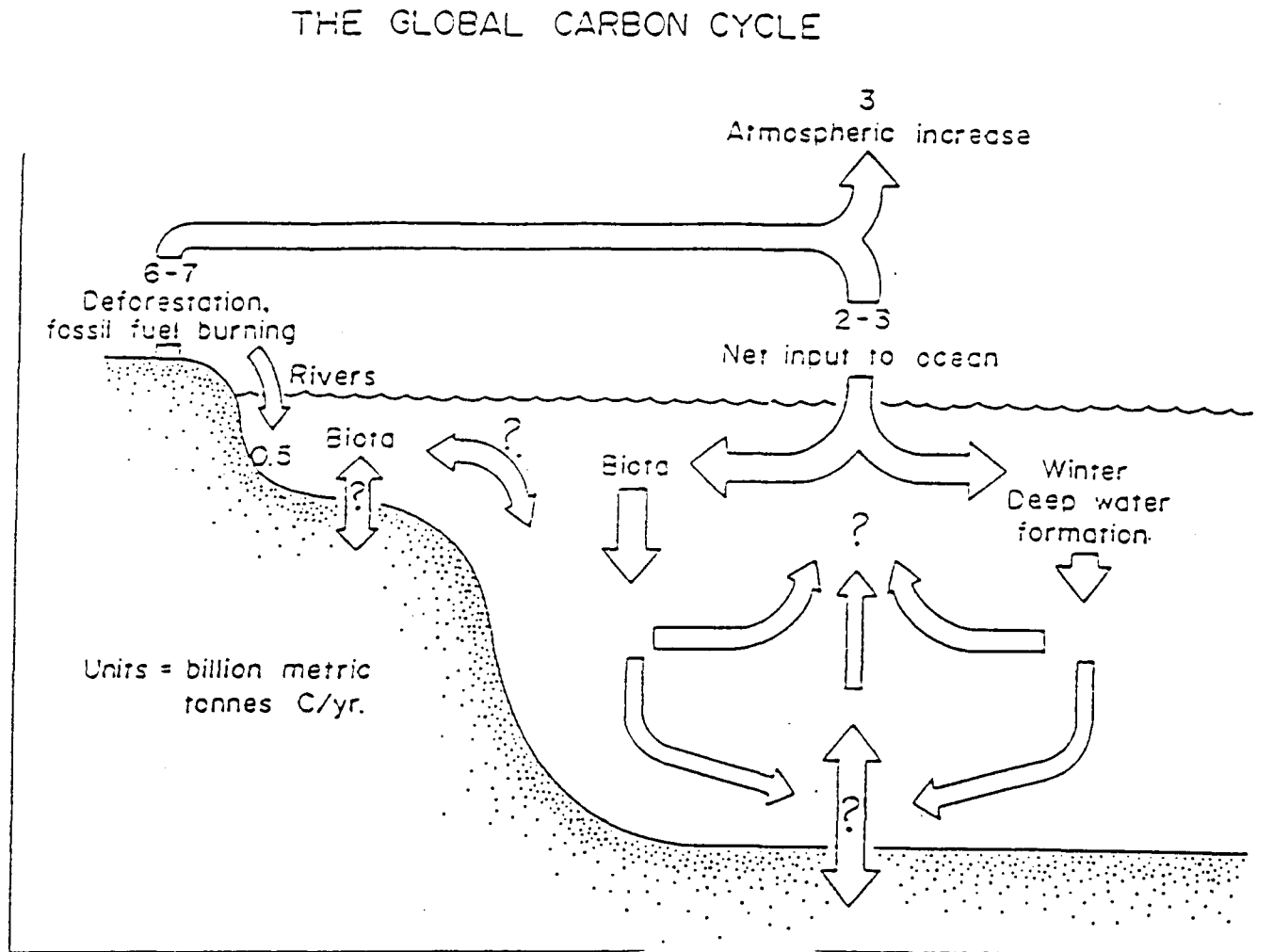
1.0.0. INTRODUCTION

1.1.0. INTRODUCTORY REMARKS

Carbon and nitrogen are very important elements in the biosphere. Both act as principal building blocks of all organic materials. Moreover, nitrogen is the essential nutrient which limits primary productivity. Apart from these roles, they act as efficient scavengers, removing many trace elements from the hydrosphere, as well as regulators of atmospheric temperatures and the global stratospheric ozone shield in the form of oxides (Rosswall, 1981; Ramanathan et al., 1985; Watson et al., 1990; Shine et al., 1990; Johnson et al., 1992). Thus, the amounts of these elements and their compounds present in the atmosphere and hydrosphere, partly controls the earth's climate and metal concentrations, respectively. Therefore, a knowledge of their input and output to various reservoirs is essential in understanding changes in primary productivity, climate and metal accumulation. However, as illustrated in Fig. 1.1, little is known on the input and output of organic matter (OM) in the deep ocean.

With the exception of primordial carbon and nitrogen, the carbon and nitrogen inputs to the atmosphere result primarily from the decomposition of OM through metamorphism, and combustion processes. Since the industrial revolution, the input of carbon dioxide and nitrogen compounds to the atmosphere through fossil fuel combustion and industrial emissions has been steadily increasing. Another mechanism of carbon and nitrogen input to the atmosphere is diagenesis (decay of organic material). Both anoxic and oxic decomposition of OM generate CO_2 whereas molecular nitrogen is generated during denitrification which is also linked to OM decomposition. A substantial fraction of freshly produced OM and eroded fossil plant materials becomes oxidized to CO_2 and N_2 and escapes to the atmosphere. Degradation of OM takes place in the soil, water column, at the

Fig. 1.1. Simplified conceptual model of the role of oceans in global carbon cycle (Source: JGOFS Canada, 1989).



sediment-water interface and within the sediments. The only global sink or output of carbon and nitrogen occurs when OM is incorporated into the sediments and sedimentary rocks of the earth's crust, principally in the form of carbonates and OM such as coal, oil, natural gas and kerogen (finely disseminated OM in sediments).

Oceans, which cover about 71% of the earth's surface, are major regulators of nitrogen and carbon exchange with the atmosphere. They also regulate long term climate change through the transport of heat and moisture from the tropics to the polar regions, and are the locii of carbon and nitrogen storage in sediments. Although attempts have been made to estimate various fluxes of OM

in the ocean (Fig. 1.1), notably at the sea floor, the processes controlling its burial rate in the marine sediments are not well understood (Oslen et al., 1985). Because of high differences in climatic conditions between glacial and interglacial periods, particularly in high altitude areas, there is also a need to investigate changes in burial rates of OM in the ocean in relation to drastic climatic changes of the Quaternary.

Although high primary productivity causes an increased flux of OM to the seafloor, only a small portion is preserved. A large part of OM is degraded while in the water column, and during early diagenesis at the sediment-water interface and through late diagenetic processes within the sediments. Oxidation of OM occurs in sequence with the oxidant that produces most free energy change per mole of organic carbon oxidized being consumed first (Fig. 1.2). Among five oxidants of OM (O_2 , NO_3 , MnO_2 , $FeO(OH)$ and SO_4), the O_2 content of the water column and sediments is considered to be the most important factor controlling preservation of OM (Canfield, 1989; Froelich et al., 1979; Emerson and Hedges, 1988; Dean et al., 1994). The role of oxygen content in the sediments as a primary factor controlling preservation of OM has been questioned based on (1) the observation of high degradation of OM of equal magnitude by sulphate reduction and nitrate reduction (Canfield, 1989; Dean et al., 1994; Lee, 1992); and (2) the lack of correlation between sedimentary organic carbon content and bottom water oxygen concentrations (Calvert, 1987; Reimers et al., 1992; Pedersen et al., 1992; Pedersen and Calvert, 1990; Calvert and Pedersen, 1992). A compilation of carbon preservation data by Canfield (1994) shows that OM can be preserved in both oxic and anoxic environments depending on the circumstance of deposition. Overall, it was concluded that sediment deposition rate is the most important factor influencing preservation. At sediment deposition rates greater than $\sim 0.04 \text{ g cm}^{-2} \text{ yr}^{-1}$ (equal to 0.04 cm yr^{-1} with a porosity of 0.6) similar preservation is observed for deposition in both oxic and anoxic environments, while at sedimentation rates below $\sim 0.04 \text{ g cm}^{-2} \text{ yr}^{-1}$, enhanced preservation is

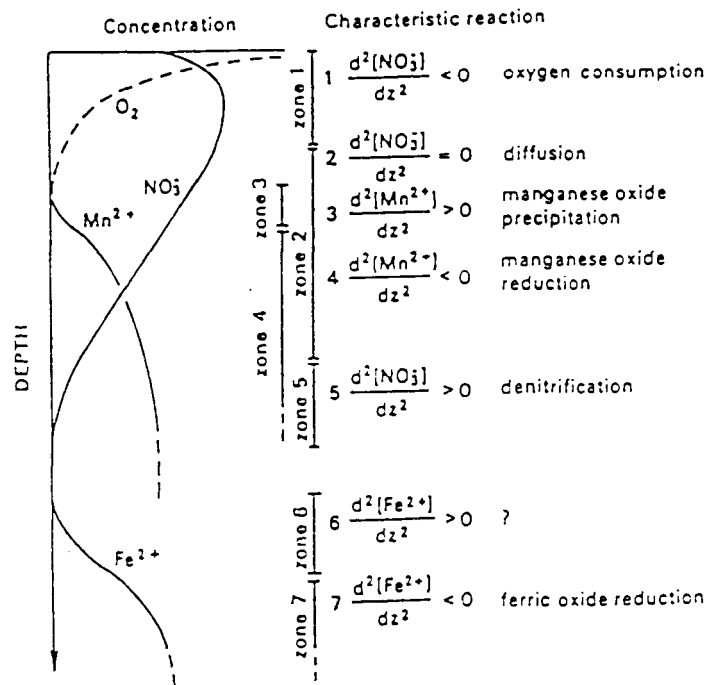


Fig. 1.2. Schematic representation of trends in pore-water profiles, showing the sequence of redox reactions involved in oxidative degradation of organic matter (modified after Van der Weijden, 1992).

observed for sediments deposited in both low- O_2 and euxinic environments (Canfield, 1994). Therefore, the burial rate of OM in the oceans is a function of the rate of sedimentation, biological mixing of surface sediments and diagenesis. Other probable factors include water current strength, vertical and lateral fluxes of allochthonous OM input as well as authigenic OM input, which is largely dependent on the primary productivity in the euphotic zone. Thus it is important to establish or quantify the importance of these factors before estimating burial rates of OM in any sedimentary basin. However, to fully understand these processes a multidisciplinary investigation is required. Because the OM buried in the sediments is only a fraction that escaped diagenesis, the extent of diagenesis needs to be evaluated in order to make correct estimates of the relationship between temporal changes in paleoproductivity and OM accumulation in sediments.

1.1.1. Definition and Objectives of the Research Project

In high latitude areas, the magnitude of variability of environmental conditions and surface area covered by sea ice is high during glacial period (de Vernal et al., 1994). Therefore, there is a several orders of magnitude difference in primary productivity and burial rates of OM between glacial and interglacial periods. Moreover, the production of OM by phytoplankton is one of the transitory sinks of atmospheric CO₂. As a result, carbon and nitrogen fluxes including their burial rates with associated diagenetic changes in subarctic basins, play major roles in climate change. Therefore, the major objective of present work is to provide quantitative estimates of burial rates of OM in the subarctic marine environment of the Labrador Sea and Gulf of St. Lawrence while establishing the relationship to climatic changes over the past 30 ka. The stable isotopic compositions of organic carbon and nitrogen, C/N ratios and organic carbon, nitrogen and CaCO₃ contents of sediments in cores collected during four separate cruises (HU-90-028, HU-90-031, HU-90-013, HU-91-045) of the SS Hudson are used to achieve this objective.

Walsh et al. (1981) and Walsh (1991) suggested that continental margins are major repositories of organic carbon and nitrogen. Off the eastern Canadian coast, no systematic studies had been conducted to evaluate the relative role of these regions with respect to the storage of OM. Such a study constitutes the second objective of this study.

As pointed out previously, autochthonous OM buried in the marine sediments is responsible for the direct removal of carbon and nitrogen from the atmosphere. Therefore, prior to estimation of burial rates using sedimentary organic carbon and nitrogen, it is important to evaluate and quantify the sources of OM in a particular environment. In the Labrador Sea and Gulf of St. Lawrence, large variations in the proportion of allochthonous OM occur during glacial and interglacial periods. During the decay of the Laurentide Ice Sheet, enormous amounts of fresh meltwater and icebergs were introduced into the Labrador Sea and the Atlantic Ocean through the

Hudson Strait, Gulf of St. Lawrence and Gulf of Mexico (Fulton and Prest, 1987; Teller, 1990; Anderson and Lewis, 1992; Dyke and Prest, 1987; Rodrigues et al., 1993). Inflow of fresh meltwater to the area undoubtedly was associated with enhanced input of terrestrial material. Therefore, the third objective of this study is to delineate various sources of organic carbon and nitrogen using stable isotopes of organic carbon and nitrogen and C/N ratios.

One method for the estimation of paleoproductivity relies on the organic carbon preserved in the sediments. However, as pointed out previously, only a small fraction of organic carbon produced in the euphotic zone is preserved in the sediments. Owing to diagenetic alteration of OM, estimates of burial rate may not be able directly to be related to the paleoproductivity. Therefore, it is also important to evaluate the extent of OM degradation. Total hydrolysable amino acids (THAA) in addition to organic carbon and nitrogen contents and C/N ratios are used to assess the diagenetic changes of OM.

During ice ages large amount of icebergs were introduced into the Atlantic Ocean, and led to the deposition of layers known as Heinrich events (e.g. Hillaire-Marcel et al., 1994a; Bond et al., 1992; Broecker et al., 1992). The Heinrich events in the Labrador Sea and north Atlantic Ocean in general have been characterized using the contents of coarse fraction greater than 150 microns, CaCO_3 , magnetic properties and distribution of microfossils (Hillaire-Marcel et al., 1994a; Stoner et al., 1994). This study uses stable isotopes of organic carbon and nitrogen as a tool to characterize OM supply and productivity changes during the Heinrich events. Apart from being used to characterize Heinrich events, stable isotopes are used as a tool to map lateral variations in the proportions of marine/terrestrial OM.

One of the key assumptions in using stable isotopes to address environmental problems is that little or no isotopic change occurs during the diagenetic alteration of OM (e.g. Sackett, 1989). However, plant components with different isotopic compositions, are degraded at different rates, and

preferential preservation of some compounds may cause a significant alteration in the stable isotopes compositions of the bulk OM of a sediment. In this present study attention is paid to the effect of diagenesis on the stable isotopic compositions of OM.

1.1.2. Importance of the Subarctic Environment

The Labrador Sea and Gulf of St. Lawrence are good sites for this type of study for several reasons, including (1) these areas are suspected to be a depocenter of OM since the continental margins are considered to be major sinks of organic carbon and nitrogen (Walsh et al., 1981; Walsh, 1991) owing to high sedimentation rates, relatively shallow depth as well as high primary productivity. Because the study areas are associated with sedimentation rates as high as 40 cm/ka (Hillaire-Marcel et al., 1994a) and high primary productivity, large quantities of labile OM are expected to reach the sea floor. Thus high resolution records and noticeable diagenetic changes are expected in such an environmental setting.

(2) The high latitude north Atlantic is presently a major atmospheric CO₂ sink as a result of the formation of deep bottom water, primary productivity and resultant OM sedimentation (Walsh, 1989; Volk and Liu, 1988). Because production of OM by phytoplankton is one of the sinks of atmospheric CO₂, it is hypothesized that carbon and nitrogen fluxes and their burial rates (diagenetic changes) in subarctic basins play a major role in the world budget of carbon and nitrogen as well as in climate change, owing to the difference by several orders of magnitude, in primary productivity between glacial and interglacial periods. As pointed out previously, during the last glacial maximum, the Labrador Sea and adjacent land masses were largely covered by sea-ice and glaciers respectively (CLIMAP, 1976; de Vernal et al., 1994). Owing to an almost permanent ice cover, primary productivity in the area was reduced, as indicated by a low abundance of coccoliths, diatoms and dinocysts in the sediments of this age (Aksu et al., 1988; Hillaire-Marcel

et al., 1994a; de Vernal et al., 1994). At present, the Labrador Sea is one of the most productive areas of the world (Lucotte et al., 1994). As a result, the difference between glacial and interglacial primary productivity is probably very high in the subarctic marine environments. However, this conclusion is contrary to that of Sancetta (1992) who suggested that primary production in the north Atlantic was as high during the last glacial maximum as it is today.

(3) A third reason for the importance of the study areas is close proximity to the centres of formation and decay of major ice sheets. The last 30 ka have seen the growth of the Laurentide ice sheet, reaching its peak at approximately 18,000 ^{14}C years (last glacial maximum), followed by its decay (during deglaciation), which is inferred to have commenced at about 14 ka (^{14}C ages) (Keigwin et al., 1991; Fairbank, 1989; Jones and Keigwin, 1988; Broecker et al., 1988; Jansen and Veum, 1990; Keigwin and Jones, 1990). As stated before, enormous amounts of fresh meltwater and icebergs were introduced into the Labrador Sea and the Atlantic Ocean through the Hudson Strait, Gulf of St. Lawrence and Gulf of Mexico during the decay of the Laurentide Ice Sheet (Fulton and Prest, 1987; Teller, 1990; Anderson and Lewis, 1992; Dyke and Prest, 1987; Rodrigues et al., 1993). The estimated volume of water channelled through the St. Lawrence and Hudson river valleys to the Atlantic Ocean ranged between 20,300 m/sec and 65,300 m/sec (Teller, 1990). Inflow of such enormous amounts of freshwater to the area undoubtedly had various impacts, including the lowering of sea surface temperatures, reduction in salinity, increased stratification, enhanced input of terrestrial materials, and the reduction in primary productivity. Its signature may have been preserved in the sediments in the form of geochemical, paleontological and sedimentological indicators such as ice-rafted debris, organic carbon and grain size distribution.

(4) The ongoing multidisciplinary work on the palaeoceanography and palaeoproductivity of the Labrador Sea during the last climatic cycle has generated valuable complementary data required for this study. Parameters such as sedimentation rates determined through AMS ^{14}C dating

and ^{18}O isotope stratigraphy, will be essential in providing the time control required for determination of burial rates of nitrogen bearing OM in the area.

1.1.3. Parameters used in Achieving Objectives.

The burial rate of OM and paleoproductivity over time may be deduced from climatic and primary productivity indicators preserved in sediments. Some of the indicators which have been used include sedimentary enrichments in ^{230}Th or uranium, abundances of coccoliths, diatoms and dinocysts, the contents of organic carbon and nitrogen in the sediments as well as the stable isotopic compositions of organic carbon and nitrogen (Müller and Suess, 1979; Suess and Müller, 1980; Aksu et al., 1988; Hillaire-Marcel et al., 1990; Stein, 1991, 1986a,b; Stein et al., 1986, 1989a,b). Early diagenetic changes can be inferred from the downcore distribution of amino acids as well as the C/N ratios (Henrichs et al., 1984; Burdige and Martens, 1988; Cowie and Hedges, 1994). In the present study, the parameters used to achieve the above mentioned objectives include isotopic compositions of both organic carbon and nitrogen, the content of sedimentary organic carbon, nitrogen, CaCO_3 as well as total hydrolyzable amino acids (THAA). Other data also available include $\delta^{18}\text{O}$ values, content of microfossils, dry bulk density, porosity as well as Accelerator Mass Spectrometric ages (AMS). These parameters were determined on sedimentary materials collected from the Gulf of St. Lawrence-Scotia Slope and the Labrador Sea (See chapter 3).

1.2.0. THEORETICAL BACKGROUND OF APPLICATION OF STABLE ISOTOPES, ORGANIC CARBON, NITROGEN C/N RATIOS AND AMINO ACIDS.

The stable isotopic compositions of organic carbon and nitrogen have a wide field of application including indicator of sources of organic materials in marine environments (Macko, 1983; Anderson et al., 1992; Peters et al., 1978; Botello et al., 1980), food chain studies (Fry and

Sherr, 1984; Peterson and Fry, 1987), palaeoproductivity, climate and nutrient utilization (Altabet and Francois, 1994a,b; Calvert et al., 1992a; Francois et al., 1992, 1993a; Rau et al., 1991a,b, 1992). The use of these isotopes is based on the assumptions that (i) there exist distinct isotopic compositions among various OM sources, and (ii) the isotopic signatures are retained by various components of the food web and the organic composite products which have undergone biochemical and thermocatalytic induced maturation during burial in sediments (Sackett, 1989).

Because of the biological fractionation, the stable isotope compositions of carbon and nitrogen in natural organic materials are highly variable (Figs. 1.3 and 1.4). The biological fractionation of isotopes occurs during photosynthesis, nitrogen fixation, denitrification, assimilation of nitrogen compounds, and deamination as well as during other diagenetic processes.

1.2.1. Organic Carbon Stable Isotopes.

Carbon has two stable isotopes namely ^{12}C and ^{13}C whose abundance on earth is 98.89% and 1.11%, respectively. In the hydrosphere, carbon occurs as dissolved carbon dioxide, bicarbonate ion (HCO_3^{-1}) and carbonate ion (CO_3^{-2}). The CO_3^{-2} results from dissolution of atmospheric CO_2 , dissolution of CO_2 generated during the decay of OM and dissolution of carbonate (Fig. 1.5). The isotopic compositions of these species in marine environments are -7‰ (atmospheric CO_2), +2‰ (HCO_3^{-1}), and 0‰ (CO_3^{-2}) (Tan, 1989). Freshwater HCO_3^{-1} and CO_3^{-2} have light and variable $\delta^{13}\text{C}$ values partly, due to plant respiration and oxidation of plant debris in soils (Faure, 1986). Although the degree of fractionation in plants may be similar, differences in the isotopic compositions of starting materials may lead to differences in the isotopic compositions of the final product. Possibly when there was a massive input of freshwater to the ocean during disintegration of the Laurentide ice sheet to the Atlantic Ocean, the OM formed during this period was depleted in ^{13}C compared to other normal marine environmental periods. Apart from the isotopic content of the starting

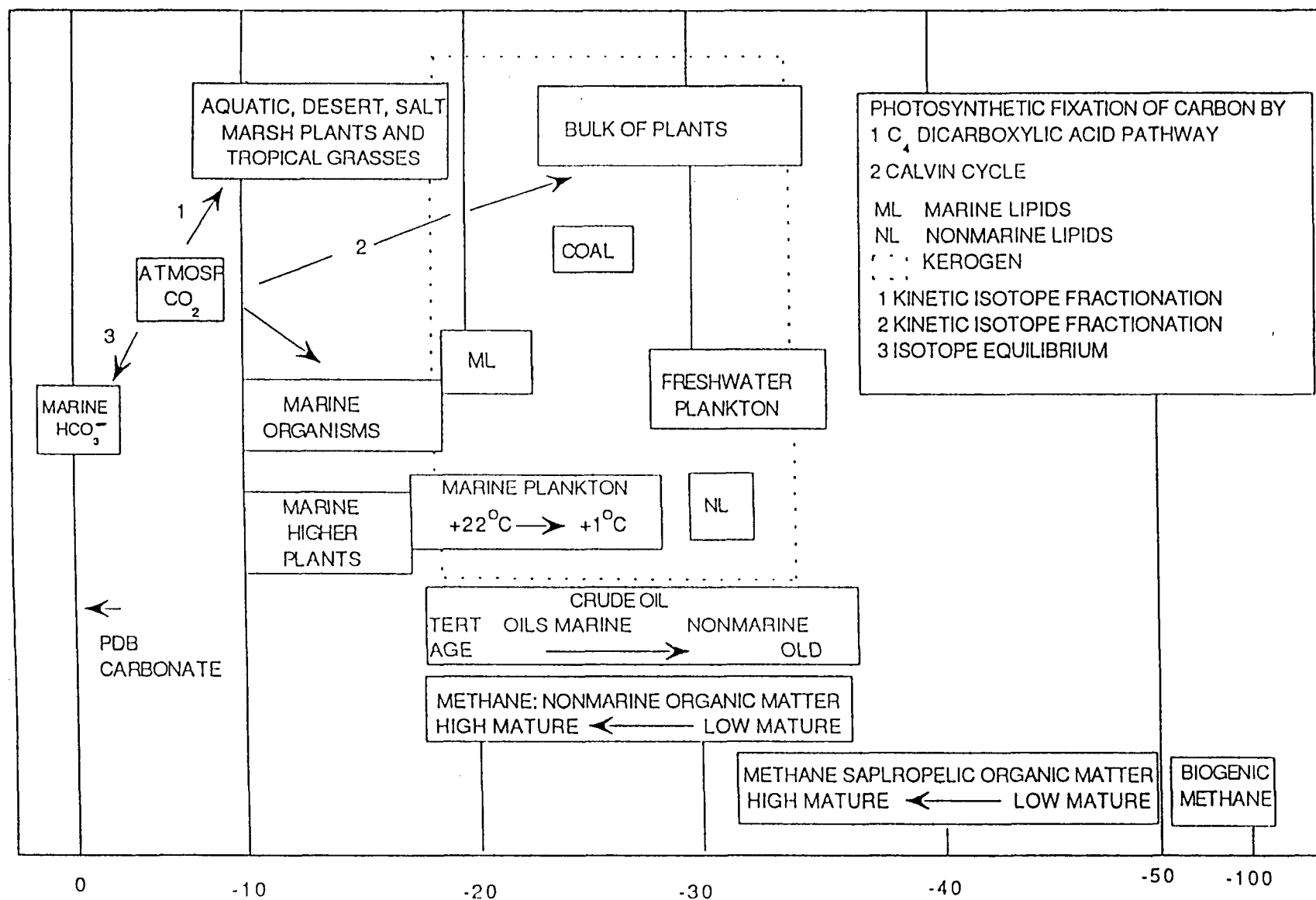
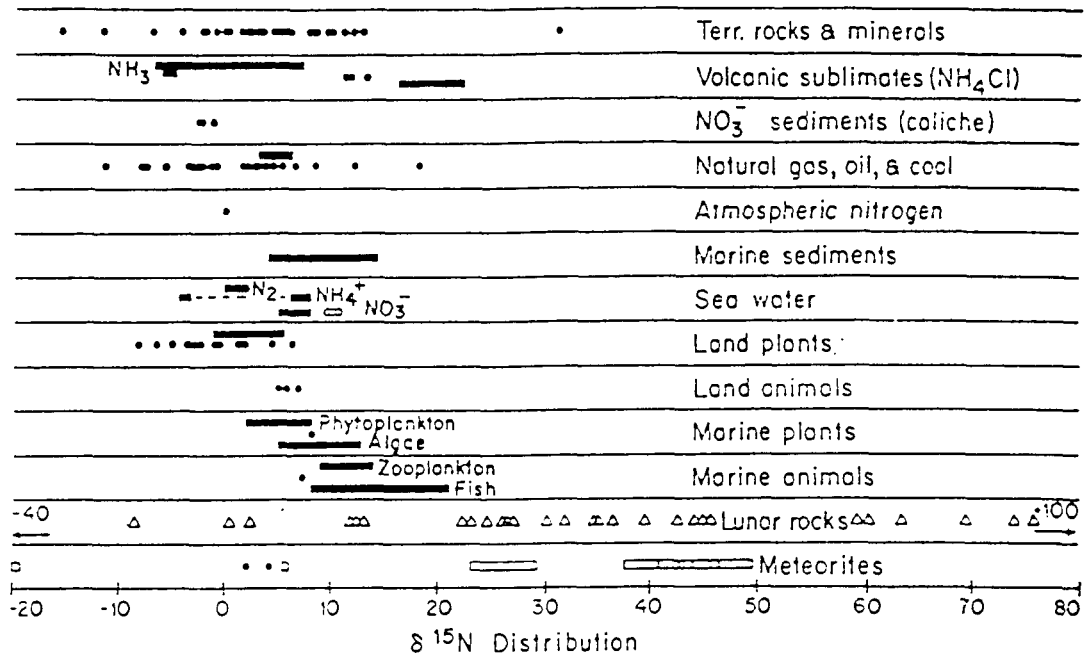


Fig. 1.3. Schematic of major sedimentary or chemical carbon components and their $\delta^{13}\text{C}$ values or ranges (modified after Anderson and Arthur, 1983).

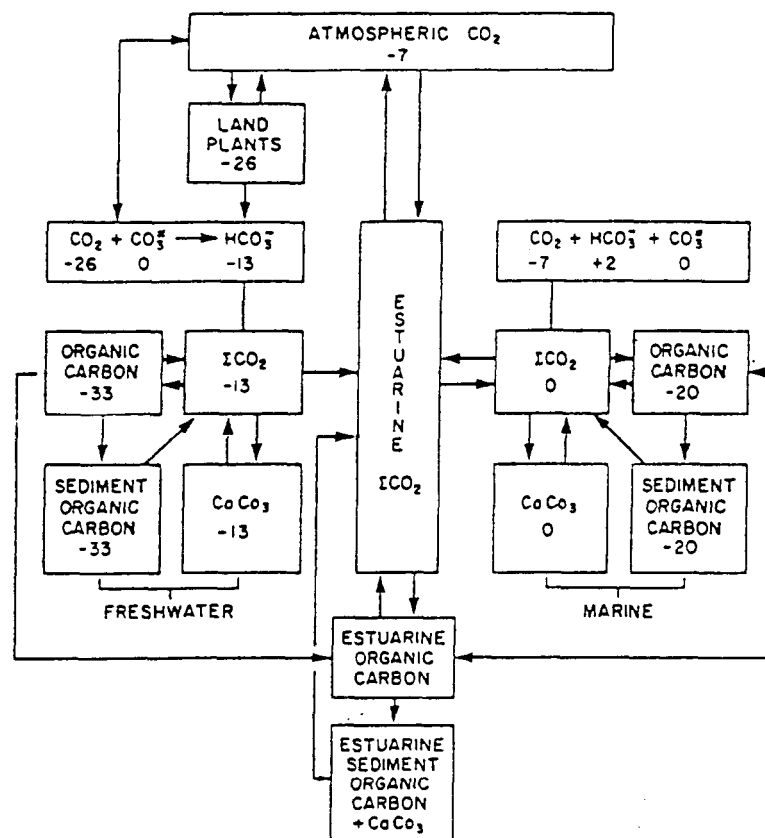
Fig. 1.4. General distribution of $\delta^{15}\text{N}$ for various natural substances (Modified after Kaplan, 1983).



materials, the isotopic compositions of organic materials are determined by the degree of fractionation occurring during synthesis and decomposition of OM. Other factors influencing the isotopic signature of OM include the concentration of CO_2 , temperature, and species diversity.

The isotopic fractionation during photosynthesis varies from one plant type to another depending on the metabolic pathway followed by the plant during photosynthesis. Smith and Epstein (1971) as well as Bender (1971) using $\delta^{13}\text{C}$ values identified two major groups of plants fixing carbon by the C_4 (Hatch-Slack) pathway and C_3 (Calvin-Benson) pathway. Plants following C_4 pathway (most tropical grasses) were found to have lower fractionation factors and their $\delta^{13}\text{C}$ values range from -9‰ to -16‰, averaging -13‰ (Deines, 1980; Fig. 1.6). High values for C_4 plants have been attributed to smaller fractionations of carbon stable isotopes by phosphoenolpyruvate (PEP) carboxylase, the closed system of Kranz anatomy characteristic of C_4 plants and depression of RuBP-oxygenase activity by high concentration within the bundle sheath cells (Wong and Sackett, 1978). Those plants having the C_3 photosynthetic pathway (most of the higher plants) were found

Fig. 1.5. Major carbon pathways in marine, estuarine and freshwater environments (source: Tan, 1989).



to have higher discriminations against ^{13}C (highest fractionation factors); their $\delta^{13}\text{C}$ values range from -23 to -33‰ averaging -26‰ (Anderson and Arthur, 1983; Fig. 1.6). A third group of plants, the CAM (Crassulacean Acid Metabolism) plants, which are succulents growing in relatively water-limited environments, utilize both types of photosynthetic pathways under varying conditions (Deines, 1980). Distribution of their isotopic compositions is bimodal (Fig. 1.6). These plants fix CO_2 at night solely through β -carboxylation of PEP with an accumulation of malic acid. In the day time, the malic acid is decarboxylated either to pyruvate or PEP. The pyruvate and PEP are subsequently converted to starch whereas atmospheric CO_2 and CO_2 released from decarboxylation of malic acid are assimilated by RuBP carboxylase through the Calvin cycle. It is the ability of CAM plants to shift the major flow of CO_2 fixation via PEP or RuBP carboxylase in response to environmental changes and the direct relationship between β -carboxylation and starch biosynthesis

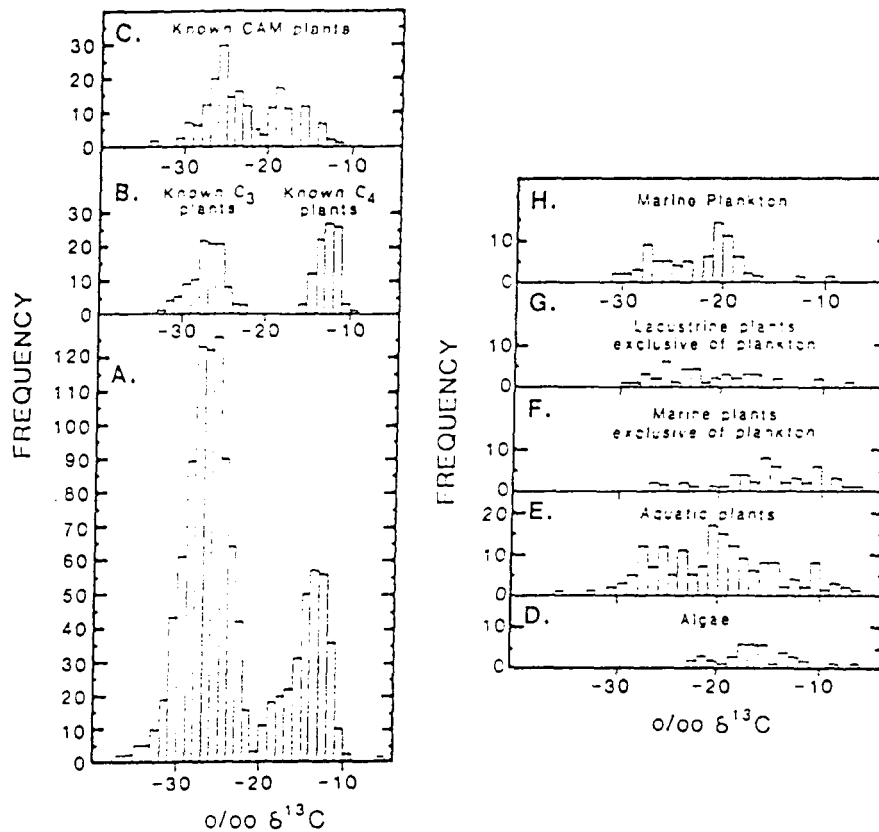


Fig. 1.6. Variations in $\delta^{13}\text{C}$ composition of photosynthetically fixed carbon . A: Terrestrial plants; B: known C_3 and C_4 plants; C: known CAM plants; D: Algae; E: Aquatic plants; F: Marine plants exclusive of plankton; H: Marine plankton. (Source: Deines, 1980).

that apparently accounts for these plants having a wide span of $\delta^{13}\text{C}$ values (Wong and Sackett, 1978).

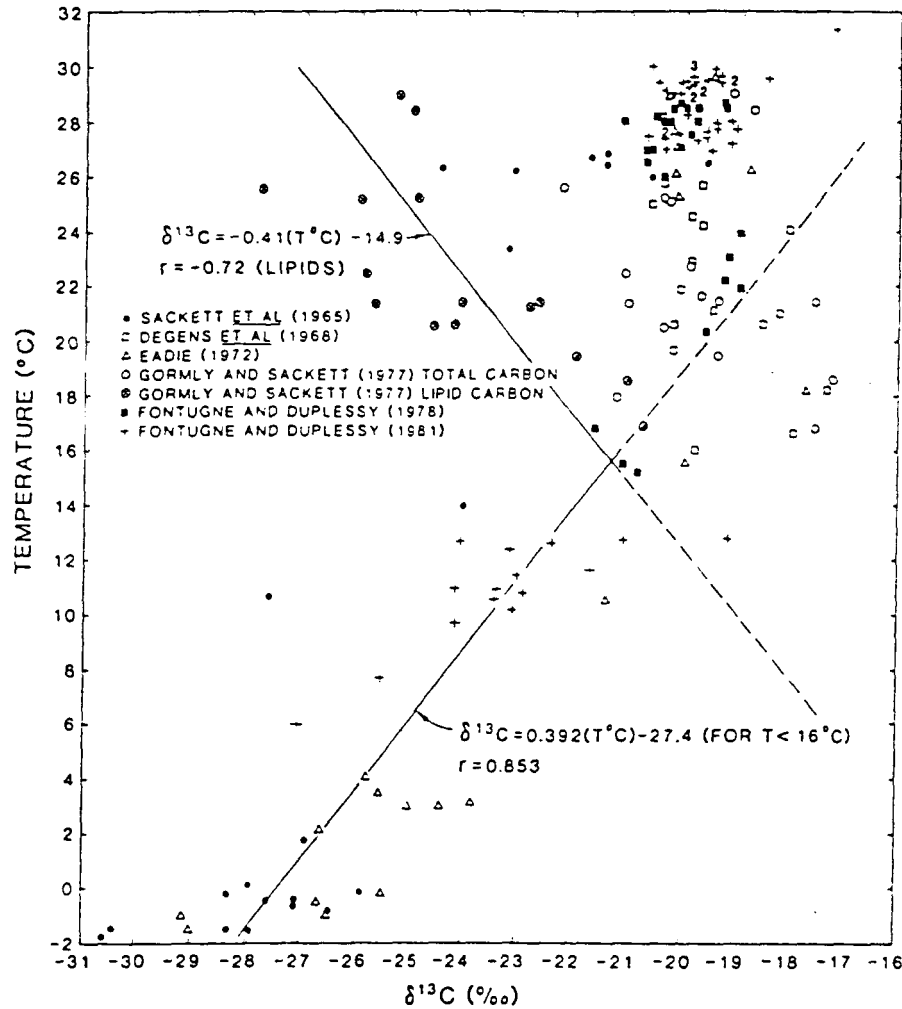
Terrestrial plants use atmospheric CO_2 which has an isotopic compositions of about -7‰ (Fig. 1.5). In contrast, in the hydrosphere, phytoplankton (C_3 plants), the major producers of oceanic or marine OM, use either dissolved carbon dioxide or bicarbonate (HCO_3^-) which are isotopically heavier than the atmospheric CO_2 . Because of isotopic compositions of the carbon sources used in the synthesis of OM, terrestrial organic material is isotopically different from that of marine OM.

In actual fact, by assuming a minor contribution of C_4 plants to the total OM found in marine sediments, the average $\delta^{13}C$ of terrestrial higher plants of -26‰ is distinct from that of phytoplankton, which ranges from -17‰ to -24‰ with an average of -21‰ (Gearing et al., 1984). These differences in the isotopic compositions of OM between high land plants and marine planktonic materials have been used widely to estimate relative contributions of terrestrial OM in the marine environment (Macko, 1983; Peters et al., 1978; Anderson et al., 1992). In estimating relative contributions of each component, a proportionation or mixing equation has been used, assuming end member values of both marine and terrestrial to be -20‰ and -26‰, respectively (Gearing et al., 1984; Macko, 1983).

However, the difference in the isotopic compositions between terrestrial higher plants and marine OM holds only for tropical and temperate areas. The isotopic compositions of organic carbon for planktonic material recovered from the southern and Arctic Oceans have been found to range from -27‰ to -35‰ (Sackett et al., 1965, 1974; Fontugne and Duplessy, 1981; Sackett, 1986; Rau et al., 1989, 1991b,c; Francois et al., 1993b; Biggs et al., 1988, 1989; Georricke and Fry, 1994). Although in some studies no correlation between temperature and isotopic compositions has been observed (Calder and Parker, 1973; Fontugne and Duplessy, 1978; Gearing et al., 1984), low $\delta^{13}C$ values in high latitude areas have been attributed partly to temperature effects (Sackett, 1989; Fontugne and Duplessy, 1981; Rau et al., 1989, 1991a,b). From analysis of widely published data, it is evident that a temperature-dependent isotope fractionation, if it exists during uptake, only exists below 16°C (Sackett, 1989; Fig. 1.7).

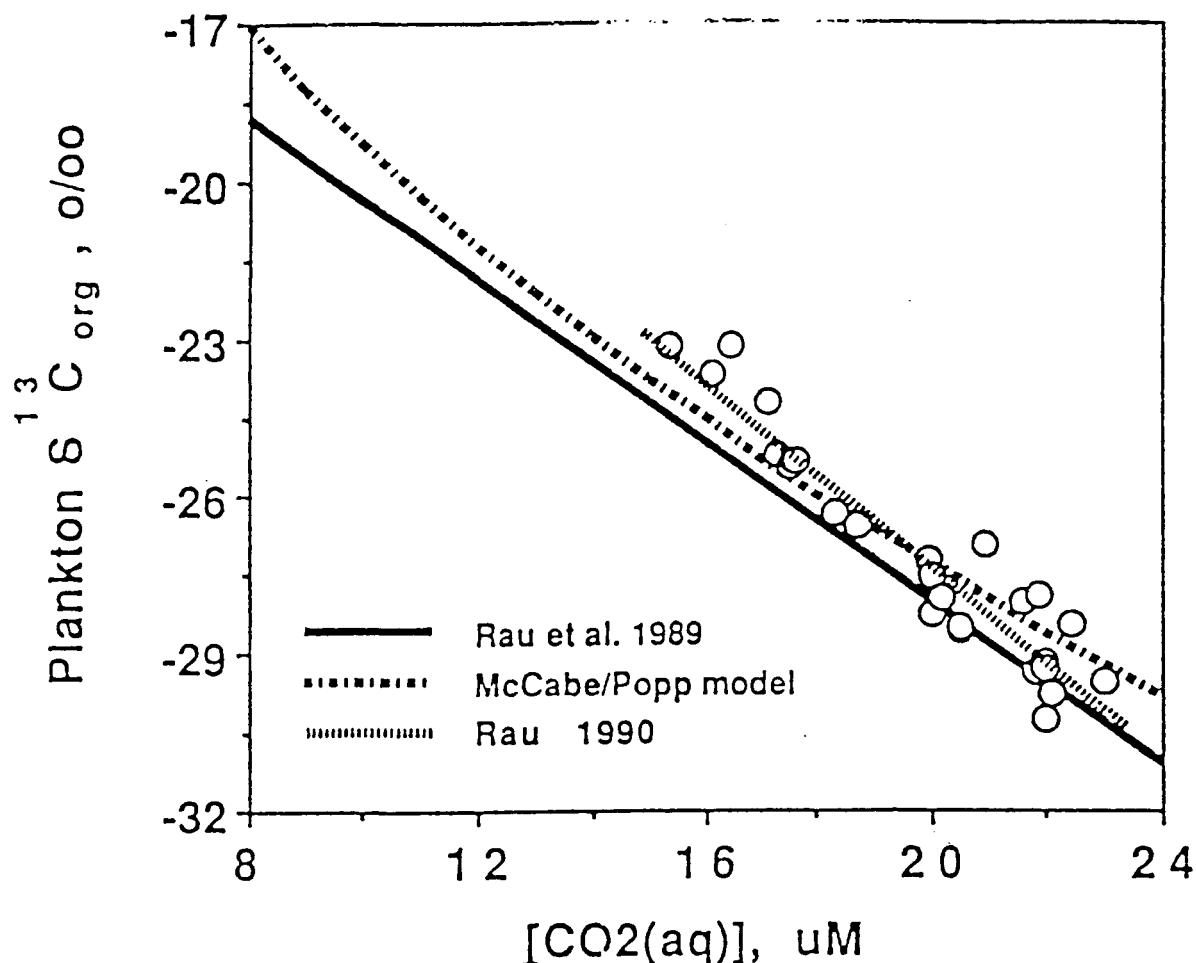
Apart from temperature effects, low $\delta^{13}C$ values in high latitudes areas have been attributed to higher concentrations of CO_2 in the surface waters (Hinga et al., 1994; Rau et al., 1991a,b,c; Goericke and Fry, 1994). This inference has been supported by latitudinal increase in dissolved CO_2 as well as inverse correlation between the isotopic compositions of particulate organic matter (POM)

Fig. 1.7. $\delta^{13}\text{C}$ compositions of plankton samples versus water temperature (Source: Sackett, 1989).



and the concentration of aqueous CO_2 (Fig. 1.8; Rau et al., 1991a; 1992). Low $\delta^{13}\text{C}$ values due to high concentrations of CO_2 is caused by high discrimination between ^{12}C and ^{13}C by plants cells, thus producing large fractionations (O'Leary, 1981). In areas where there exists high utilization of CO_2 such that the CO_2 concentrations are low, plant cells use available CO_2 for growth regardless of isotopic composition, causing less fractionation (O'Leary, 1981). Based upon this fact, downcore variations in the isotopic compositions of organic carbon have been widely used to infer changes in primary productivity in those areas where terrestrial input has been established to be minimal (e.g. Shemesh et al., 1993).

Fig. 1.8. Relationship between $[\text{CO}_2(\text{aq})]$ and stable carbon isotope abundance in the bulk organic fraction of plankton (modified after Rau et al., 1991a).



As suggested previously, another factor which may cause variation in the stable isotopic compositions of OM is a change in species assemblage. The study of Wong and Sackett (1978) has indicated that diatoms show a more pronounced temperature dependence during fractionation than calcareous species. Thus, changes from calcareous to diatomaceous species is expected to cause a pronounced isotope fractionation and thus a change in the isotopic compositions of resulting OM. Hence, low isotope values observed in high latitude areas have been partly attributed to species diversity (Sackett et al., 1974). However, it is not easy to separate temperature effects from that of changes in species. The stable isotopic compositions of organic carbon probably vary with changes

in species population.

Various components of plant material (e.g. lignin, lipids, proteins, carbohydrate) have different isotopic compositions (Fig. 1.9) and different rates of diagenetic alteration. Isotopic compositions of altered organic carbon could thus depend on the type of components removed during diagenesis. For example, diagenetic loss of ^{13}C -enriched carboxyl carbon has been proposed to account for ^{13}C depletion (Behrens and Frishman, 1971; Macko, 1981). So far, the effect of diagenesis on the isotopic compositions of OM is inconclusive (Dean et al., 1986; Sackett, 1989); in some studies changes of up to 5‰ have been attributed to diagenesis (Spiker and Hatcher, 1984; McArthur et al., 1992), possibly as a result of difficulties in isolating or constraining non-diagenetic sources of isotopic variation that may influence the vertical changes seen in sediment cores.

1.2.2. Nitrogen Stable Isotopes

Nitrogen has two stable isotopes, ^{14}N and ^{15}N , and their relative abundance in the atmosphere are 99.635% and 0.365% respectively (Wada and Hattori, 1991). Nitrogen occurs in various media (atmosphere, hydrosphere, biosphere and lithosphere) but atmospheric nitrogen is the principal reservoir of nitrogen. In aqueous environments, nitrogen occurs as dissolved molecular nitrogen, NO_3^{-2} , NH_4^{+} , N_2O , NO_2^{-} , NO_2 and organic nitrogen. Stable isotopic compositions of natural materials range from -50‰ to +100‰ (Fig. 1.4), with the isotopic compositions of natural OM ranging from -50‰ to 50‰ (Wada and Hattori, 1991). Variability in the isotopic compositions of OM is due to isotope fractionation occurring during primary production of food by photosynthesis (nitrogen assimilation) and denitrification (Montoya, 1994). Other isotopic fractionation mechanisms include nitrification, deamination, and ammonification (Montoya, 1994). Fractionation factors associated with these processes are presented in Table 1.1 (Montoya, 1994).

From the estimated fractionation factor of 1.000 to 1.004 due to nitrogen fixation, the OM

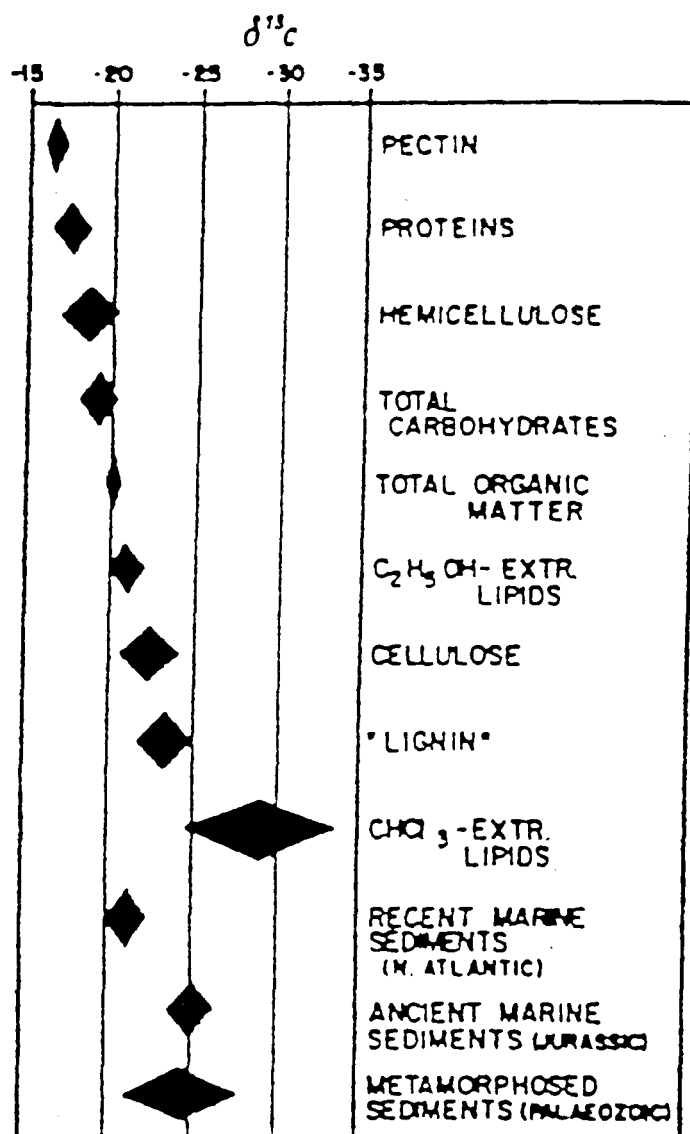


Fig. 1.9. $\delta^{13}\text{C}$ in various biochemical constituents isolated from marine plankton. The $\delta^{13}\text{C}$ for Recent and ancient sediments are included for comparison. Diamond shaped figures represent 1-sigma ranges (After Degens, 1969).

resulting from plants fixing nitrogen are expected to range from 0‰ to -4‰. Since terrestrial plants utilize fixed atmospheric nitrogen, their $\delta^{15}\text{N}$ values are expected to be close to that of atmospheric nitrogen of 0‰. Based on the compilation of Létolle, (1980) and Gearing (1988), $\delta^{15}\text{N}$ for terrestrial OM ranges from -10‰ to +10‰, averaging 2‰ (Fig. 1.10). With respect to aquatic environments,

Table 1.1: Nitrogen Isotope Fractionation in Various Biochemical Processes.

Reaction	Apparent isotope fractionation factor	Remarks
Assimilation		
$\text{NO}_3^- \rightleftharpoons \text{Organic N}$	1.000—1.019	<i>Phaeodactylum tricornutum</i>
$\text{NO}_3^- \rightleftharpoons \text{Organic N}$	1.000—1.0025	<i>Chaetoceros</i> sp.
$\text{NH}_4^+ \rightleftharpoons \text{Organic N}$	1.000—1.010	<i>Dunaliella tertiolecta</i>
		<i>Cricosphaera carterae</i>
$\text{NO}_3^- \rightleftharpoons \text{Higher plant}$	1.00027	
Nitrification		
$\text{NH}_4^+ \rightleftharpoons \text{NO}_3^-$	1.00—1.021	Marine nitrifier
Nitrate reduction		
$\text{NO}_3^- \rightleftharpoons \text{NO}_2^-$	1.000—1.029	<i>Serratia marinoirubra</i>
	1.011—1.017	Natural soil
	1.0065—1.019	Natural soil
Denitrification		
$\text{NO}_3^- \rightleftharpoons \text{N}_2$	1.000—1.021	Marine denitrifier
	1.04	The eastern tropical North Pacific Ocean
	1.014—1.023	Natural soil
	1.020	<i>Pseudomonas</i> sp.
	1.017	<i>Pseudomonas</i> sp.
	1.002	Marine denitrifier
	(0.2% KNO_3)	
	1.012(2.0% KNO_3)	
N_2 fixation		
$\text{N}_2 \rightleftharpoons \text{NH}_4^+$	0.991—1.004	<i>Azotobacter</i> spp.
	0.999—1.008	<i>Anabaena cylindrica</i>
Decomposition		
Organic N \rightleftharpoons Dissolved organic N	0.999—1.002	<i>Scenedesmus</i> sp.
	1.000—1.002	<i>Trichodesmium erythraeum</i>
	0.998—1.002	<i>Chaetoceros</i> sp.
	0.995—1.002	<i>Calanus plumichrus</i>
Organic N $\rightleftharpoons \text{NO}_3^-$	0.998—1.006	Natural soil
		mean 1.000
Amino acid synthesis	0.991—1.000	Rate for nonessential amino acid synthesis

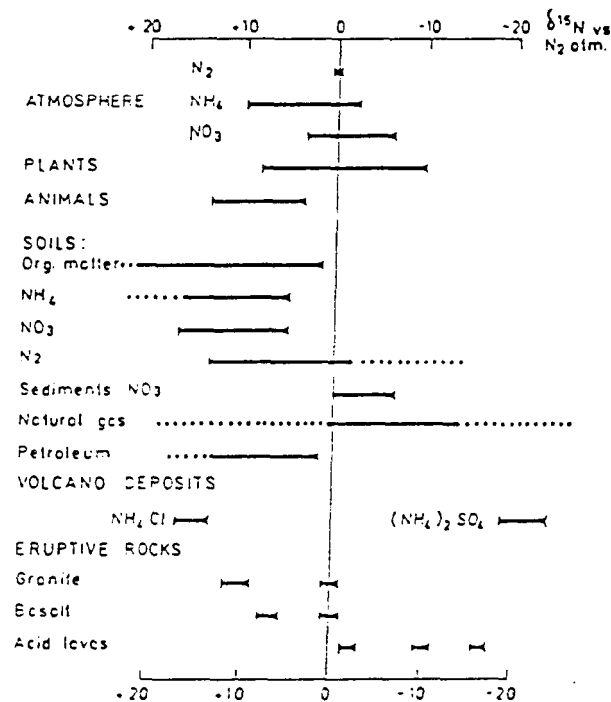


Fig. 1.10. The abundance of ^{15}N in terrestrial materials (Source: L  toll  , 1980).

phytoplankton mainly utilize dissolved inorganic nitrogen in the form of nitrate during the synthesis of OM, although other forms of nitrogen, such as dissolved molecular nitrogen, ammonium, and nitrite, are also used (Saino and Hattori, 1985). The isotopic composition of oceanic nitrate is about 6‰, although it may vary depending on the environmental conditions (Wada and Hattori, 1991). Compilation of various reported data by L  toll   (1980) has indicated that the nitrogen stable isotopic compositions of marine planktonic OM range from 4‰ to 10‰ with an average of 6‰. Because of the differences in the isotopic compositions between land and marine plants, nitrogen stable isotopic compositions of OM have also been used separately or in combination to imply the influence of terrestrial OM in the marine environment (Peters et al., 1978; Macko, 1983; Muzuka et al., 1991).

Because of variation in concentrations of nitrate in the oceans as well as the degree of utilization of nutrients, the isotopic composition of planktonic OM is highly variable. According to

Wada and Hattori (1991), isotope fractionation tends to increase with increasing nitrate concentrations, up to 0.1 moles/liter. Low as well as high values of nitrogen have been observed in the Southern Ocean, and low values have been attributed to incomplete utilization of available nutrient (Francois et al., 1992, 1993a; Altabet and Francois, 1994a,b). When the rate of nutrient utilization is low compared to the available nutrients, fractionation increases, and more depleted isotopic compositions are observed in the resulting OM. Conversely, when the rate of nutrient utilization is high, phytoplankton utilize all available nutrients regardless of their isotopic compositions, and hence a low fractionation is observed. Based on these facts, downcore variations in the stable isotopic compositions of nitrogen in the oceans have been used to imply changes in primary productivity as well as nutrient utilization (Shemesh et al., 1993; Francois et al., 1992, 1993a; Calvert et al., 1992a; Altabet and Francois, 1994a,b).

Alteration of the isotopic composition of nitrogen starts in the water column and probably continues in the sediments. The nitrogen stable isotopic compositions of POM have been determined in the Atlantic Ocean (Altabet, 1988; Altabet and McCarthy, 1985, 1986, Montoya et al., 1992), Pacific Ocean (Saino and Hattori, 1985; 1987) and in the Indian Ocean (Saino and Hattori, 1980). These studies have indicated that the $\delta^{15}\text{N}$ values of POM range from -3 to 30‰, and that vertical profiles show a subsurface minimum associated with a maximum concentration of particulate nitrogen near the base of the mixed layer, followed by an increase in $\delta^{15}\text{N}$ that is associated with a decrease in the concentration of particulate nitrogen. A minimum below the mixed layer has been attributed to isotopic fractionation during uptake of NO_3^- under the low light levels and relatively high NO_3^- concentrations often found at the top of the thermocline, whereas high increases in $\delta^{15}\text{N}$ below this zone have been ascribed to isotopic fractionation in the course of remineralization of particulate nitrogen (Montoya et al., 1992). High values (>30‰) have been attributed to isotopic fractionation during the decomposition of, and resulting loss of nitrogen from, particles sinking

through the water column (Montoya et al., 1992, Montoya, 1994). Because vertical profile show inverse relationships between $\delta^{15}\text{N}$ and the concentration of particulate nitrogen, isotopic fractionation during the mineralization of particulate nitrogen is thought to be important determinant of the $\delta^{15}\text{N}$ of particulate nitrogen in the water column. The estimated average isotope fractionation factor for the mineralization of organic nitrogen is 1.003 (Montoya et al., 1992).

Since various compounds contained in the OM have different isotopic compositions of nitrogen (Macko et al., 1983; Benner et al., 1987), diagenetic changes can be expected to cause alteration of the stable isotopes of nitrogen, and resulting $\delta^{15}\text{N}$ values will be influenced by what types of organic compounds have been removed. The type and quantity of clay minerals present in the sediments also affect $\delta^{15}\text{N}$ values. This is because interaction of clay minerals with nitrogen species, especially NH_4^+ through adsorption, ion exchange and substitution processes is associated with isotopic fractionation (Hubner, 1986; Karamanos and Rennie, 1978). Owing to differences in the residue charge, the ability of clay minerals to fix NH_4^+ varies, with illite and vermiculite having the highest fixation capacity and kaolinite the lowest. However, the effect of clay mineral content in the marine sediments on the isotopic compositions of nitrogen has been little studied.

The mineralization of OM has been found to be associated with small isotopic changes of both nitrogen and carbon (Fig. 1.11; Macko, 1981; Spiker and Hatcher, 1984; Peters et al., 1981; Velinsky et al., 1991; McArthur et al., 1992). Lack of major changes in isotopic composition has nitrogen is remineralized compared been attributed to mass effect (selective degradation) where small fractions of the particulate to the total particulate nitrogen (McArthur et al., 1992). Another possible reason is an extensive decomposition of OM while in the water column, which would leave behind refractory material which would alter slightly in the sediments. Owing to high flux of labile OM to the sea floor and shallow depths, noticeable diagenetic changes are expected in areas of continental margins with high primary productivity.

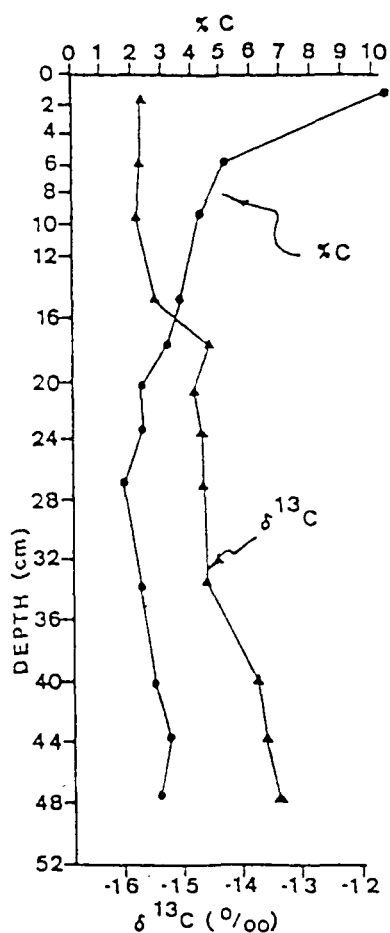


Fig. 1.11a

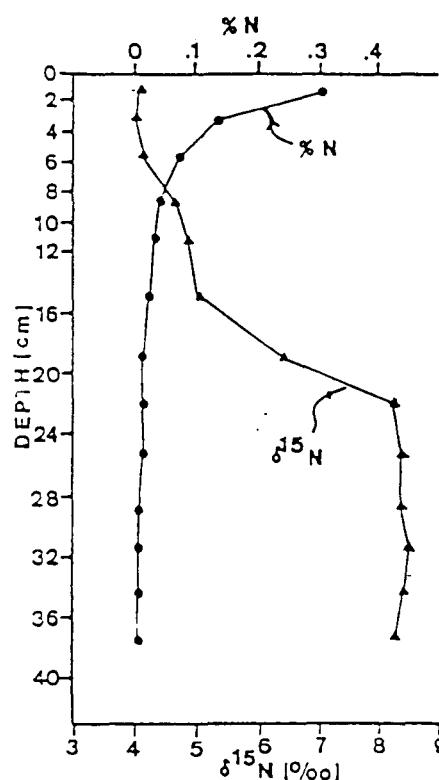


Fig. 1.11b

Fig. 1.11 (a) Variation in $\delta^{13}\text{C}$ and $\%C$ with depth in a sedimentary core from the Baffin Bay, Texas, algal mat laminations. (b) Variation in $\delta^{15}\text{N}$ and $\%N$ with depth in a sedimentary core from a Laguna Madre, Texas, seagrass bed. (Source: Macko et al., 1993).

1.2.3. Content of organic carbon and nitrogen

The distribution of particulate organic carbon content in the marine sediments has been found to reflect surface primary productivity (Romankevich, 1984). This observation has been the basis for using organic content as an indicator of productivity history. However, the application of this parameter to the interpretation of past environments is difficult. Simply mapping present distributions is not straightforward, because of the rapid change of organic carbon content in the

uppermost few centimetres of sediment. Burial of organic carbon is largely independent of oxygenation, unless one deals with anaerobic conditions, combined with low sedimentation rates (Berger and Herguera, 1992). There is great uncertainty as to the amount of organic carbon within slope sediments that is brought in through re-deposition, by bottom-near transport, rather than by delivery from primary production above. In places, much of the carbon may, in fact, be derived from productivity on the shelf, and from continental erosion. Estimates of paleoproductivity are affected by the decay of OM within the sediment. Decay proceeds rapidly first, in sediments close to the sea floor, and then progressively more slowly, as the more accessible (and more labile) material is removed (Froelich et al., 1979). Apart from these problems, the organic carbon preserved in the sediments is a good measure of primary productivity in the euphotic zone (Berger and Herguera, 1992; Müller and Suess, 1979; Sarnthein et al., 1987, 1988).

1.2.4. C/N Ratios

C/N ratios have been used as source indicators under the assumption that algal and land-plant have different C/N ratios (Stevenson and Cheng, 1972; Müller, 1977; Jasper and Gagosian, 1990; Meyers, 1994). Algae typically have atomic C/N ratios between 4 and 10, whereas vascular land plants have C/N ratios of ≥ 20 (Meyers, 1994). This difference arises from a lack of cellulose in algae and its abundance in vascular plants. Selective degradation of OM components during early diagenesis can potentially modify the C/N ratio of OM. Because of this, the C/N ratios do not necessarily represent the C/N ratios of decomposing matter (Müller, 1977). However, Meyers (1994), has indicated that early diagenesis does not significantly alter the signature, and the difference between two groups can be easily identified.

Assuming a steady state input of OM with a constant C/N ratio, constant fixed (plus exchangeable) NH_4^+ , and constant non-metabolizable organic carbon, the slope of a linear C/N

relationship in the sediments would be equal to the C/N ratio of OM being oxidized. A non-linear C/N relationship would reflect a changing C/N ratio or variation in the fixed NH_4^+ or non-metabolizable carbon. A nonzero intercept would indicate unavailable N or C depending on the sign (Grundmains and Murray, 1982). If the intercept is on the total nitrogen (TN) axis, it would suggest that there is inert nitrogen in sediments, possibly fixed NH_4^+ in the clays, because aerobic sediments contain little exchangeable ammonia (Müller, 1977; Stevenson and Cheng, 1972).

1.2.5. Amino acids.

Amino acids are the building blocks of proteins and are generally the largest component of organic nitrogen in most organisms. They are the major forms of organic nitrogen and important components of organic carbon in most marine organisms. Amino acids occur as dissolved free amino acids and total hydrolysable amino acids (THAA) bound in humic substances or as proteinaceous material. In marine sediments, amino acids are found both as proteinaceous material and humic substances, and represent significant fractions of OM where they may account for 40 to 60% of the OM (...). Amino acids are simple molecules having at a minimum one carboxylic acid (COOH) and one amino functional group (NH_2). Although the number of different kinds of amino acids theoretically possible is almost unlimited, only 20 commonly occur in proteins of organisms (Kvenvolden, 1975). Many other amino acids occur naturally in organisms, and because they usually are not commonly found in proteins they are classified as non-protein amino acids. Most of the protein amino acids are α -amino derivatives of carboxylic acids and are optically active. With the exception of glycine, all are characterized by at least one centre of asymmetry at α -carbon position, to which is attached an amino ($-\text{NH}_2$), α -carboxyl ($-\text{COOH}$), a proton ($-\text{H}$), and $-\text{R}$ group. The $-\text{R}$ group substituent is different for each of the twenty amino acids. Based on the side chain present on the amino acid, the amino acids are commonly grouped into neutral, secondary, aromatic, acidic

and basic amino acids (Hare, 1969).

The THAA are major constituents of both organisms and sediment OM and undergo significant diagenesis in near-surface sediments (Kvenvolden, 1975; Schroeder and Bada, 1976). Downcore variations of amino acids in marine sediments has been observed to decrease exponentially with increasing sediment depth (Burdige and Martens, 1988). They are typically labile components relative to bulk organic carbon and nitrogen and account for a considerable portion of the particulate organic carbon and nitrogen recycled in both the water and sediments (Haugen and Lichtentaler, 1991; Burdige and Martens, 1988). Thus the study of amino acids distributions may help to gain valuable information on early diagenesis of OM.

Because amino acids make up the major fraction of labile organic nitrogen in marine sediments, they are of importance to the overall nitrogen cycling in marine ecosystems. Studies of amino acids diagenesis in coastal marine environments have demonstrated that amino acids may account for 40 to 90% of the total nitrogen being mineralized in sediments (Henrichs and Farrington, 1987; Burdige and Martens, 1988) and 13 to 40% of the total nitrogen mineralized in fjords (Haugen and Lichtentaler, 1991). Few cores of deep ocean surface sediment have been analyzed for amino acids (Hare, 1973; Aizenshtat, 1973; Rittenberg et al., 1963; Whelan, 1977; Henrichs et al., 1984).

Downcore variations in the amino acids in marine environments have been used as a tracer of diagenetic changes and to a lesser extent as sources indicators of OM. The distribution of amino acids in sediments and particulate matter in the water column of aquatic environments have not been extensively used as source indicators. This is due to the fact that amino acids are generally widely distributed with a uniform composition. Apart from this handicap, amino acids have been used successfully either in combination with other biochemical classes or separately in situations where there are very limited numbers of sources. For example, amino acids have been used separately and also in conjunction with stable isotopic compositions of organic carbon in Saanich Inlet (British

Columbia, Canada) to infer sources of OM in the area (Cowie et al., 1992; Cowie and Hedges, 1992). Their use as indicators is based on the premise that total OC-normalized amino acid yields for unaltered vascular plant tissues are distinct from those of more protein-rich plankton, bacteria and fungi. The OC-normalized amino acid yields for unaltered vascular plant tissues range from 0.4 to 1.3 mg (100 mg OC)⁻¹ for wood, 7 to 17 mg (100 mg OC)⁻¹ for leaves, grasses and needles whereas for plankton, bacteria and fungi the OC-normalized amino acid yields are >50 mg (100 mg OC)⁻¹ (Cowie et al., 1992).

Also, amino acids have been used as source indicators based on the fact that land-derived humic compounds have high abundances of acidic amino acids (aspartic and glutamic acids) including the neutral amino acids (glycine, alanine and serine) (Haugen and Lichtentaler, 1991). The dominant amino acids in plankton are: glycine, alanine, and glutamic and aspartic acids (Degens and Mopper, 1976). However, Cowie and Hedges (1992) analyzed various vascular plant components, macrophytes, phytoplankton, zooplankton and bacteria, and found similar but highly variable amino acid compositions within individual groups, with no amino acid which was unique to any source (Fig. 1.12). When the total hydrolysable amino acid yields were scaled to OC [mg (100 mg OC)⁻¹], vascular plants produced lower yields <18 mg (100 mg OC)⁻¹ while yields for protein-rich organisms ranged from 50 to 140 mg (100 mg OC)⁻¹. Similarly, in a study conducted in Cape Lookout Bight (North Carolina), the mole fraction of individual amino acids in sediments was not found to be different between vascular salt marsh plants and marine plankton (Burdige and Martens, 1988), and it was concluded that amino acids do not appear to be good biomarkers for sources of sedimentary OM owing to their relatively invariant distribution in a wide range of naturally occurring organic materials.

The compositions of amino acids can provide three potentially valuable indicators of diagenetic alteration: (1) In all species other than woody vascular plant tissues, the percentage of total nitrogen

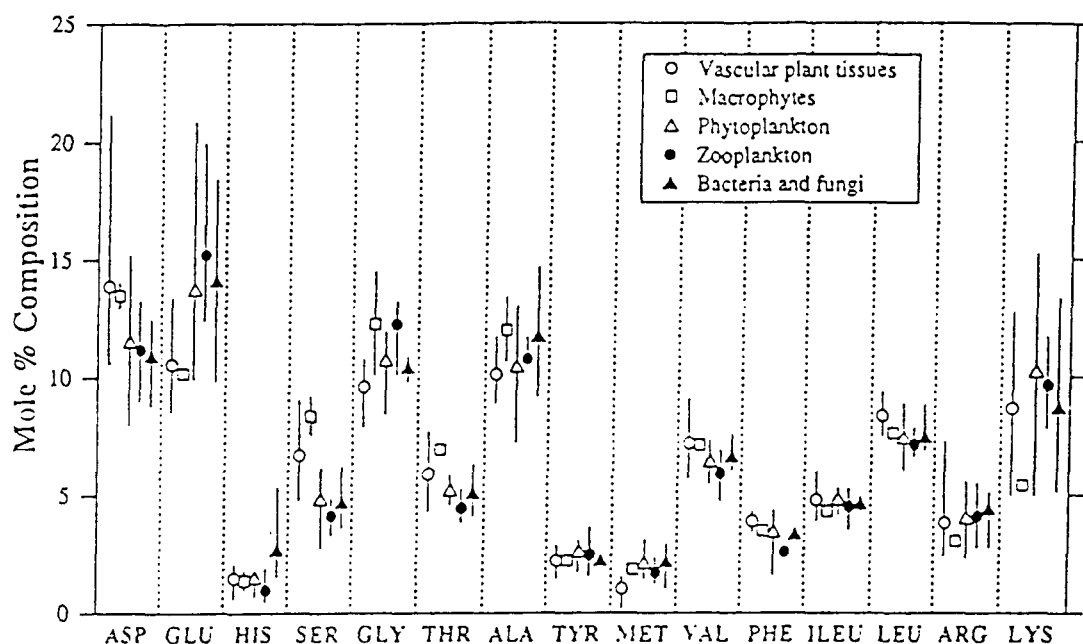


Fig. 1.12. Means and ranges for mole % protein amino acid compositions of different groups of source organisms. Abbreviations: ASP aspartic acid; GLU, glutamic acid; HIS, histidine; SER, serine; GLY, glycine; THR, threonine; ALA, alanine; TYR, tyrosine; MET, methionine; VAL, valine; PHE, phenylalanine; ILE, isoleucine; LEU, leucine; ARG, arginine; and LYS, lysine (Source: Cowie and Hedges, 1992).

represented by amino acids (%AA-N) is >38% and can be as high as 84%. This parameter is diagenetically sensitive and has generally been found to decrease as degradation progresses, for example with depth in marine sediment cores (Whelan, 1977; Henrichs et al., 1984; Burdige and Martens, 1988). (2) The non-protein amino acids (β -alanine, α -aminobutyric acid, γ -aminobutyric acid, and ornithine) are thought to be of mainly diagenetic origin (Lee and Cronin, 1982; Cowie and Hedges, 1994) and are generally absent or present at trace levels in living organisms. Whelan (1977) and Cowie and Hedges (1994) observed high levels of the non-protein amino acids β -alanine and γ -aminobutyric acid in marine sediments, and partly attributed this to be a product of diagenetic reactions. Thus, elevated levels of these compounds can indicate diagenetic alteration. (3) Major deviations from the nearly uniform amino acid compositions observed in living resources offers an indicator of selective alteration. Another class of non-protein amino acids that result from diagenetic processes in sediments includes amino acids of D-stereoisomeric configuration occurring during racemization (Kvenvolden, 1975).

CHAPTER 2

2.0. STUDY AREA DESCRIPTION AND PREVIOUS WORK DONE.

The Labrador Sea and Gulf of St. Lawrence are marginal basins located in the northwestern Atlantic Ocean. The Labrador Sea is one of the seaways linking the northwestern Atlantic Ocean with Arctic Ocean whereas the Gulf of St. Lawrence is a waterway linking the Atlantic Ocean and the Great Lakes.

2.1.0. GULF OF ST. LAWRENCE.

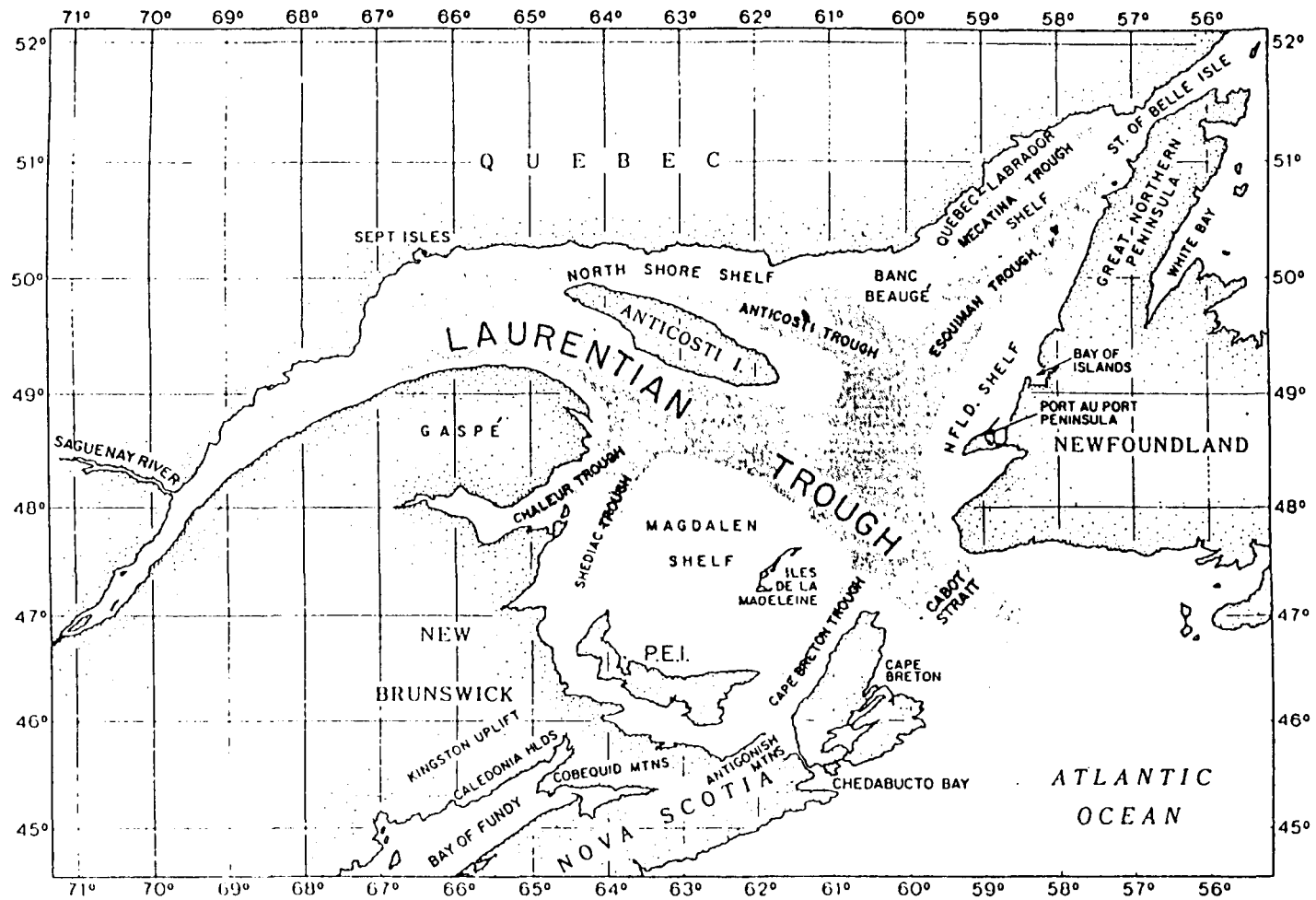
2.1.1. Location and Physiography.

The Gulf of St. Lawrence is located on the east coast of Canada and is located between latitudes 46°N and 52°N and longitudes 65°W and 68°W (Fig. 2.1). It is an inland sea, which covers an area of approximately 250,000 km² and is dissected by the long, deep Laurentian, Anticosti and Esquiman troughs (Fig. 2.1). The trough-shaped submarine valleys with water depths ranging from 200 to 500 m are the most prominent features of the submarine topography. The Laurentian trough is the longest of all, about 1200 km long, 37 to 89 km wide and extending from the Scotia shelf edge to a position off the mouth of the Saguenay river in the upper St. Lawrence estuary. The troughs are flanked by five major shelves, the Northshore, Anticosti, Quebec-Labrador, Magdalen and Newfoundland (Fig. 2.1).

2.1.2. Physical and Geological Setting

Three water masses have been identified in the Gulf of St. Lawrence: a warm surface layer, a cold intermediate layer and a warm bottom water (Sunby, 1974; Tang, 1980, Strain, 1988; Keen et al., 1966). The thickness of the upper two layers is highly variable, and during winter these two

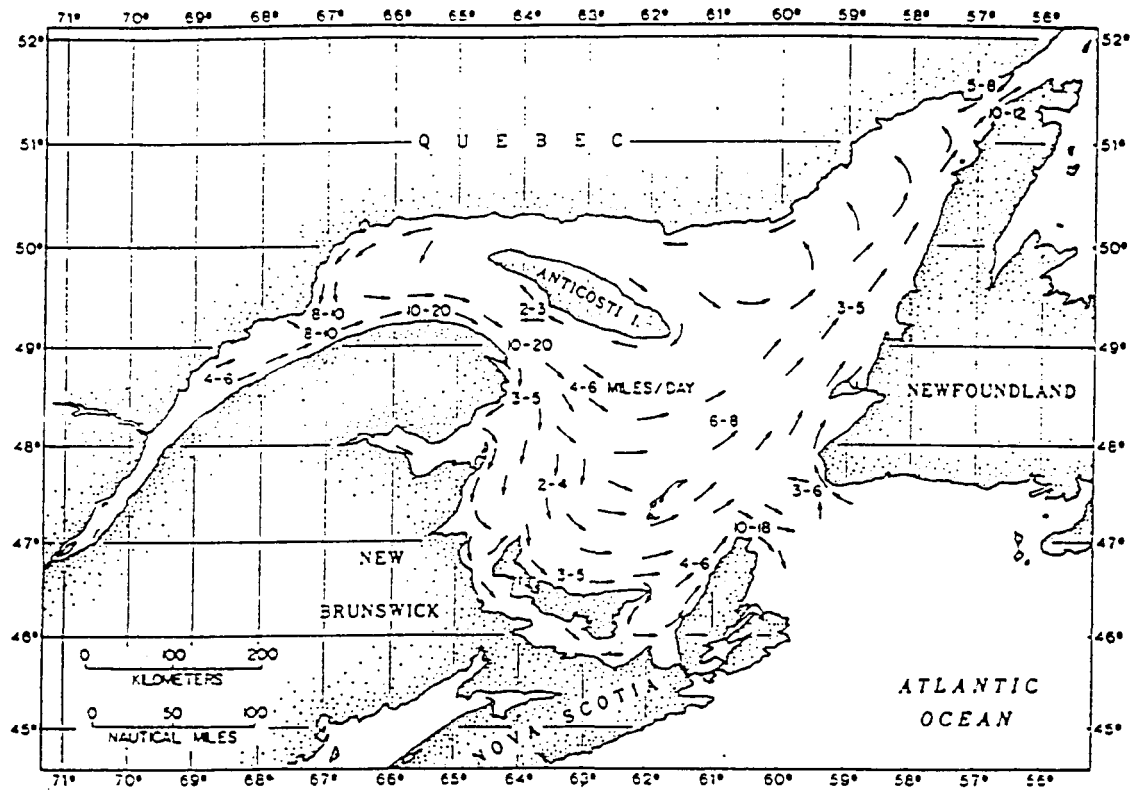
Fig. 2.1. Physiographic elements of the Gulf of St. Lawrence (Source: Loring, 1975).



layers may merge to form a two layer system (Sunby, 1974; Tang, 1980; Strain, 1988; Keen et al., 1966).

The circulation pattern in the Gulf of St. Lawrence, which is linked to the Atlantic Ocean by Belle Isle Strait to the north and Cabot Strait to the south and extends inland to Point-de Monts, has been described by El-Sabh (1976, 1979), Sunby (1974), Tang (1980) and Keen et al. (1966). The main circulation patterns are counterclockwise in the centre of the Gulf, a permanent seaward current flow between Gaspé Peninsula and Anticosti Island known as Gaspé Current and a current flowing landward below the Gaspé Current (Fig. 2.2; Tang, 1980; Keen et al., 1966). Water movements in the Cabot Strait are dominated by an outward surface flow, strongest around Cape North on the Nova Scotian side, and an inward flow off Cape Ray, Newfoundland side. The annual input of the Atlantic waters to the Gulf through Belle Isle Strait is low owing to the shallow depth (60 m) and narrow strait (16 km) (Sunby, 1974). However, the annual input through the Cabot Strait amounts to 11.99 km^3 of water, in which the estimated mass transport of organic material from the Atlantic Ocean to the Gulf amounts to $10.24 \times 10^6 \text{ Ta}^{-1}$ (Pocklington, 1988). According to Pocklington (1988), the gross annual transport of the total OM is one quarter of the autochthonous production in the Gulf, and is two times that contributed by OM fixation on the Scotian shelf adjacent to the North Atlantic ($5.25 \times 10^6 \text{ Ta}^{-1}$). Similarly, the annual output through the same Strait amounts to 12.48 km^3 of water in which the estimated mass transport of organic material from the Gulf to the Atlantic Ocean is $14.03 \times 10^6 \text{ Ta}^{-1}$ (Pocklington, 1988). The estimated net seaward transport of particulate material ($4 \times 10^6 \text{ Ta}^{-1}$) at the Cabot strait by Pocklington (1988) is in agreement with those of Sunby (1974) of $5.5 \times 10^6 \text{ Ta}^{-1}$. Thus, the exchange of waters and particulate materials between the Gulf and the Atlantic Ocean through the Cabot Strait, which is 104 km wide and 480 m deep, is high. However, these estimates are higher compared to those made by Yeats (1988) $1.6 \times 10^6 \text{ Ta}^{-1}$.

Fig. 2.2. Typical summer-surface circulation pattern in the Gulf of St. Lawrence (After Sundby, 1974).



The Quaternary geology of the Gulf of St. Lawrence has been described by Syvitski and Praeg (1989) based on high resolution seismo-stratigraphy. Other works worth noting are those of Loring, (1971, 1975) and Loring and Nota (1973). Generally, the unconsolidated Quaternary sediments in the Gulf are characterized by glacial (Winsconsinian glaciation) and post glacial (Holocene) deposits. The glacial deposits, which are the oldest unconsolidated unit in the Gulf, consist of tills, glaciomarine pelites and glaciolacustrine clays (Loring, 1971, 1975; Loring and Nota, 1973). They are unevenly distributed and overlay the bedrock. The postglacial deposits, which are composed of pelites, sands and gravels, overlay the glacial deposits and occupy the floors of the major troughs, shelf valleys, trough slopes and adjacent shelves (Loring, 1971, 1975; Loring and Nota, 1973).

2.1.3. Paleoproductivity and Burial Rates

Nutrient inputs to the Gulf of St. Lawrence are derived from hinterland through rivers such as the St. Lawrence river, local upwelling (vertical mixing) and diffusion mechanisms, and regeneration (Yeats, 1988; Coote and Yeats, 1979; Therriault and Lacroix, 1976; Lucotte and d'Anglejan, 1988; d'Anglejan et al., 1973; Sinclair et al., 1976). A nutrient rich landward moving current through the Cabot Strait produces high concentrations of nutrients at intermediate depths in the Gulf (Yeats, 1988; Coote and Yeats, 1979). The influx of nutrients from the Atlantic Ocean through the strait of Cabot during the summer is relatively high compared to outflux (Yeats, 1988; Coote and Yeats, 1979). Because of high supplies of nutrients, the primary productivity in the Gulf is high and the estimated productivity is as high as $385 \text{ gCm}^{-2}\text{yr}^{-1}$ (Steven, 1975). Although much is known about recent nutrient fluxes and productivity, paleoproductivity and burial rates of OM are poorly known.

2.1.4. Sources of Organic Matter

Several studies have been conducted to evaluate sources and their relative contribution of OM in the Gulf of St. Lawrence and its estuary (Pocklington, 1976, 1988; Tan and Strain, 1979a, b, 1983, 1988; Pocklington and Tan, 1987; Lucotte, 1989; Lucotte et al., 1991). These studies have utilized stable isotopic compositions of organic carbon, total organic carbon content for both suspended and sedimentary particulate matter and C/N ratios. However, there is a lack of high resolution data on temporal variations in the stable isotopic compositions of organic carbon, and total contents of organic carbon and nitrogen for sedimentary OM. The nitrogen stable isotope compositions of OM in the Gulf and its estuary have not been examined, and the present study presents the first data covering large part of the Laurentian channel. Generally, the terrestrial influence decreases with increasing distance from the continent offshore (Fig. 2.3; Pocklington, 1976; Tan and Strain, 1979a, b, 1983; Pocklington and Tan, 1987; Lucotte et al., 1991). The organic

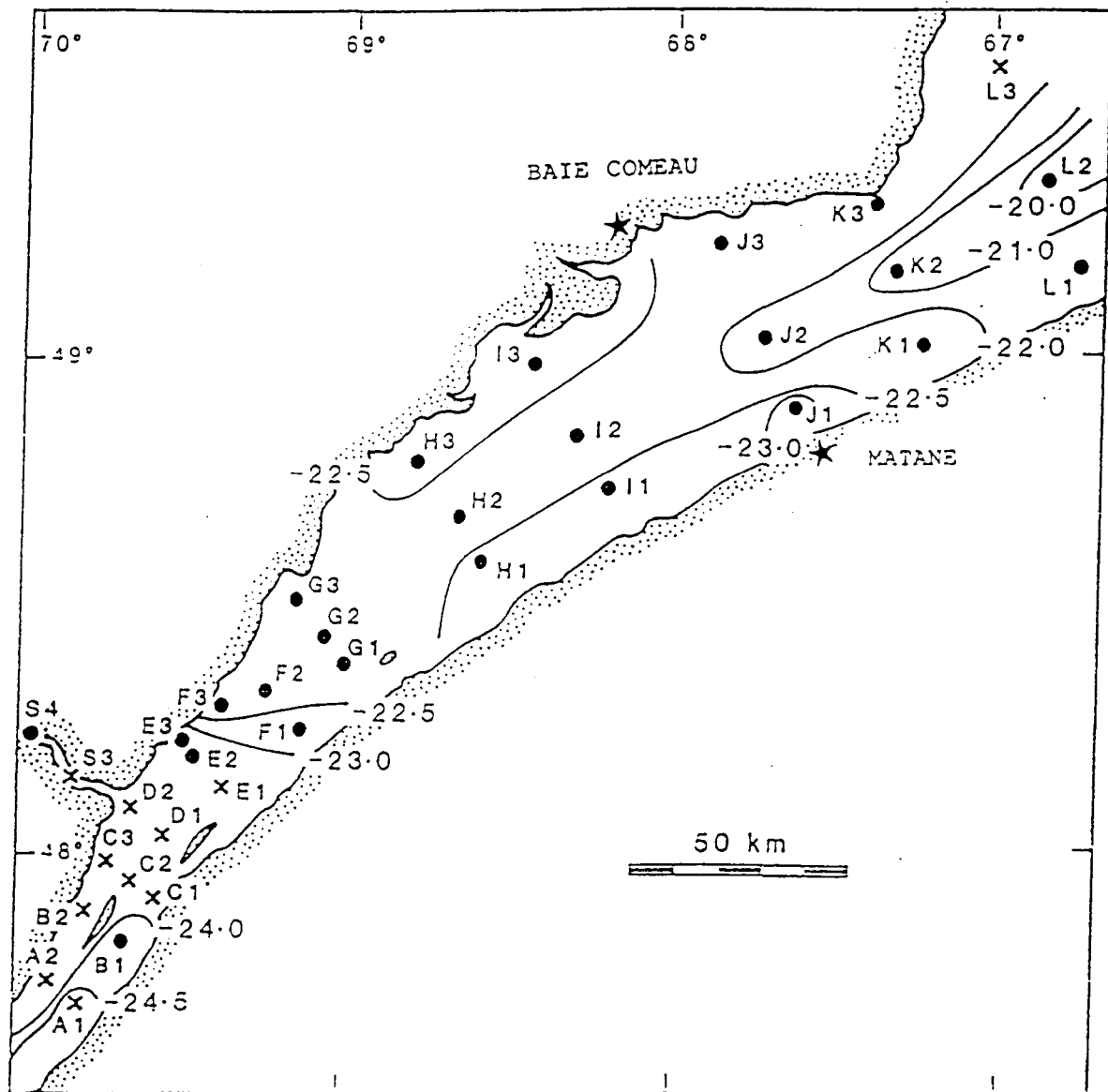


Fig. 2.3. Average $\delta^{13}\text{C}$ (‰) of the particulate organic carbon in the top centimetre of the sediments from the lower estuarine of St. Lawrence (Modified after Lucotte et al., 1991).

carbon stable isotopic compositions of POM in the Gulf where the terrestrial influence is minimal, averages $-24.9 \pm 0.5\text{‰}$ while that on the Scotia shelf and slope averages $-25.1 \pm 1.4\text{‰}$ (Tan and Strain, 1979b). In contrast, lateral variation in the isotopic compositions of surficial organic carbon in the Gulf is low and has an average of -22.4‰ (Tan and Strain, 1979a). Such isotopic

composition of particulate matter leaves one to wonder why and how the isotopic compositions in the water column are not reflected in the sediment.

2.1.5. Diagenetic Changes

Regardless of the carbon content of the material measured in the traps, the organic carbon content of the surficial sediments in the lower estuary was observed to be 2% by weight (Silverberg et al., 1985). The carbon loss was estimated to be 30% of total carbon in the OM. The C/N ratio of surface sediments was observed to be higher than particulate matter trapped in sediment traps (Silverberg et al., 1985) and was attributed to diagenetic changes. Moreover, the freshly deposited solids in the estuary of the St. Lawrence are being homogenized by bioturbation processes (Silverberg et al., 1985, 1986). The organic carbon content below the mixing zone was found to be less variable. With regard to the distribution of amino acids, there are no studies in the area that have been conducted using this parameter to trace diagenetic changes.

2.2.0. LABRADOR SEA

2.2.1. Physical and Geological Setting

The surface circulation in the Labrador Sea is characterized by a northward flowing current off the Greenland coast known as the West Greenland Current, and the Labrador Current which flows southward off Baffin Island and Labrador (Fig. 2.4; Ichiye, 1966; Plutchak, 1966). The West Greenland Current, which is composed of subpolar waters, is a mixture of Arctic overflow water from the East Greenland Current and temperate North Atlantic Drift (McCartney, 1992; Lucotte and Hillaire-Marcel, 1994). The Labrador Current, which sweeps along the Labrador Shelf, is a mixture of the Arctic overflow water through the Hudson strait and the Baffin Land current (Ichiye, 1966; Plutchak, 1966). Because of this circulation pattern, the Labrador Sea plays a major role in the

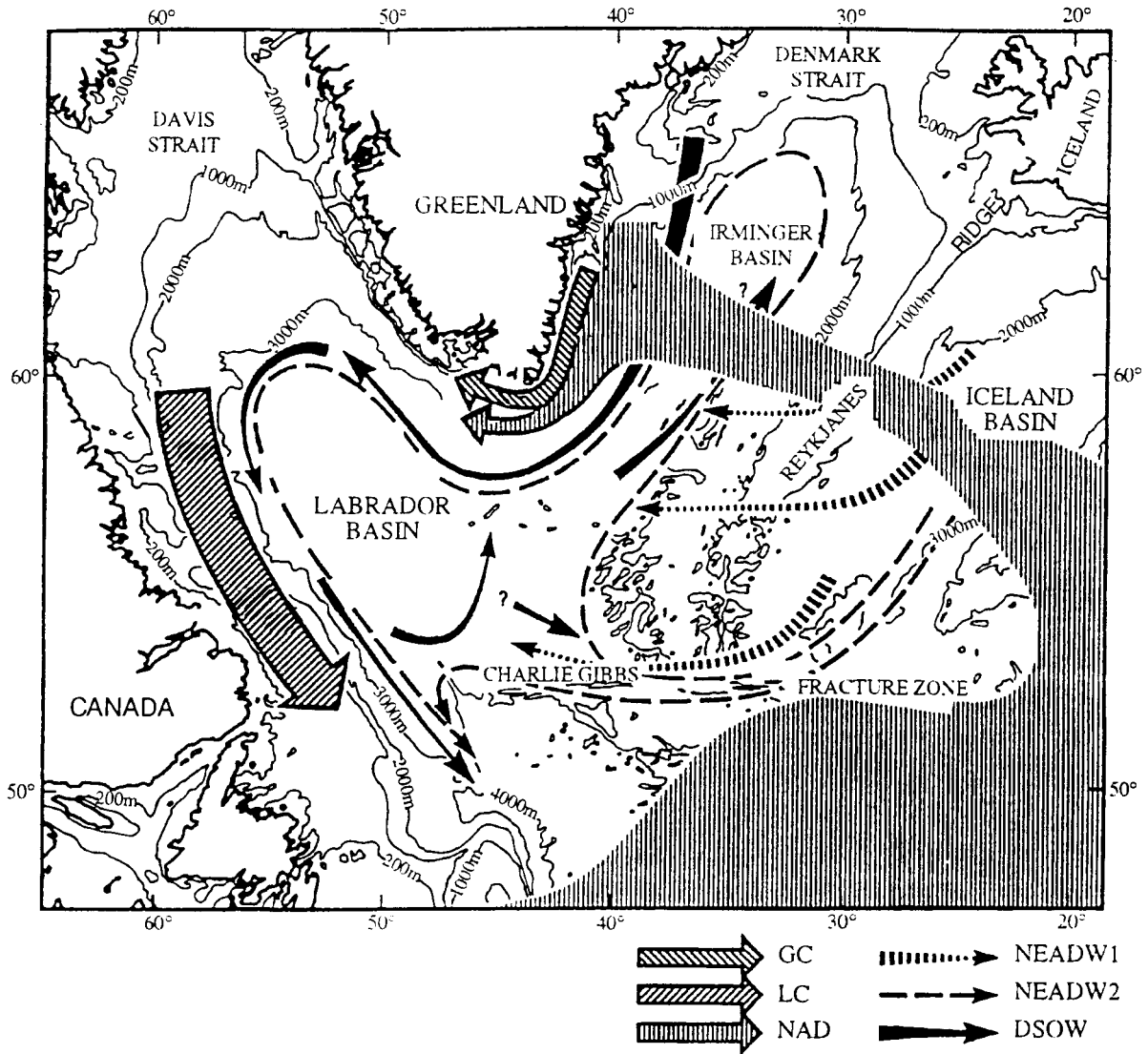


Fig. 2.4. A map showing bathymetry and the present-day surface water circulation of the northwest Atlantic Ocean (Source: Lucotte and Hillaire-Marcel, 1994). Abbreviations: DSOW, Denmark Strait Overflow Water; GC, Greenland Current; LC, Labrador Current; NAD, North Atlantic Drift; NEADW, North East Atlantic Deep Water.

transport of heat and moisture between the atmosphere and the ocean (Fillon and Duplessy, 1980; Aksu et al., 1992). The intermediate water formed by sinking of surface waters, flows southward into the Atlantic Ocean (Ichiye, 1966; McCartney, 1992; Haye, 1993).

Another strong circulation system is the western boundary undercurrent (WBUC). The waters of the WBUC are a mixture of waters from the Norwegian Sea, Irminger and Labrador seas east and west of Greenland (McCartney, 1992; Lucotte and Hillaire-Marcel, 1994). The Norwegian Sea waters enters the Labrador Sea through two passages namely, the Denmark Strait and the Faroe-Scotland channel between Faroe Island and Lousy Bank (Heezen and Hollister, 1971). Waters through the Denmark Strait flows south at abyssal depths of 2000 to 3000 m around the southern tip of Greenland. The waters through the Faroe-Scotland channel flow in a southwesterly direction parallel to the bathymetric contours along the eastern side of the Mid-Atlantic ridge. At approximately 53°N the current is deflected westward through the Charlie Gibbs fracture zone, then turns northeast due to Coriolis force, and finally flows northward along the northwestern flank of Reykjanes Ridge, where it mixes with waters from the Irminger and Labrador seas east and west of Greenland (McCartney, 1992; Lucotte and Hillaire-Marcel, 1994). From there on it flows north at a depth along the west Greenland margin, around the Labrador Sea margin and finally flows south along the lower slope and upper rise off eastern Canada. The core of the WBUC has been suggested to occur at a depth of approximately 2800 m, east of Newfoundland (Carter et al., 1979). The speed of the WBUC is high (20 cms¹) and areas it sweeps are characterized by coarse sediments (gravelly muddy sand) and current induced bed forms (Carter et al., 1979; Heezen et al., 1966).

Various workers have described the geology of the Labrador Sea (Piper et al., 1990 and references therein). The Labrador inner shelf is studded by a thin cover of till and of sediments derived from till by wave and iceberg reworking (Grant, 1972; Josenhans et al., 1986). The outer shelves of both Labrador and Greenland contain sequences of till and overlying stratified muddy

sediments of up to 300 m (Grant, 1972; Funder and Larsen, 1989; Josenhans et al., 1986). Generally, the deep Labrador Sea surficial sediments consist of hemipelagic material intercalated with ice-rafted debris derived from Greenland, Baffin Island and Labrador (Piper et al., 1990).

The allochthonous material in the Labrador Sea basin can be transported by turbidity currents through the Northwest Atlantic Mid-Ocean Channel (NAMOC), a submarine channel which traverses the continental slope and rises off Hudson Strait as submarine canyons and deep basins of Labrador and Newfoundland and continues as far as the Sohm Abyssal Plain (Hesse et al., 1987). The NAMOC crosses the Labrador Basin approximately along its median line, but it turns east near Orphan Knoll at about 52°N where it follows the westernmost part of the Charlie Gibbs Fracture Zone for about 90 km before entering the Newfoundland Basin to the south (Hesse et al., 1987; Myers and Piper, 1988). This giant channel is connected with a system of tributary and satellite channels, especially on the Labrador side, where spilled over sediments are deposited (Hesse et al., 1987; Myers and Piper, 1988). The NAMOC has been inferred to have been very active during glacial-transition periods (Hesse et al., 1987, 1990; Myers and Piper, 1988).

2.2.2. Paleoproductivity and Burial Rates

The major sources of nutrients in the Labrador Sea are regeneration, upwelling off the coast of Greenland, cross-shelf mixing on the Labrador Shelf and advection of nutrient rich waters from Baffin Bay and Hudson Bay (Sutcliffe et al., 1983). The paleoproductivity in the Labrador Sea has been inferred from the content of organic carbon and nitrogen and the abundance of coccoliths, foraminifera and dinoflagellates (Macko, 1989; Stein, 1991; Stein et al., 1989a; Hillaire-Marcel et al., 1990, 1994a,b; Aksu et al., 1992). The coccoliths and dinoflagellates and partly the planktonic foraminifera, are the largest contributors of biogenic particulate matter in the area (Aksu et al., 1992). The abundance (productivity) of foraminifera in the sediments between 16 and 13Ka is low relative to other periods (Aksu et al., 1992). The low rate of OM flux (primary productivity) has

been attributed to low rates of nutrient supply owing to a reduction in oceanic circulation (Aksu et al., 1992). Based on the data from ODP Sites 646 and 647, the estimated productivity during the Tertiary-Quaternary period range from 100 to 170 $\text{gCm}^{-2}\text{y}^{-1}$ and between 40 and 160 $\text{gCm}^{-2}\text{y}^{-1}$ respectively (Stein et al., 1989a). Concentrations of dinocysts, which reflect levels of primary productivity in marine environments, have been observed to be higher during interglacial periods (Aksu et al., 1992; Hillaire-Marcel et al., 1994b) and are associated with an enrichment in uranium in the sediments (Hillaire-Marcel et al., 1990).

The stable isotopic compositions of nitrogen in conjunction with that of organic carbon have been used to infer paleoproductivity in the Labrador Sea (Macko, 1989). This particular study indicates a constant influx of OM from Miocene to Present with a lack of relationship between isotope stages and these parameters (Macko, 1989).

2.2.3. Sources of Organic Matter

Although nitrogen stable isotopes have been successfully used as source indicators (Macko, 1983; Peters et al., 1978; Sweeney and Kaplan, 1980; Muzuka, 1990; Muzuka et al., 1991), this approach has not been widely applied in the Labrador Sea. The only notable work in the area, in which stable isotopic compositions of nitrogen in combination with that of organic carbon were used as source indicators of OM, is that of Macko (1989) and Rogers et al. (1972). The study of Macko (1989), which utilized material recovered at ODP Sites 646 and 647, indicates a dominance of marine OM over that of terrestrial OM. A similar conclusion was reached by Stein et al., (1989a) who used C/N ratios to infer sources of OM in the area. Rogers et al. (1972) reported very low resolution isotopic compositions data for sedimentary OM recovered at various sites in the Labrador Sea during the Deep Sea Drilling Program.

2.2.4. Diagenetic Changes

Recent work in the area on early diagenetic changes include that of Lucotte et al. (1994) and Gariépy et al. (1994). These studies address the question of diagenesis using reactive and nonreactive iron and phosphorous, as well as uranium. Apart from these recent works little has been done to determine the diagenetic changes of nitrogen and carbon in the area.

2.3.0. WHAT REMAINS TO BE DONE

As stated previously in section 1.1.1., burial of autochthonous marine OM is one of the processes involved in the removal of carbon and nitrogen from the atmosphere. Therefore, it is important to evaluate relative proportions of various sources prior to making burial rate estimates based on organic carbon preserved in the sediments. Although sedimentation processes such as turbidity currents, iceberg deposition, strong WBUC in the Labrador Sea, as well as riverine input of OM to the Gulf of St. Lawrence, may cause different distribution patterns of terrestrial OM, little has been done to delineate spacial and temporal sources of OM in these areas. From the literature review presented above, the only notable works where downcore variations in C/N ratios, ^{13}C and/or ^{15}N were used as source indicators in the Labrador Sea and Gulf of St. Lawrence is that of Stein (1989a), Rogers et al. (1972), Macko (1989), Lucotte et al. (1991), Tan and Strain (1979a,b 1983) and Pocklington (1976). Most of the work in the Gulf of St. Lawrence and its estuary, which focused mainly on surficial and particulate OM, was largely conducted in the estuary. Data on temporal variations in the relative proportions of marine/terrestrial OM, and stable isotopic compositions of organic carbon and nitrogen for the Gulf of St. Lawrence are lacking. Furthermore, information on lateral distribution of nitrogen stable isotopes compositions of sedimentary OM in the Gulf and its estuary is lacking. The present study intend to provide the first high resolution data on spacial and temporal variations in the relative proportions of marine/terrestrial OM, and stable isotopes of organic carbon and nitrogen.

In the Labrador Sea, low resolution studies on temporal variations in the paleoproductivity, burial rate, and stable isotopic compositions of organic carbon and nitrogen are confined to a few cores collected during the Ocean Drilling Program and the Deep Sea Drilling Program. High resolution data on spacial and temporal variations in the sources of OM and stable isotopic compositions of organic carbon and nitrogen are lacking. Thus, high resolution data are required to asses relative proportions of marine/terrestrial OM and sediment dispersion patterns caused by turbidity currents, iceberg deposition, and strong WBUC in the Labrador Sea.

Although high latitude areas are considered to be very important in regulating the earth's climate, burial rates and primary productivity, which are some of the processes regulating the amount of CO₂ and N₂ present in the atmosphere, are poorly known. In the Labrador Sea and Gulf of St. Lawrence (subarctic areas), few studies have been conducted to document differences in burial rate and paleoproductivity between glacial and interglacial periods (e.g. Stein, 1989a). There are no systematic studies which have been conducted to document lateral variations in burial rate and paleoproductivity off eastern Canada.

Diagenetic alteration of OM may alter the signatures of paleoproductivity indicators such as organic carbon and stable isotopes of organic carbon content. One way of evaluating extent of diagenesis is through the use of diagenetic models, compositions of amino acids and stable isotopes of sedimentary organic carbon and nitrogen. As shown in the literature review, little is known on the diagenetic changes of OM from the diagenetic model, stable isotopic compositions and amino acids contents perspectives. It is clear that, there is a lot to be done in order to better understand spacial and temporal variations in burial rates, paleoproductivity and sources of OM, as well as degree of OM degradation. The present work addresses these issues using high resolution results of geochemical analysis of short cores as well as long cores, that covers a much wider area than previous studies.

CHAPTER 3

3.0. MATERIAL AND METHODS

3.1.0. MATERIAL.

The sedimentary materials used in this study were collected during four cruise missions, two (HU-90-028 and HU-90-031) in the Gulf of St. Lawrence-Scotia slope, and two (HU-90-13 and HU-91-045) in the Labrador Sea. The type of cores, geographic location and water depths are given in Table 3.1, and Figs 3.1 and 3.2. Abbreviations for cores given in Table 3.1 are used in this and all proceeding chapters.

3.1.1. Core description: Labrador Continental Margin

Cores 05 BC and 14 BC were collected from the upper Labrador continental slope off the Hamilton Bank in the Cartwright Channel. Other cores recovered from the northern part of the Hamilton spur on the mid to lower continental slope are 16 BC, 18 BC and 23 BC. Core 28 BC was recovered in the Labrador basin, while cores 93 BC and 94 PC were recovered from the southern Labrador Sea. Site 28 BC is within the tributaries and satellite channels of the NAMOC. The character, colour, number of samples analyzed and core length of the sediment cores recovered from the Labrador continental margin and basin are given in appendix 9.1.0., Table 3.2. The upper 640 cm of the sediment core recovered at site 94 PC was analyzed. Based on ^{14}C AMS ages, the analyzed core section covers material deposited over the last 31,000 years (Hillaire-Marcel et al., 1994a).

The sampling interval was (i) 1 cm at sites 14 BC and 93 BC, (ii) 2 cm at sites 18 BC and 28 BC, and (iii) 10 cm at site 94 PC. The samples at sites 05 BC and 16 BC were collected every 1 cm in the upper 7 cm and 16 cm, respectively, followed by a 2 cm sampling interval to the base of the core. The sampling interval at site 23 BC was typically 2 cm for the upper 14 cm, followed by a 1 cm sampling

Table 3.1. Cores used in this study

CRUISE/CORE	ABBRE	LATITUDE AND LONGITUDE		W/D	No.	LOCALITY
HU-91-045-05 BC	05 BC	54°42.47 N	56°26.96 W	530	1	Labrador Shelf; off the Hamilton Bank in the Cartwright Channel
HU-91-045-14 BC	14 BC	54°44.50 N	53°43.98 W	340	2	Labrador Shelf; off the Hamilton Bank in the Cartwright Channel
HU-91-045-16 BC	16 BC	54°49.27 N	52°52.03 W	1364	4	Labrador Slope; northern part of the Hamilton spur
HU-91-045-23 BC	23 BC	54°54.04 N	52°44.72 W	1984	4	Labrador Slope; northern part of the Hamilton spur
HU-91-045-18 BC	18 BC	55°02.06 N	52°07.78 W	2648	5	Labrador Slope; northern part of the Hamilton spur
HU-91-045-28 BC	28 BC	56°36.99 N	49°45.01 W	3992	6	Labrador Basin within the tributaries and satellite channels of the NAMOC
HU-90-013-13 PC	13 PC	58°12.59 N	48°22.40 W	3380	7	SW Greenland Continental Margin
HU-90-013-11 BC	11 BC	58°54.85 N	47°05.13 W	2805	8	SW Greenland Continental Margin
HU-91-045-38 TWC	38 TWC	58°45.81 N	44°52.59 W	2052	9	Eirik Ridge; SW Greenland Continental Margin
HU-90-045-40 LHC	40 LHC	58°47.83 N	43°57.07 W	1559	10	Eirik Ridge; SW Greenland Continental Margin
HU-91-045-93 BC	93 BC	50°12.28 N	45°41.15 W	3448	11	Western Labrador Sea
HU-91-045-94 PC	94 PC	50°12.26 N	45°41.14 W	3448	11	Western Labrador Sea
HU-90-031-13 BC	13 BC	49°25.42 N	66°19.45 W	322	12	Gulf of St. Lawrence; at the mouth of the lower estuary
HU-90-031-17 BC	17 BC	49°17.44 N	63°59.57 W	373	13	Gulf of St. Lawrence; SW of the Anticosti Island
HU-90-031-29 BC	29 BC	48°31.51 N	61°10.21 W	408	14	Gulf of St. Lawrence; SE of the Anticosti Island
HU-90-031-34 BC	34 BC	47°09.15 N	60°32.54 W	174	15	Gulf of St. Lawrence; NW of Cape Breton Island close to the Cabot Strait
HU-90-028-06 BC	06 BC	47°39.54 N	59°43.31 W	521	16	Gulf of St. Lawrence; within the Cabot Strait
HU-90-031-41 BC	41 BC	46°59.56 N	59°04.46 W	448	17	Gulf of St. Lawrence; within the Cabot Strait
HU-90-031-59 BC	59 BC	45°50.36 N	58°34.19 W	268	18	Gulf of St. Lawrence; SE of Cape Breton Island
HU-90-031-45 BC	45 BC	45°51.17 N	57°35.51 W	473	19	Gulf of St. Lawrence; south of the Cabot Strait
HU-90-031-43 PC	43 PC	44°49.19 N	56°29.47 W	387	20	Scotia Continental Shelf at one of the end members of the Laurentian Channel
HU-90-031-44 PC	44 PC	44°39.42 N	55°37.13 W	1378	21	Scotia continental slope

NOTE: BC = Box core; PC = Piston core; TWC = Trigger weight core; LH = Le high core; ABBRE = core abbreviation; W/D = water depth (m), No. = numbers indicated in Figs. 3.1 and 3.2.

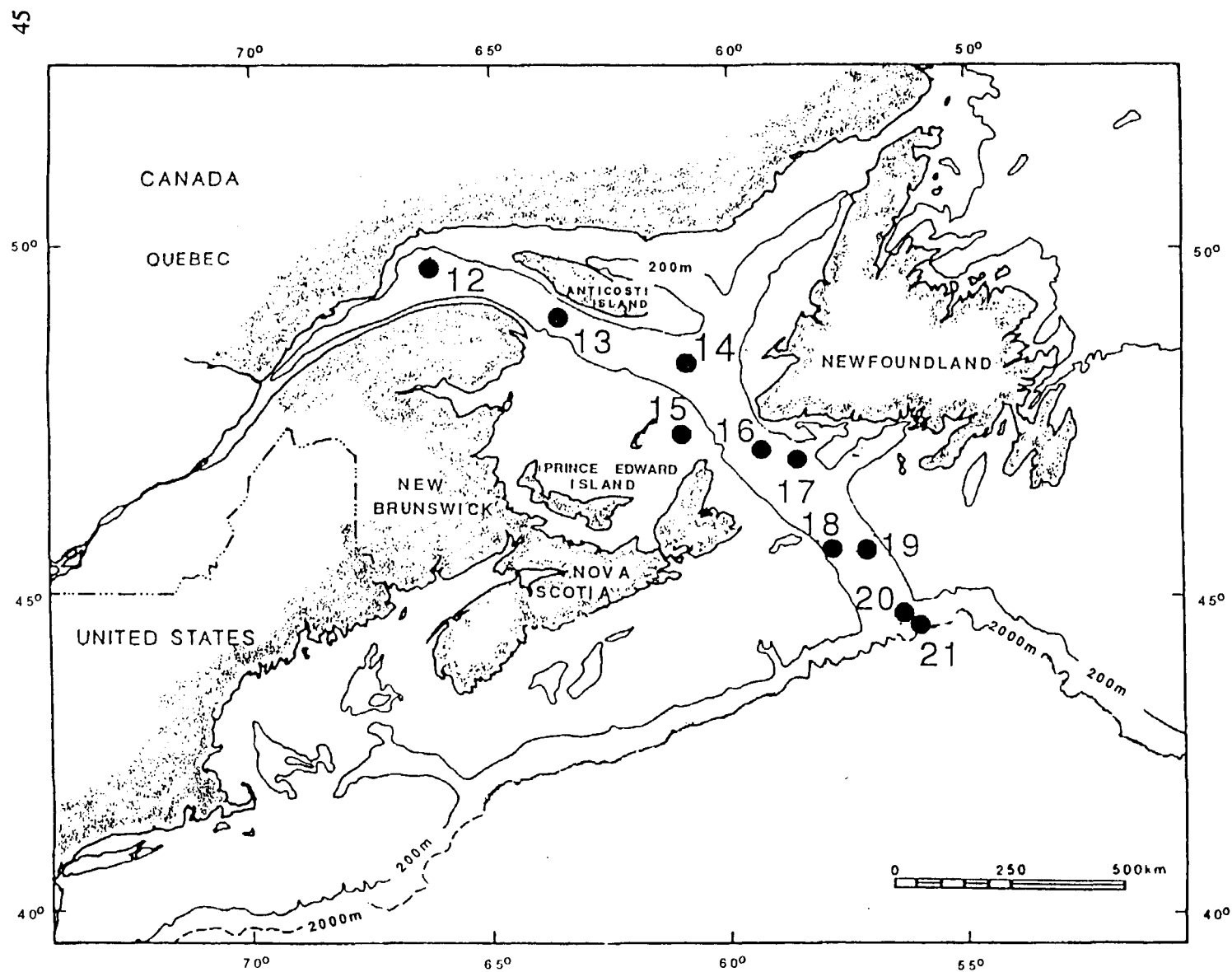
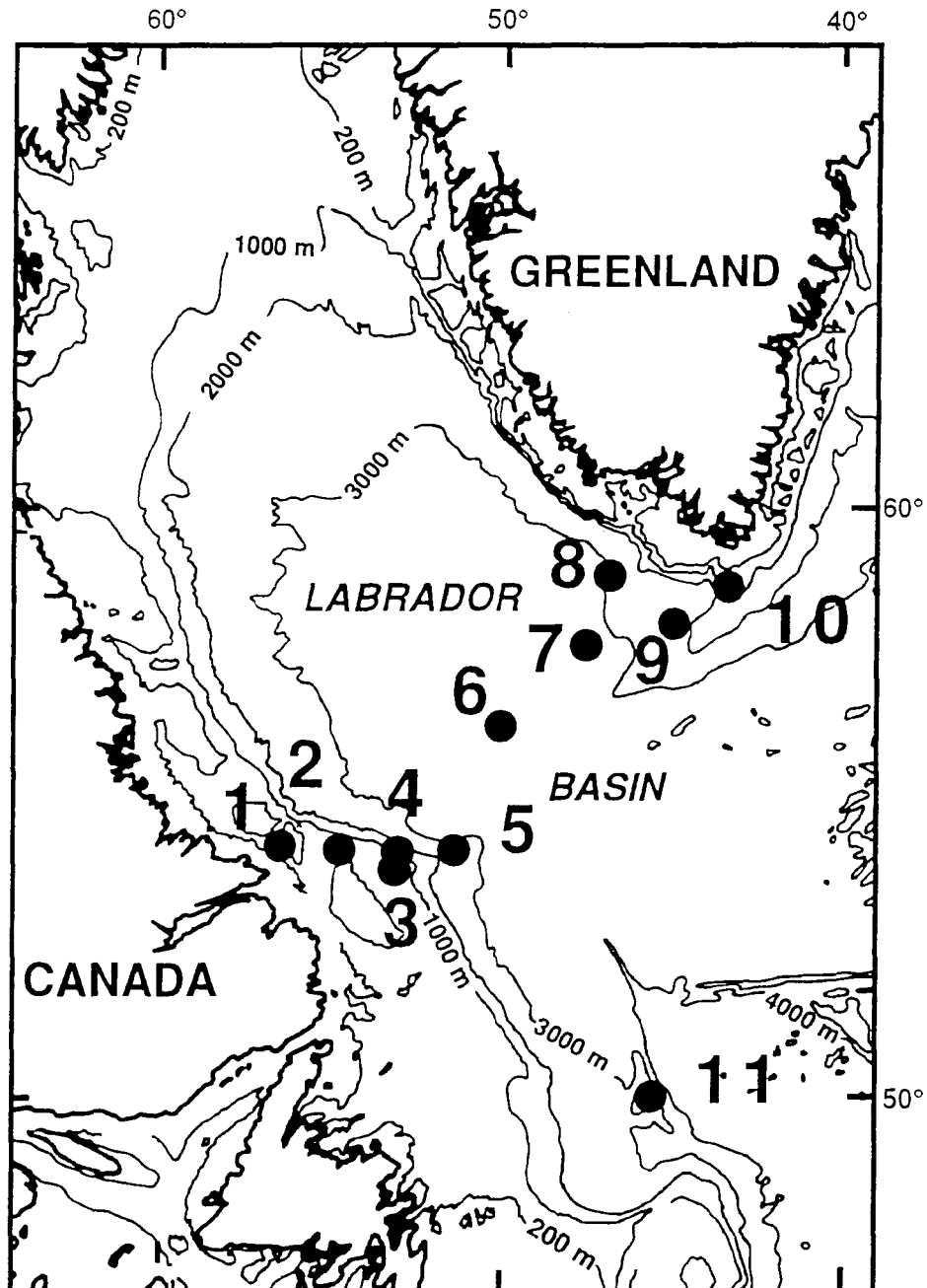


Fig. 3.1. A map showing sampling sites in the the Gulf of St. Lawrwence-Scotian slope

Fig. 3.2. A map showing sampling sites in the Labrador Sea.



to about 18 cm. A core section between 18 and 22 cm was sampled every 2 cm, whereas that below 22 cm was typically 1 cm.

Based on ^{14}C ages, the estimated sedimentation rate at site 23 BC for the Holocene period is 2.8 cm/ka, while that of site 28 BC is 3.5 cm/ka (Hillaire-Marcel et al., 1994b). Because cores 93 BC and 94 PC were collected from the same spot, the Holocene sedimentation rate of 18 cm/ka determined for core 94 PC (Hillaire-Marcel et al., 1994b), has been taken as a representative value for core 93 BC. The mean sedimentation rate including the Heinrich events at site 94 PC is about 20 cm/ka (Hillaire-Marcel et al., 1994a). There are no estimates of sedimentation rate for the other sites.

The redox potential (Eh) is positive in the upper few cm at sites 05 BC and 14 BC, and in the whole core at sites 16 BC, 18 BC, 23 BC, 28 BC and 93 BC (Fig. 3.3). The downcore distribution of the Eh in all cores shows a general downcore decrease, except core 18 BC that has the most positive and nearly constant Eh values (Fig. 3.3).

3.1.2. Core Description: Greenland Continental Margin

The CTD-profiles where cores 11 BC and 13 PC were collected revealed three water masses. These water masses are: (a) a surface layer with a temperature of about 3.25°C, and which extended to approximately 100 m; (b) the Labrador Sea water mass which extends down to 1700 m with a minimum temperature of about 3°C; and (c) a deep water mass showing a strong temperature gradient from 3.3 to 1.75°C (Hillaire-Marcel and Rochon, 1990; Lucotte and Hillaire-Marcel, 1994).

Cores 13 PC and 11 BC were recovered off southwest Greenland coast, while cores 38 TWC and 40 LHC were recovered on the Eirik ridge in the eastern Labrador Sea. The character, colour, number of samples analyzed and core length of the sediment cores recovered from the Greenland continental margin are given in appendix 9.1.0., Table 3.2. The upper 620 cm of the core 13 PC was analyzed. Based on ^{14}C AMS ages, the analyzed core section covers material deposited over the last 30,000 years

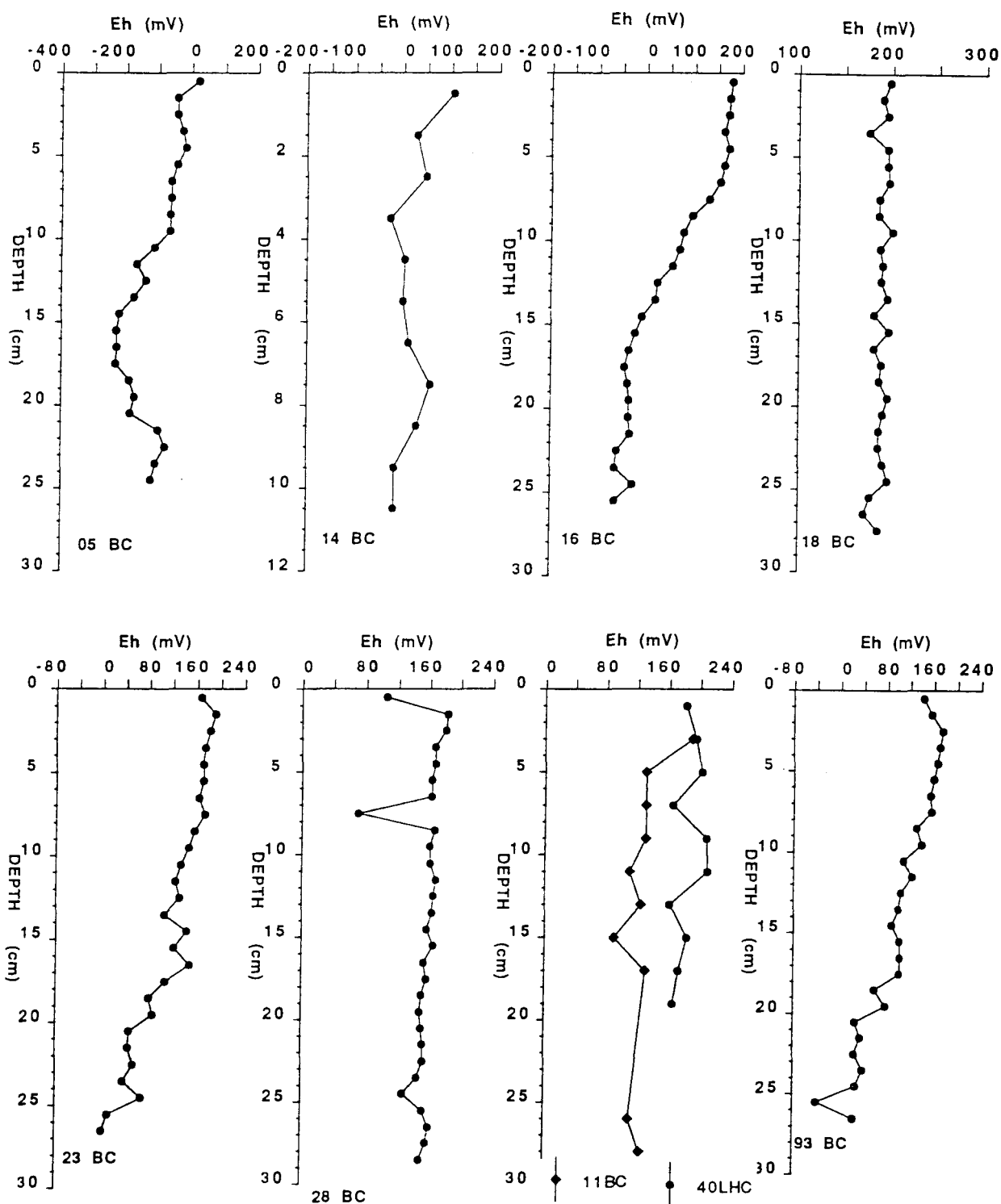


Fig. 3.3. Onsite redox potential (Eh in mV) for short cores collected from the Labrador Sea.

(Hillaire-Marcel et al., 1994a).

The ^{14}C AMS ages for the sediments recovered at site 11 BC indicates that the core penetrated material deposited over the last 12,500 years (Hillaire-Marcel et al., 1994a ; Wu and Hillaire-Marcel, 1994). The sediments at the surface have been dated at 4000 years, an indication of intense erosion or non-deposition of sediments (Hillaire-Marcel et al., 1994a ; Wu and Hillaire-Marcel, 1994). The ^{14}C ages in the upper 5 cm of this core are constant, which indicates bioturbation activity in the area. A simple two-box model has indicated that the mixed layer is about 11 cm deep (Hillaire-Marcel et al., 1994a; Wu and Hillaire-Marcel., 1994).

Based on the ^{14}C ages, the sedimentation rate at site 11 BC is about 2.3 cm/ka in the upper 15 cm followed by high sedimentation rate of 15 cm/ka (Hillaire-Marcel et al., 1994a). The sedimentation rates at site 13 PC range from 9 to 32 cm/ka (Hillaire-Marcel et al., 1994a). There are no estimates of sedimentation rate for the other two sites. The Eh values at sites 11 BC and 40 LHC are positive, and they show a slight downcore decrease (Fig. 3.3).

The sampling interval at sites 11 BC and 40 LHC was 2 cm, while at site 13 PC was typically 10 cm. The sample collection at site 38 TWC was irregular with at least 1 sample per two centimetres. Each sample at all sites represent a homogenate of 2 cm.

3.1.3. Core Description: Gulf of St. Lawrence

The samples analyzed from the Gulf of St. Lawrence-Scotia slope were collected from a transect along the Laurentian channel. The character, colour, number of samples analyzed and core length of the sediment cores recovered from the Gulf of St. Lawrence-Scotia slope are given in appendix 9.1.0., Table 3.2. The surface sediments at site 29 BC, which are usually brownish in colour, are suspected to have been washed out during retrieval (Thibaudeau and Curie, 1990). Based on the ^{14}C AMS ages and ^{18}O stratigraphy (unpublished data), the longest core analyzed in the area (44 PC) extends back to

about 14,000 years.

Except for core 29 BC, the sampling interval for all box cores was typically 1 cm in the upper 5 cm followed by a 2 cm sampling interval below it. A sample in the upper 5 cm represents a homogenate of 1 cm, while that below 5 cm represents a homogenate of 2 cm. The sampling interval at site 29 BC was typically 2 cm. Upper 39 cm of the core 43 PC was analyzed in this study, and sampling interval was 2 cm for the upper 18 cm, followed by a 5 cm sampling interval below it. The samples at site 44 PC were collected every 10 cm and each sample represent a homogenate of 2 cm.

The sedimentation rate as determined using excess ^{210}Pb at site 13 BC is 0.17 cm/yr, and the mixed zone is about 6 cm (Jennane, 1992). The estimated mixing (bioturbation) coefficient at this site is 15 cm²/yr. A core section of 37 cm analyzed in this study represents sediments deposited for the past 200 years. Similarly, the estimated sedimentation rate using the same method at site 17 BC is about 0.13 cm/yr, and the effect of bioturbation is minimal (Jennane, 1992). The sedimentation rate for site 29 BC has been estimated to be 0.11 cm/yr (Jennane, 1992). The estimated sedimentation rate at site 41 BC is about 0.44 cm/yr. Based on the ^{14}C AMS ages and ^{18}O stratigraphy (unpublished data), site 44 PC is associated with a very high sedimentation rate of up to 300 cm/ka (see section 3.2.2). There are no estimates of sedimentation rate for the other sites.

Based on the on-site determination of Eh, the upper 1-3 cm has positive values (slightly oxic) at sites 13 BC, 17 BC and 06 BC, with the remaining part of the cores having a negative Eh values (Fig. 3.4). All remaining cores have negative Eh values. The Eh values show a downcore decrease to the base of the core at sites 17 BC, 41 BC and 06 BC (Fig. 3.4). The Eh at site 29 BC is highly variable and shows a slight increase downcore to about 17 cm. From 17 cm to the base of the core, the Eh values remains relatively constant (Fig. 3.4). Site 34 BC has the most negative Eh, and shows a general trend of decreasing downcore to about 30 cm, followed by a slight increase to the base of the core (Fig. 3.4). At site 45 BC, the values of Eh decrease with depth in upper 5 cm followed by a slight

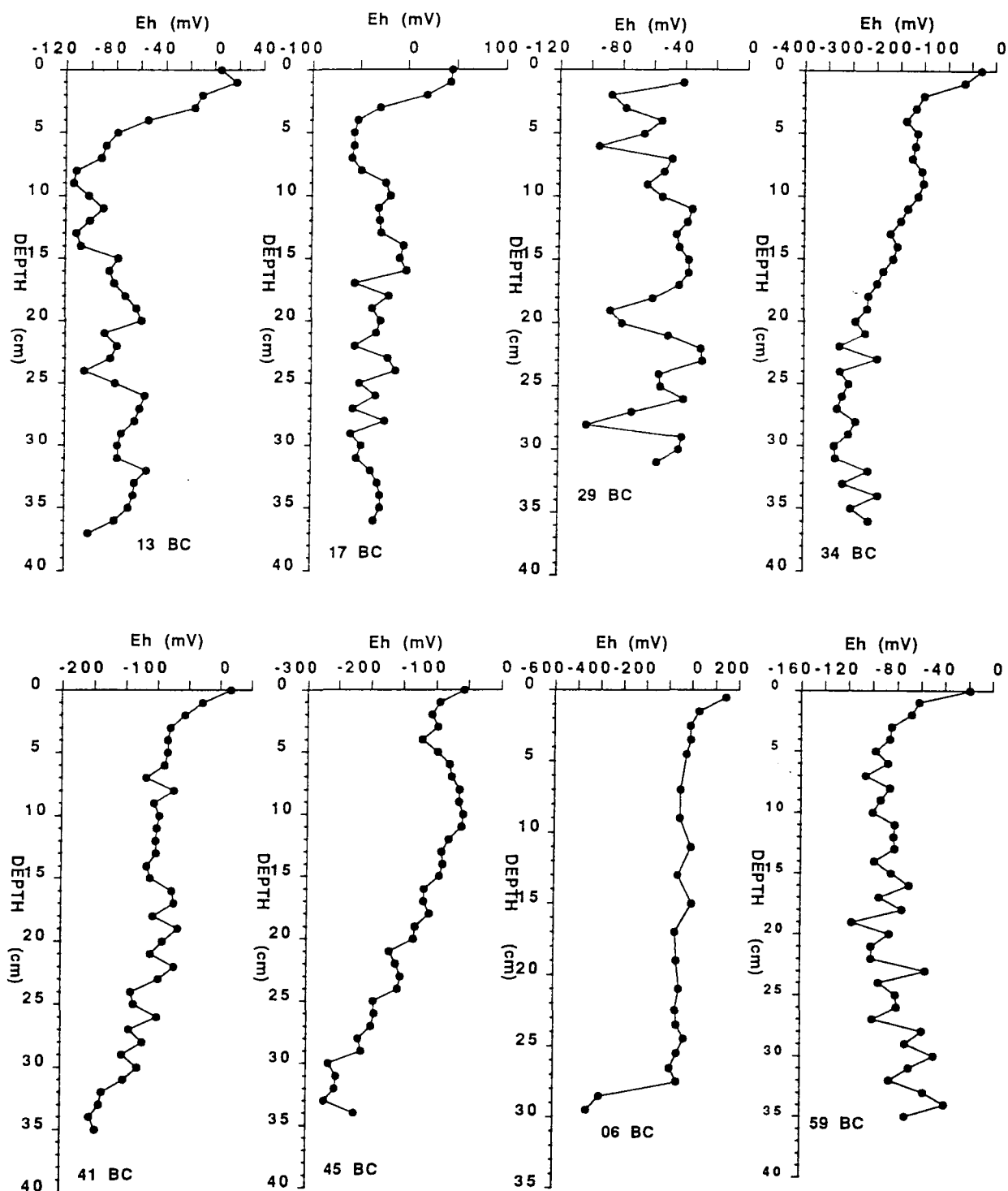


Fig. 3.4. Onsite redox potential (Mv) for short cores collected from the Gulf of St. Lawrence.

increase to about 15 cm. Below 15 cm, the redox potential decrease with depth to the base of the core (Fig. 3.4). With regard to site 59 BC, the Eh decreases with depth in the upper 10 cm, followed by a slight increase to the base of the core (Fig. 3.4).

3.2.0. METHODOLOGY

The stable isotopic compositions of sedimentary organic carbon and nitrogen for all box cores, one Le High Core, one piston core (43 PC) and one trigger weight core (Table 3.1) are used in this study to establish or delineate lateral variation in the sources of OM in the Labrador Sea and Gulf of St. Lawrence-Scotia slope (Chapter 4). The contents of CaCO_3 , organic carbon and nitrogen, as well as the isotopic compositions of both organic carbon and nitrogen in cores 13 PC, 94 PC, 44 PC and 11 BC are used to estimate the inputs of terrestrial OM, burial rates of organic carbon and nitrogen and changes in primary productivity during glacial and interglacial periods (Chapter 5). Since the nitrogenous compounds are preferentially removed relative to carbonaceous compounds during biodegradation, the extent of diagenetic changes of organic nitrogen is partly inferred from the downcore variation of the C/N ratios in all box cores and downcore variation in the content of amino acids in cores 17 BC, 29 BC, 45 BC and 43 PC (Chapter 6). A multi G-model of Berner (1980) and Weistrich and Berner (1984) was used to estimate first order rate constant that indicate rate of OM decomposition using a MATLAB fitexp curve fitting method. Assumptions and equations used are given in section 3.2.3.

3.2.1. Geochemical Analysis

Samples for all geochemical analysis were dried at 60°C and then ground to a fine powder using an agate mortar. Part of each ground sample was acidified twice with 1M HCl to remove carbonate, washed, dried, and then divided into two portions for isotopic analysis and determination of residual

organic carbon content.

Aliquots for isotopic analysis were combusted in a quartz tube for 1 hr at 850°C in the presence of purified cupric oxide wire and high quality granular copper (Macko, 1981). The N₂ and CO₂ gases obtained were cryogenically isolated from other combustion products and analyzed on a V.G. micromass PRISM stable isotope ratio mass spectrometer. On the basis of replicate analysis of samples, the reproducibility in combustion and measurement is within $\pm 0.2\%$. Isotope data are reported in δ -notation as:

$$\delta^Z(N,C) = \left[\frac{R_{sample}}{R_{standard}} - 1 \right] \times 10^3 \quad (1)$$

where z is either 13 for carbon or 15 for nitrogen, and R is the abundance ratio of the heavy to light isotope; the standards for carbon and nitrogen are the PDB and atmospheric nitrogen respectively.

The percentages of total carbon and nitrogen, the organic carbon and the CaCO₃ contents were determined using a carbo erba nitrogen/carbon analyzer, model NA1500 Series 2. Total carbon and nitrogen were determined on an untreated portion of each sample. The residue organic carbon content was determined on acidified material.

Analysis of the amino acids for cores 29 BC, 45 BC, 43 PC and 17 BC was performed using high performance liquid chromatography (HPLC). Aliquots (10-35 mg) for amino acid analysis were hydrolyzed by adding equal amount by volume of DL-Norleucine (DL-2-aminohexanoic acid) and 6M HCl and sealed in the presence of nitrogen and hydrolyzed at 110°C for 22 hours. Hydrolyzed samples were dried on a rotary drier and dissolved to a pH of 2, and then directly injected into the HPLC analyzer. Peak calibration was achieved by using Beckman standard system 6300 hydrolyzate.

3.2.2. Estimation of Burial Rates and Paleoproductivity

The OM flux to the sea floor (F_i) is primarily a function of primary productivity (P) and the water depth (Z). The relationship between primary production, OM flux and water depth is non-linear because consumption of OM occurs at any given depth in the ocean below the euphotic zone (Suess, 1980; Taylor and Karl, 1992). The relationship between F_i , P and Z can be expressed as:

$$F_i = KP^a Z^b \quad (2)$$

where K , a and b are constants. Various workers have determined values of these constants using sediment trap data (appendix 9.1.0., Table 3.3; Suess, 1980; Suess and Müller, 1980; Taylor and Karl, 1992; Sarnthein et al., 1987, 1988).

The mass or total accumulation rate of biogenic material AR_{Ci} is a function of paleoproductivity, water depth, and bulk sedimentation rate (SR) and is given by:

$$AR_{Ci} = KF_i SR^d \quad (3)$$

Where d is a constant (see appendix 9.1.0., Table 3.3 for the estimated values by various workers). The total sediment accumulation rate (AR in $g\ cm^{-2}ky^{-1}$) may be calculated using the following equation:

$$AR = SR \times DBD \quad (4)$$

Where DBD is dry bulk density (g/cm^3), and SR is linear sedimentation rate ($cm\ ky^{-1}$). The mass accumulation rate of organic carbon, nitrogen or carbonate (AR_{Ci}) is a product of total sedimentation rate and the carbon content (in percentage) in the sediments (C_i) i.e.

$$AR_{Ci} = AR \times (\%C_i) \times 10^{-2} \quad (5)$$

Therefore, the flux of organic carbon or nitrogen is given by:

$$F_i = K \times AR \times (\%C_i) \times 10^{-2} SR^{-d} \quad (6)$$

Substituting equation 1 and 4 into 2 yields

$$AR \times (\%C_i) \times 10^{-2} = KP^a Z^b SR^d \quad (7)$$

Substituting equation 3 into equation 5 yields

$$SR \times DBD \times (\%C_i \times 10^{-2}) = KP^a Z^b SR^d \quad (8)$$

$$P = SR^{\left(\frac{1-d}{a}\right)} (DBD)^{\frac{1}{a}} (\%C_i \times 10^{-2})^{\frac{1}{a}} Z^{\frac{b}{a}} \quad (9)$$

The quantity of terrestrial OM contributed to the marine environment was determined using a mass balance equation under the assumption that the $\delta^{13}\text{C}$ values of marine and terrestrial end members for these high latitude areas are -21 and -26‰ respectively (Gearing, 1988; Fry and Sherr, 1984; Gearing et al., 1984). The mass accumulation of marine OM ($MART_{OM}$) was determined using the following equation:

$$MART_{OM} = AR_{Cr} \times T_{OM} \times 10^{-2} \quad (10)$$

Where T_{OM} is marine organic carbon content. The $MART_{OM}$ was used to estimate paleoproductivity of each component.

Note: The dry bulk density was estimated under the assumption that the water content for all piston core is 50%, while that of box cores is about 60%, that the grain density of mineral matter is about 2.68 g/cm³, the density of interstitial water of 1.025 g/cm³, and that the density of OM is 0.9 g/cm³. The contribution of OM to the dry bulk density was considered negligible because of low organic carbon content in most of the cores. To estimate new production, an equation of Sarthein et al. (1988) that is similar to equation 9 was used.

Sedimentation rates used in the estimation of paleoproductivity and burial rates for cores 11 BC, 13 PC and 94 PC are those reported by (Hillaire-Marcel et al., 1994a). Because of high variability in the sedimentation rate at site 44 PC, the sedimentation rates were determined by an exponential curve fitting (fitexp) method using Matlab (Fig. 3.5); and the resulting equation was:

$$y=1.018^{11}x\exp(-0.9482x)-12084x\exp(-0.01268x)+10941x\exp(0.0002532x) \quad (11)$$

where y and x are ^{14}C age and depth respectively. For comparison, the ^{14}C age data (unpublished data) were also transformed into calendar years using the following equations:

(1) For ages younger than 10,000 ^{14}C yr B.P.(Bond et al., 1992a)

$$y=-173.1+1.118x(^{14}\text{C}_{age})+1.416x10^{-5}(^{14}\text{C}_{age})^2-1.373x10^{-9}(^{14}\text{C}_{age})^3 \quad (12)$$

(2) For the period 10,000-20,000 ^{14}C yr BP. (Bard et al., 1993).

$$y=-840+1.24x(^{14}\text{C}_{age}) \quad (13)$$

and then interpolated using the following equation resulting from fitexp method.

$$y=5.505x10^{10}x\exp(-0.9359x)-13889x\exp(-0.01079x)-13076x\exp(0.0002323x) \quad (14)$$

Values of sedimentation rates using both methods are similar (Fig. 3.5). Equations 11 and 14 are applicable for depths ≥ 18 cm.

3.2.3. Diagenetic Model

Both field observations and laboratory experiments have indicated that the various types of OM undergo decomposition at widely different rates. Because of this, Berner (1980) proposed a model for the multiple "pools" (multiple G-model) of OM in sediments being decomposed at different rates. Estimation of the rate of OM decomposition using the multi G-model was made under the assumption that the system had reached a steady state condition, constant porosity, constant sedimentation rate, and first order kinetics for the oxidation of OM. Samples from the Labrador Sea were excluded from modelling owing to high probability of their turbidite origin. The shapes of the organic carbon and nitrogen profiles that showed a downcore decline in the Gulf of St. Lawrence-Scotia slope were used in the modelling process. Because of the irregular distribution of nitrogen, rates of nitrogen

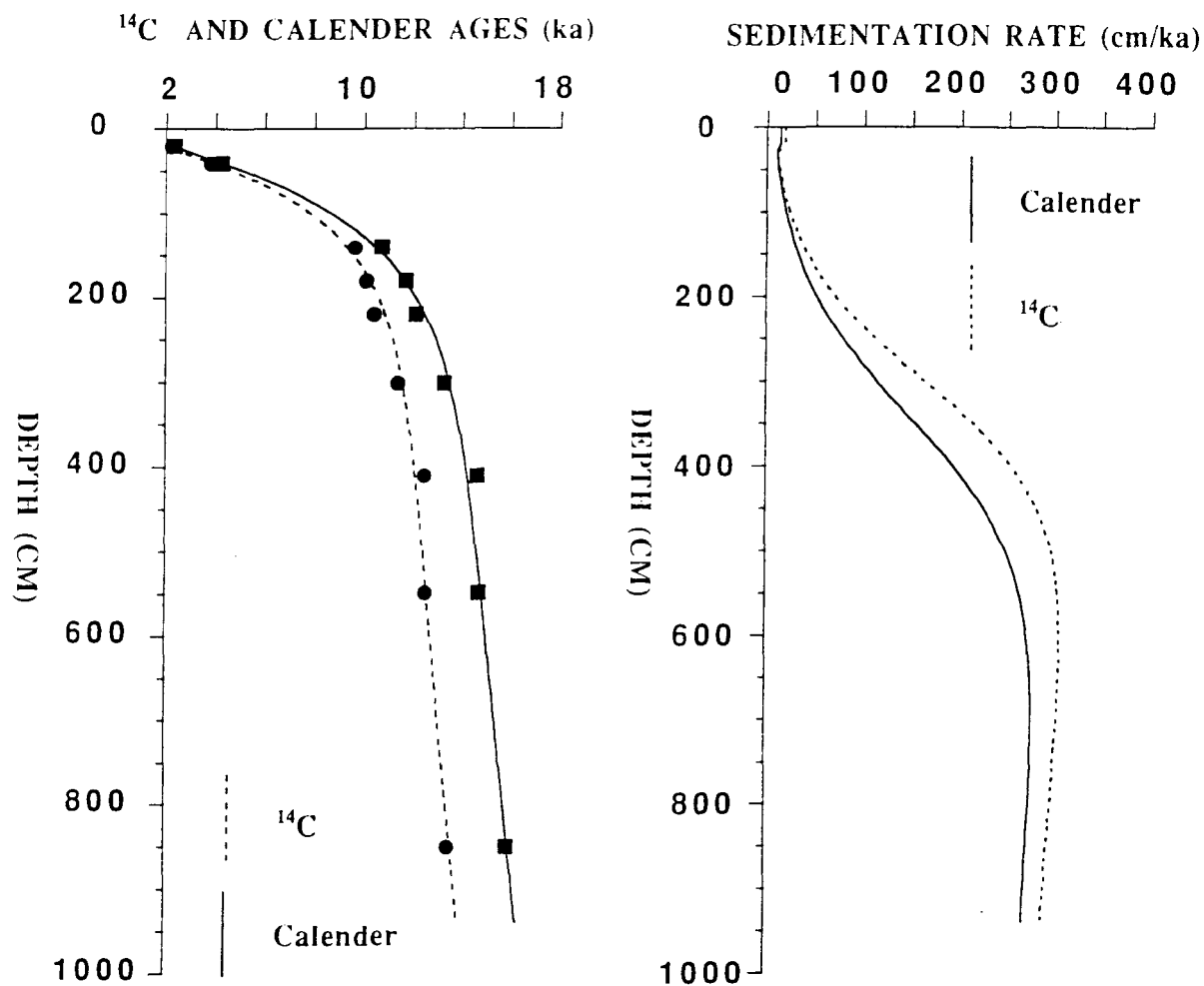


Fig. 3.5. Curve fitting results for ^{14}C and calendar ages (left), and downcore variations in the estimated sedimentation rates based on ^{14}C and calendar ages (right) at site HU-90-031-44 PC.

decomposition have been determined at Sites 44 PC, 43 PC, 17 BC and 29 BC. In addition to these four sites, rates of degradation of organic carbon were determined at sites 41 BC and 45 BC. Results of the exponential fit are presented in chapter 6. Owing to lack of accurate sedimentation rates, the model presented here provides a first order results for the rate of OM degradation.

The adopted multi G-model, classifies or arranges total OM (G_T) into the most to the least metabolizable fractions (G_i), such that:

$$G_T = \sum_{i=0}^n G_i \quad (15)$$

As pointed out previously, each group denoted as G_i is assumed to degrade via first-order kinetics such that

$$\frac{dG_i}{dt} = -k_i G_i \quad (16)$$

Thus,

$$-\frac{dG_T}{dt} = \sum_{i=0}^n k_i G_i \quad (17)$$

where k_i = the first order decay constant for decomposition of metabolizable fraction, and n = the number of individual metabolizable fractions, with boundary conditions of: $G_i = G_0$ at $t = 0$; $G_i = 0$ at $t = \text{infinity}$.

Thus for each individual fraction the time dependency of the inventory of the metabolizable organic fraction is given by the integral of equation 16 under the stated boundary conditions, and the result of integration is:

$$G_{i(t)} = G_{i(0)} [\exp(-k_i t)] \quad (18)$$

From equation 15 the pool of decomposing organic matter is given by:

$$G_T = G_{1(0)} [\exp(-k_1 t_1)] + G_{2(0)} [\exp(-k_2 t_2)] + \dots + G_{NR} \quad (19)$$

Although during curve fitting more than two fractions of reactive material were assumed, utmost three were significant. Thus the final equation obtained is of the form:

$$G_T = G_{1(0)}[\exp(-k_1 t_1)] + G_{2(0)}[\exp(-k_2 t_2)] + G_{3(0)}[\exp(-k_3 t_3)] \quad (20)$$

Since sedimentation rate has been assumed to be constant, time t can be expressed in terms of Z (sediment depth positive down wards) such that $t = Z/SR$, where SR is sedimentation rate. Thus the resulting equation is:

$$G_T = G_{1(0)}[\exp(-\frac{k_1}{SR}Z_1)] + G_{2(0)}[\exp(-\frac{k_2}{SR}Z_2)] + G_{3(0)}[\exp(-\frac{k_3}{SR}Z_3)] \quad (21)$$

Letting $k_i/SR = B_i$, equation 21 can be written as:

$$G_T = G_{1(0)}[\exp(-B_1 Z_1)] + G_{2(0)}[\exp(-B_2 Z_2)] + G_{3(0)}[\exp(-B_3 Z_3)] \quad (22)$$

Sedimentation rate is one of the major limitations of the model presented here. Assumption of a constant sedimentation rate is not easily met in nature. For example, sedimentation rates at site 44 PC are highly variable (more than one order of magnitude). Apart from this, there is a high uncertainty in the determined values of sedimentation rates for the Gulf of St. Lawrence. Another limitation of the model is the steady state conditions, where in nature it is not easily met. Therefore, the model values for first order rate constants (k) of OM decomposition are first order estimates.

CHAPTER 4

4.0. LATERAL VARIATION IN SOURCES OF CARBON AND NITROGEN IN THE LABRADOR SEA AND GULF OF ST. LAWRENCE.

The estimation of marine paleoproductivity using sedimentary organic matter (OM) has been made by many workers (eg. Müller and Suess, 1979; Sarthein et al., 1987, 1988, 1992; Pedersen et al., 1991). The major problem encountered when using OM is the way in which various sources of OM are delineated. Relative contributions of terrestrial OM to the marine environment has been determined from lignin contents (Hedges et al, 1988), C/N ratios (Stevenson and Cheng, 1972; Müller, 1977; Thornton and McManus, 1994), as well as from the stable isotopic compositions of both organic carbon and nitrogen (Peters et al., 1978; Macko, 1983; Cifuentes et al., 1988; Thornton and McManus, 1994). Because one of the objectives of this study is to estimate paleoproductivity in the Labrador Sea and the Gulf of St. Lawrence-Scotia slope, it is important to establish various sources and estimate their relative contributions before any inference on past paleoproductivity based on OM can be made. This chapter presents high resolution geochemical results of the stable isotopic compositions of OC and nitrogen, the content of OC and nitrogen, as well as the C/N ratios, and discusses its implications in relation to the sources and diagenetic changes of OM.

4.1.0. GEOCHEMICAL RESULTS FOR SHORT CORES FROM THE LABRADOR SEA.

4.1.1. Organic Carbon Stable Isotopes

The geochemical results and descriptive statistics for all short cores from the Labrador Sea are presented in appendix 9.2.0, Table 4.1. The range of organic $\delta^{13}\text{C}$ values is small and is within analytical error at sites 05 BC and 93 BC (appendix 9.2.0., Table 4.1; Figs. 4.1 and 4.2). A downcore increase in organic $\delta^{13}\text{C}$ values to the base of the core is observable at site 14 BC (Fig. 4.3). However,

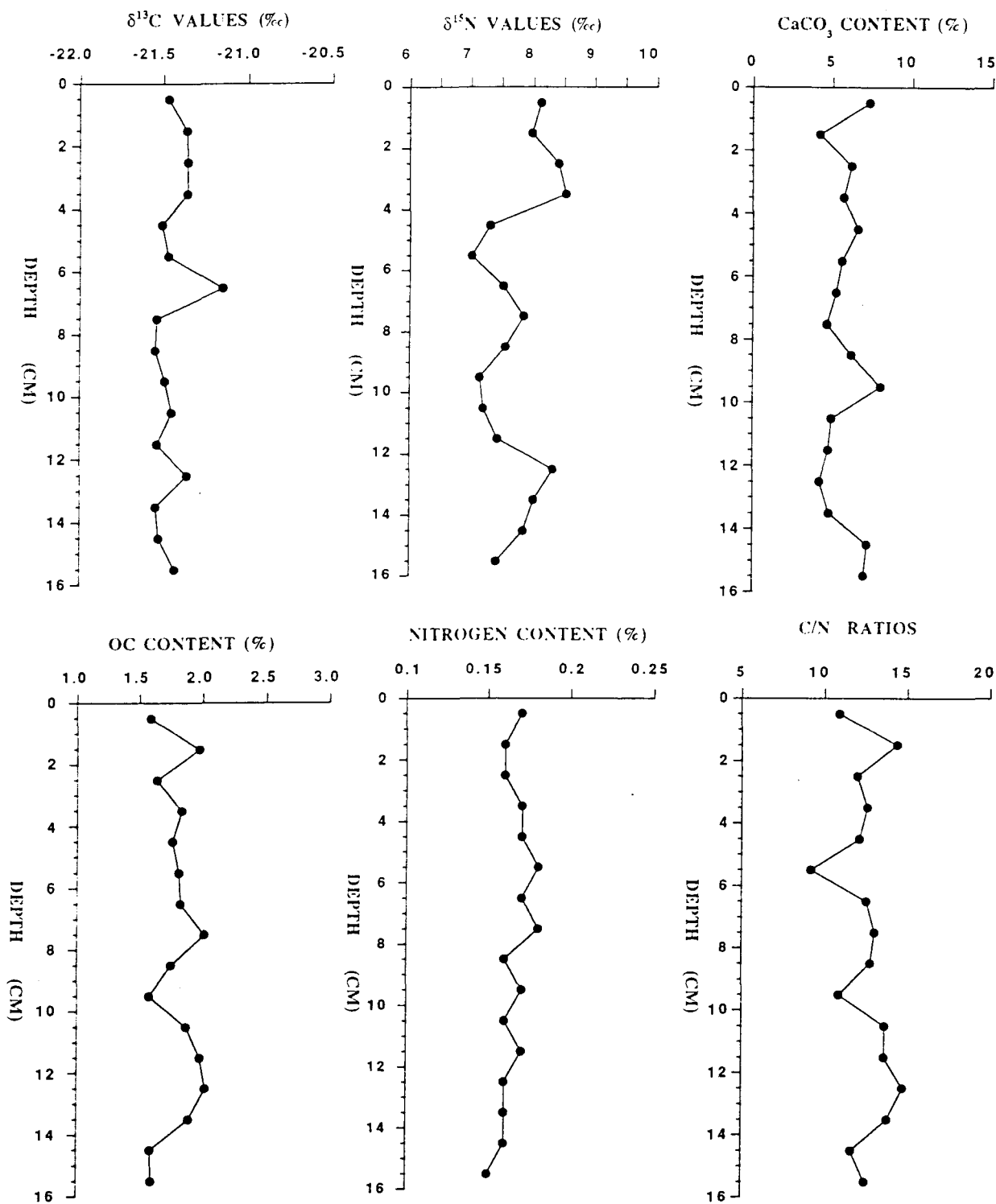


Fig. 4.1. Downcore variation in $\delta^{13}\text{C}$, $\delta^{15}\text{N}$, CaCO_3 , organic carbon, nitrogen and C/N ratios for core

HU-91-045-05 BC.

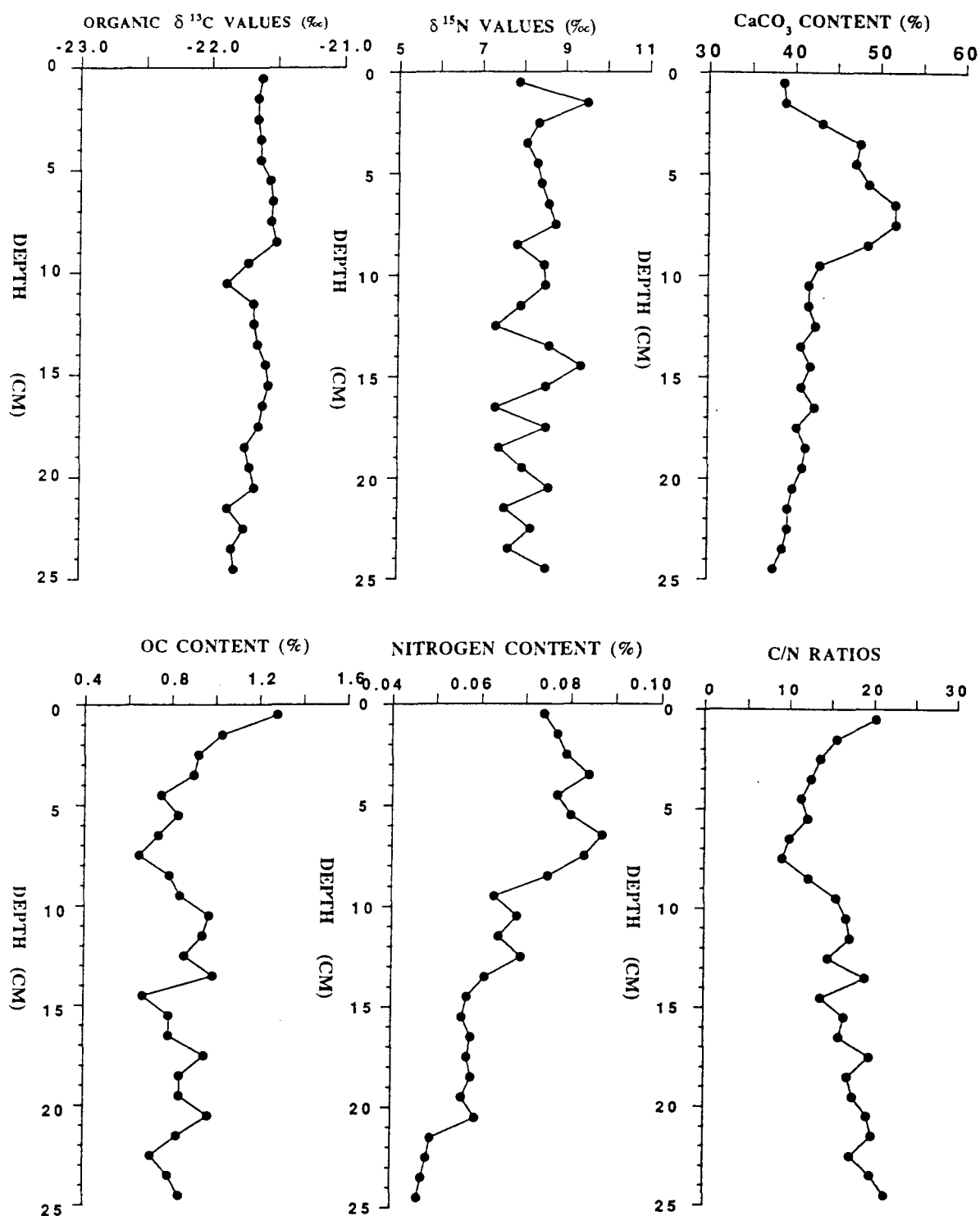


Fig. 4.2. Downcore variation in $\delta^{13}\text{C}$, $\delta^{15}\text{N}$, CaCO_3 , organic carbon, nitrogen and C/N ratios for core HU-91-045-93 BC.

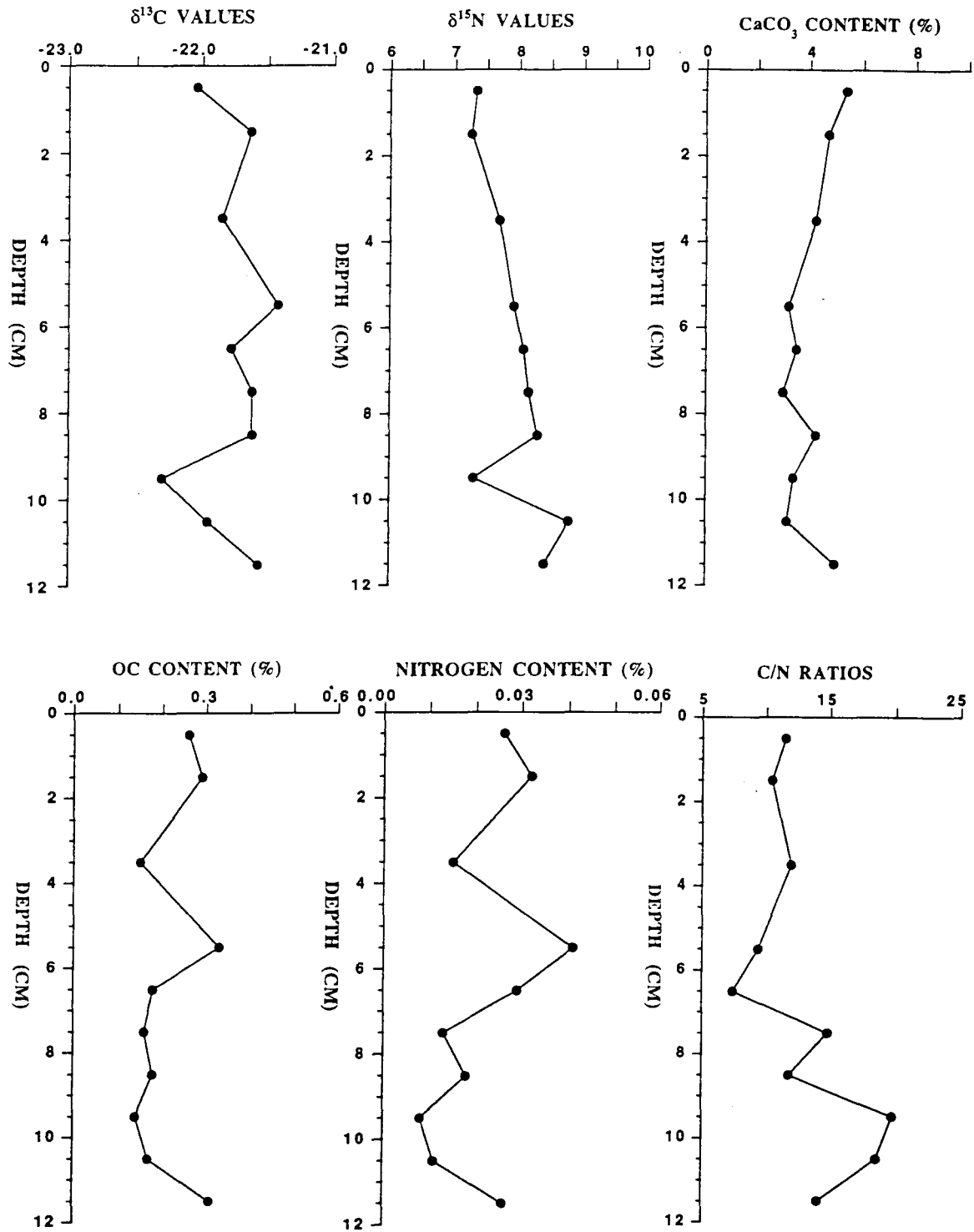


Fig. 4.3. Downcore variation in $\delta^{13}\text{C}$, $\delta^{15}\text{N}$, CaCO_3 , organic carbon, nitrogen and C/N ratios for core HU-91-045-14 BC.

the $\delta^{13}\text{C}$ values at this site (14 BC) are highly variable.

The organic $\delta^{13}\text{C}$ values at sites 16 BC, 18 BC, 23 BC, 38 TWC and 40 LHC show a general downcore decrease to the base of the core (Figs. 4.4, 4.5, 4.6, 4.7 and 4.8). A similar downcore decrease is observable below 4 cm at site 28 BC (Fig. 4.9). The most depleted values at site 28 BC are confined below 23 cm (Fig. 4.9).

The stable isotopic composition of organic carbon for core 11 BC increase slightly (0.4‰) downcore for the upper 10 cm, followed by a systematic decrease of up to 2‰ to about 15 cm (Fig. 4.10). This trend of decreasing ^{13}C with depth is interrupted by a sudden increase in ^{13}C enrichment (of up to 0.6‰) at approximately 10.5 ka (^{14}C age) (Younger Dryas). This is followed by relatively constant values (at around -23‰) down to the base of the core (Fig. 4.10).

4.1.2. Nitrogen Stable Isotopes

The $\delta^{15}\text{N}$ values at site 05 BC increases with depth from the core surface to 4 cm, followed by a decrease, of up to 1‰, to about 6 cm (Fig. 4.1). Below 6 cm, there is an irregular distribution pattern (Fig. 4.1).

With the exception of interruption at a depth of 9.5 cm, the $\delta^{15}\text{N}$ values at site 14 BC increases downcore to the base of the core (Fig. 4.3). A similar downcore distribution in the $\delta^{15}\text{N}$ values is observable at site 28 BC (Fig. 4.9), between 6 and 15 cm at site 18 BC (Fig. 4.5), and in the upper 13 cm at site 38 TWC (Fig. 4.7).

The downcore variations in the $\delta^{15}\text{N}$ values at sites 16 BC, 23 BC and 40 LHC show a general decrease to the base of the core (Fig. 4.4, 4.6 and 4.8). A similar downcore decrease in $\delta^{15}\text{N}$ is observable (i) below 13 cm at site 38 TWC (Fig. 4.7), and (ii) in the upper 6 cm as well as below 15 cm at site 18 BC (Fig. 4.5).

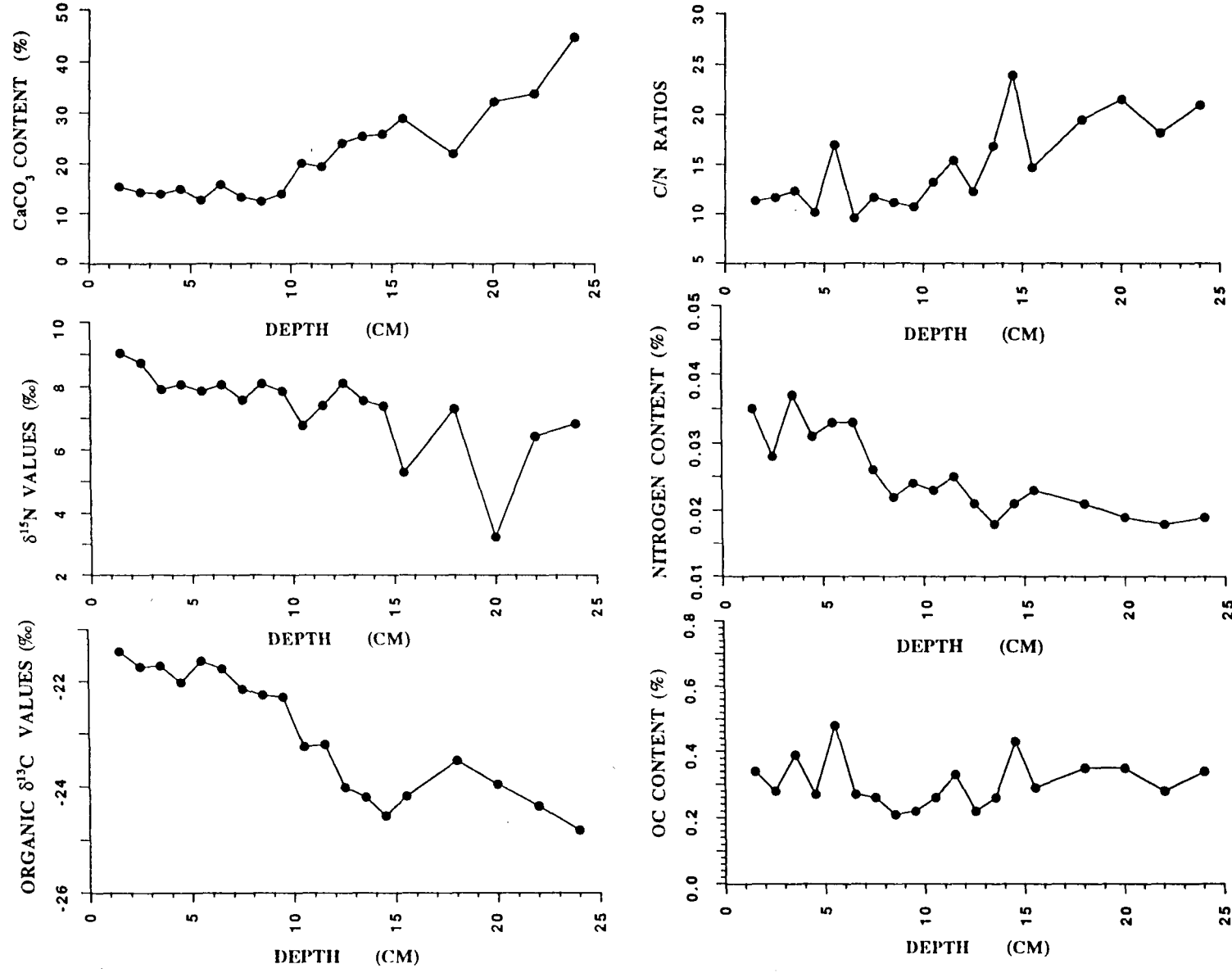


Fig. 4.4. Downcore variation in $\delta^{13}\text{C}$, $\delta^{15}\text{N}$, CaCO_3 , organic carbon, nitrogen and C/N ratios for core

HU-91-045-16 BC.

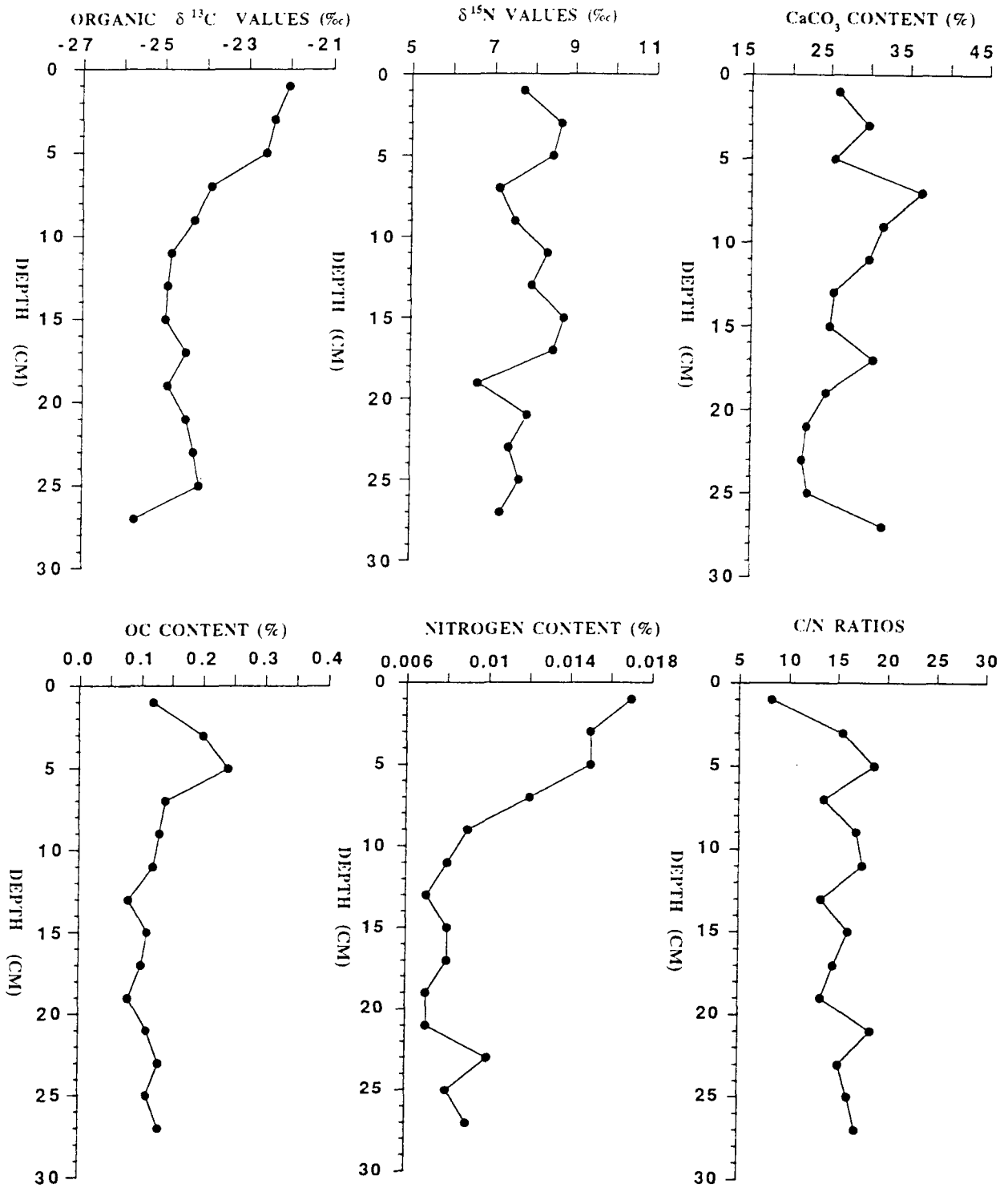


Fig. 4.5. Downcore variation in $\delta^{13}\text{C}$, $\delta^{15}\text{N}$, CaCO_3 , organic carbon, nitrogen and C/N ratios for core

HU-91-045-18 BC.

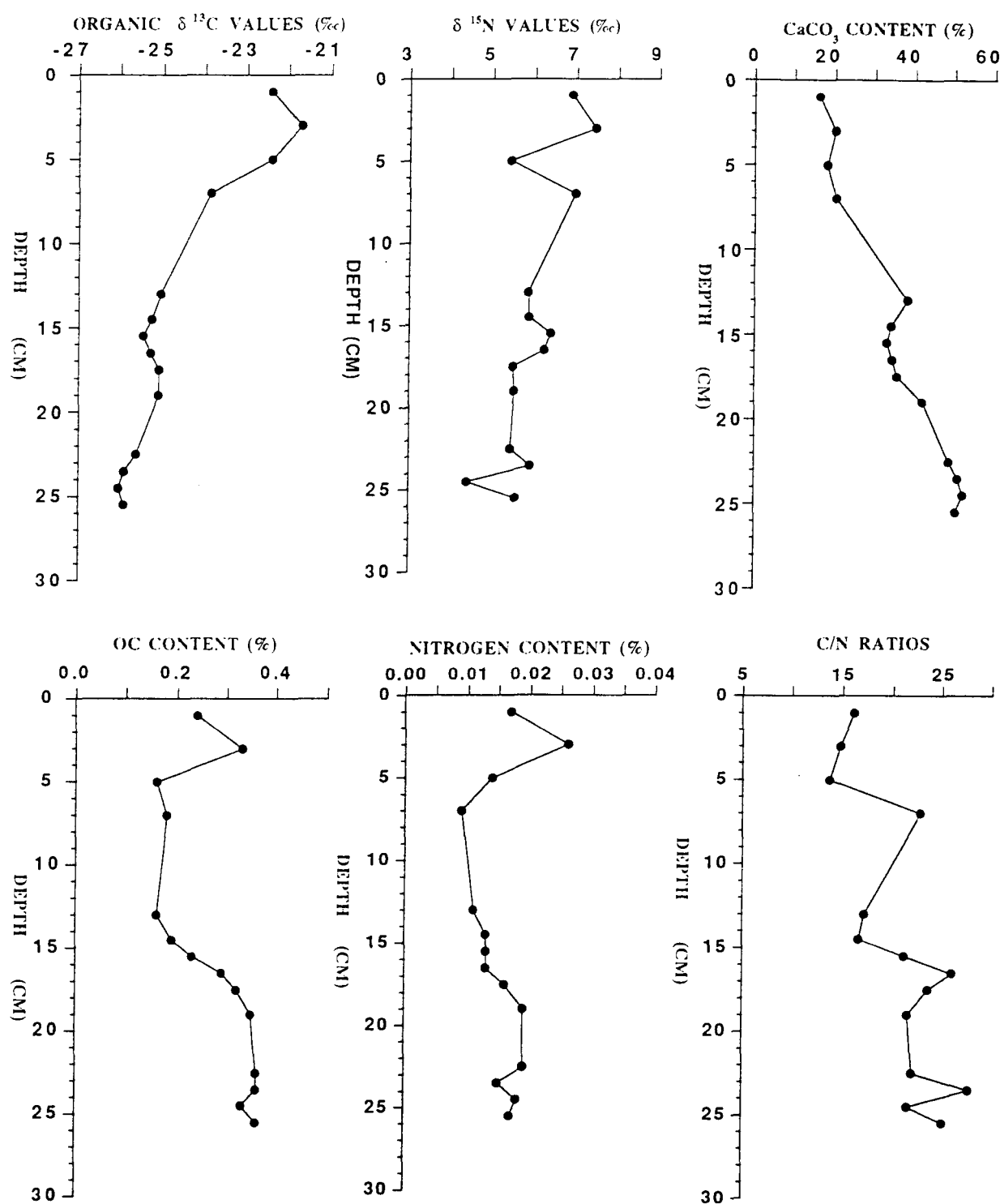


Fig. 4.6. Downcore variation in $\delta^{13}\text{C}$, $\delta^{15}\text{N}$, CaCO_3 , organic carbon, nitrogen and C/N ratios for core HU-91-045-23 BC.

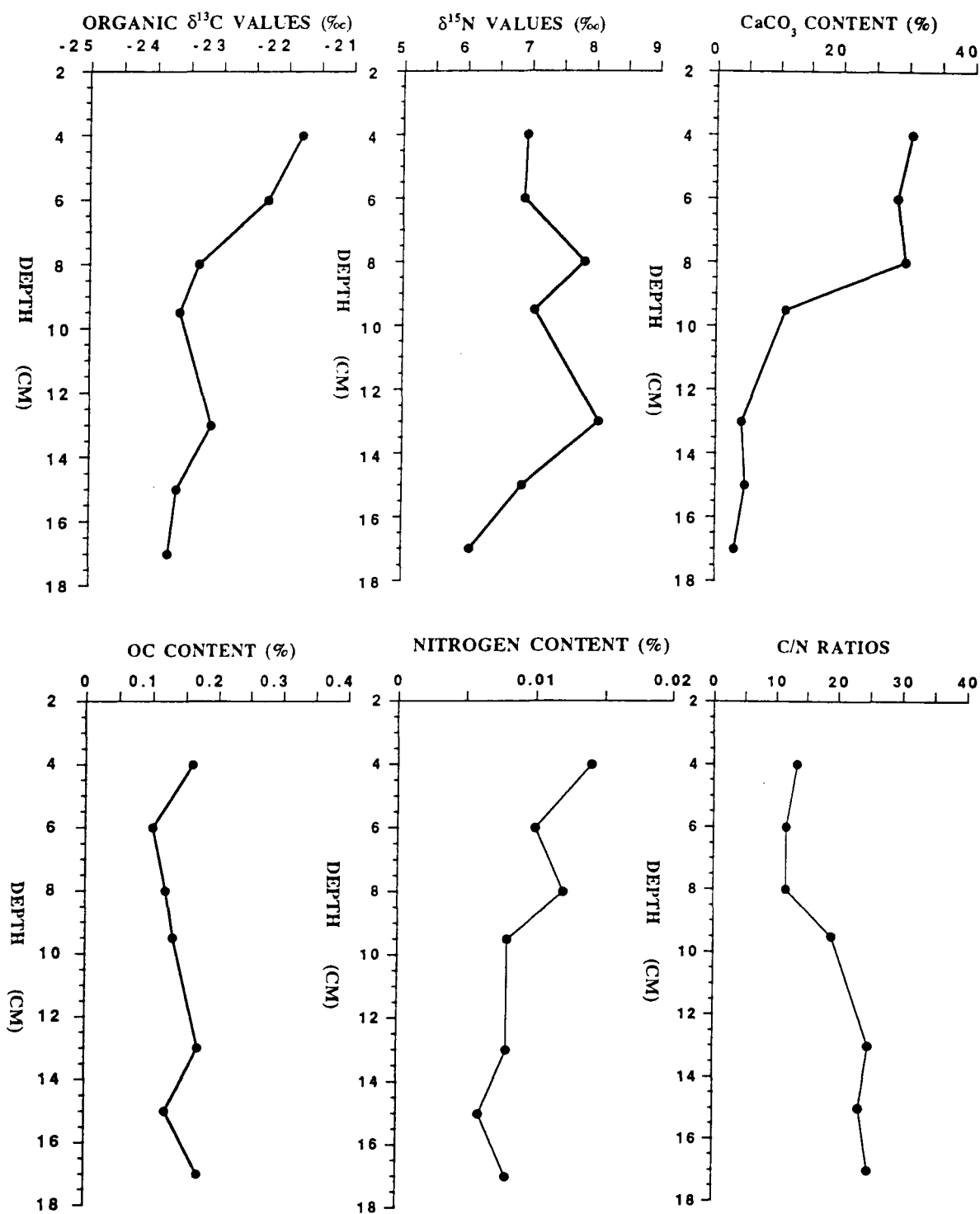


Fig. 4.7. Downcore variation in $\delta^{13}\text{C}$, $\delta^{15}\text{N}$, CaCO_3 , organic carbon, nitrogen and C/N ratios for core

HU-91-045-38 TWC.

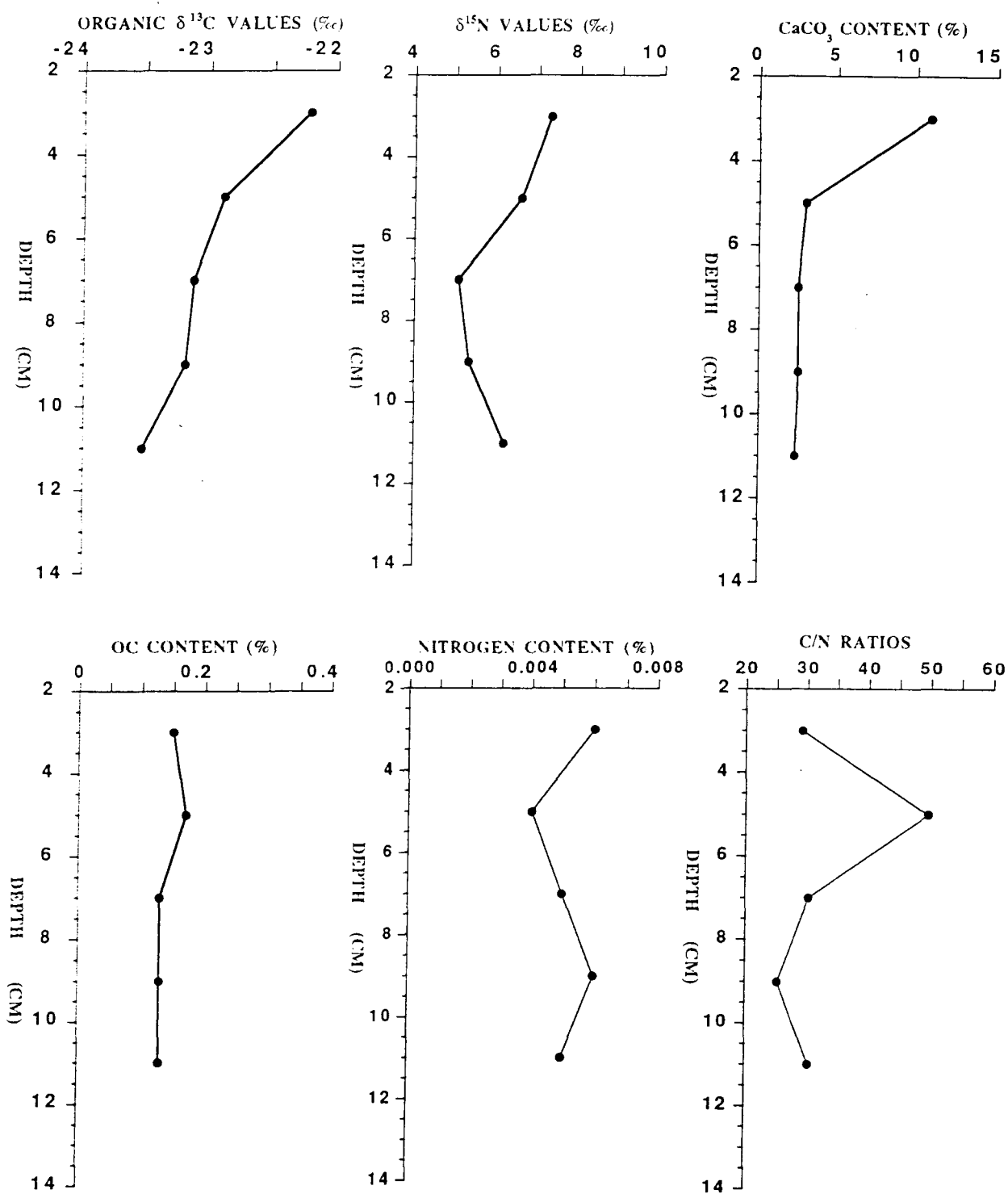


Fig. 4.8. Downcore variation in $\delta^{13}\text{C}$, $\delta^{15}\text{N}$, CaCO_3 , organic carbon, nitrogen and C/N ratios for core HU-91-045-40 LHC.

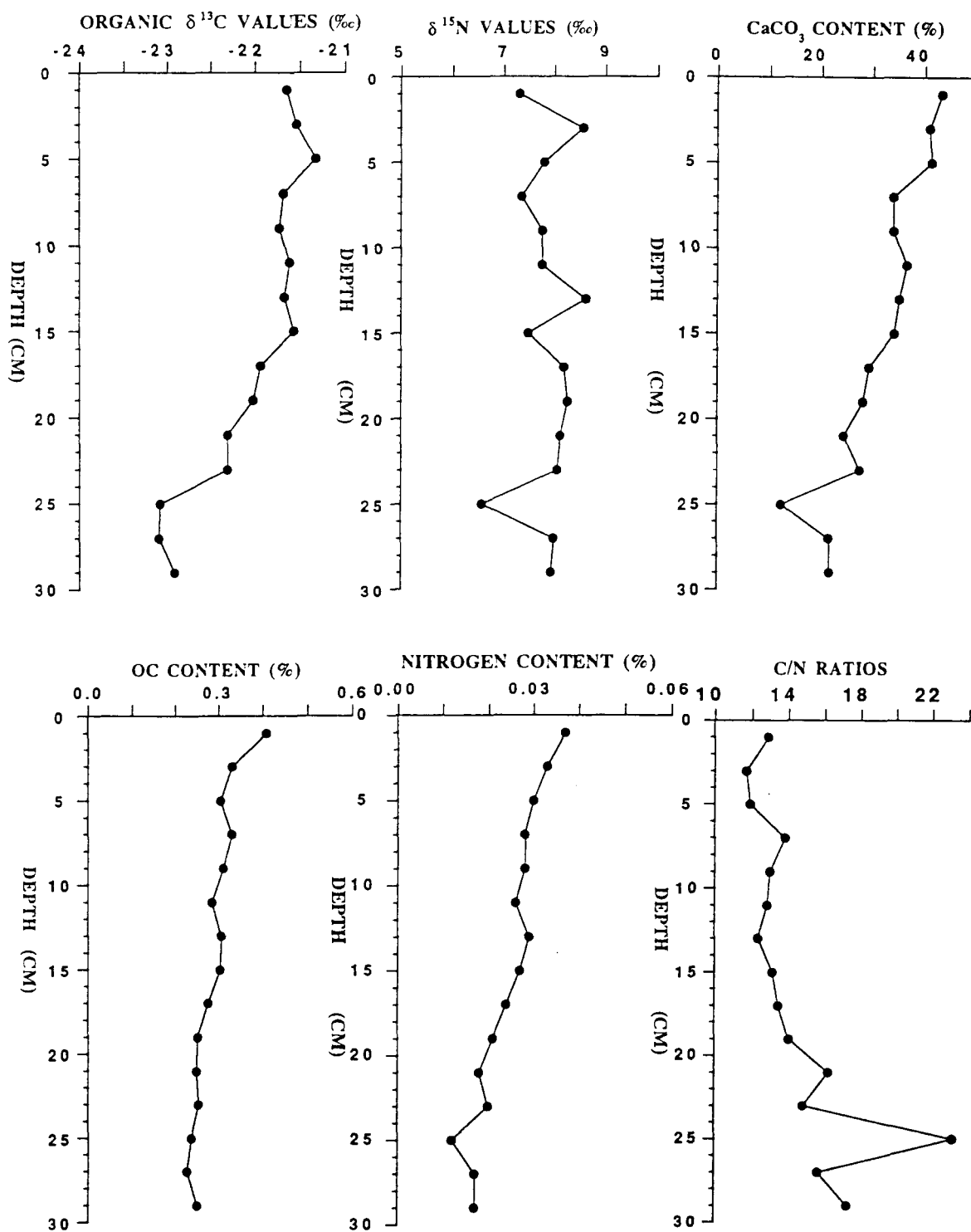


Fig. 4.9. Downcore variation in $\delta^{13}\text{C}$, $\delta^{15}\text{N}$, CaCO_3 , organic carbon, nitrogen and C/N ratios for core

HU-91-045-28 BC.

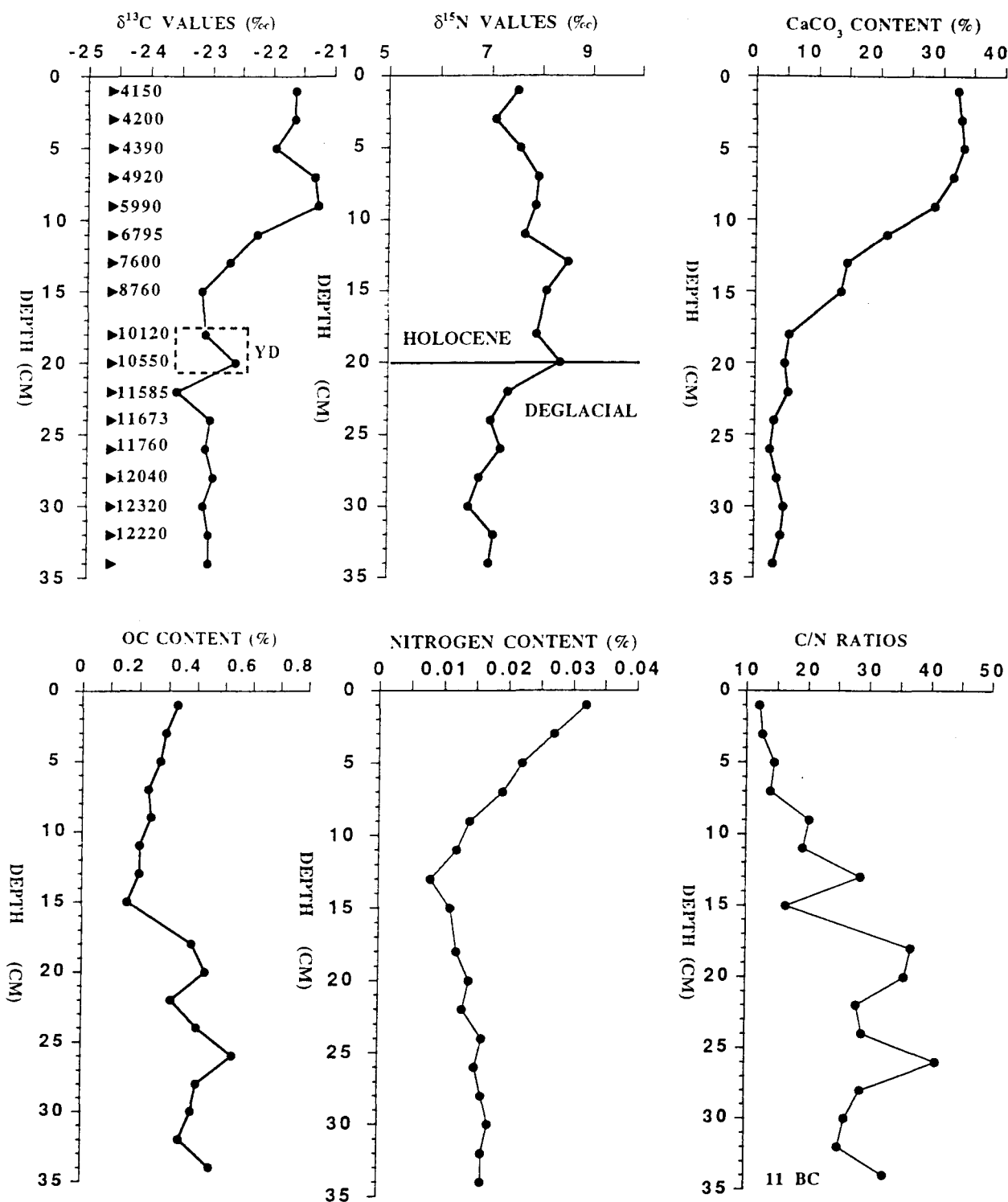


Fig. 4.10. Downcore variation in $\delta^{13}\text{C}$, $\delta^{15}\text{N}$, CaCO_3 , organic carbon, nitrogen and C/N ratios for core HU-90-013-11 BC. Numbers in the $\delta^{13}\text{C}$ plot are ^{14}C ages, while YD is abbreviation for the Younger Dryas.

The $\delta^{15}\text{N}$ values at a dated site 11 BC (Wu and Hillaire-Marcel, 1994) show an enrichment in ^{15}N in the Holocene section than the Late Pleistocene section. There is an increase in $\delta^{15}\text{N}$ values with depth to approximately 13 cm at an ^{14}C AMS age of about 7.5 ka (Fig. 4.10). Below this depth, there is a decrease in $\delta^{15}\text{N}$ values of approximately 0.6‰ through to the base of the core (Fig. 4.10).

4.1.3. Organic Carbon Content

The organic carbon content at site 11 BC is lower in the Holocene period compared to that of the late Pleistocene period (Fig. 4.10). Excluding site 05 BC, the content of organic carbon for all sites is less than 1% (appendix 9.2.0., Table 4.1). Apart from low organic carbon content in the Labrador Sea, the organic carbon content at sites 14 BC, 38 LHC and 28 BC show a general decrease with depth to the base of the core (Figs. 4.3, 4.7, and 4.8). A similar downcore decrease in the organic carbon is observable (i) in the upper 8 cm at site 93 BC (Fig. 4.2), (ii) below 5 cm at site 18 BC (Fig. 4.5), and (iii) in the upper 15 cm at site 11 BC (Fig. 4.10).

A slight downcore increase in organic carbon content to the base of the core is observable at sites 05 BC, 23 BC and 38 TWC (Figs. 4.1, 4.6, and 4.7). A similar downcore increases in the organic carbon is observable (i) below 7 cm at site 16 BC (Fig. 4.4), and (ii) in the upper 5 cm at site 18 BC (Fig. 4.5). The organic carbon content at site 16 BC is highly variable. Other downcore increases in the organic carbon contents are observable bellow 8 cm at site 93 BC (Fig. 4.2)

4.1.4. Nitrogen Content

The nitrogen content is low for all sites, and only slightly high values occur at site 05 BC (appendix 9.2.0., Table 4.1). The nitrogen content observed at site 05 BC is similar to that of 0.13 reported by Vilks et al. (1974) for a core recovered from the same area. Apart from low contents, a downcore decrease in the nitrogen content to the base of the core is observable at sites 14 BC, 16

BC, 18 BC, 28 BC and 38 TWC (Figs. 4.3, 4.4, 4.5, 4.7 and 4.9). A similar downcore decrease in the contents of nitrogen is observable (i) below 8 cm at site 93 BC (Fig. 4.2), (ii) in the upper 5 cm at site 23 BC (Fig. 4.6), and (iii) in the upper 13 cm at site 11 BC (Fig. 4.10).

A downcore increase in the nitrogen content is observable (i) in the upper 8 cm at site 93 BC (Fig. 4.2), (ii) below 5 cm at site 23 BC (Fig. 4.6), and (iii) below 13 cm at site 11 BC (Fig. 4.10). Contrary to the downcore increase, downcore distribution of nitrogen content at sites 05 BC and 40 LHC is relatively invariant (Figs. 4.1 and 4.8).

4.1.5. Calcium Carbonate Content

The CaCO_3 content is low during the glacial period at a well-dated core (11 BC). Downcore variation of CaCO_3 show a general increase to the base of the core at sites 16 BC and 23 BC (Figs. 4.4 and 4.6). Other downcore increases in the CaCO_3 are observable in the upper (i) 8 cm at site 93 BC (Fig. 4.2), and (ii) 10 cm at site 18 BC (Fig. 4.5).

The CaCO_3 content shows a downcore decrease to the base of the core at sites 38 TWC, 28 BC, and 11 BC (Figs. 4.7, 4.9 and 4.10). A similar downcore decrease in the contents of CaCO_3 is observable (i) below 8 cm at site 93 BC (Fig. 4.2), (ii) in the upper 6 cm at site 14 BC (Fig. 4.3), and (iii) below 10 cm at site 18 BC (Fig. 4.5).

With the exception of the uppermost point for core 40 LHC, the percent CaCO_3 content at this site as well as at site 05 BC is relatively invariant with depth (Figs. 4.1, and 4.8). A similar invariant values are observable below 6 cm at site 14 BC (Fig. 4.3).

4.1.6. C/N Ratios

Generally, the values of C/N ratio are greater than 10 at all sites (appendix 9.2.0., Table 4.1). The highest C/N ratios are observable at site 40 LHC (appendix 9.2.0., Table 4.1). There is a general

downcore increase in the C/N ratios at sites 05 BC, 14 BC, 16 BC, 18 BC, 23 BC, 38 TWC, 28 BC, and 11 BC (Figs. 4.1, 4.3, 4.4, 4.5, 4.6, 4.7, 4.9, and 4.10). The C/N ratios at site 93 BC shows a general downcore decrease to about 8 cm, followed by an increase to the base of the core (Fig. 4.2). At site 40 LHC, the C/N ratios are relatively invariant with depth (Fig. 4.8).

4.2.0. GEOCHEMICAL RESULTS FOR SHORT CORES FROM THE GULF OF ST. LAWRENCE

4.3.1. Organic Carbon Stable Isotopes

The range of the isotopic compositions of organic carbon for sedimentary OM recovered from the Gulf of St. Lawrence is either close to or within the analytical error (appendix 9.2.0, Table 4.2). Apart from a small range, the organic $\delta^{13}\text{C}$ values at site 45 BC shows a slight downcore increase to the base of the core (Fig. 4.11). A similar downcore distribution of organic $\delta^{13}\text{C}$ values is observable in the upper (i) 10 cm at site 29 BC (Fig. 4.12), (ii) 8 cm at site 34 BC (Fig. 4.13), (iii) 15 cm at site 41 BC, (Fig. 4.14), and (iv) 20 cm at site 59 BC (Fig. 4.15). Furthermore, there is a slight downcore enrichment in ^{13}C between (i) 6 cm and 15 cm at site 17 BC (Fig. 4.16), and (ii) 5 cm and 8 cm at site 43 PC (Fig. 4.17).

A downcore decrease in the organic $\delta^{13}\text{C}$ values is observable (i) below 15 cm at site 41 BC (Fig. 4.14), (ii) below 20 cm at site 59 BC (Fig. 4.15), and (iii) in the upper 8 cm at site 13 BC (Fig. 4.18). The organic $\delta^{13}\text{C}$ values show a slight downcore decrease (i) of about 0.3‰ in the upper 6 cm, as well as below 15 cm at site 17 BC (Fig. 4.16), and (ii) of about 0.5‰ in the upper 5 cm as well as below 8 cm at site 43 PC (Fig. 4.17).

A downcore distribution of the organic $\delta^{13}\text{C}$ is similar to that of the redox potential at sites 13 BC (Fig. 3.4) and 17 BC (Fig. 3.4). Furthermore, the $\delta^{13}\text{C}$ and $\delta^{15}\text{N}$ values are the lowest at site 34 BC relative to other sites.

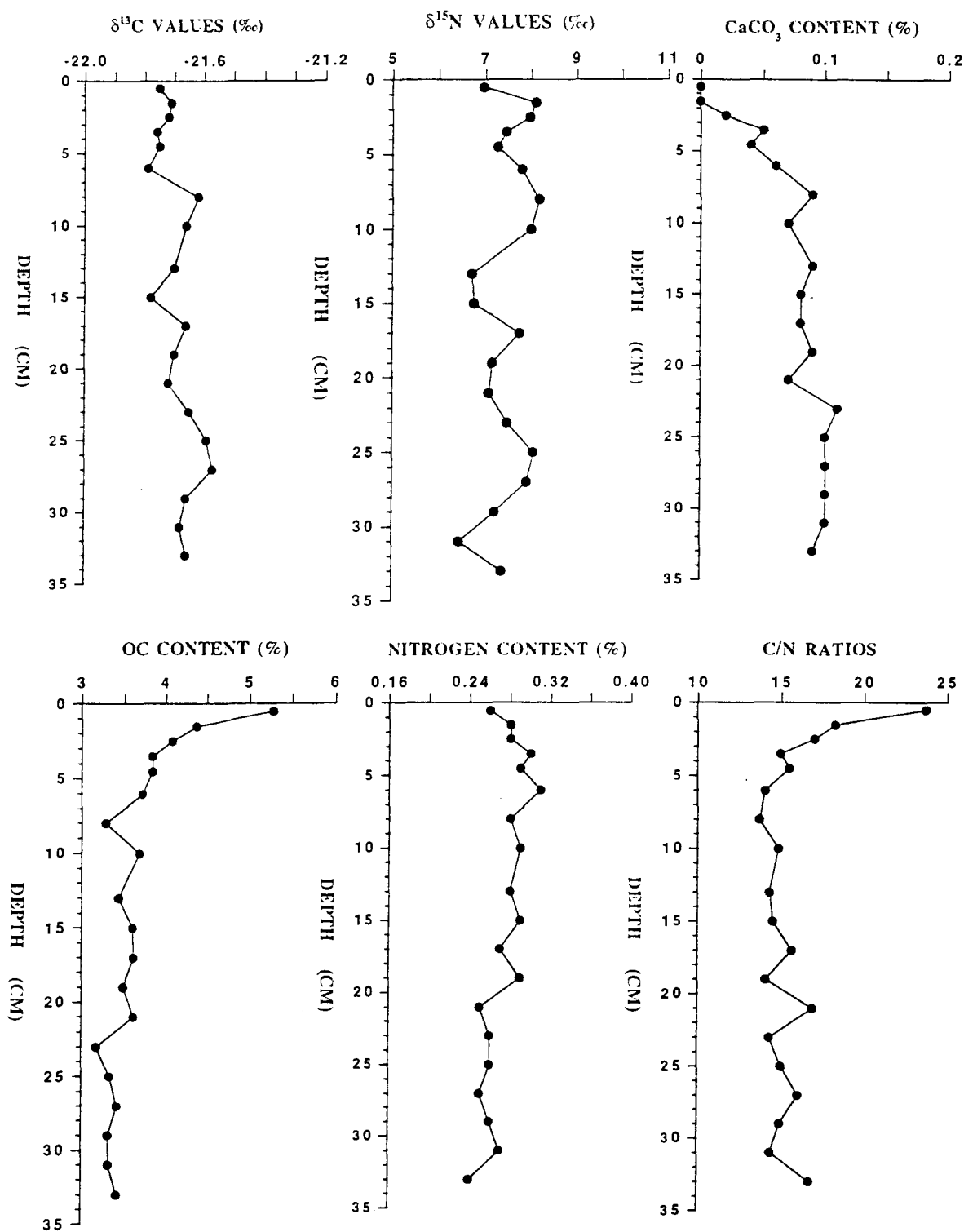


Fig. 4.11. Downcore variation in $\delta^{13}\text{C}$, $\delta^{15}\text{N}$, CaCO_3 , organic carbon, nitrogen and C/N ratios for core

HU-90-031-45 BC.

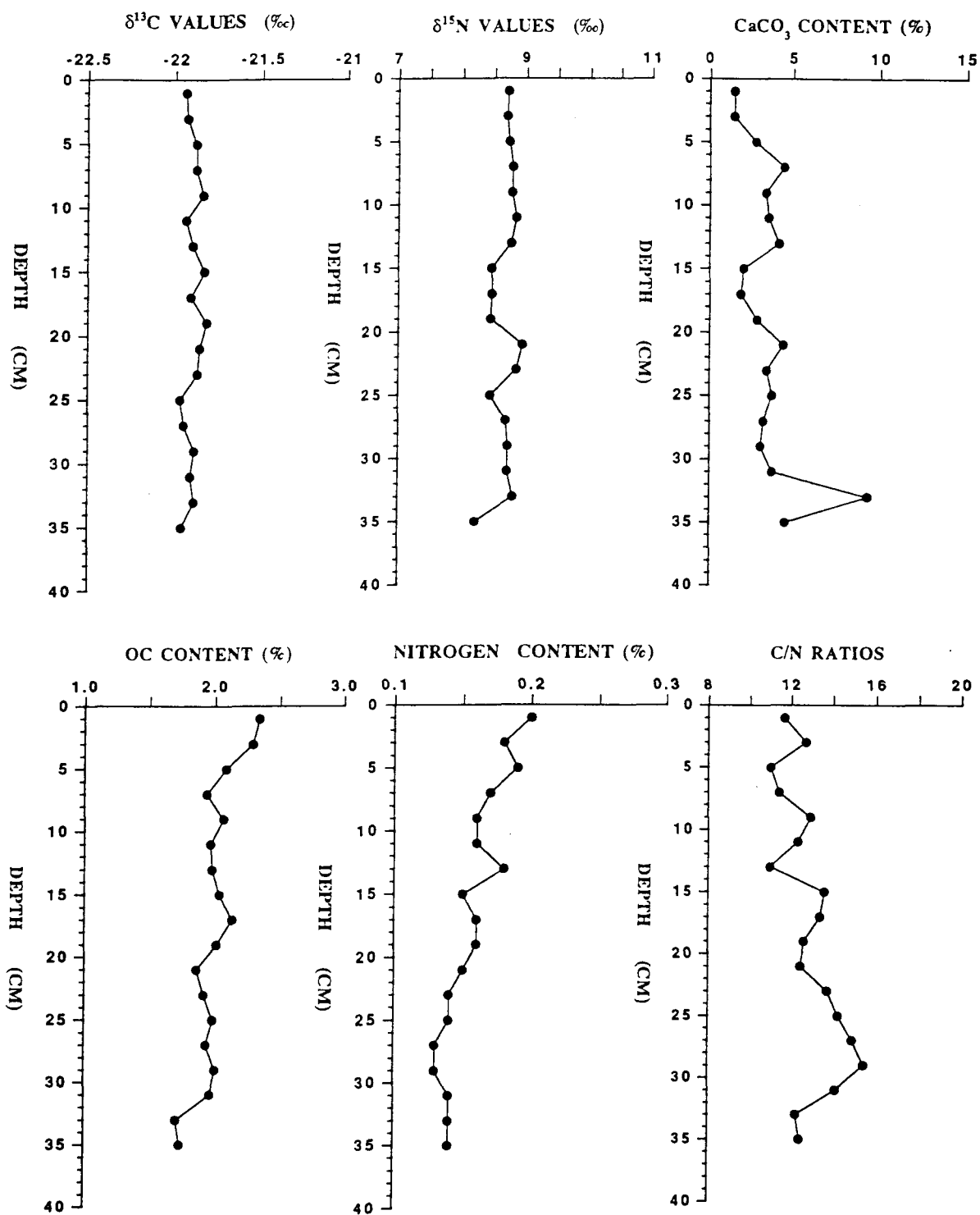


Fig. 4.12. Downcore variation in $\delta^{13}\text{C}$, $\delta^{15}\text{N}$, CaCO_3 , organic carbon, nitrogen and C/N ratios for core

HU-90-031-29 BC.

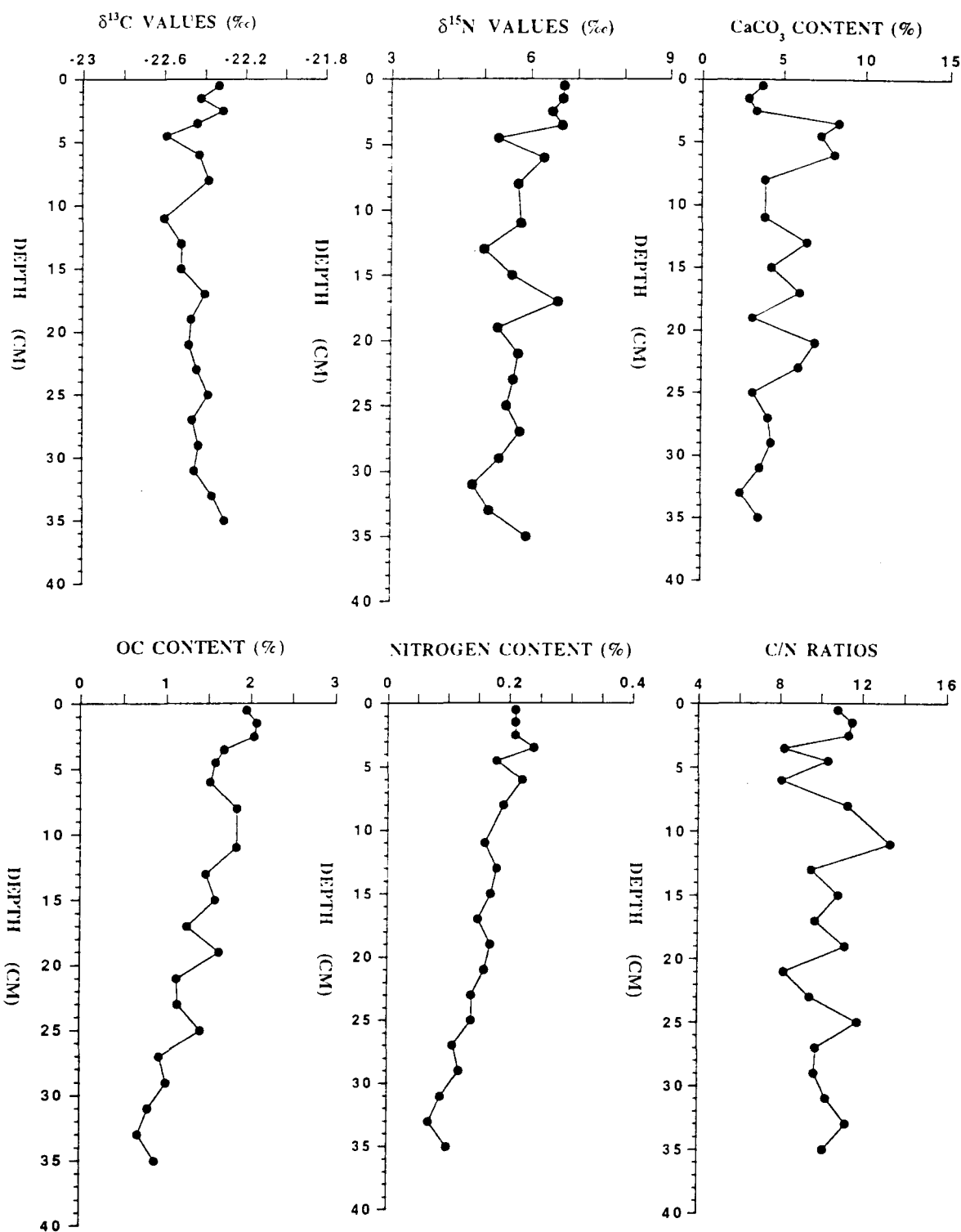


Fig. 4.13. Downcore variation in $\delta^{13}\text{C}$, $\delta^{15}\text{N}$, CaCO_3 , organic carbon, nitrogen and C/N ratios for core

HU-90-031-34 BC.

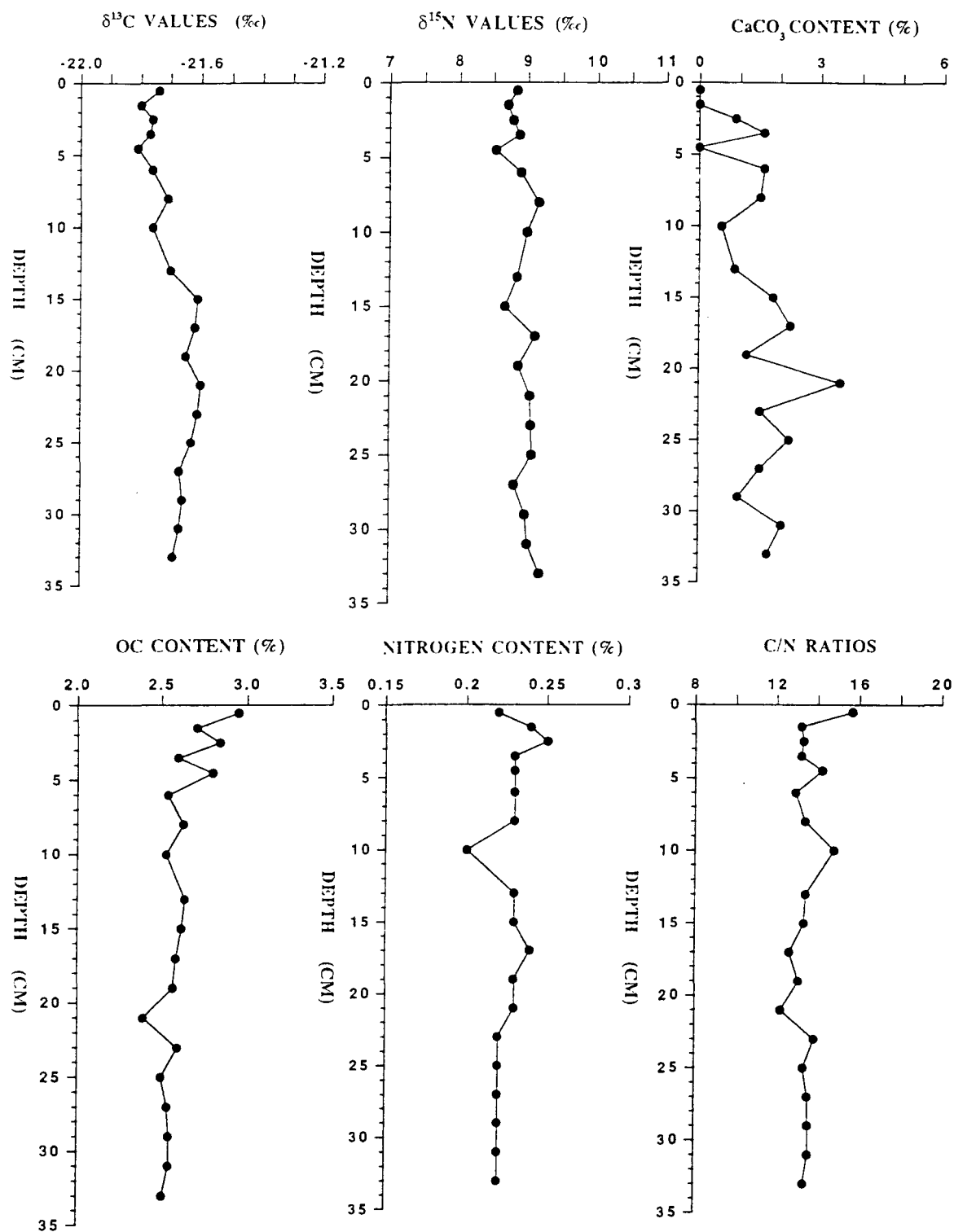


Fig. 4.14. Downcore variation in $\delta^{13}\text{C}$, $\delta^{15}\text{N}$, CaCO_3 , organic carbon, nitrogen and C/N ratios for core

HU-90-031-41 BC.

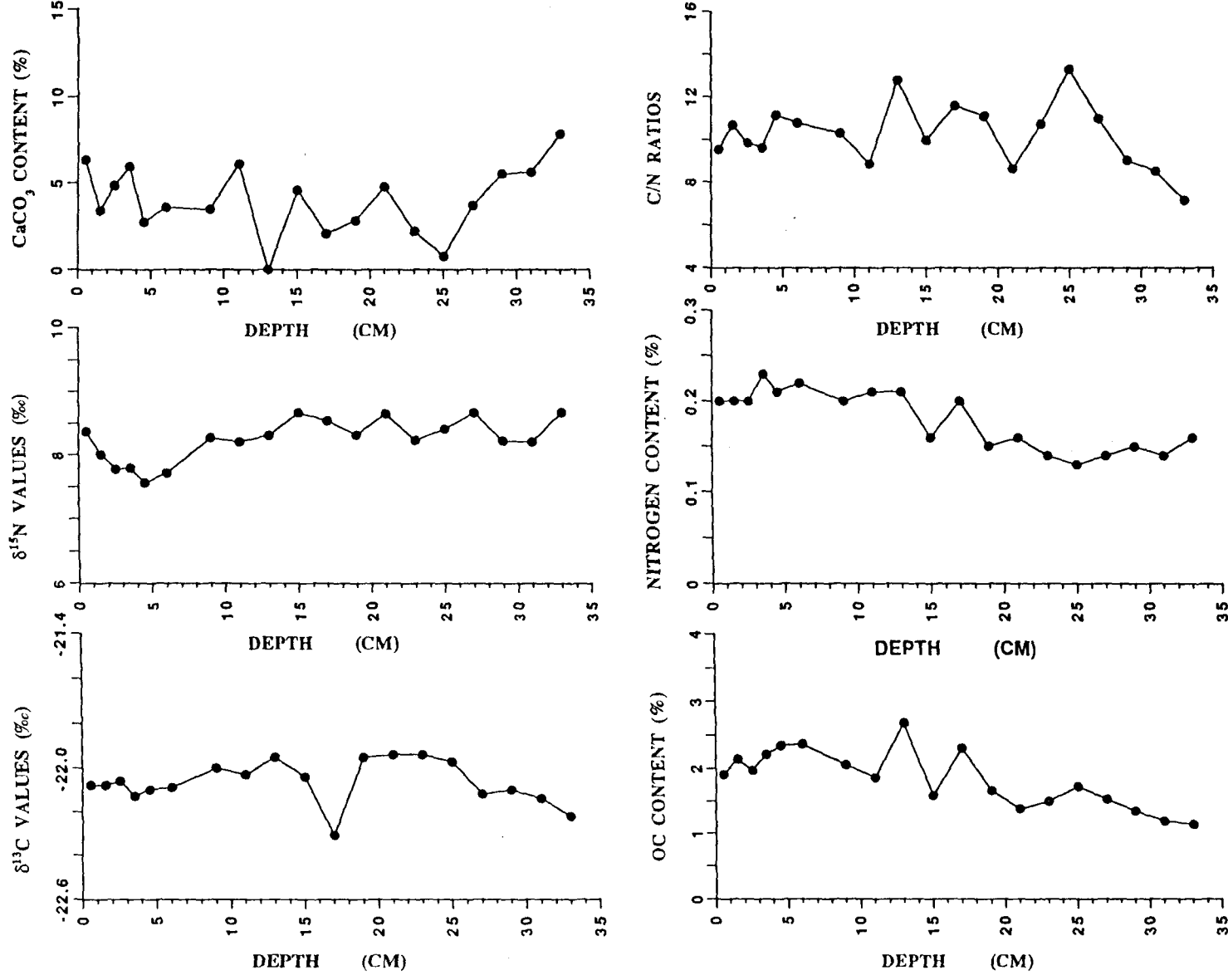


Fig. 4.15. Downcore variation in $\delta^{13}\text{C}$, $\delta^{15}\text{N}$, CaCO_3 , organic carbon, nitrogen and C/N ratios for core

HU-90-031-59 BC.

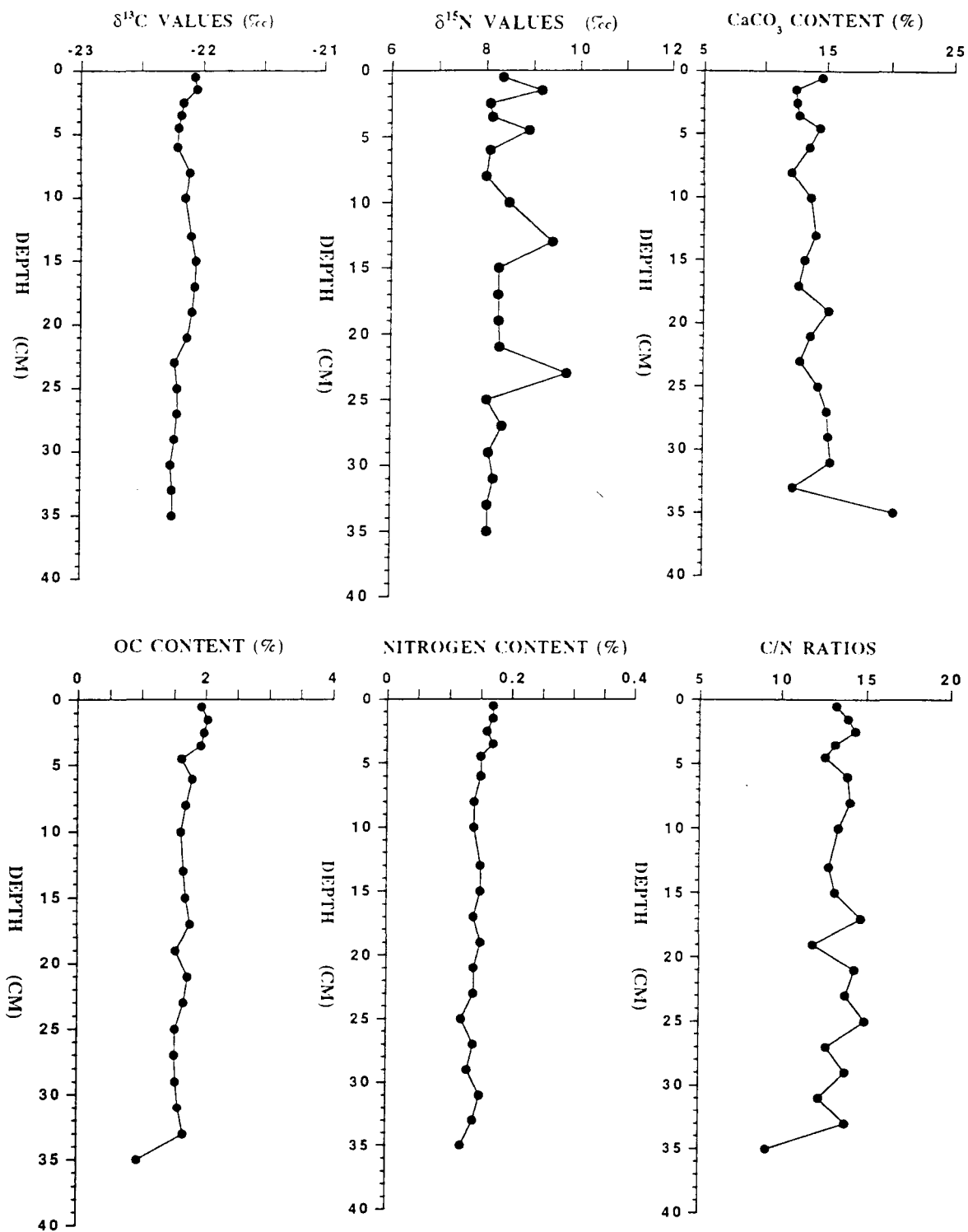


Fig. 4.16. Downcore variation in $\delta^{13}\text{C}$, $\delta^{15}\text{N}$, CaCO_3 , organic carbon, nitrogen and C/N ratios for core

HU-90-031-17 BC.

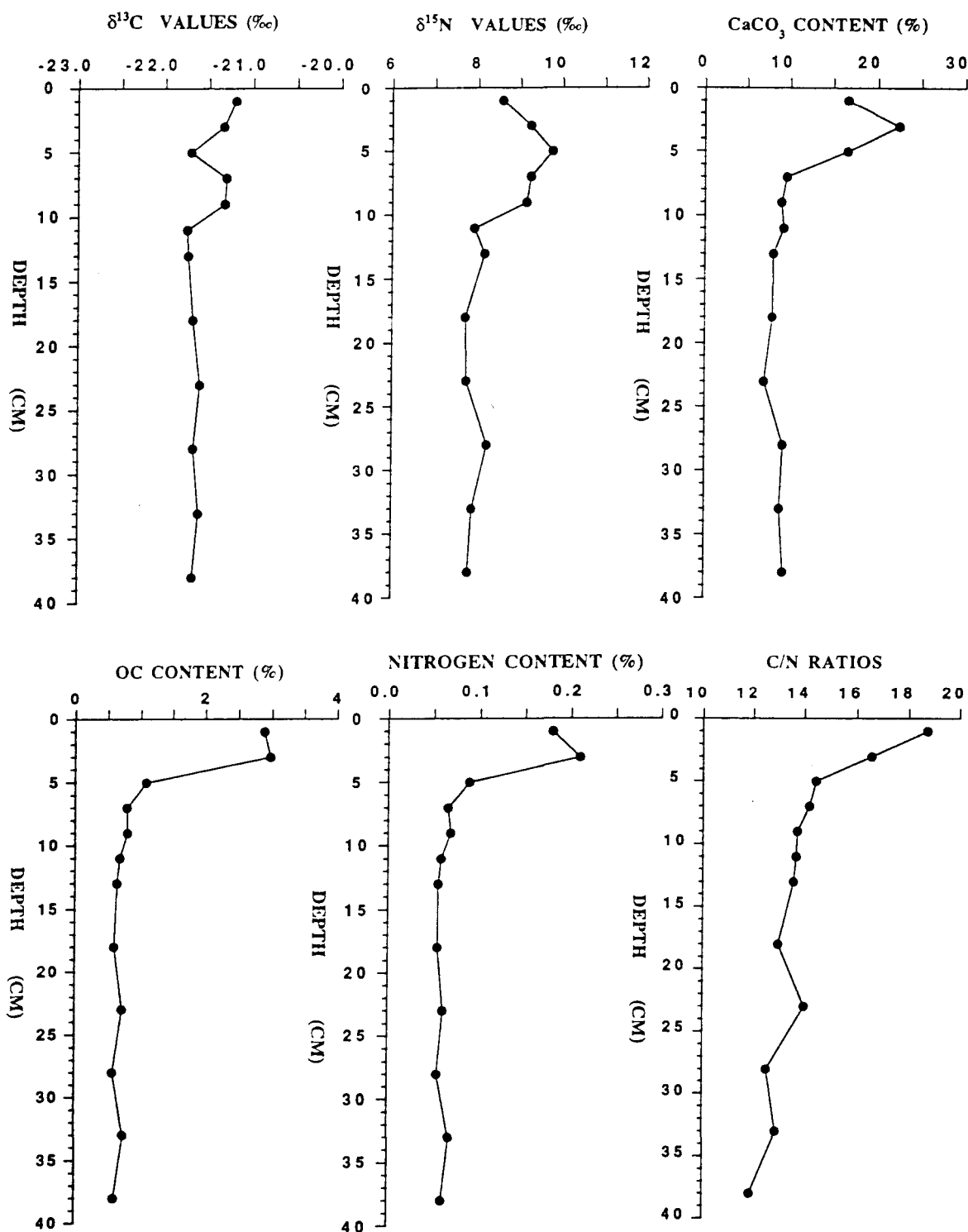


Fig. 4.17. Downcore variation in $\delta^{13}\text{C}$, $\delta^{15}\text{N}$, CaCO_3 , organic carbon, nitrogen and C/N ratios for core

HU-90-031-43 PC.

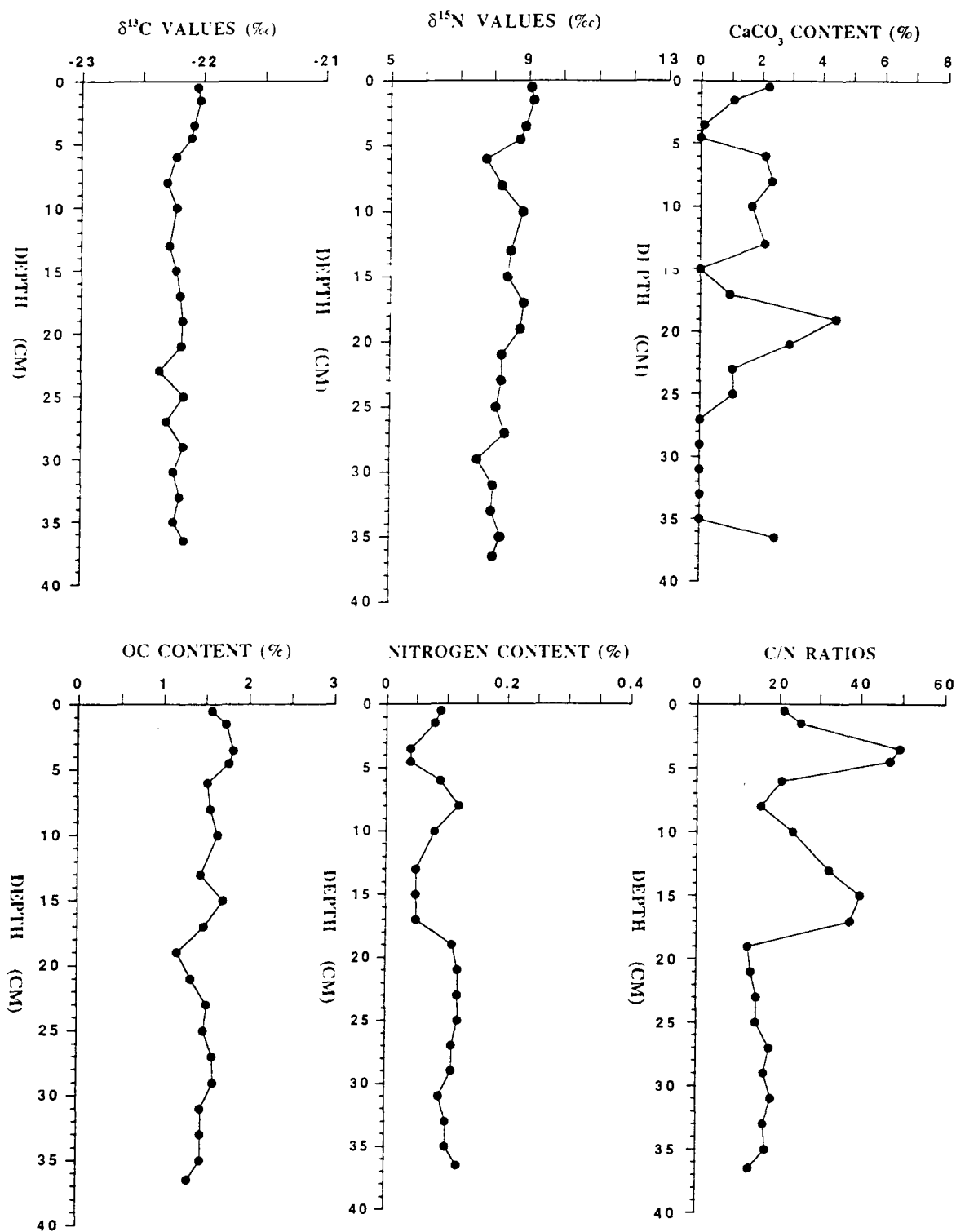


Fig. 4.18. Downcore variation in $\delta^{13}\text{C}$, $\delta^{15}\text{N}$, CaCO_3 , organic carbon, nitrogen and C/N ratios for core

HU-90-031-13 BC.

The organic $\delta^{13}\text{C}$ values at site 06 BC shows a nearly constant downcore variation (Fig. 4.19). A similar downcore distribution of organic $\delta^{13}\text{C}$ values is observable (i) below 10 cm at site 29 BC (Fig. 4.12), (ii) in the upper 8 cm at site 34 BC (Fig. 4.13), and (iii) below 8 cm at site 13 BC (Fig. 4.18).

4.2.2. Nitrogen Stable Isotopes

Excluding core 34 BC, the $\delta^{15}\text{N}$ values for sedimentary OM from the Gulf of St. Lawrence-Scotia slope are higher than 8‰ (appendix 9.2.0., Table 4.2). The $\delta^{15}\text{N}$ values shows a general downcore decrease to the base of the core at site 13 BC (Fig. 4.18). A similar downcore trend is observable (i) in the upper 13 cm as well as below 18 cm at site 34 BC (Fig. 4.13), and (ii) in the upper 5 cm at site 59 BC (Fig. 4.15). Other downcore decreases in $\delta^{15}\text{N}$ values are observable between (i) 5 cm and 18 cm at site 43 PC (Fig. 4.17), and (ii) 4 cm and 11 cm at site 06 BC (Fig. 4.19).

The $\delta^{15}\text{N}$ values shows a downcore increases to the base of the core at site 41 BC (Fig. 4.14). A similar downcore increases is observable (i) between 13 cm and 18 cm at site 34 BC (Fig. 4.13), (ii) below 5 cm at site 59 BC (Fig. 4.15), (iii) in the upper 5 cm at site 43 PC (Fig. 4.17), and (iv) in the upper 4 cm at site 06 BC (Fig. 4.19). The $\delta^{15}\text{N}$ values below 4 cm at site 06 BC, shows a two steps increases with a break at about 16 cm (Fig. 4.19).

The nitrogen stable isotope values for sedimentary OM from the Gulf of St-Lawrence-Scotia slope are invariant downcore at sites 45 BC, 29 BC and 17 BC (Figs. 4.11, 4.12 and 4.16). A similar downcore distribution of $\delta^{15}\text{N}$ values is observable below 18 cm at site 43 PC (Fig. 4.17).

4.2.3. Organic Carbon Content.

The organic carbon content shows a general downcore decrease to the based of the core at sites 29 BC, 41 BC and 17 BC (Figs 4.12, 4.14 and 4.16). A similar downcore distribution of organic carbon is observable (i) in the upper 10 cm at site 45 BC (Fig. 4.11), (ii) below 5 cm at site 59 BC

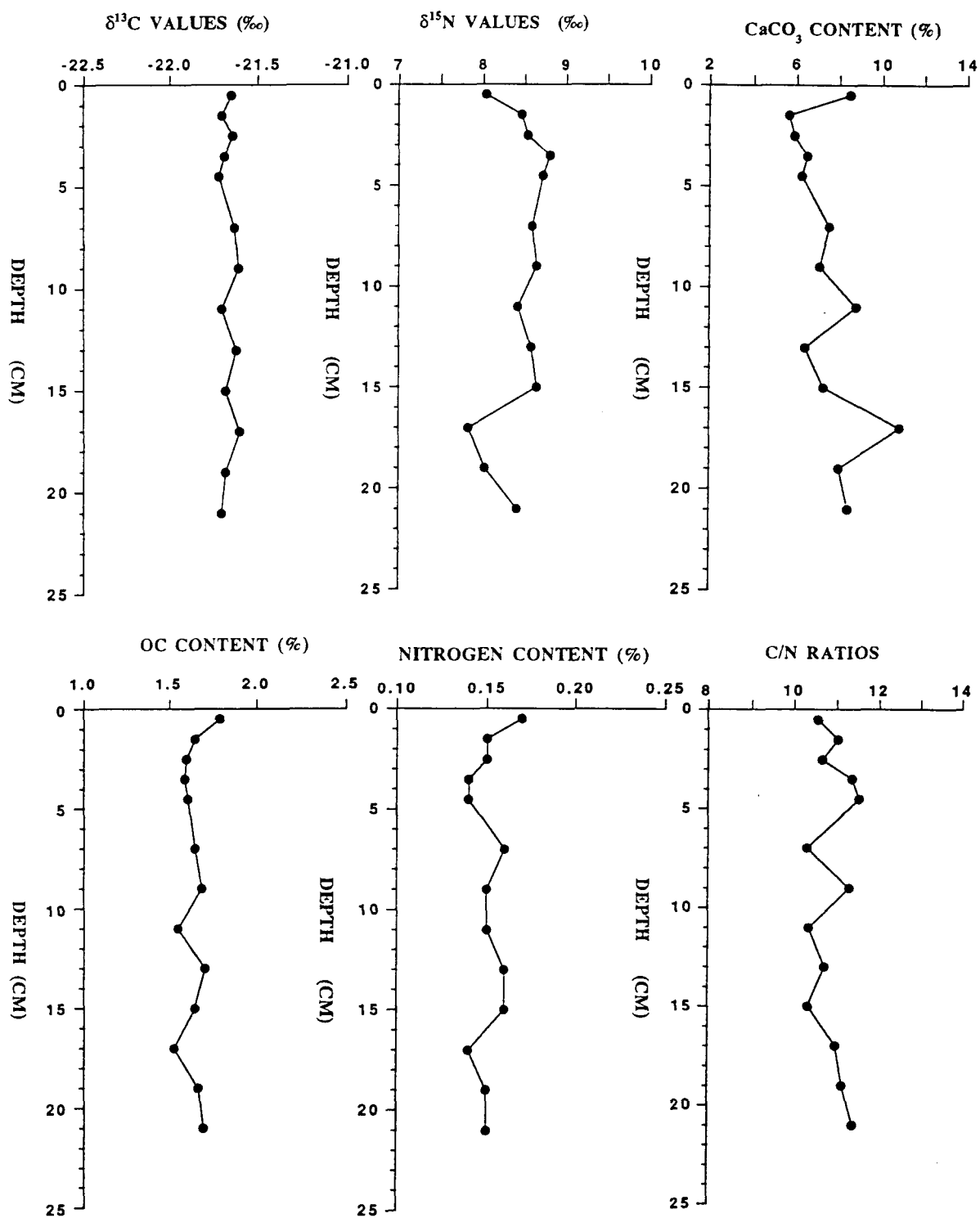


Fig. 4.19. Downcore variation in $\delta^{13}\text{C}$, $\delta^{15}\text{N}$, CaCO_3 , organic carbon, nitrogen and C/N ratios for core

HU-90-028-06 BC.

(Fig. 4.15), (iii) in the upper 5 cm at site 43 PC (Fig. 4.17), (iv) below 29 cm at site 13 BC (Fig. 4.18), and (v) in the upper 5 cm as well as between 13 and 17 cm at site 06 BC (Fig. 4.19). Moreover, there is a two steps downcore decrease in the organic carbon content, with a break centred at 6 cm, at site 34 BC (Fig. 4.13).

The organic carbon content shows a general downcore increase (i) in the upper 5 cm at site 59 BC (Fig. 4.15), (ii) in the upper 5 cm as well as between 16 cm and 29 cm at site 13 BC (Fig. 4.18), and (iii) between 5 cm and 13 cm as well as below 17 cm at site 06 BC (Fig. 4.19). Moreover, the organic carbon content is relatively invariant downcore (i) below 10 cm at site 45 BC (Fig. 4.11), (ii) below 5 cm at site 43 PC (Fig. 4.17), and (iii) between 5 cm and 16 cm at site 13 BC (Fig. 4.18).

4.2.4. Nitrogen Content

A downcore decrease in the nitrogen content to the base of the core is notable at sites 17 BC, 29 BC, 34 BC and 41 BC (Figs. 4.16, 4.13 and 4.14). A similar downcore decrease in the nitrogen content is observable (i) below 6 cm at site 45 BC (Fig. 4.11), (ii) below 5 cm at site 59 BC (Fig. 4.15), (iii) in the upper 5 cm at sites 43 PC, 13 BC and 06 BC (Figs. 4.19, 4.18 and 4.17), and (iv) between 9 cm and 17 cm at site 13 BC (Fig. 4.18).

The nitrogen content for core 06 BC show a general two steps downcore increase below 5 cm with a break centred at about 16 cm (Fig. 4.19). Other slight downcore increases in the nitrogen contents are observable (i) in the upper 6 cm at site 45 BC (Fig. 4.11), (ii) in the upper 5 cm at site 59 BC (Fig. 4.15) and (iii) between 5 cm and 9 cm at site 13 BC (Fig. 4.18). Nearly constant values of nitrogen content, which are invariant downcore, are observable below (i) 5 cm at site 43 PC (Fig. 4.17), and (ii) 17 cm at site 13 BC (Fig. 4.18).

4.2.5. CaCO_3 Content

The CaCO_3 content shows a downcore increase to the base of the core at sites 45 BC, 29 BC, 41 BC, 17 BC, and 06 BC (Figs. 4.11, 4.12, 4.14, 4.16, and 4.19). A similar downcore distribution of CaCO_3 values is observable (i) in the upper 6 cm at site 34 BC (Fig. 4.13), and (ii) below 25 cm at sites 59 BC (Fig. 4.15) and 43 PC (Fig. 4.17). In contrast, the CaCO_3 shows a downcore decrease (i) below 6 cm at site 34 BC (Fig. 4.13), (ii) in the upper 25 cm at site 43 PC (Fig. 4.17), and (iii) in the upper 5 cm at site 13 BC (Fig. 4.18). Relatively constant values of CaCO_3 are observable in the upper 25 cm at site 59 BC (Fig. 4.15), while irregular distribution is observable below 5 cm at site 13 BC (Fig. 4.18).

4.2.6. C/N Ratios.

The C/N ratios are slightly higher than 10 but are generally indicative of phytoplanktonic sources. The highest C/N ratios are observable at site 13 BC (appendix 9.2.0., Table 4.2; Fig. 4.18). The C/N ratios shows a constant downcore variation at sites 41 BC and 17 BC (Fig. 4.14 and 4.18). A similar downcore distribution is observable (i) in the upper 25 cm at site 59 BC (Fig. 4.15), and below 17 cm at site 13 BC (Fig. 4.18). However, the values of C/N ratio are highly variable with a lack of any tendency of increasing or decreasing with depth at site 34 BC (Fig. 4.13).

There is an increase in the C/N ratios downcore to the base of the core at site 29 BC (Fig. 4.12). A similar downcore increase in the C/N ratios is observable (i) below 8 cm at site 45 BC (Fig. 4.11), (ii) in the upper 5 cm as well as between 9 and 17 cm at site 13 BC (Fig. 4.18), and (iii) in the upper 5 cm as well as below 15 cm at site 06 BC (Fig. 4.19).

The C/N ratios decreases abruptly downcore in the upper 5 cm followed by a gradual decrease with depth to the base of the core at site 43 PC (Fig. 4.17). A downcore decrease in the C/N ratios is further observable (i) in the upper 8 cm at site 45 BC (Fig. 4.11), (ii) below 25 cm at site 59 BC (Fig.

4.15), (iii) between 5 cm and 9 cm at site 13 BC (Fig. 4.18), and (iv) between 5 cm and 15 cm at site 06 BC (Fig. 4.19). The upper 5 cm of core 45 BC have the highest C/N values that are greater than 17 (Fig. 4.15).

4.3.0. LATERAL VARIATIONS

4.3.1. Labrador Sea

To avoid inclusion of sediments deposited during the last glacial period, the upper 5 cm for all cores was taken as a representative of a part or complete section of material deposited during the Holocene. The average organic $\delta^{13}\text{C}$ values for the upper 5 cm off the Labrador coast decrease slightly with increasing water depth to a depth of about 2800 m (-21.42‰ to -22.32‰), and then start to increase down to the Labrador basin (3994 m, Fig. 4.20). The mean organic $\delta^{13}\text{C}$ values off the Greenland coast increase with increasing water depth (Fig. 4.20), indicating either a reduction in the transport of terrestrial material with increasing distance offshore or low primary productivity at the nearshore sites. The stable isotopic compositions of OM below 5 cm show high inputs of terrestrial OM at sites 16 BC, 18 BC, 23 BC, 38 TWC and 40 LHC, sites which are situated at a water depth interval of 1300-2800 m. On the Labrador shelf, the influence of the continental OM is minimal and input of OM to the sea floor seems to be dominated by marine primary productivity.

With the exception of core 23 BC (which has the lowest mean value), the mean $\delta^{15}\text{N}$ values of OM for the upper 5 cm are relatively constant at about 8‰ on the Labrador side (Fig. 4.20). As was the case with the stable isotopic compositions of OC, the mean $\delta^{15}\text{N}$ values increase slightly with water depth off the Greenland coast (Fig. 4.20).

With the exception of sites 05 BC and 93 BC, which have relatively high OC contents (1.79% and 0.69% respectively), the mean OC content percentage is very low on both sides of the Labrador Sea basin (Fig. 4.20). Relatively high sedimentary OC values at these two sites may indicate either

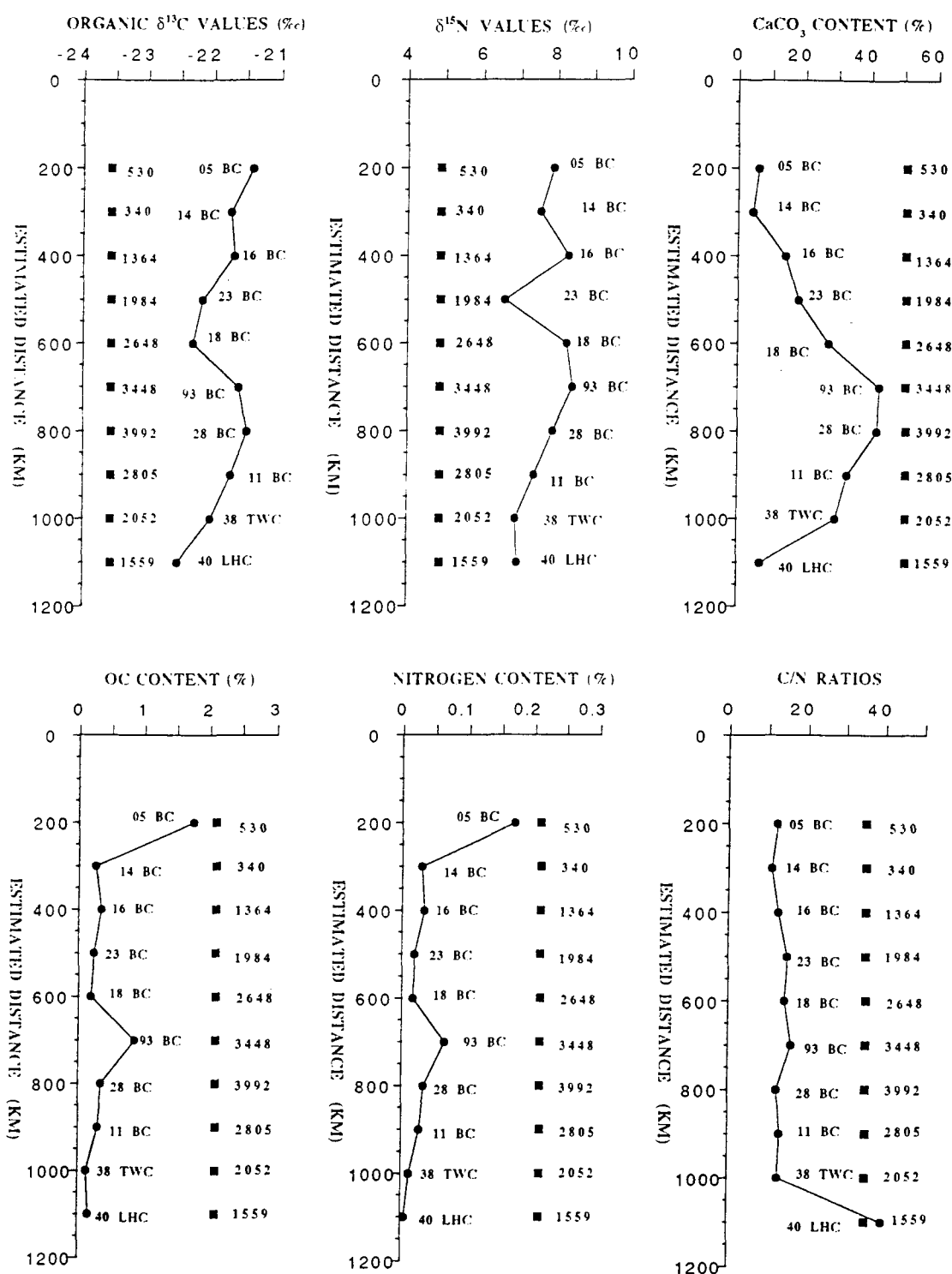


Fig. 4.20. A transect from SW Labrador Shelf to NE Greenland slope showing variation in $\delta^{13}\text{C}$, $\delta^{15}\text{N}$, CaCO_3 , organic carbon, nitrogen and C/N ratios. Shaded rectangles and corresponding numbers are water depths (m), and sites abbreviations are given in Table 3.1.

enhanced preservation or high primary productivity.

The mean CaCO_3 off the Labrador coast is high, and increases with increasing water depth to the basin of the Labrador Sea (Fig. 4.20). In contrast, the mean CaCO_3 content is low off the Greenland coast, and shows a slight increase with increasing water depth (Fig. 4.20). The CaCO_3 content on the Labrador continental margin is higher than on the Greenland side, most likely due to the differences in the sources. There is a large component of detrital carbonate off the Labrador coast, whereas off the Greenland coast it is mainly derived from planktonic production. An increase in the contents of CaCO_3 with water depth associated with an enrichment in ^{13}C may be an indication of high primary productivity at sites located further offshore.

With the exception of core 05 BC, mean nitrogen contents for the upper 5 cm are relatively low, with slightly high values in deep water (Fig. 4.20). All in all, they show a decrease with increasing water depth (Fig. 4.20). In contrast, the mean C/N ratios show a slight increase with water depth on the Labrador Margin (Fig. 4.20). Excluding site 40 LHC, which has high C/N ratios, this parameter is relatively constant on the Greenland Margin (Fig. 4.20).

4.3.2. Gulf of St. Lawrence

Because all cores contain Holocene sediments, mean values are used to evaluate lateral variation in these parameters. The mean isotopic compositions of OC for cores collected from the Gulf of St. Lawrence show a general increase with increasing water depth (Fig. 4.21). The mean nitrogen stable isotope values show a similar trend, although values for a cross-section across the Cabot Strait increase towards the Newfoundland side (Fig. 4.21). With the exception of site 06 BC which is located in the centre of the Cabot Strait, the mean OC content increases with depth (Fig. 4.21). Mean nitrogen contents show lateral distribution which are similar to the OC contents (Fig. 4.21). The mean C/N ratio values are higher at deeper sites than at more shallow sites (Fig. 4.21). The highest mean CaCO_3 occurs at site 17 BC, and the lowest occurs at site 45 BC (Fig. 4.21).

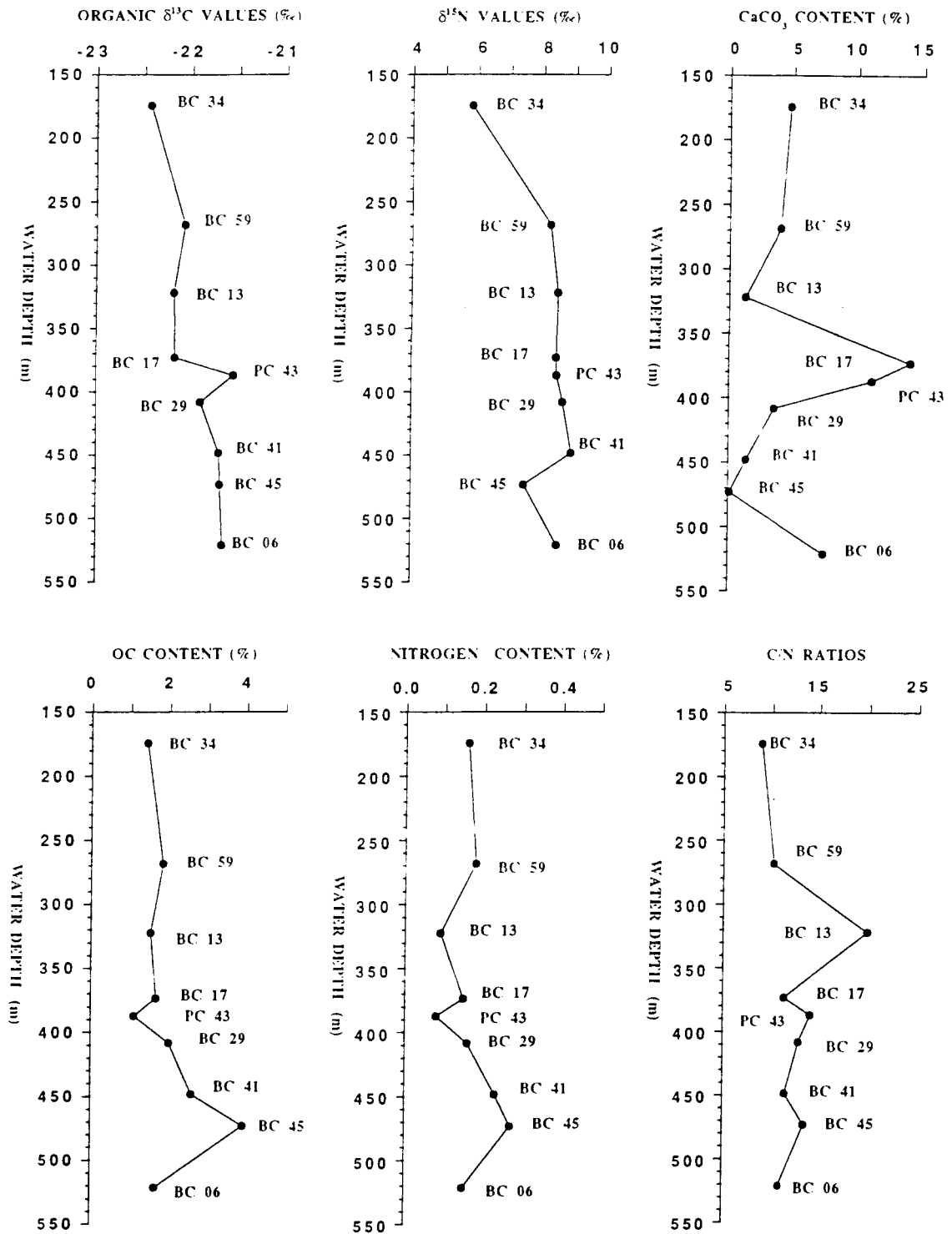


Fig. 4.21. Lateral variation in $\delta^{13}\text{C}$, $\delta^{15}\text{N}$, CaCO_3 , organic carbon, nitrogen and C/N ratios in the Gulf of St. Lawrence-Scotia slope.

4.4.0. DISCUSSION

4.4.1. Labrador Sea

A downcore increase in $\delta^{15}\text{N}$ values of at about 1‰ and $\delta^{13}\text{C}$ values of about 0.4‰ at sites 14 BC and 28 BC, which are associated with a downcore increase in the C/N ratios can be attributed to a diagenetic changes. A downcore enrichment in ^{13}C and ^{15}N can be attributed to a peptide bond hydrolysis followed by bacterial utilization of free amino acids or shorter-chain peptide, and a preferential preservation of ^{13}C enriched compounds like proteins and carbohydrates during diagenesis (Behrens and Frishman, 1971; Macko, 1981; Macko et al., 1993, 1994). The effects of diagenesis are supported by a significant negative correlation between (i) C/N ratios and nitrogen content at these sites (Figs. 4.22 and 4.23), (ii) $\delta^{13}\text{C}$ and C/N ratios at site 28 BC (Fig. 4.23), and (iii) CaCO_3 and C/N ratios at sites 28 BC and 11 BC (Figs. 4.22 and 4.23). A significant positive correlation between contents of nitrogen and carbon at sites 14 BC and 28 BC (Figs. 4.22 and 4.23) may be an indication of equal rate of removal of nitrogen and carbon during diagenesis (Grundimains and Murray, 1982).

Downcore decreases in $\delta^{13}\text{C}$ values similar to the one observed at sites 16 BC, 18 BC, 23 BC, 38 TWC and 40 LHC (Figs. 4.4, 4.5, 4.6, 4.7, and 4.8), have been observed in the Pigmy Basin (Gulf of Mexico) (Jasper and Gagosian, 1989), in Mangrove Lake Bermuda (Spiker and Hatcher, 1984; Hatcher et al., 1983), and in the southern ocean (Singer and Shemesh, 1995; Shemesh et al., 1993). Several factors can be invoked as the cause of the downcore decrease in the isotopic compositions of organic carbon of at least 2‰ observed at the above mentioned sites. These factors include (i) a diagenetic alteration of labile OM, (ii) a change in the rate of nutrient utilization (shift in primary productivity) between late Pleistocene and Holocene, and (iii) a change in the proportion of land-derived and marine-derived OM. Similarly, these factors can be used to explain the downcore decrease in the $\delta^{15}\text{N}$ values observed at sites 16 BC, 23 BC and 40 LHC (Figs. 4.4, 4.6 and 4.8).

The oxygen content of sediments is one of the major factors governing rates of OM degradation (Froelich et al., 1979; Emerson and Hedges, 1988; Dean et al., 1994). Based on the result

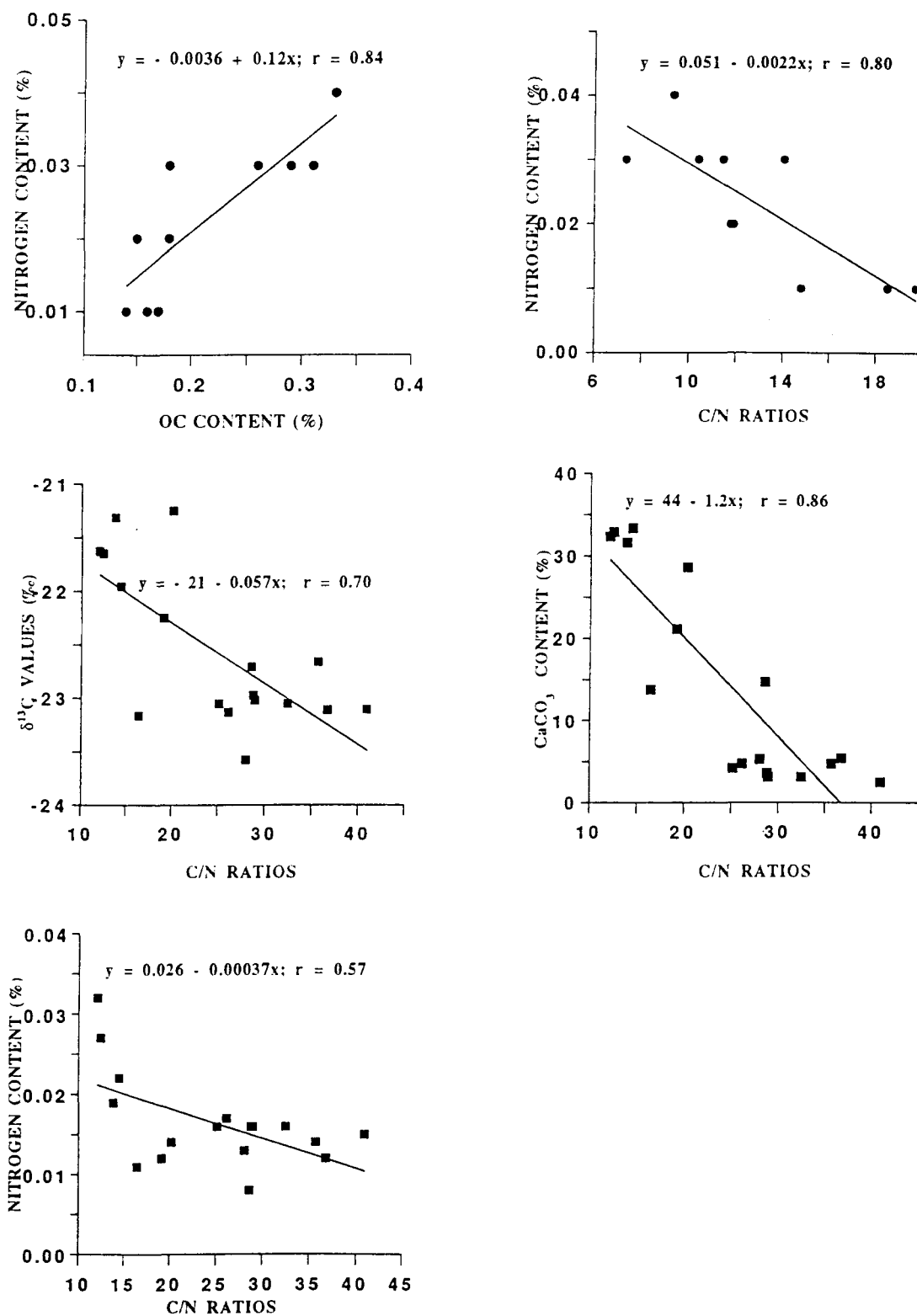


Fig. 4.22. Scatter plots for cores HU-91-045-14 BC (solid circle), and HU-90-013-11 BC (solid rectangle). These correlations among parameters are significant at the 95% confidence level.

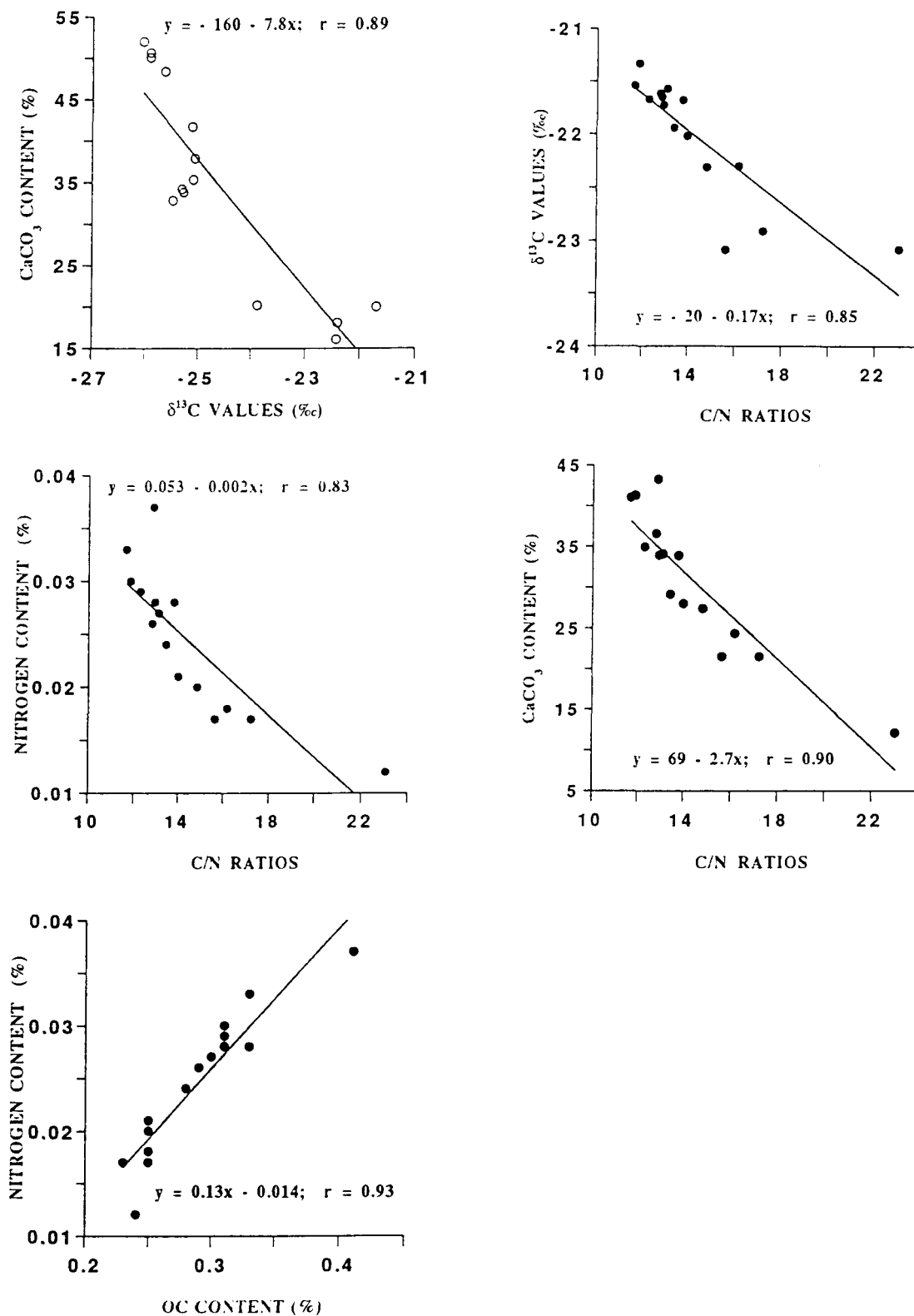


Fig. 4.23. Scatter plots for cores HU-91-045-23 BC (open circle), and HU-91-045-28 BC. These correlations among parameters are significant at the 95% confidence level.

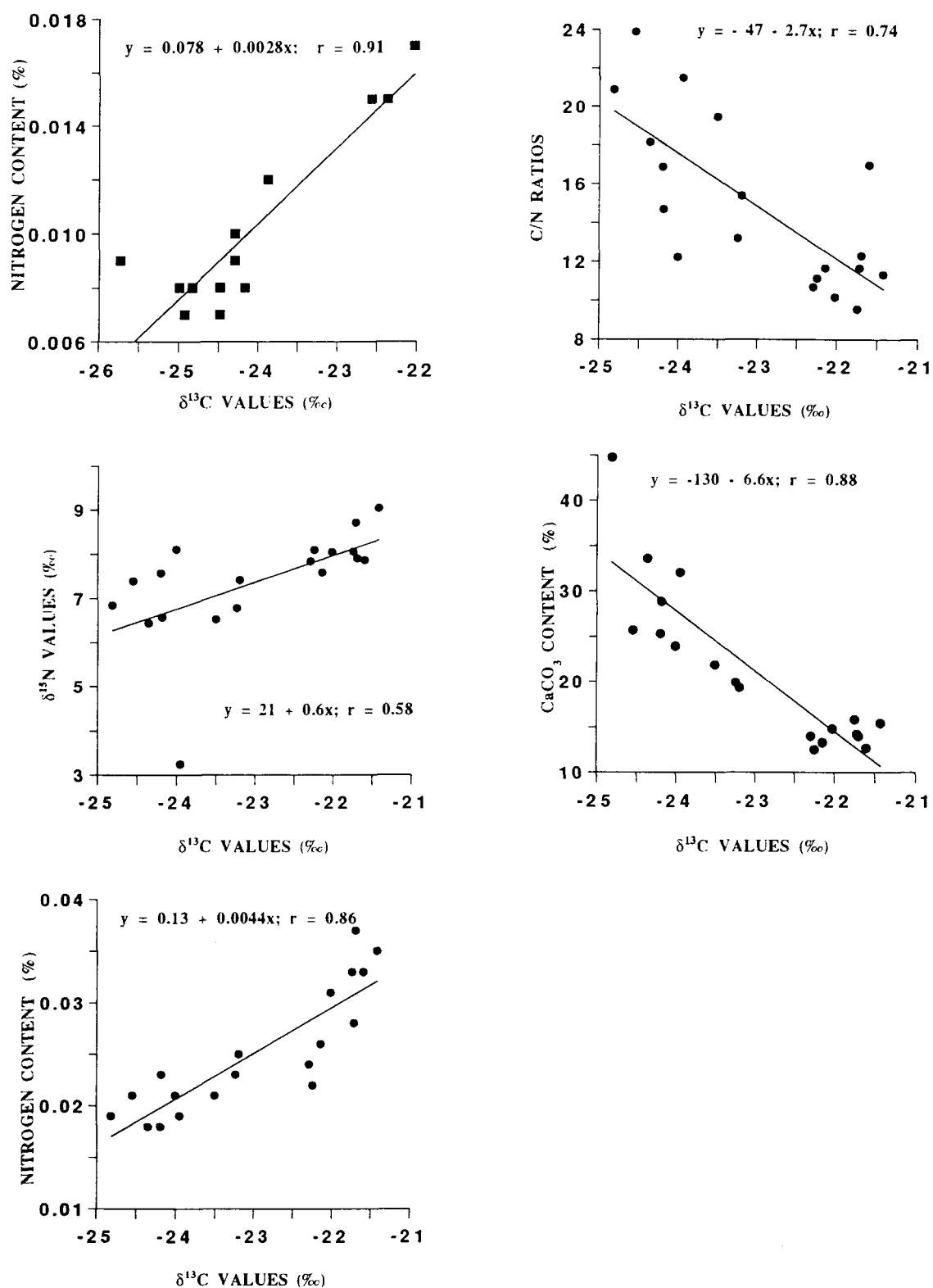


Fig. 4.24. Scatter plots for cores HU-91-045-16 BC (solid circle), and HU-91-091-18 BC (solid rectangle). These correlations among parameters are significant at the 95% confidence level.

of on-site determination of redox potential (Fig. 3.3.), the oxygen penetration depth is high in the Labrador Sea. High penetration depth of oxygen has a potential of altering the isotopic compositions of OM during diagenesis. A study by McArthur et al., 1992, has indicated that when sediments are re-exposed to oxic conditions, the shift in the organic carbon isotopic compositions towards lower (lighter) values can be as high as 2‰. Apart from this work, studies conducted to trace the effect of early diagenesis on the stable isotopes of organic carbon have shown downcore depletions in ^{13}C (Hatcher et al., 1983, Spiker and Hatcher, 1984). A downcore decrease in $\delta^{13}\text{C}$ values has been partly attributed to the preferential loss of carbohydrate that is enriched in ^{13}C (Hatcher et al., 1983, Spiker and Hatcher, 1984, 1987). Therefore, a downcore decrease in $\delta^{13}\text{C}$ observed in this study can partly be attributed to a diagenetic loss of ^{13}C enriched compounds like carbohydrates and proteins or humification process. However, the issue of isotopic alteration is controversial. In some work, no shift or slight shift in the isotopic compositions has been observed (Velinsky et al., 1991; Macko et al., 1994; Meyers, 1994; Altabet and Francois, 1994b). Because of this it has been concluded that diagenetic alteration of labile OM has little effect on the bulk OM (Meyers, 1994; Altabet and Francois, 1994b; Rau et al., 1987). Although the effect of diagenesis can not be quantified in this study, the observed downcore variations is unlikely to have been wholly caused by diagenetic alteration.

Another factor which might have caused the observed downcore decrease in $\delta^{13}\text{C}$ values is a change in the rate of nutrient utilization (low during the late glacial maximum and high during the Holocene). The available estimates of sedimentation rates (Chapter 3; Hillaire-Marcel et al., 1994b) indicate that sites located between water depths of 1300 m and 2800 m have low sedimentation rates (Hillaire-Marcel et al., 1994b). Owing to low sedimentation rates, the analyzed cores most likely represent material deposited since the late Pleistocene. The core sections with the most depleted values are a representative of the late Pleistocene period. Because newly formed OM is enriched in ^{13}C and

^{15}N whenever nutrients in the euphotic zone are fully utilized owing to a small fractionation, difference between glacial and Holocene periods in $\delta^{13}\text{C}$ may reflect a change in the rate of nutrient utilization (shift in primary productivity). A thin cover of recent sediments (6-10 cm) on the slope and rise areas can be attributed to erosion or non-deposition of sediments caused by the strong WBUC. This inference is supported by high content of sand fraction >63 microns (Bilodeau et al., 1994), on the Labrador and the Greenland continental margins.

A downcore decrease in both $\delta^{13}\text{C}$ and $\delta^{15}\text{N}$ values of diatomic OM in the Southern Ocean has been used as an indicator of reduced primary productivity during the glacial period (Singer and Shemesh, 1995; Shemesh et al., 1993). This is based on the observation that newly formed OM is enriched in ^{13}C and ^{15}N whenever nutrients in the euphotic zone are fully utilized owing to a small fractionation, and is depleted in both ^{13}C and ^{15}N when the rate of utilization of available nutrients is low (Altabet and Francois, 1994a,b; Calvert et al., 1992a; Francois et al., 1992; Rau et al., 1991,1992). A similar reasoning can be applied to the Labrador Sea. There is ample evidence that the Labrador Sea experienced a significant change in the primary productivity as the climatic conditions changed from cold (glacial) to warmer (Holocene) conditions (Hillaire-Marcel et al., 1994b). During the glacial period, a large part of the Labrador Sea was covered by ice for a large period of the year (de Vernal et al., 1994), and was characterized by low primary productivity. Evidence for low primary productivity is found in the distribution of dinocysts in a dated core (11 BC), in which dinocyst abundances are lower during the glacial period than during the Holocene (Hillaire-Marcel et al., 1994b). A change in primary productivity from low (glacial-transition period) to high (Holocene) is further supported by an increase in the concentration of dinoflagellate cysts off southwest Greenland and in the Labrador Sea in general (Rochon and de Vernal, 1994; Hillaire-Marcel et al., 1994b). Therefore, enrichment in ^{15}N and ^{13}C during the late Holocene is an indication of high nutrient demand during photosynthesis, thus high primary productivity. Although there are no data on downcore

distribution of various primary productivity indicators at other sites, high values in the upper 5-10 cm of the cores located between water depths of 1300 m and 2800 m may be an indication of high rates of nutrient utilization and hence primary productivity.

Although downcore variation in the isotopic compositions of OM can partly be explained by the changes in primary productivity and diagenesis, high C/N ratios and very low values (less than -23.0‰) observed at these sites, particularly at sites 16 BC, 18 BC, 23 BC, 38 TWC, and 40 LHC point to another mechanism. Excluding diagenetic changes, high C/N ratios for autochthonous marine OM can only result in areas with high primary productivity that are associated with limited nitrate availability (Meyers, 1992). The OM produced under such conditions would be lipid-rich and nitrogen-poor, with the C/N ratios that are less than those of terrestrial OM. But such conditions entail elevated ^{15}N values, because all available nitrates will be consumed. In contrast, the $\delta^{15}\text{N}$ values for most of the cores decrease downcore. High C/N ratios associated with both depleted ^{15}N and ^{13}C particularly at sites 16 BC, 18 BC and 23 BC can partly be explained by an increase in the proportion of land-derived OM over the marine-derived OM. A significant positive correlation at 95% confidence level between $\delta^{15}\text{N}$ and $\delta^{13}\text{C}$ at site 16 BC (Fig. 4.24), negative correlation between (i) C/N ratios and $\delta^{13}\text{C}$ at sites 16 BC and 11 BC (Figs. 4.22 and 4.24), and (ii) CaCO_3 and $\delta^{13}\text{C}$ at sites 16 BC and 23 BC (Figs. 4.23 and 4.24) may be a further indication of the influence of the terrestrial OM. Since terrestrial OM is poor in nitrogen relative to marine OM, a significant positive correlation between nitrogen and $\delta^{13}\text{C}$ at sites 16 BC and 18 BC (Fig. 4.24), and a significant negative correlation between nitrogen and C/N ratios at site 11 BC (Fig. 4.22) may partly be an indication of changes in the proportions of terrestrial OM in the area. All three factors ((i) a diagenetic alteration of labile OM, (ii) a change in the rate of nutrient utilization (shift in primary productivity) between late Pleistocene and Holocene, and (iii) a change in the proportion of land-derived and marine-derived OM) invoked to explain downcore decrease in $\delta^{13}\text{C}$ values observed in this study are possible. However, it is difficult to quantify contribution of each factor.

This work has indicated that high enrichments in ^{13}C and ^{15}N are confined to sites close to the continent (05 BC, and 14 BC) and deep water sites (93 BC and upper 23 cm of the core 28 BC). The inferred high proportion of land derived OM over that of marine derived OM below 5-10 cm, particularly at sites 16 BC, 18 BC, 23 BC, 38 TWC, and 40 LHC is contrary to various studies that have indicated increase in the δ -values of OM with increasing distance offshore (Macko, 1983; Sackett and Thompson, 1963; Schultz and Calder, 1976; Gearing, 1988; Lucotte et al., 1991). As pointed out previously, one possible explanation is that cores at shallow depth as well as deeper sites have not penetrated far enough to reach the late Pleistocene deposits. A thin cover of the Holocene deposits at sites located between water depths of 1300 m and 2800 m can be attributed to a winnowing process caused by the fast moving WBUC, which has been inferred to have intensified during the Holocene (Bilodeau et al., 1994; Hillaire-Marcel et al., 1994b).

Processes that might have caused enhanced input of terrestrial OM during the late Pleistocene include deposition of reworked slope sediments by the WBUC (contourite facies), slumping, turbidity currents, meltwater plumes and icebergs. Although it is a localized process, slumping of sediments on the continental shelf off the Labrador coast is one of the major mechanisms responsible for sediment transport to deeper areas (Hesse, 1992). However, cross-shelf transport of sedimentary OM is not sufficient to explain the observed basinwide distribution of terrestrial OM below 6-10 cm for sites located between 1300 m and 2800 m.

Sediment deposition by turbidity currents into tributaries and satellite channels of submarine canyons (on the slope) during the late Pleistocene could be one of the major mechanisms responsible for transport of terrestrial OM at these depth intervals. The turbidity currents have been inferred to have been very active during the glacial-interglacial transition times, and a considerable amount of shelf and slope materials were transported through NAMOC (Myers and Piper, 1988; Hesse et al., 1987, 1990). Most of the glacial turbidite deposits are currently studded by recent pelagic sediments.

Low organic $\delta^{13}\text{C}$ values in the lower part of core 28 BC may be an indication of a turbidite deposit blanketed by recent marine OM. Downcore increases in CaCO_3 to the base of the core at sites 16 BC, 18 BC and 23 BC (Figs. 4.4, 4.5 and 4.6), that correspond to low organic $\delta^{13}\text{C}$ and $\delta^{15}\text{N}$ values as well as high C/N ratios (greater than 12) may be an indication of turbidity current deposition of fine carbonate particles mixed with terrestrial OM into tributaries and satellite channels of the submarine canyons. Negative correlation between $\delta^{13}\text{C}$ and CaCO_3 content at sites 16 BC and 23 BC (Figs. 4.23 and 4.24) might be an indication of continental sources of organic carbon that was rich in carbonate.

Another possible mechanism responsible for the above is the iceberg transport and melting of land based ice in the Labrador region. The sampling sites are located within the observed maximum seaward extent of abundant icebergs for the past 90 years (Ruddiman, 1977). The icebergs are transported to the area by the Labrador current, and all slope as well as rise sites are located within the influence of the Labrador current.

Because of poor preservation (very low %OC) of OM in the basin, the inferred allochthonous OM may be partly a refractory material derived from the continent through wind transport and/or reworked Cretaceous sedimentary rocks from Baffin Bay. The contents of *Pinus*, *Sphagnum* and *Lycopodium* palynomorphs in surficial sediments of the analyzed cores increase with increasing distance offshore (Rochon and de Vernal, 1994), an indication of atmospheric influence. Similarly, the possibility of reworked Cretaceous rocks is supported by the wide spread presence of reworked Arctic palynomorphs in many analyzed cores from the Labrador Sea and Baffin Bay (de Vernal and Mudie, 1989a,b; Hillaire-Marcel et al., 1989, 1994a). Baffin Bay is the most probable source of refractory material because of occurrence of Cretaceous rocks in the area.

On the Greenland side, there is a measurable input of terrestrial material at site 11 BC in the lower part of the core section (Late Pleistocene and early Holocene) of similar magnitude as the two shallower depths cores (38 TWC and 40 LHC). The coring site 11 BC experienced low sedimentation

rate or erosion by the WBUC during the Holocene (Hillaire-Marcel et al., 1994a) and all three sites may be subjected to the same sedimentation process. This is because it has been indicated that deep currents were active upslope as far as 1100 m during the late Holocene (Hillaire-Marcel et al., 1994a). However the question which arises is the source of OM in the area. Currently, continental primary productivity on the Greenland is low owing to almost permanent coverage of ice throughout the year. Marine primary productivity is the major source of OM in the area. Thus, the sedimentary OM off the western Greenland coast is likely to be a reworked Cretaceous sediments from either the Greenland shelf or Europe carried to the site by the surface current, WBUC and/or icebergs. This inference is supported by a work of Henrich et al. (1995) who observed low $\delta^{13}\text{C}$ values in the Norwegian-Greenland Sea, and attributed it to ice rafting deposition of continental derived OM.

Basing on the terrestrial end member values for $\delta^{15}\text{N}$ commonly used, which range from 0-4‰, the nitrogen stable isotopic compositions of OM recovered at these sites would seem not to indicate a measurable input of terrestrial OM. For obtaining the same terrestrial fraction represented by $\delta^{13}\text{C}$ values, the $\delta^{15}\text{N}$ terrestrial end member value has to be at least 5‰. Thus, the nitrogen stable isotopes seem not to be a best indicator of the sources of OM in the Labrador Sea.

This study has also demonstrated that lateral variations in $\delta^{13}\text{C}$ decrease slightly with increasing water depth to a depth of about 2800 m off the Labrador coast. The possible explanations include isotope fractionation (due to temperature effect, and changes in species assemblages), as well as differences in primary productivity between nearshore and offshore sites. Although in some studies no correlation between temperature and isotopic compositions was observed (Calder and Parker, 1973; Fontugne and Duplessy, 1978; Gearing et al., 1984), $\delta^{13}\text{C}$ values of particulate OM and sedimentary OM collected from high latitude areas as low as -30‰ (Sackett et al., 1965; Sackett et al., 1974; Fontugne and Duplessy, 1981; Sackett, 1986, 1991; Rau et al., 1989, 1991; Francois et al., 1993b; Biggs et al., 1988, 1989; Rogers et al., 1972) have been attributed partially to temperature effect. The

difference in sea surface temperature between marginal and central areas of the Labrador Sea is small (Isemer and Hasse, 1985), thus, not sufficient enough to explain the observed differences in the isotopic compositions. However, the effect of temperature is controversial, recently Fogel and Cifuentes (1993) have concluded that there is no temperature effect on the carbon isotopes.

Although it has been observed that the stable isotopic compositions of OC may vary with changes in species diversity (Sackett et al., 1974; Wong and Sackett, 1978; Gearing et al., 1984; Georik and Fry, 1994), this factor is unlikely to have caused the observed lateral trend. As pointed out in chapter 1, high fractionation of carbon isotopes occurs when species assemblage changes from calcareous to siliceous producer (Sackett et al., 1974). Albeit there is a high species diversity of dinoflagellates (Rochon and de Vernal, 1994), no major changes (from calcareous to siliceous producing organisms) have been reported across the transect.

The observed trend is likely to have been caused by differences in utilization of available nutrients between nearshore and offshore sites. The density of nannofossils and dinocysts in surficial sediments (de Vernal et al., 1994), which are indicators of surface primary productivity, water temperature and salinity, is high (e.g. >1000 cysts/cc) and shows a slight increase with increasing water depth in the Labrador sea. High concentration of these productivity indicators in surficial sediments in association with high $\delta^{15}\text{N}$ values in all cores, indicate enhanced utilization of nutrients in the area. An increase in productivity indicators with increasing water depth is not likely to be an indication of high utilization of nutrients at sites located further offshore. This is because, high concentrations of primary productivity at sites located further offshore are likely to have been caused by sediment focusing. Thus, differences in the rate of primary productivity is the most probable explanation of the observed depletion in ^{13}C with increasing distance off the Labrador coast.

An enrichment of OM in ^{13}C and ^{15}N in the Holocene core section at site 11 BC is an indication of increased primary productivity. This inference is supported by the high content of CaCO_3

during the same time interval and other productivity indicators such as dinoflagellate cyst and benthic foraminifers which are also high (Rochon and de Vernal, 1994; de Vernal et al., 1994; Bilodeau et al., 1994). This indicate an improvement in the surface water temperature and increase in the supply of nutrients to the euphotic zone.

An increase in OC and nitrogen contents with depth in the upper 4 cm, at sites 05 BC which is associated with increase in organic $\delta^{13}\text{C}$ and $\delta^{15}\text{N}$ values, may be attributed to increased primary productivity and/or bioturbation processes which transport labile material downwards and refractory material upwards. High contents of OC and nitrogen may indicate that the area is under the influence of high primary productivity or enhanced preservation of OM. As pointed out above, a downcore decrease in nitrogen content associated with a slight increase in C/N ratios below 4 cm may be an indication of diagenetic changes caused by preferential loss of nitrogen containing compounds over that of carbon.

4.4.2. Gulf of St. Lawrence

The stable isotopic compositions of OC and nitrogen as well as the C/N ratios indicate little influence of the terrestrial OM to the area and OM is made up mainly of phytoplanktonic debris. Although core 13 BC was collected close to the lower estuary, the terrestrial input at this site is minimal. This indicate that most of the terrestrial OM transported by the river of St. Lawrence and its distributaries are deposited or trapped within the estuary, as pointed out by previous workers (Lucotte et al., 1991; Tan and Strain, 1983, 1979a,b; Pocklington, 1976). However, this is contrary to the work of de Vernal and Giroux (1991) who observed high concentration of pollen and spores in the Gulf. A lack of records of terrestrial OM in the Gulf could partly be explained by the high primary productivity, where the effect of terrestrial input is overprinted (diluted) by high flux of marine autochthonous OM.

Distribution of the isotopic compositions of particulate OM in the upper 50 m of the water column in the Gulf of St. Lawrence is characterized by very low values (less than -24‰) indicative of terrestrial source (Tan and Strain, 1979b). Although the POM have $\delta^{13}\text{C}$ values indicative of a terrestrial source, it has been concluded that they are actually of marine origin (Tan and Strain, 1979b). In contrast, the results of this work (Fig. 4.21), and previous work (Tan and Strain, 1979a, 1983), indicate that surficial sedimentary OC in the Gulf of St. Lawrence is enriched in ^{13}C and homogeneous ($-21.7 \pm 0.2\text{‰}$) compared to the POM. The differences between particulate material and sedimentary OM is probably due to size of trapped particulate material and/or diagenetic effects. Fast falling particulate material such as fecal pellets, which make up large fraction of OM that reach the sea floor, are likely to have not been sampled by 12L Niskin bottles as pointed out by Tan and Strain (1979b). The isotopic compositions of the fast falling particulate matter has been observed to be lower than that of suspended particulate matter (Altabet, 1988). Thus, the observed $\delta^{13}\text{C}$ values for sedimentary OM should be even more depleted than the surface particulate matter. Therefore, selective trapping of fine particles, that might be rich in pollen and spores may be the reason behind low δ -values of the particulate OM.

The lowest values of $\delta^{15}\text{N}$ and $\delta^{13}\text{C}$ observed at site 34 BC, may be attributed to a slight input of terrestrial material to the area, high fractionation resulting from high concentration of nutrients, diagenetic effects or high input of macrophytic material that are depleted in ^{13}C and ^{15}N . Although input of terrestrial material is likely because of close proximity to the land mass (Cape Breton Island), low C/N ratios indicative of marine sources of OM exclude this possibility. Furthermore the high content of OC excludes the possibility that the C/N ratios are low due to the release of adsorbed inorganic nitrogen as it has been reported for organic lean sediments (Müller, 1977).

During sample collections, macrophytes were observed at site 34 BC. The macroalgae are one of the major producers of OM in high latitude areas (Ostrom and Macko, 1992 and references

therein). Isotope values of macroalgae have been observed to fall within wide ranges; -20‰ to -12‰ (^{13}C) and 5‰ to 10‰ (^{15}N) (Stephenson et al., 1984). The $\delta^{13}\text{C}$ and $\delta^{15}\text{N}$ values of a dominant species of *Laminaria solidungula* in waters off Newfoundland were taken to be representative of the macroalgae, and their $\delta^{13}\text{C}$ and $\delta^{15}\text{N}$ values were -20.3‰ and 4.6‰ respectively (Ostrom and Macko, 1992). The isotopic compositions of macrophytes at this site might be lower than the published ones, and the results of the isotopic compositions of OC and nitrogen are a mixture of the organic material produced by macrophytes and phytoplankton. Thus, the observed values are likely due to a mixing of macrophytes and planktonic organic material as well as diagenetic effects. The diagenetic effects are supported by a positive correlation between (i) Eh and OC contents (Fig. 4.25), and (ii) Eh and nitrogen content at this site (34 BC) (Fig. 4.25). Because of a significant positive correlation between organic carbon and nitrogen (Fig. 4.25), the rate of decomposition of these two elements is equal. Low values of $\delta^{13}\text{C}$ and $\delta^{15}\text{N}$ can also be the result of incomplete utilization of available nutrients.

The range of the organic $\delta^{13}\text{C}$ at all sites is very small and is either within or close to analytical error. Apart from this, a slight downcore increase in $\delta^{13}\text{C}$ in either the upper few cm or whole core at sites 29 BC, 34 BC, 41 BC, 43 PC, 45 BC and 59 BC may be attributed to diagenetic effects. Enrichment in ^{13}C during early diagenesis might have resulted from the preferential loss of isotopically depleted (lipids) components (Macko et al., 1993 and references therein).

A slight downcore decrease in organic $\delta^{13}\text{C}$ either in the upper few cm or whole core at sites 13 BC and 17 BC may be attributed to diagenetic effects. A shift toward more depleted values in organic $\delta^{13}\text{C}$ of the same magnitude (0.3‰) was observed in carbonate turbidite "a" where up to 35% of OM was inferred to have been oxidized (McArthur et al., 1992). Furthermore, laboratory experiments have shown a depletion of 2.8‰ for a mixture of marine sediments and seagrass (Macko et al., 1994). These variations in isotopic compositions during early diagenesis might have resulted from the preferential loss of isotopically enriched components such as carbohydrates (Spiker and

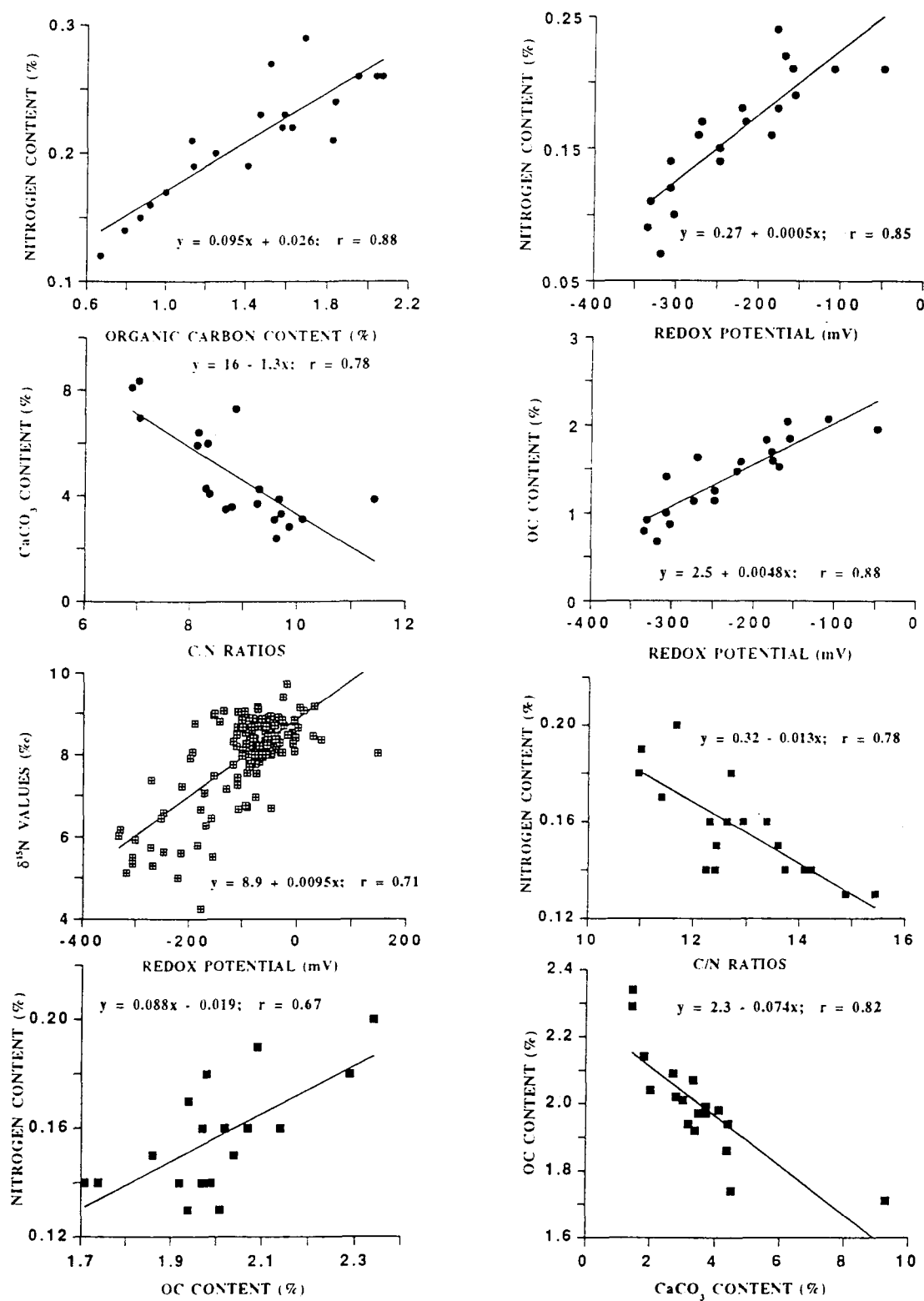


Fig. 4.25. Scatter plots for cores HU-90-031 34 BC (solid circle), All Gulf data (crossed rectangle) and HU-90-031-29 BC (solid rectangle).

Hatcher, 1984, 1987; McArthur et al., 1992), preservation of depleted (lipids) components, peptide bond hydrolysis, deamination, decarboxylation and condensation reactions (Macko et al., 1994; Qian et al., 1992).

Although an increase in $\delta^{13}\text{C}$ of up to 2‰ of organic rich sediments have been attributed to anaerobic decomposition by bacteria (Behrens and Frishman, 1971), the small range of $\delta^{13}\text{C}$ values observed in this study indicates that the $\delta^{13}\text{C}$ values in the Gulf of St. Lawrence-Scotia slope are conservative tracers that do not change significantly as diagenesis progresses. However, as it has been observed that the isotopic composition of the POM in the Gulf of St. Lawrence is about -25‰, the observed values might be the result of diagenetic changes either prior to or immediately after deposition.

Studies trying to identify effects of nitrogen diagenesis on its isotopic composition indicated a lack of significant isotope effects during particulate nitrogen remineralization (Velinsky et al., 1991; Macko et al., 1994). However, nitrogen isotopes may be affected by diagenetic processes involving peptide bond rupture (Silfer et al, 1992; Macko et al., 1994). Macko (1981) observed a downcore enrichment in ^{15}N of OM in a seagrass bed which was attributed to diagenesis resulting from deamination or hydrolysis reactions with preferential bond rupture or loss of ^{14}N amines. Laboratory experiments have also indicated enrichment in ^{15}N in the residue during condensation of amino acids and sugars (Maillard reactions) which is one of the possible diagenetic pathways involved in the formation of humic substances in sediments (Qian et al., 1992). Furthermore, the isotopic compositions of particulate OM has been observed to increase with depth in the oceans following diagenetic loss of ^{14}N enriched materials (Altabet and McCarthy, 1988, 1986; Altabet et al, 1991; Libes and Deuser, 1988; Wada, 1980). Hence, an increase in $\delta^{15}\text{N}$ in either the upper few cm or whole core at sites 06 BC, 41 BC, 43 PC, and 59 BC may be attributed to the diagenetic effect. A diagenetic effect is partly supported by a downcore decrease in the content of THAA at site 43 PC (Chapter 6).

Laboratory experiments have indicated that biological degradation of OM can sometimes deplete the residue OM in ^{15}N (Macko and Estep, 1984; Wada, 1980). Depletion of the residue in ^{15}N have been attributed to deamination. A decrease in $\delta^{15}\text{N}$ either in the upper few cm or whole core, of up to 1‰, at sites 13 BC, 34 BC, and 59 BC may be attributed to the diagenetic effects. A similar process can be invoked to explain the downcore decrease in $\delta^{15}\text{N}$ below 5 cm, of up to 1.8‰, at site 43 PC.

A downcore decrease in $\delta^{15}\text{N}$ also can partly be explained by the preferential removal of ^{15}N enriched amino acids. The most stable amino acids, which are the major component of sedimentary nitrogen in many marine areas, are ornithine, serine, leucine, glycine and aspartic acids (Degens, 1967). Glutamic acid, threonine, and alanine are slightly diagenetically more stable than the rest of the amino acids. The isotopic compositions of these stable amino acids is lower than those that are less stable (Macko et al., 1983). Thus, preferential removal of these less stable compounds that are enriched in ^{15}N may have led to low $\delta^{15}\text{N}$ values.

Excluding site 45 BC, the stable isotopic compositions of nitrogen for the Gulf of St. Lawrence are slightly low in shallower areas off Cape Breton Island (34 BC and 59 BC), and relatively high as well as homogeneous in the Laurentian channel. Distribution of the nitrogen stable isotopes along the Laurentian channel shows a slight increase with increasing water depth. Homogeneous and high $\delta^{15}\text{N}$ values along the Laurentian channel may indicate that the isotopic compositions of nitrogen in the Gulf of St. Lawrence are controlled by primary productivity as well as the diagenetic changes taking place.

The $\delta^{15}\text{N}$ values for all cores from the Gulf of St. Lawrence are positively correlated with the redox potential (Fig. 4.25). A significant positive correlation between the nitrogen stable isotope values and the redox potential (Fig. 4.25, $r=0.7$, $n = 148$), indicate that as redox conditions change from oxic to reducing conditions, the OM becomes more depleted in ^{15}N .

With the exception of site 13 BC, the mean C/N ratios in this study fall within the intermediate zone (8-14) previously reported by Pocklington (1976). However, these C/N ratio values are slightly higher than those of particulate matter in the water column (9.4) and in surficial sediments in the troughs and channel (9.1) previously reported by Pocklington (1976). Elevated values may indicate an effect of a selective loss of nitrogen bearing compounds during early diagenesis, or the influence of materials poor in proteinaceous components like terrestrial OM. The influence of terrestrial material in the Gulf of St. Lawrence is minimal, as is indicated by the stable isotopic compositions of OC and nitrogen. Thus, the elevated values of C/N ratios are likely due to diagenetic changes. This inference is supported by a strong negative correlation between C/N and nitrogen content at sites 13 BC, 29 BC, and 41 BC (Figs 4.25 and 4.26), which is associated with a significant positive correlation at the 95% confidence level between C/N ratios and OC content (Figs 4.25 and 4.26). A negative correlation between C/N ratios and nitrogen content at these sites (Figs. 4.25 and 4.26) may be a further indication of preferential removal of nitrogen bearing compounds. This is because when there is preferential removal of nitrogen bearing compounds, the C/N ratios increase. A significant positive correlation between OC and C/N ratios that is associated with significant negative correlation between OC and CaCO_3 at sites 13 BC, 17 BC, 41 BC, 45 BC, and 59 BC (Figs. 4.26 and 4.27), may be a further indication of the effects of diagenesis.

The differences in the mean isotopic compositions of nitrogen of up to 1‰ for sites located at or near the Cabot Strait (34 BC, 41 BC, 06 BC, 45 and 59 BC) may indicate differences in the rate of nutrient utilization. Water movements in the Cabot strait are dominated by an outward surface flow, which are strongest around Cape North on the Nova Scotian side, and an inward flow off Cape Ray on the Newfoundland side. A landward moving current through the Cabot strait from the Atlantic Ocean is rich in nutrients, thus causing high concentrations of nutrients at intermediate depths in the Gulf (Yeats, 1988; Coote and Yeats, 1979). The influx of nutrients from the Atlantic Ocean through

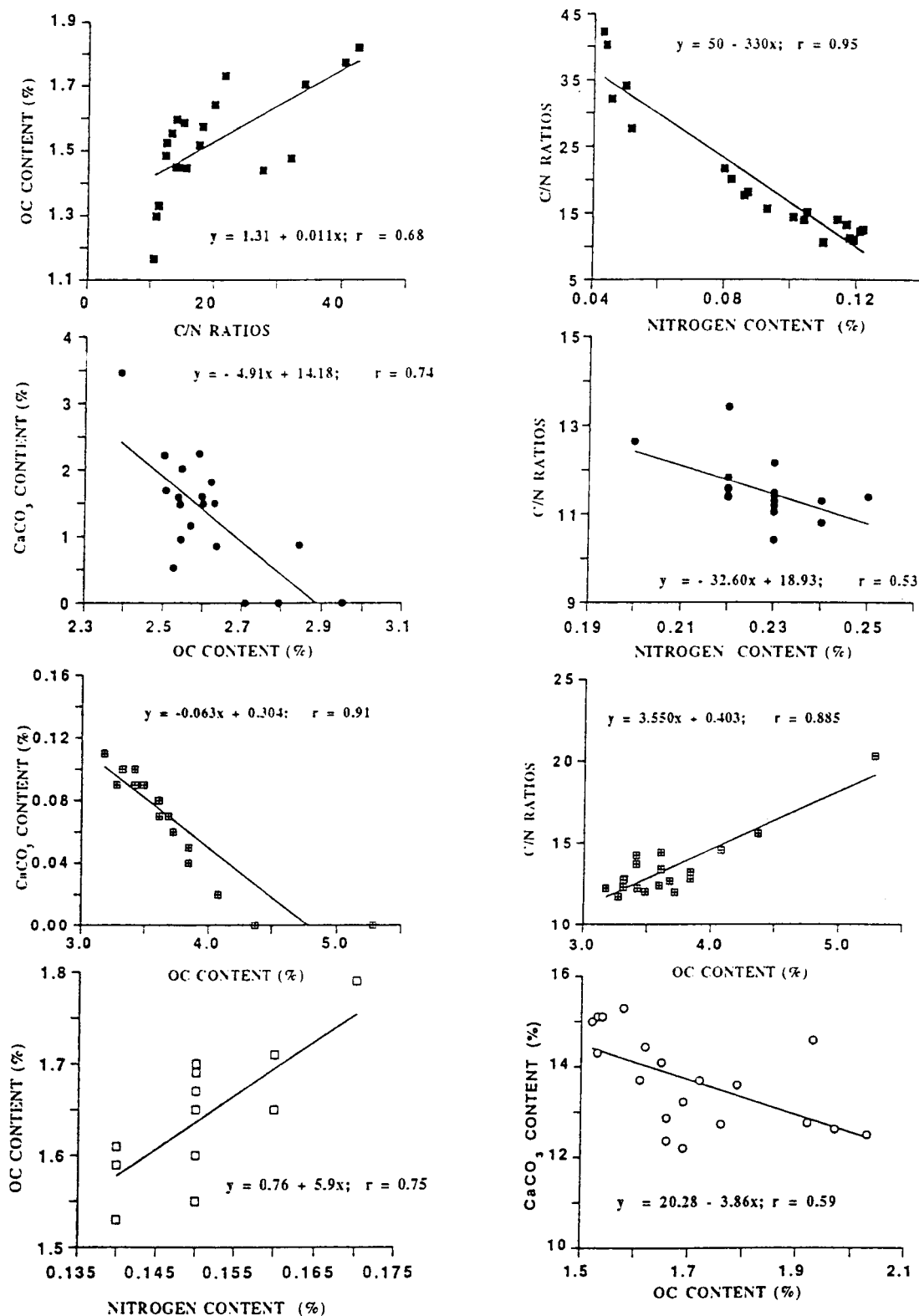


Fig. 4.26. Scatter plots for cores HU-90-031-13 BC (solid rectangle), HU-90-031-45 BC (crossed rectangle), HU-90-031-41 BC (solid circle), HU-90-031-17 BC (open circle) and HU-90-031-06 BC (open rectangle).

the strait of Cabot during the summer is relatively high compared to outflux (Yeats, 1988; Coote and Yeats, 1979). Hence, high concentrations of nutrients from the Atlantic Ocean on the Newfoundland side may be the cause of high $\delta^{15}\text{N}$ values, owing to complete utilization of available nutrients associated with high primary productivity. This inference is supported by a high content of OC at sites 06 BC and 41 BC relative to 34 BC. Low $\delta^{15}\text{N}$ values in conjunction with a high content of OC and nitrogen at 45 BC may be an indication of high primary productivity associated with incomplete utilization of nutrients.

Exclusion of sites 34 BC and 45 BC, results in mean $\delta^{15}\text{N}$ values which are higher than 8‰. The OM in the Gulf is generally isotopically heavier than that of the Labrador Sea. This can be attributed to denitrification processes or a high rate of utilization of available nutrients. Although denitrification processes cause an enrichment of ^{15}N in the residue, a positive correlation between ^{15}N and redox potential (Fig. 4.25), which may indicate preferential removal of compounds that are enriched ^{15}N during early diagenesis, excludes this possibility. However, a positive correlation might have been caused by low $\delta^{15}\text{N}$ values at site 34 BC which is associated with the lowest redox potential. Thus, most probably, a high rate of utilization of nutrients as indicated by high organic carbon content and recent primary productivity values that are higher than in the Labrador Sea (Stevenson, 1975), may be the cause of such differences in the isotopic compositions. Diagenetic changes alone can be excluded because isotopic alteration resulting from OM degradation could have led to higher values in the Labrador Sea where OM is highly degraded. This is because decomposing planktonic material has been found to be associated with enrichment in ^{15}N (Wada, 1980). Similarly, downcore increases in the degree of degradation of OM has been observed to be associated with enrichment in ^{15}N (Macko, 1981). However, no major diagenetic alteration of stable isotopes have been reported by various workers (e.g. Velinsky, 1991; Rau et al., 1987).

An increase in the content of OC with depth in the upper 5 cm at sites 13 BC and 59 BC may

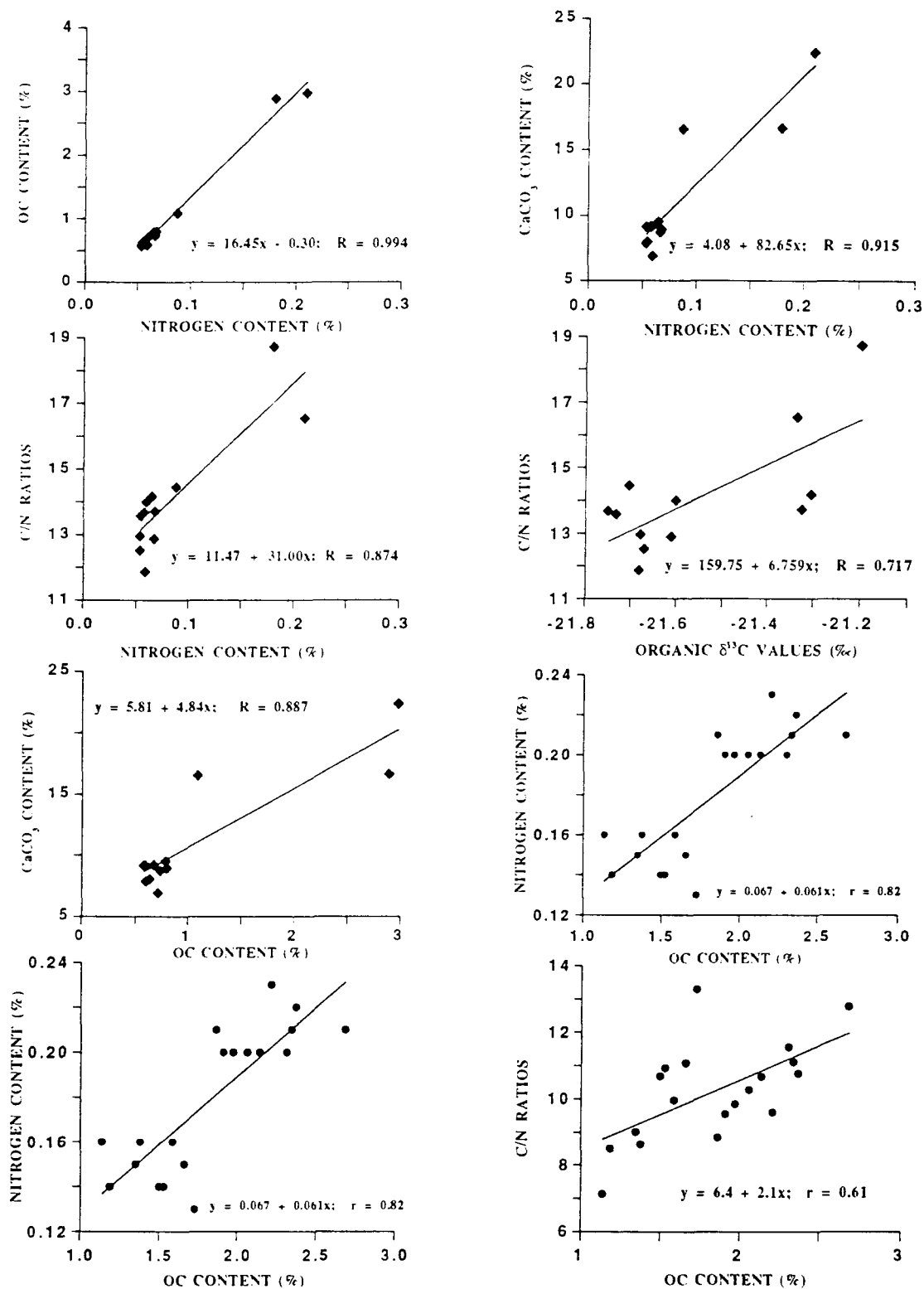


Fig. 4.27. Scatter plots for cores HU-90-031-43 PC (solid diamond), and HU-90-031-59 BC (solid circle).

be attributed to mixing by benthic organisms that transport labile material to a greater depth. The depth of 5 cm is close to the estimated mixed layer of 6 cm at site 13 BC (Jennane, 1992).

A systematic decrease in the content of OC and nitrogen with depth, as well as a slightly high C/N values (greater than 10), at sites 17 BC, 29 BC and 41 BC can be interpreted as an indication of diagenetic changes. The effects of diagenesis are exemplified by the significant negative correlation between OC and CaCO_3 at the 95% confidence level at these sites (Figs. 4.25 and 4.26). A negative correlation between OC content and CaCO_3 is expected particularly in areas with low content of CaCO_3 , because CO_2 released during early diagenesis is used to dissolve CaCO_3 owing to an increase in the acidity.

A constant C/N ratios at sites 17 BC, and 41 BC might indicate that the rate of degradation of carbon and nitrogen is the same. This inference is further supported by the positive correlation among nitrogen and carbon at these two sites (Fig. 4.26). Owing to a significant positive correlation between nitrogen and organic carbon at the 95% confidence level at sites 06 BC, 34 BC, and 59 BC (Figs. 4.25, 4.26 and 4.27), it is inferred here that there are equal rates of losses of carbon and nitrogen during early diagenesis at these sites.

Preferential loss of nitrogen over carbon is inferred here to occur at sites 13 BC, 29 BC, and 45 BC. Evidence of preferential loss of nitrogen over carbon for cores 29 BC and 45 BC is provided by the elevated values of C/N ratios which are associated with a decrease in the contents of both organic carbon and nitrogen. Lack of and/or a weak positive correlation between OC and nitrogen at these two sites, the negative correlation between C/N and nitrogen content at site 29 BC (Fig. 4.25), as well as a positive correlation between organic carbon and C/N ratios at site 45 BC (Fig. 4.26) may be a further indication of a slight preferential loss of the nitrogen bearing compounds than of carbon containing compounds. However, a downcore decrease of both organic carbon and nitrogen that is associated with an increase in the C/N ratios at site 29 BC may be an indication of downcore decrease

in the input of nitrogen rich OM. A preferential loss of nitrogen over carbon at site 13 BC is supported by an inverse relationship between organic carbon and nitrogen, positive correlation between organic carbon content and C/N ratios (Fig. 4.26), as well as negative correlation between nitrogen content and the C/N ratios (Fig. 4.26).

Diagenetic changes are intense in the upper 5 cm at site 43 PC, probably due to high refractory material, below 5 cm. A decrease in the C/N ratios with depth can be caused by a higher rate of loss of carbon containing compounds than of nitrogen containing compounds during diagenesis. However, a positive correlation between OC content and nitrogen content at this site indicate equal rate of loss of carbon and nitrogen during early diagenesis. Furthermore, a positive correlation between (i) contents of OC and CaCO_3 (Fig. 4.27), (ii) contents of CaCO_3 and nitrogen (Fig. 4.27), (iii) C/N and nitrogen content (Fig. 4.27), and (iv) C/N and $\delta^{13}\text{C}$ values (Fig. 4.27) may indicate that various parameters at this site are equally affected by the same processes of either diagenesis or primary productivity. In the upper 3-5 cm (which is associated with a decrease in ^{13}C), the contents of OC and nitrogen as well as an enrichment in ^{15}N may be due to diagenetic changes. The diagenetic changes are associated with a preferential removal of organic compounds enriched in ^{13}C such as proteins and carbohydrates (Hoef, 1982). It is most probable that the material which is enriched in lipids (which in turn is enriched in ^{12}C with respect to total plant material), and possibly the material which is rich in acidic amino acids (which is enriched in ^{15}N compared to other amino acids), contributes more than 30% of the total nitrogen. Macko et al. (1994) observed a decrease in ^{13}C content in glutamic acid, alanine, valine and glycine during decomposition experiments. The most dominant amino acids at this site are glutamic acid, glycine and aspartic acid, all of which are depleted in ^{13}C .

4.5.0. CONCLUSION

4.5.1. Labrador Sea

The result of this work indicates that there is a thin cover of the Holocene sediments for all cores that are located between water depths of 1300 m and 2800 m. The late Pleistocene sections are characterized by low values of organic carbon and nitrogen stable isotopes. A thin Holocene layer can be attributed to erosion and or non-deposition of sediments caused by the strong WBUC.

A downcore decrease in δ -values of organic carbon and nitrogen at sites located between water depths of 1300 m and 2800 m can be attributed to (i) diagenetic effects, (ii) changes in the rate of the utilization of nutrients between the late Pleistocene and the Holocene, and (iii) relative changes in the proportion of terrestrial OM during the late Pleistocene. A high concentration of terrestrial OM in the late Pleistocene core sections can be attributed to turbidity currents that were channelled through the NAMOC and its tributary as well as satellite channels, erosion or non deposition of OM caused by the strong WBUC which currently sweeps the Labrador Sea continental slope and rise. Low values of both $\delta^{13}\text{C}$ and $\delta^{15}\text{N}$ between 1300 m and 2800 m can also be attributed to deposition of reworked Cretaceous sediments from the Baffin Island as indicated by high content of reworked palynomorphs.

The offshore decrease in the isotopic compositions of organic carbon for the upper 5 cm off the Labrador coast most likely indicates lateral variations in the utilization of available nutrients. Furthermore, the result of the isotopic compositions of OC and nitrogen indicates that marine OM is confined to the upper 6-10 cm for sites located between 1300 m and 2800 m, as well as for all sites located on the Labrador shelf and deep basin.

Slight downcore increase in the C/N ratios at sites 05 BC, 14 BC, 28 BC and 93 BC can be interpreted as indication of preferential loss of nitrogen containing compounds. Furthermore, there is improvement in climatic conditions associated with increase in primary productivity during the Holocene as indicated by high enrichment in $\delta^{13}\text{C}$ and $\delta^{15}\text{N}$ at site 11 BC.

4.5.2. Gulf of St. Lawrence

1. Although the St. Lawrence river is one of the major rivers in the world, the influence of OM transported as suspended load to the Gulf of the St. Lawrence is minimum. Most of riverine allochthonous OM are trapped in the lower and upper estuary.
2. The results of the contents of organic carbon and nitrogen as well as the C/N ratios have indicated preferential loss of the nitrogen containing compounds over that of carbon containing compounds at several sites in the Gulf of St. Lawrence. This shows effect of diagenetic changes on the nitrogen bearing OM. This is further supported by a downcore decrease in the concentrations of THAA (Chapter 6).
3. Equal rates of nitrogen and carbon losses during early diagenesis occur at sites several sites in the Laurentian Channel.
4. A downcore decrease in C/N ratios, and contents of organic carbon and nitrogen at a sites located on the Scotian continental slope suggest a slightly higher rate of loss of carbon over nitrogen. Diagenetic model estimates of remineralized fractions organic carbon (Table 6.5) is about 6-8% higher than that of nitrogen.
5. Lower values of organic carbon and nitrogen stable isotopes observed at a site close to Cape Breton Island are partly due to high mixing of phytoplanktonic debris and macrophytes in the area that are likely to have lower isotopic values. This suggest that macrophytes might be one of the major contributors of organic carbon in the Gulf of St. Lawrence.
6. There is a high range of nitrogen stable isotopes values relative to that of organic carbon at each site, most probably due to susceptibility of nitrogen stable isotopes during microbial mineralization of OM.
7. Although there are slight shifts in the stable isotopic compositions of organic carbon that can be attributed to diagenetic changes, small ranges of $\delta^{13}\text{C}$ at many sites indicates that this parameter is a conservative tracer in the Gulf of St. Lawrence.

CHAPTER 5

5.0. GLACIAL-INTERGLACIAL VARIATIONS IN SOURCES OF ORGANIC MATTER, PALEOPRODUCTIVITY AND BURIAL RATES OF NITROGEN AND CARBON.

The primary productivity of OM by phytoplankton in the oceans is partly a function of the availability of nutrients such as nitrates and phosphates. A high concentration of nutrients in the euphotic zone resulting from upwelling, river runoff and regeneration result in a high primary productivity and thus high flux of OM to the sea floor. The nutrient supply in the ocean is governed by the oceanic circulation, which is further controlled by the prevailing climatic conditions.

The OC and nitrogen preserved in the sediments are related to bulk sedimentation rate and water depth (Suess, 1980; Ibach, 1982; Müller and Suess, 1979; Suess and Müller, 1980; Bertzer et al., 1984; Taylor and Karl, 1992). Similarly, the sedimentary OM is enriched in ^{13}C and ^{15}N when supplied dissolved CO_2 and NO_3^- are fully utilized during photosynthesis resulting in low fractionation. Because of this, various workers have used total OC content, stable isotopic compositions of OC and nitrogen and other productivity indicators preserved in the sediments to infer paleoproductivity and fluxes of particulate OM in the oceans (Pedersen, 1983; Stein, 1986a,b, 1991; Müller and Suess, 1979; Glenn and Arthur, 1985; Fontugne and Duplessy, 1986; Bonifay and Giresse, 1992; Howell and Thunell, 1992; Berger and Herguera, 1992; Sarnthein et al., 1987, 1988; Stein et al., 1986, 1989a,b; Littke et al., 1991; Cremer et al., 1992; Lyle et al., 1992; Paetsch et al., 1992; Reimers et al., 1992). Müller and Suess (1979) were the first researchers to use OC preserved in the sediments to quantitatively estimate paleoproductivity. Their equations have since been modified (Sarnthein et al., 1987, 1988, 1992; Stein et al., 1986, 1989a,b). The derivation of the formulas used to estimate paleoproductivity and fluxes of OM in this study is given in chapter 3. This chapter present geochemical results and estimated spacial and temporal paleoproductivity and burial rates of carbon and nitrogen.

5.1.0. GEOCHEMICAL RESULTS

5.1.1. HU-91-045-94 PC

The geochemical results of this core are presented in appendix 9.3.0, Table 5.1. The stable isotopic compositions of OC from the upper 640 cm of the core 94 PC show a general downcore decrease to approximately 120 cm, followed by a slight enrichment in ^{13}C to about 180 cm (Fig. 5.1). A minimum at about 120 cm which has been dated at approximately 8410 ± 80 ^{14}C ages (Hillaire-Marcel et al., 1994a), fall within a region with high contents of reworked palynomorphs (Fig. 5.2) and low contents of planktonic foraminifer and coccoliths per cm^3 (Hillaire-Marcel et al., 1994a). Omitting areas which are characterized by very low $\delta^{13}\text{C}$ values, the δ -values are relatively constant at approximately -23‰ between 180 and 500 cm. Below 500 cm to the base of the analyzed core section, an increase in ^{13}C values of up to 1‰ is noticeable. Five zones that are characterized by low $\delta^{13}\text{C}$ values are easily recognizable (Fig. 5.1) and correspond to zones of relatively high CaCO_3 content as well as low OC content. Four of the five zones occurring in interval 178-192, 220-250, 340-390 and 550-600 cm have been interpreted as Heinrich layers (H0, H1, H2 and H3), that were deposited during massive discharge of icebergs (Hillaire-Marcel et al., 1994a). Based on the ^{14}C ages the fifth zone is considered to be a result of turbidity deposition (Hillaire-Marcel et al., 1994a).

The Holocene section contain organic material enriched in ^{15}N relative to the upper Pleistocene section (Fig. 5.1). Generally, the $\delta^{15}\text{N}$ values increase downcore reaching an apex at about 100 cm (Fig. 5.1). Excluding zones corresponding to the Heinrich layers, the $\delta^{15}\text{N}$ values decrease with increasing depth from 100 cm to a depth of about 200 cm where they remains relatively constant down to the oxygen isotope stage 3/2 boundary at about 500 cm (Fig. 5.1). From there on there is a slight increase in $\delta^{15}\text{N}$ values down to the bottom of the analyzed core section. Apart from this general trend, there is a small zone depleted in ^{15}N at 120 cm (Fig. 5.1). Based on

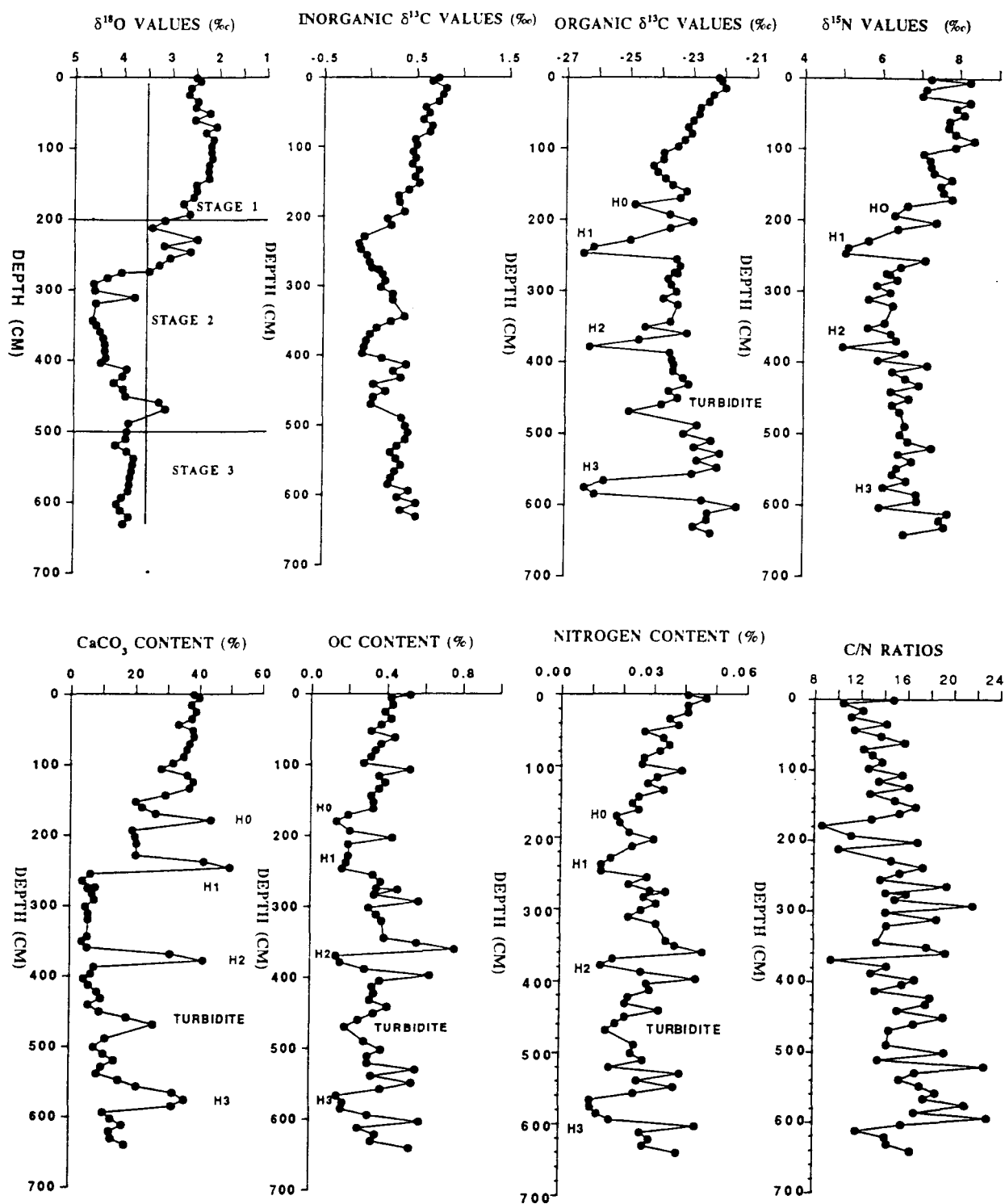


Fig. 5.1. Downcore variation of various geochemical parameters for core HU-91-045-94 PC.

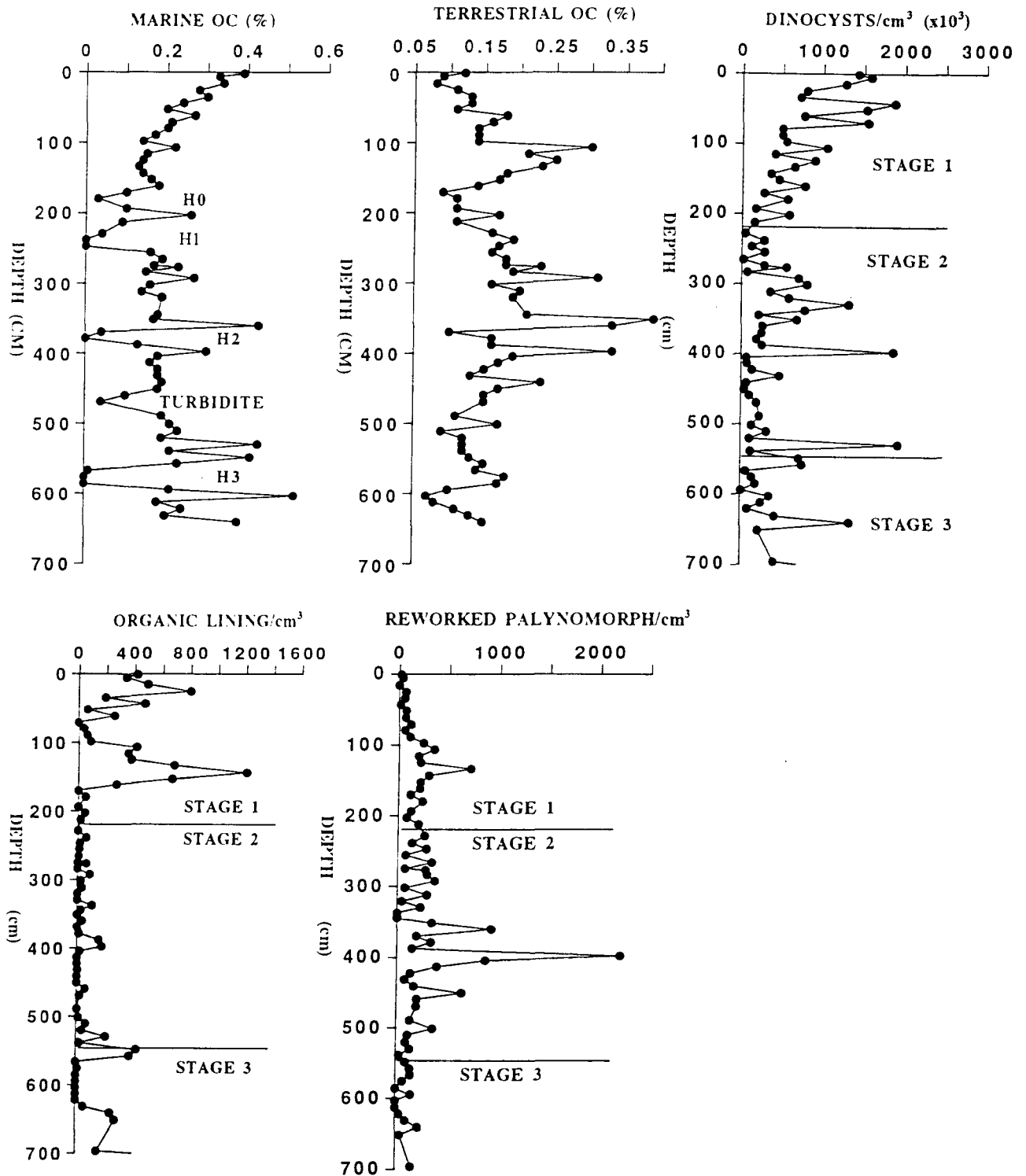


Fig. 5.2. Downcore variations in the contents of reworked palynomorphs, marine and terrestrial OM, dinocysts and organic lining of benthic foraminifera for core HU-91-045-94 PC (Source of micropalaeontological data: Hillaire-Marcel et al., 1994a).

this parameter alone, H1 and H2 have the lowest $\delta^{15}\text{N}$ values (less than 5.5‰) that correspond to low $\delta^{13}\text{C}$ values. The $\delta^{15}\text{N}$ values during H3 event are not significantly different from those above and below it. The $\delta^{15}\text{N}$ values for H0 and H3 are greater than 6‰ and may point to a different source of reworked materials. H0 most likely originated in areas which had marine deposits or reworked marine sediments.

The percent OC content is relatively low (appendix 9.3.0, Table 5.1). As with the case of OC stable isotopes, five zones of very low OC content corresponding to the Heinrich layers and turbidite can be easily identified (Fig. 5.1). With the exception of Heinrich layers, there is no significant difference in OC content between glacial and interglacial periods. However, using a two component mixing equation with -21‰ and -26‰ as marine and terrestrial end members respectively, core sections above 100 cm and below 500 cm, which fall within interglacial periods, contain a high proportion of marine OM (Fig. 5.2). Furthermore there is a systematic decrease in marine OC content with increasing depth down to about 200 cm at which point it remains relatively constant for the whole glacial interval (Fig. 5. 2). The proportion of terrestrial material increases with depth from the core surface reaching a local maxima at about 130 cm where it is followed by a decrease in OC content to about 200 cm (Fig. 5.2). From 200 cm there is a systematic increase in terrestrial OC content with depth down to about 450 cm, followed by a decrease to 641 cm (Fig. 5.2). The section representing materials deposited during the glacial period contains high proportion of terrestrial materials. A local maxima at 130 cm corresponds to a high proportion of reworked palynomorphs from Arctic Canada (Fig. 5.2; Hillaire-Marcel et al., 1994a) which may be an indication of re-initiation of the WBUC and/or the final stage of retreat of the Laurentide ice sheet.

The CaCO_3 content is higher in the interglacial core section than during glacial periods (Fig. 5.1). The upper 640 cm of the core contains five zones anomalously rich in CaCO_3 at the following core depths: 179 cm, 246 cm, 380 cm, 490 cm, and 590 cm (Fig. 5.1). The first layer, which

correspond to low $\delta^{13}\text{C}$ and $\delta^{15}\text{N}$ values, was deposited during the Younger Dryas when the climate changed abruptly from a deglaciation to glacial mode. Three layers at 246 cm, 380 cm and 590 cm were deposited during episodes of massive discharge of icebergs now known as the Heinrich layers.

The nitrogen contents are very low, and shows a general downcore decrease to about 200 cm, followed by a slight increase, reaching a local maxima at about 390 cm (Fig. 5.1). From this depth to about 470 cm there is a slight decrease in the nitrogen content, followed by an increase to the bottom of the analyzed core section (Fig. 5.1). Generally, there are no differences in nitrogen content between glacial and interglacial periods, and zones identified as Heinrich events also correspond to low nitrogen content (Fig. 5.1). In contrast, the C/N ratios does not show records of the Heinrich events, and shows a general two step increase with depth with a break near 300 cm below sea floor (Fig. 5.1).

5.1.2. HU-90-O13-13 PC

The sedimentological and geochemical data such as magnetic properties, inorganic $\delta^{13}\text{C}$, $\delta^{18}\text{O}$, abundance of benthic and planktonic foraminifers have been reported previously (Hillaire-Marcel et al., 1994a; Stoner et al., 1994a; Bilodeau et al., 1994; Wu and Hillaire-Marcel, 1994). This work provides additional geochemical results (appendix 9.3.0, Table 5.2). The $\delta^{13}\text{C}$ values of sedimentary OM at this site show a general downcore decrease, reaching a minimum at 279 cm (Fig. 5.3). The extrapolated age at this minima is about 8400 years, and corresponds to a minima observed at site 94 PC. Below 300 cm, these isotopic results indicate a general two step downcore increase to 618 cm (Fig. 5.3). A break separating these two steps occurs at 420 cm. Apart from this general trend, there are low $\delta^{13}\text{C}$ values recorded at about 350 cm and 400 cm. The extrapolated age for the record at 350 cm is about 9,000 B.P., while that of 400 cm represents the Younger Dryas event. Two zones of low $\delta^{13}\text{C}$ values, which have been previously interpreted as Heinrich events

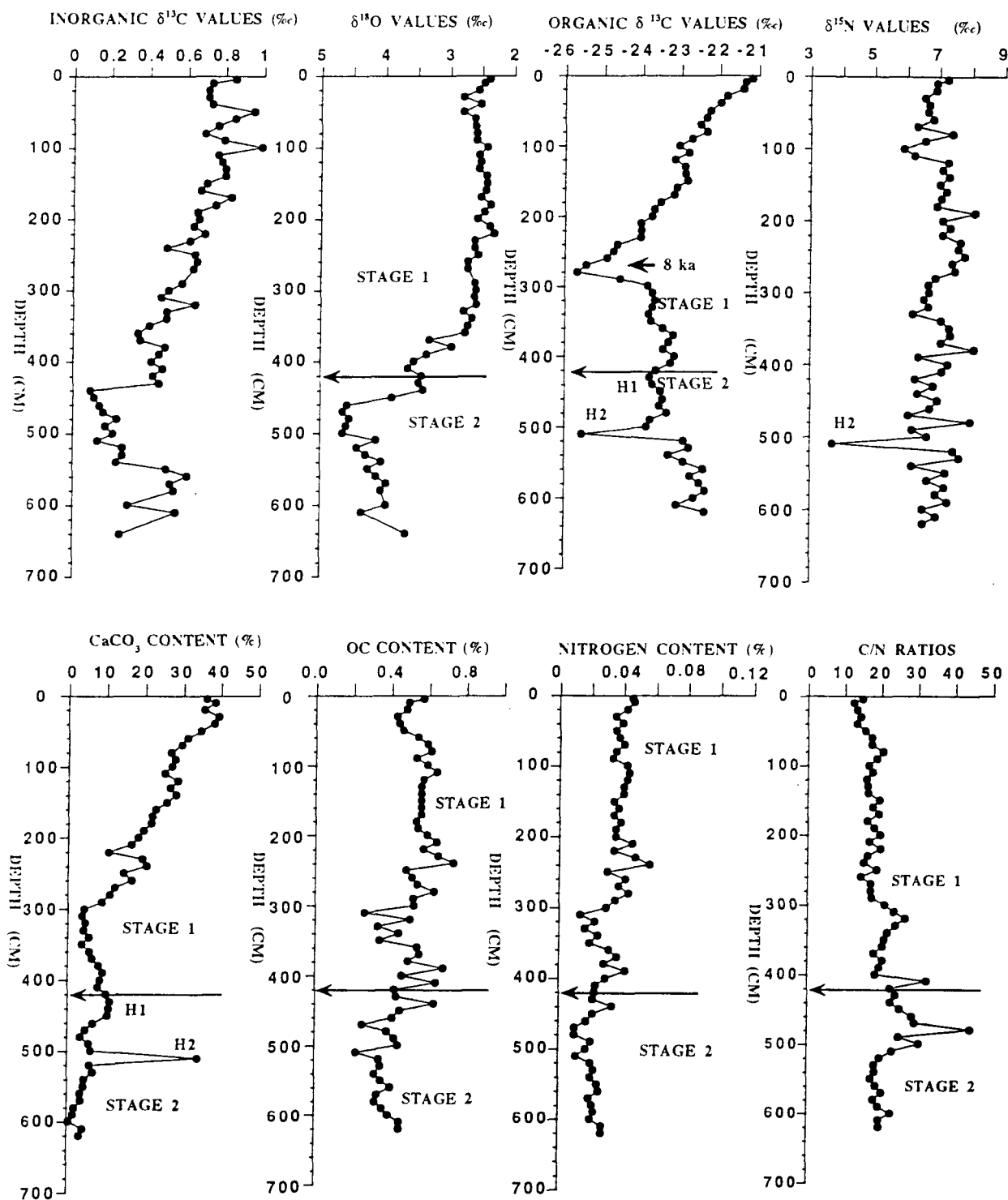


Fig. 5.3. Downcore variation of various geochemical parameters for core HU-90-013-13 PC.

based on the coarse fraction $>150\mu$ content and/or anomalously high CaCO_3 (Hillaire-Marcel et al., 1994a), occurs at 420 cm and 510 cm (Fig. 5.3).

The $\delta^{15}\text{N}$ values at this site decrease with depth in the upper 100 cm (Fig. 5.3). This depletion in ^{15}N with depth is followed by a slight downcore increase to ~250 cm, followed by a slight decrease to about 340 cm (Fig. 5.3). The $\delta^{15}\text{N}$ values shows high variability below this depth down to the base of the analyzed core (Fig. 5.3). Although the $\delta^{15}\text{N}$ values are highly variable, the Younger Dryas and two previously identified Heinrich events are characterized by low $\delta^{15}\text{N}$ values (Fig. 5.3). The Holocene period has slightly higher $\delta^{15}\text{N}$ values than the glacial period (oxygen isotope stage 2).

The CaCO_3 content is higher in the Holocene period than during the last glacial maximum (Hillaire-Marcel et al., 1994a; Fig. 5.3). This parameter show a general downcore decrease to about 300 cm, followed by a slight increase to about 450 cm (Fig. 5.3). Below 450 cm, it decreases to 620 cm (Fig. 5.3). The CaCO_3 content at 510 cm is anomalously high and correspond to low $\delta^{13}\text{C}$ and $\delta^{15}\text{N}$ values (Fig. 5.3). This interval, dated at about 20 ka, has been correlated to the Heinrich event H2 (Hillaire-Marcel et al., 1994a). Low CaCO_3 content occurs near 200 cm and 300-450 cm (Fig. 5.3). The event at 300-350 cm predate the most depleted ^{13}C values which is centred at about 279 cm (Fig. 5.3). Heinrich event H1 is marked by slightly higher CaCO_3 content (Fig. 5.3).

The OC content at this site is highly variable. Owing to the high variability, smoothing using a three point moving average method was performed. Generally, the last glacial maximum contains low OC contents compared to the Holocene period (Fig. 5.3). The core section between 329 and 350 cm has a low OC content while the intervals centred at 200 cm, 279 and 400 cm have relatively high OC contents (Fig. 5.3).

Total nitrogen at this site is very low, and Holocene core sections contain slightly more nitrogen (Fig. 5.3). This result is similar to that previously reported by Hall et al (1989) from nearby

site 646, ODP Leg 105. Two Heinrich events identified in this study are characterized by low nitrogen contents. The interval between 300 and 350 cm contains the lowest total nitrogen (Fig. 5.3). With regard to the C/N ratios, which have a mean value of 19.9 ± 5.0 , a general downcore increase is observable (Fig. 5.3). Events between 300-350 cm and 400-510 cm have relatively high C/N ratios (Fig. 5.3).

5.1.3. HU-90-031-44 PC

All geochemical results for this core are presented in appendix 9.3.0, Table 5.3. The $\delta^{13}\text{C}$ values decrease with depth in the upper 80 cm followed by a slight increase to about 180 cm (Fig. 5.4). The interval between 180 cm and 200 cm (younger dryas) is characterized by low OC stable isotope values relative to sections above and below it (Fig. 5.4). Below 200 cm the organic $\delta^{13}\text{C}$ decrease with depth to approximately 800 cm followed by an increase down to the base of the core (Fig. 5.4). The Holocene core section contains OM which is most enriched in ^{13}C relative to the late Pleistocene period. Moreover, core sections older than 12,400 years (Fig. 5.4; appendix 9.3.0, Table 5.3) contain the most depleted values, while the core section that ranges from 10,000 to 12,400 years (^{14}C ages) has organic $\delta^{13}\text{C}$ values which range from -22.2‰ to -23.3‰ and average value of -22.7‰ .

The $\delta^{15}\text{N}$ values in the upper 150 cm are greater than 7.5‰ , and increase slightly with depth (Fig. 5.4). There is an abrupt change in the isotopic composition of nitrogen at about 160 cm (Fig. 5.4). The interpolated age of this sharp change in the stable isotopic compositions is about 10,000 B.P. The nitrogen isotope values below 160 cm show a general downcore decrease with depth to approximately 800 cm, followed by a slight increase to the base of the core (Fig. 5.4). The core section older than 12,000 years contains the most depleted $\delta^{15}\text{N}$ values.

The OC content increases slightly in the upper 20 cm then decreases to about 100 cm (Fig.

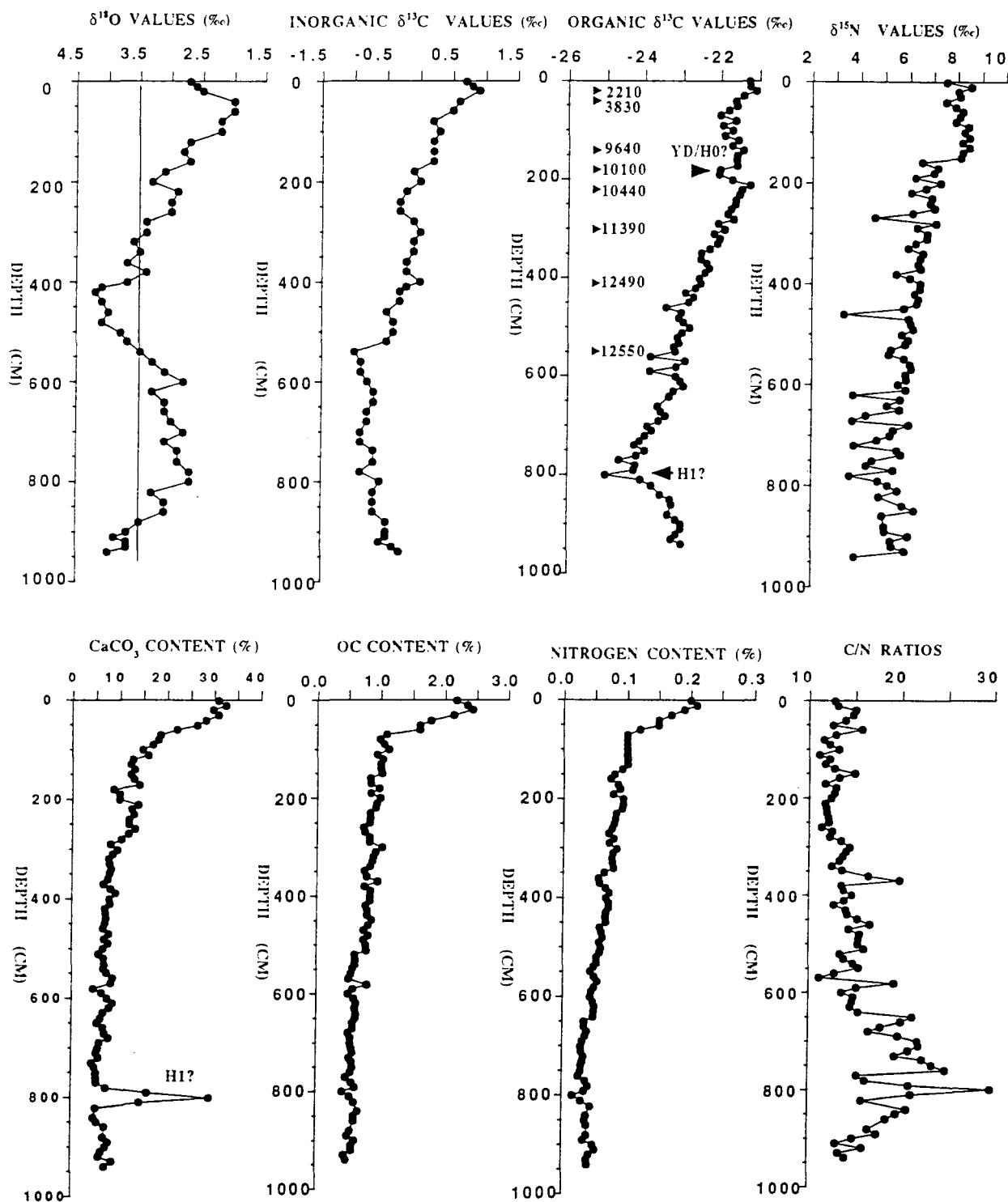


Fig. 5.4. Downcore variation of various geochemical parameters and ^{14}C ages for core HU-90-031-44 PC. H0?

and H1? possibly represent Heinrich Events, while YD is an abbreviation for the Younger Dryas.

5.4). Below 100 cm, there is a gradual decrease down to the base of the core (Fig. 5.4). Similarly, nitrogen content decreases sharply in the upper 100 cm followed by a gradual downcore decrease to the base of the core (Fig. 5.4). The lowest value occurs at about 800 cm. This depth interval is associated with low $\delta^{13}\text{C}$ value and high C/N ratios as well as high CaCO_3 .

Like OC and nitrogen contents, CaCO_3 decrease sharply in the upper 100 cm, followed by a gradual decrease to the base of the core (Fig. 5.4). Apart from this general trend, there is a high peak at 800 cm (Heinrich event H1?) below sea floor (Fig. 5.4). This peak corresponds to relatively low $\delta^{13}\text{C}$ values. A peak at 800 cm may be indicative of detrital carbonate derived from the St. Lawrence platform where limestones of Cambro-Ordovician to Silurian rocks occur (Loring, 1975). Similarly, downcore variation in the C/N ratios show a general increase, reaching its peak at about 800 cm (Fig. 5.4). Below 800 cm, the C/N ratios decrease with depth (Fig. 5.4).

5.2.0. VARIATION IN ACCUMULATION RATES AND PRIMARY PRODUCTIVITY

5.2.1. Lateral Variation in Accumulation Rates

Excluding site 41 BC which has the highest accumulation rate of OC and nitrogen, the accumulation rate of OC in the Gulf of St. Lawrence-Scotia slope decreases with increasing water depth along the Laurentide channel (Fig. 5.5). Similarly, the burial rate of nitrogen decreases with increasing water depth along the same transect (Fig. 5.5). By comparison, accumulation rates of both OC and nitrogen are higher in the Gulf than in the Labrador Sea. Accumulation of both OC and nitrogen in the Labrador Sea is highest at sites located at greater depths (Fig. 5.5). The estimated accumulation rates of OC and nitrogen in the upper few cm of cores from the Gulf-Scotia slope ranges from 400.3 to 621.5 $\text{mgC/m}^2/\text{yr}$, whereas that of nitrogen range from 28.3 to 55.0 $\text{mgN/m}^2/\text{yr}$ (appendix 9.3.0, Table 5.4). Similarly, the estimated accumulation rate of OC in the Labrador Sea ranges from 12.6 to 188.2 $\text{mgC/m}^2/\text{yr}$, while that of nitrogen range from 1.0 to 33.7 $\text{mgN/m}^2/\text{yr}$ (appendix 9.3.0, Table 5.4).

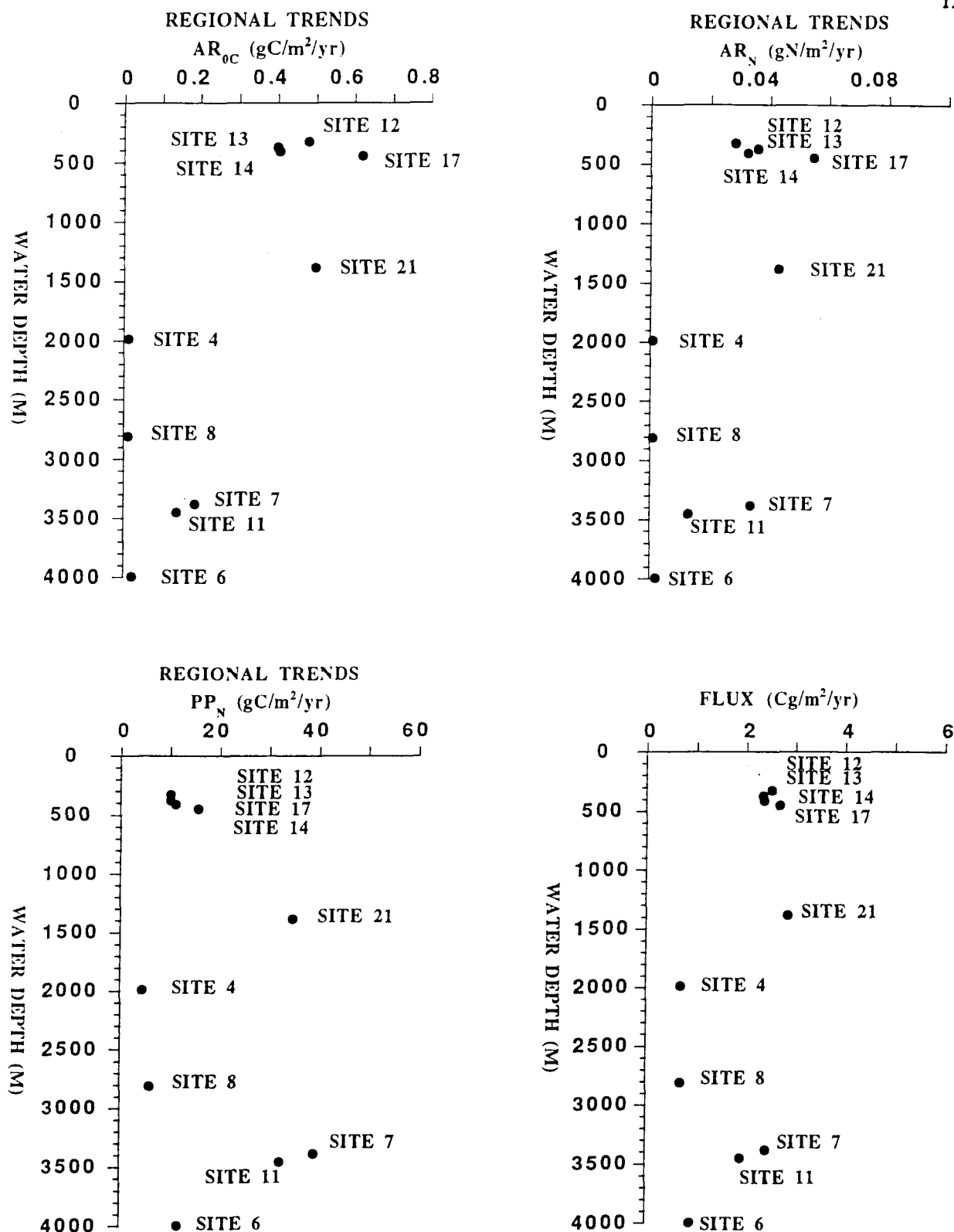


Fig. 5.5. Regional variation in burial rates of total organic carbon (AR_{OC} (gC/m²/yr) and nitrogen (AR_N (gN/m²/yr), paleoproductivity and paleoflux in the Labrador Sea and Gulf of St. Lawrence-Scotia slope. For location of sites refer to Figs. 3.1 and 3.2.

The estimated lateral variation in the primary productivity is higher in the Gulf than in the Labrador Sea (Fig. 5.5). Primary productivity for the Gulf of St. Lawrence ranges from 63.4 to 117.8 gC/m²/yr, while that of the Labrador Sea ranges from 42.6 to 125 gC/m²/yr (appendix 9.3.0, Table 5.4). Differences in the burial rate, primary productivity, and flux of OC between the Labrador Sea and the Gulf of St. Lawrence are due to the differences in supplies of nutrients and preservation efficiency of OM between the two areas. Owing to many sources of nutrients in the Gulf of St. Lawrence compared to the Labrador Sea (see Chapter 2), concentrations of nutrients are likely to be higher in the Gulf of St. Lawrence than in the Labrador Sea.

As stated previously in section 1.1.0., sedimentation rate has been pointed out to be one of the factors controlling preservation of OM (Canfield, 1994). Lower sedimentation rates for most of the cores from the Labrador Sea relative to that of the Gulf of St. Lawrence, requires preservation of OM in a reducing environment. However, the on-site determination of redox potential has indicated that the oxygen penetration depth is high compared to the Gulf of St. Lawrence, which is mainly reducing (Figs. 3.3 and 3.4). Therefore, differences in the oxygen penetration depth as well as supplies of nutrients, may explain the observed differences in burial rate and paleoproductivity. The high burial rates of OM in the Labrador Sea at sites 13 PC and 94 PC can be attributed to the sediment focusing, i.e. fine sediments eroded from the continental slope by the strong WBUC are deposited down slope (Hillaire-Marcel et al., 1994b).

5.2.2. Glacial-Interglacial Variation in Burial Rate

The estimated burial rate for the total OC at site 11 BC ranges from 5 to 16 mgC/m²/yr, while that of marine OM ranges from 2.8 to 9.6 mgC/m²/yr (appendix 9.3.0, Table 5.5). The burial rate of nitrogen ranges from 0.25 to 0.99 mgN/m²/yr (appendix 9.3.0, Table 5.5). Similarly the estimated new primary productivity in the euphotic zone ranges from 2.4 to 5.3 gC/m²/yr (appendix

9.3.0, Table 5.5). Total paleoproductivity values range from 31 to 46 gC/m²/yr. Based on these results, the paleoflux of the marine autochthonous OC to the sea floor ranges from 0.45 to 0.77 gC/m²/yr. From the above estimates, about 0.02% of the OM produced in the euphotic zone is buried, while only about 1.6% of OM reaching the sea floor is preserved.

The estimated marine primary productivity decrease downcore to about 15 cm (~8700 years) followed by a slight increase to the base of the core (Fig. 5.6). Furthermore, there are no significant differences in the estimated primary productivity between the glacial-interglacial transition and the middle to late Holocene (Fig. 5.6). Lack of differences in the estimated primary productivity between the Holocene and the late Pleistocene is contrary to various primary productivity indicators, which indicate high primary productivity during the Holocene and low levels during the late Pleistocene (Fig. 5.7). The differences may be due to large quantities of reworked marine OC during the late Pleistocene which can not be separated from unreworked material using stable isotopes of OC and nitrogen. This might explain the high values of $\delta^{15}\text{N}$. Various primary productivity indicators preserved in the sediments suggest that the onset of high primary productivity was at about 8500 BP, and the late Pleistocene was associated with low primary productivity. Because of large differences in the sedimentation rates, unequivocal comparisons of primary productivity between the last glacial maximum and the Holocene cannot be made. However, high OC content below 15 cm may indicate preferential preservation of OM owing to high sedimentation rate.

The burial rate of nitrogen decreases downcore to about 13 cm, followed by a slight increase to the base of the core (Fig. 5.6). The burial rate of nitrogen is higher during the Holocene period than during the late Pleistocene. In contrast, the burial rate of marine OC is slightly higher during the late Pleistocene than during the Holocene (Fig. 5.6). Higher burial rates of nitrogen during the Holocene over the late Pleistocene indicate a preferential preservation of nitrogen during the Holocene than during the late Pleistocene period. This can be attributed to an increase in primary

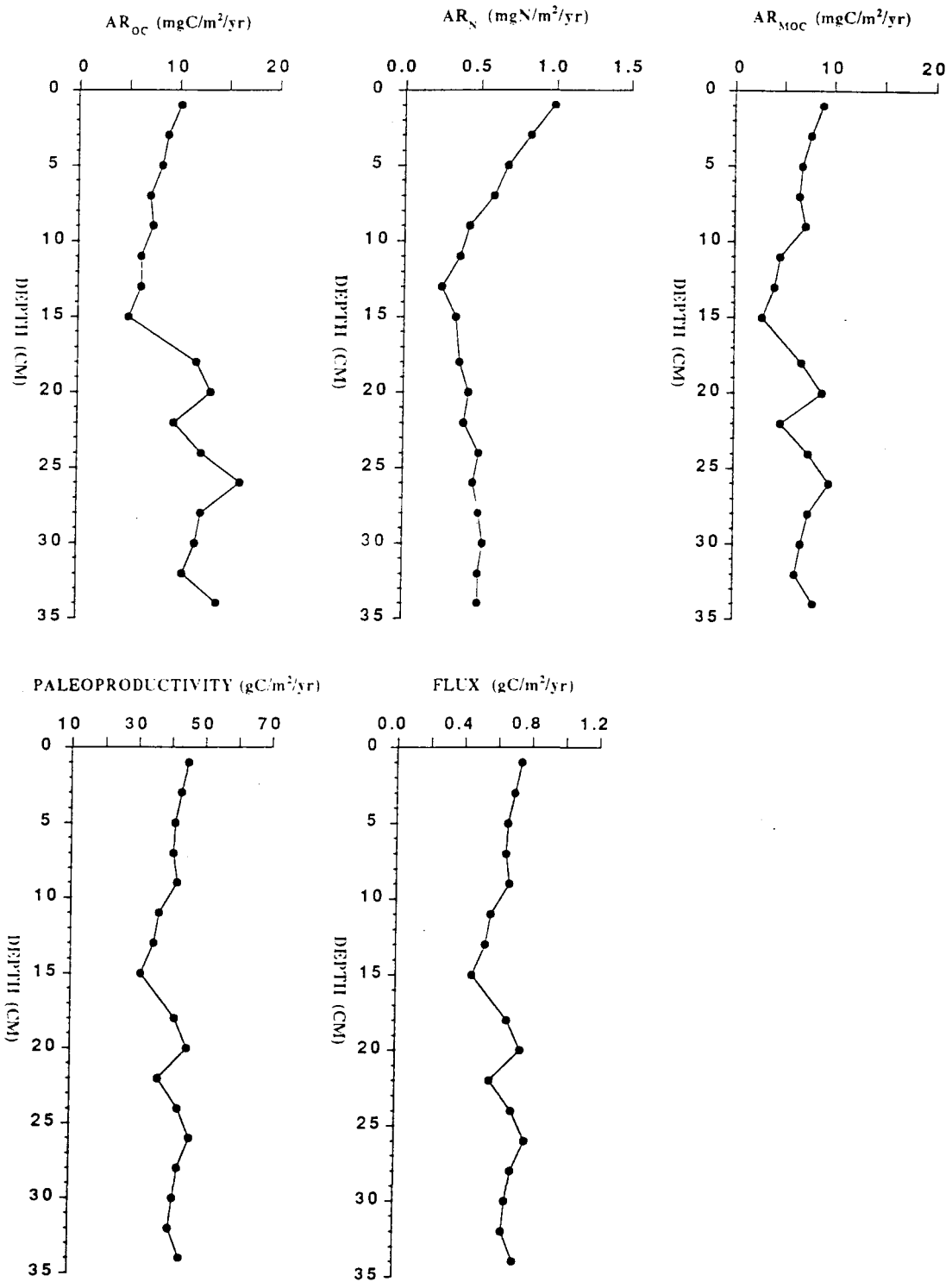


Fig. 5.6. Downcore variation in burial rates of total organic carbon (AR_{OC} (gC/m²/yr) nitrogen (AR_N (gN/m²/yr) and marine organic carbon (AR_{MOC} (gC/m²/yr), paleoproductivity and paleoflux at site HU-90-013-11 BC.

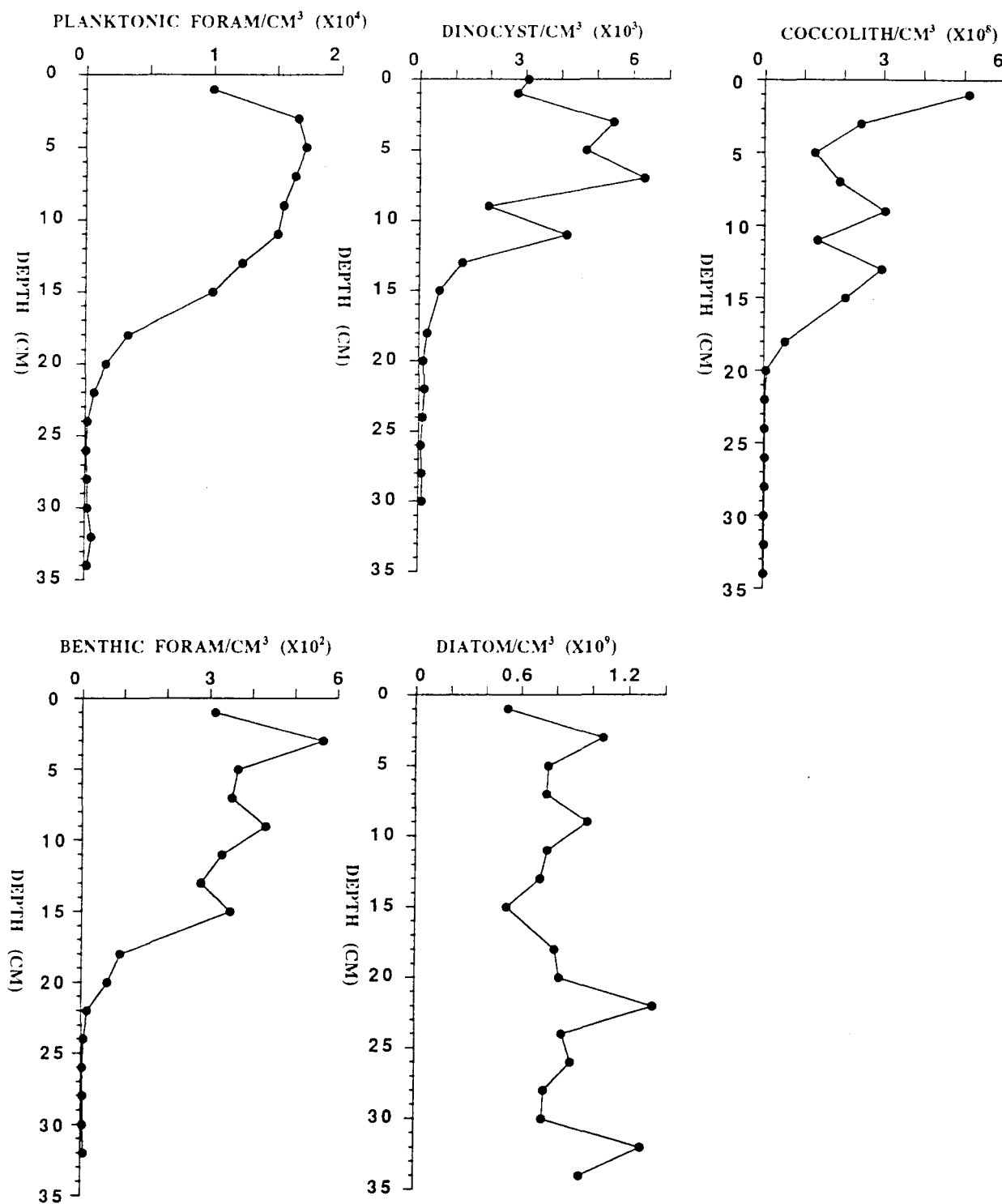


Fig. 5.7. Downcore variation in various primary productivity indicators at Site HU-90-013-

11 BC (Source Hillaire-Marcel et al., 1994b).

productivity and/or preferential downcore diagenetic loss of nitrogen, as partly indicated by a downcore increase in the C/N ratios (Fig. 4.10).

The estimated burial rates of the total OC for core 94 PC which are presented in appendix 9.3.0, Table 5.6, range from 38 to 204 mgC/m²/yr, while those of autochthonous marine organic carbon are as high as 139 mgC/m²/yr. The burial rate of nitrogen ranges from 3 to 13 mgN/m²/yr. The paleoproductivity at this site is as high as 115 gC/m²/yr. Similarly the flux of the autochthonous marine OM is as high as 2.33 gC/m²/yr. From these estimations, about 0.07% of the OM produced in the euphotic zone is preserved. About 4% of autochthonous OM reaching the sea floor is buried.

With the exception of the upper 100 cm, there are no significant differences in the estimated primary productivity, fluxes as well as burial rates of OM at this site (Fig. 5.8). The burial rate of nitrogen is slightly higher during the Holocene period than during the last glacial maximum (Fig. 5.8). The high burial rate of total OC during the glacial period can be attributed to high input of terrestrial OM that is resistant to degradation after entering the marine environment.

Results of estimated paleoproductivity and burial rates of nitrogen and carbon for rate of marine OM ranges from 5 to 246 mgC/m²/yr. The flux of marine OM ranges from 0.55 to 2.93 gC/m²/yr. With respect to the estimated paleoproductivity, which ranges from 39 to 136 gC/m²/yr, the OM which reaches the sea floor is about 2%, and the material buried is about 0.1% of the total productivity. About 6% of the autochthonous OM that reaches the sea floor is preserved. These results are in agreement with those of Stein et al. (1989a), who estimated that the burial rate of site 13 PC are presented in appendix 9.3.0, Table 5.7. The estimated burial rate for the total OC at site 13 PC ranges from 34 to 566 mgC/m²/yr, whereas that of nitrogen ranges from 1.3 to 43 mgN/m²/yr. The burial marine OM in the Labrador Sea is lower than 300 mg/cm²/ky. Similarly the total primary productivity estimated in this study falls within the range estimated by the same author for the Pleistocene.

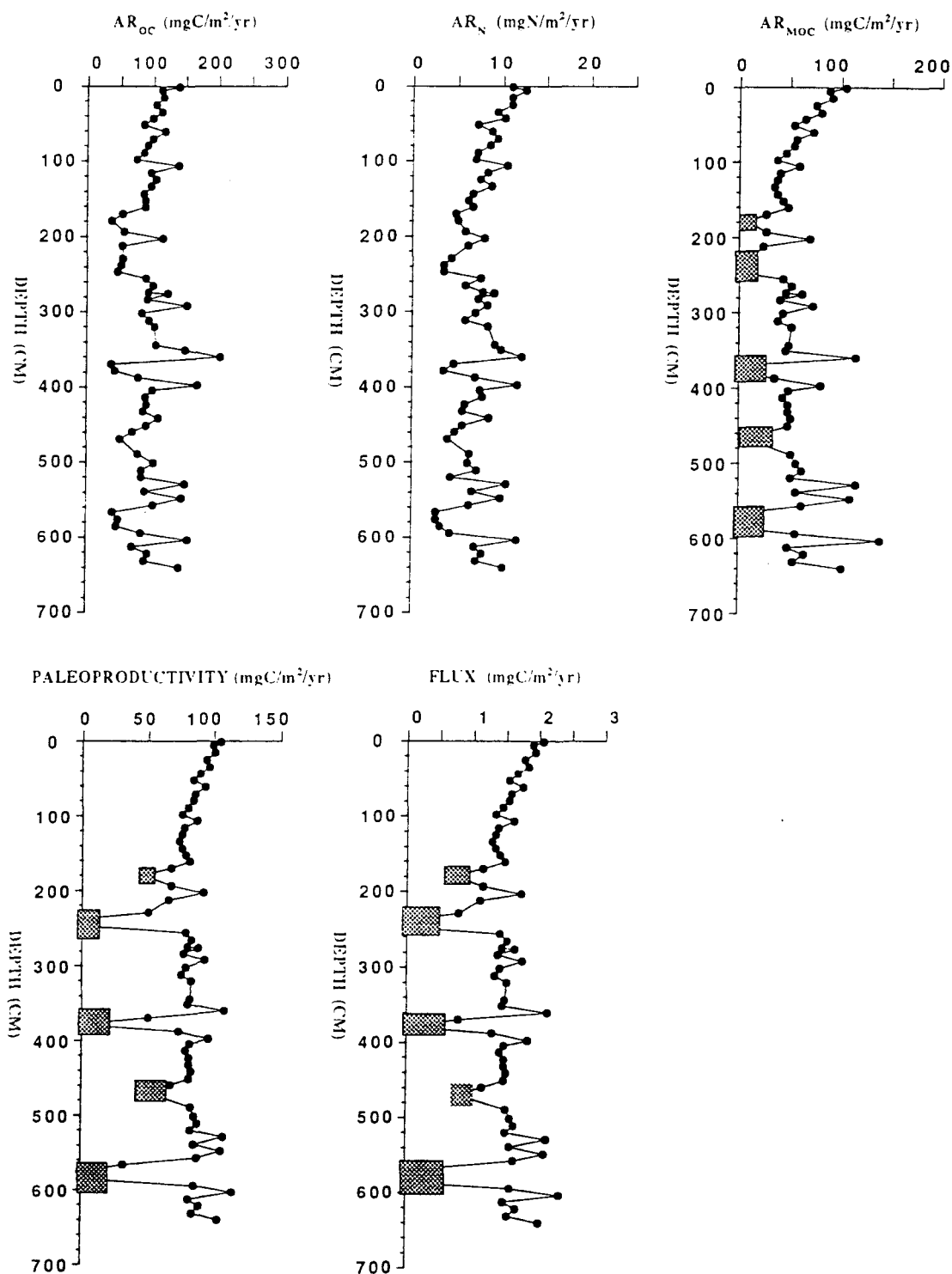


Fig. 5.8. Downcore variation in burial rates of total organic carbon (AR_{OC} ($gC/m^2/yr$), nitrogen (AR_N ($gN/m^2/yr$)) and marine organic carbon (AR_{MOC} ($gC/m^2/yr$), paleoproductivity and paleoflux at Site HU-91-045-94 PC.

The estimated primary productivity at site 13 PC is higher during the Holocene period (particularly after 7500 ^{14}C ages) than it was during the last glacial maximum (Fig. 5.9). Similarly, the burial rate is higher during the Holocene period than that of the last glacial maximum (Fig. 5.9). Low primary productivity is estimated between 8800 and 7700 ^{14}C ages. The estimated flux of marine OM is higher during the Holocene than during the late Pleistocene, and decrease downcore to the base of the core. Higher burial rates, paleoproductivity and fluxes during the Holocene are in accord with the downcore distribution of primary productivity indicators (Fig. 5.11).

The estimated burial rate, paleoproductivity and flux of OC for core 44 PC are given in appendix 9.3.0, Table 5.8. The total accumulation rate of OC at site 44 PC ranges from 0.28 to 3.6 $\text{gC/m}^2/\text{yr}$, and has burial rates of autochthonous marine OM which range from 0.23 to 2.11 $\text{gC/m}^2/\text{yr}$. The burial rate of nitrogen ranges from 0.02 $\text{gN/m}^2/\text{yr}$ to 0.26 $\text{gN/m}^2/\text{yr}$. The total primary productivity ranges from 91 to 181 $\text{gC/m}^2/\text{yr}$. The estimated total paleoproductivity ranges from 21 to 82 $\text{gC/m}^2/\text{yr}$. The fraction of autochthonous OM preserved in the sediments is about 0.8% of the total primary productivity in the euphotic zone. The OM produced in the euphotic zone which reaches the sea floor is about 4% at the most. The burial rate, fluxes and paleoproductivity increase downcore to about 450 cm, followed by a decrease to the base of the core (Fig. 5.10). The Holocene period has lower estimated burial rate and primary productivity compared to the late Pleistocene (Fig. 5.10). High primary productivity during the late Pleistocene at this site can be attributed to either high input of nutrients during meltwater discharge or reworking of marine OM.

The lack of differences in the estimated primary productivity and accumulation rates between glacial and interglacial periods (prior to about 8 ka) at sites 11 BC and 94 PC is in agreement with the work of Coppedge and Balsam (1992) who observed lack of difference in the OC content between glacial and interglacial periods. This may either indicate that the area experienced similar

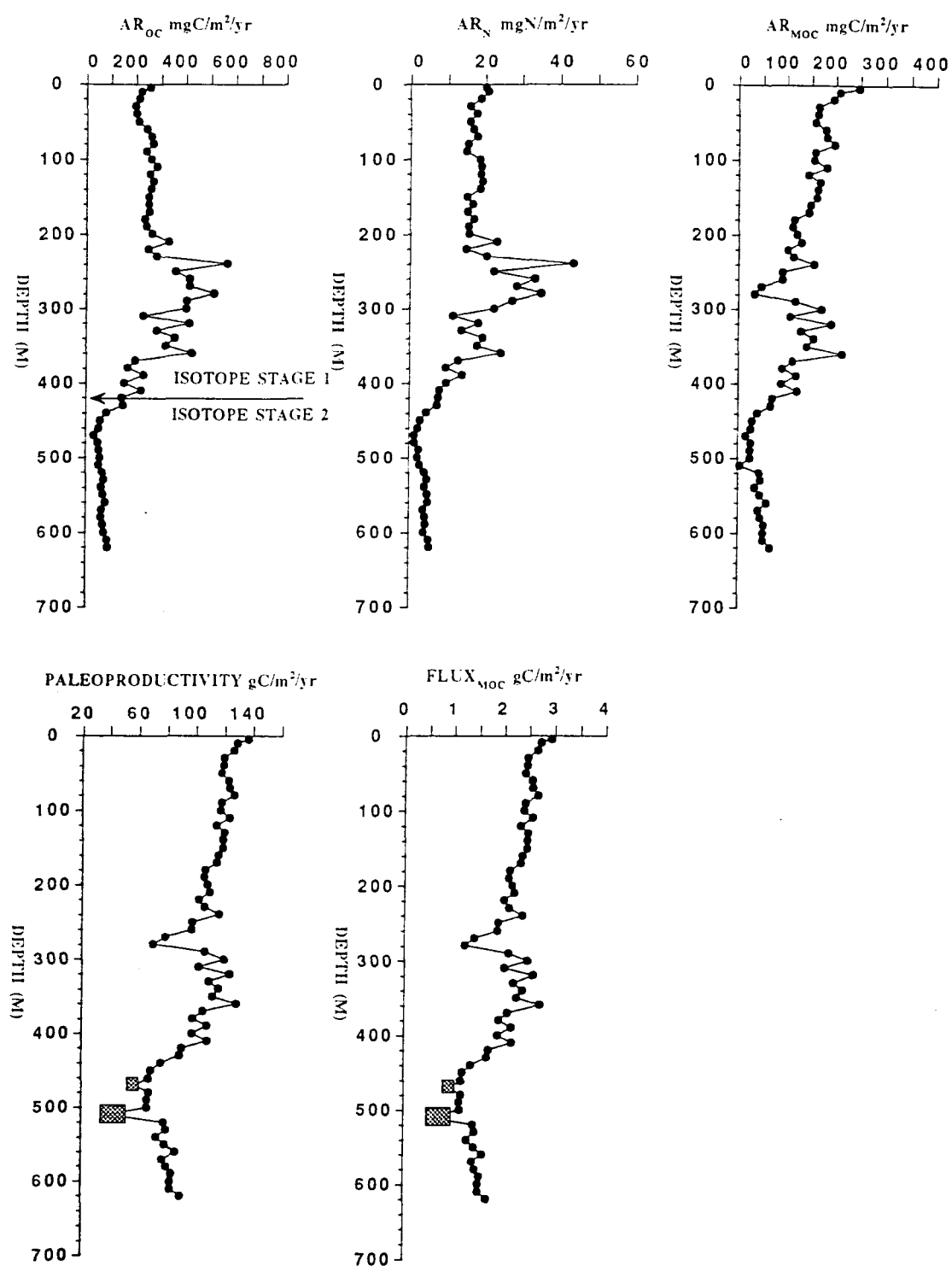


Fig. 5.9. Downcore variation in burial rates of total organic carbon (AR_{OC} (gC/m²/yr) nitrogen (AR_N (gN/m²/yr) and marine organic carbon (AR_{MOC} (gC/m²/yr), paleoproductivity and paleoflux at Site HU-90-013-13 PC.

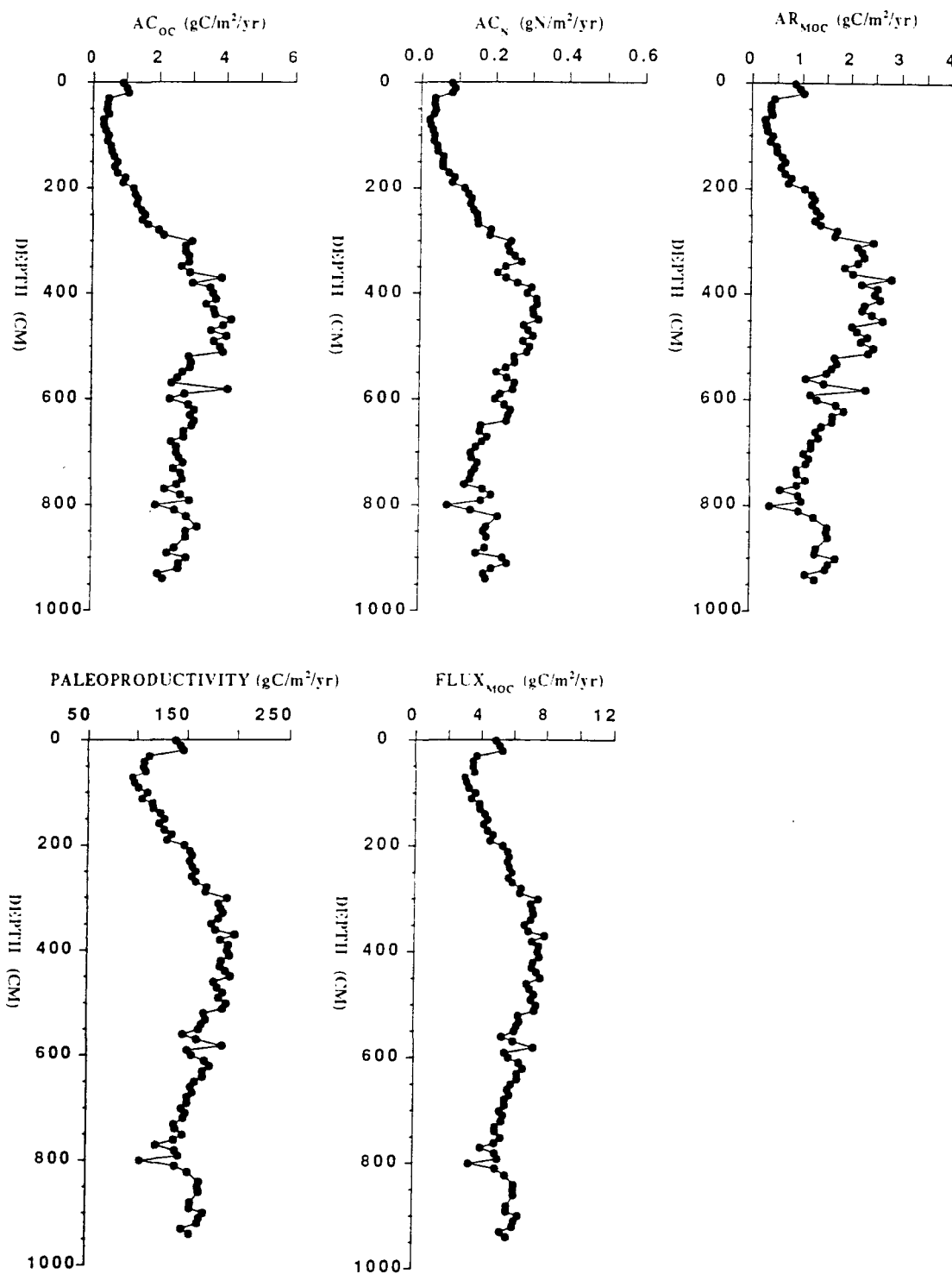


Fig. 5.10. Downcore variation in burial rates of total organic carbon (AR_{OC} ($gC/m^2/yr$), nitrogen (AR_N ($gN/m^2/yr$), and marine organic carbon (AR_{MOC} ($gC/m^2/yr$), paleoproductivity and paleoflux at Site HU-90-031-44 PC.

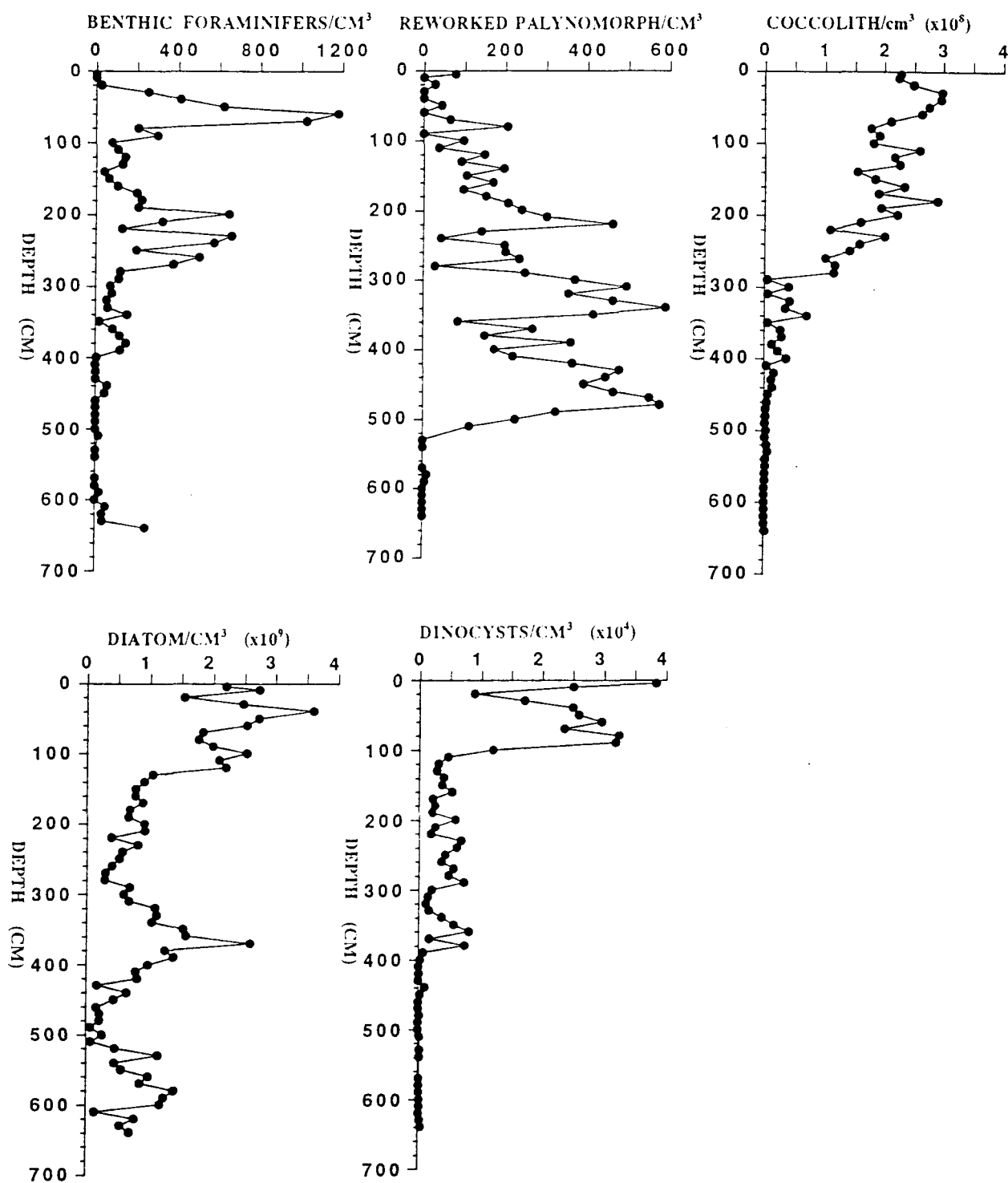


Fig. 5.11. Downcore variation in reworked palynomorph and various primary productivity indicators at Site HU-90-013-13 PC (Source Hillaire-Marcel et al., 1994b).

magnitude of production but under different physical/chemical conditions or the primary productivity was low during glacial period but preservation of reworked marine OM (which can not be separated from unreworked material using stable isotopes and C/N ratios) was high. Based on the diatom assemblages, Sancetta (1992) concluded that plankton biomass was at least as high as it is today in the North Atlantic. He hypothesized that the presence of numerous icebergs, possibly associated with sea ice, supported high production by physical mechanisms such as turbulent mixing and enhanced density stratification and/or biogeochemical ones such as supply of major nutrients. The diatom concentration is high and shows no differences between glacial and interglacial concentrations at site 11 BC (Fig. 5.7). A high concentrations of diatoms occurs in the upper 120 cm at site 13 PC (Fig. 5.11), below, there are no major differences in the concentration of diatoms. In contrast, concentrations of other primary production indicators are low. This might be an indication that during the glacial period, compared to the Holocene period, diatoms were major producers of OM. This inference is in accord with that of Sancetta (1992). The concentration of diatoms per cm³ is very high compared to other primary productivity indicators, which implies that diatoms in the Labrador Sea have been and still are the major producers of OM.

High primary productivity during the glacial period is most unlikely. High values of estimated primary productivity during glacial and transition periods can be attributed to the deposition of reworked marine OM that can not be easily distinguished from unreworked using stable isotopes of OC and nitrogen as well as the C/N ratios. A low primary productivity is supported by low abundances of various primary productivity indicators including dinocysts, benthic foraminifers and dinoflagellate at all sites.

The OM preserved in the sediments at these four sites is less than 1%. High rates of OM oxidation occur at site 11 BC, while a slight preferential preservation of OM occurs at site 13 PC. Differences in preservation of OM in the Labrador sea as well as the Gulf of St. Lawrence-Scotia

slope can be attributed to differences in primary productivity and sedimentation rates. The estimated low sedimentation rate at site 11 BC have partially been attributed to the strong bottom current of the WBUC which sweeps the area.

5.3. DISCUSSION

5.3.1. HU-91-045-94 PC

The isotopic results in conjunction with contents of CaCO_3 , OC and nitrogen indicate that the previously identified Heinrich events H0, H1, H2 and H3 at this site (Hillaire-Marcel et al., 1994a) are characterized by very low $\delta^{13}\text{C}$ and $\delta^{15}\text{N}$ values, low contents of OC and nitrogen as well as high contents of CaCO_3 . Low δ -values observed at this site during episodes of ice rafting of debris can be attributed to high inputs of terrestrial OM, most probably derived from eastern Canada. Based upon the Nd-Sr isotopic compositions of material constituting different Heinrich events, H1 and H2 have been inferred to have a large component of material from eastern Canada (Grousset et al., 1993). The inference of an eastern Canadian source area is further supported by a marked westward increase in the thickness of the carbonate layers (Bond et al., 1992; Dowdeswell et al., 1995). Based on inverted ^{14}C AMS ages, the event at 460-670 cm depth interval has been interpreted as a turbidite (Hillaire-Marcel et al., 1994a). However, this event may correlate to the Heinrich event H2a inferred from ice core records by Mayewski et al. (1994).

In estimating the proportion of terrestrial OM, the terrestrial end member value of -26‰ was used. The use of this value is supported by the isotopic compositions of zones rich in the Arctic reworked palynomorphs in the Labrador Sea that have isotopic compositions of about -25‰ (Macko, 1989). Thus, the isotopic compositions of both OC and nitrogen for the sections that contains high proportions of pre-Quaternary reworked palynomorphs in Baffin Bay (Macko, 1989) justify the use of -26‰ as the end member for the inferred terrestrial material. Because a two component mixing

equation has indicated minor inputs of marine OM in all sections containing ice rafted debris (Fig. 5.2), low contents of OC and nitrogen indicate that the terrestrial source areas of these materials contained low OM, were probably highly refractory and underwent little diagenetic change after entering the marine environment. Lack of major differences in the C/N ratios between sections containing large fractions of marine OM and ice rafted episodes, may be an indication of high differential losses of nitrogen in marine OM during early diagenesis.

The stable isotopic compositions of OC indicate measurable inputs of allochthonous material from the continent and continental shelf areas through turbidity current, meltwater plumes and iceberg. A question which immediately emerges is that of the source of OM. During the last glacial-transition periods, the land masses surrounding the Labrador Sea were permanently covered by the Laurentide and Greenland ice sheets. The ice coverage implies that terrestrial primary productivity was halted in these areas. Thus, the material inferred to have been transported into the Labrador Sea definitely is not of Late Pleistocene and Holocene. The OM most probably is reworked Tertiary and Cretaceous sediments, whose formations outcrop in many parts of eastern Canada or material deposited during the last interglacial period.

Based on the low organic $\delta^{13}\text{C}$ values, the Heinrich layers are inferred here to have been associated with low primary productivity. This is supported by the low abundances of dinocysts (Fig. 5.2), coccoliths, benthic and planktonic foraminifers (Hillaire-Marcel et al., 1994a,b), the low contents of OC and nitrogen (Fig. 5.1) as well as the low burial rates for OC and nitrogen (Fig. 5.9). Low primary productivity is likely because these events were associated with a turbid surface layer that might have hindered penetration of light required for photosynthesis. Furthermore, reduction in primary productivity could have been a result of lower sea surface temperature (cold conditions owing to melting of icebergs), and low salinity, which has been inferred to have been associated with the Heinrich events (Bond et al., 1992) and supported by low $\delta^{18}\text{O}$ and inorganic

$\delta^{13}\text{C}$ values (Fig. 5.1).

Episodes of ice rafted debris have been inferred to have associated with high sedimentation rates. According to Francois and Bacon (1994), Heinrich events lasted for about 700 years. Although sedimentation rate has been suggested to be the primary factor controlling preservation of OM (Canfield, 1994), inferred high sedimentation rates during all episodes of ice rafted debris were associated with low accumulation rates of carbon and nitrogen. This is probably due to low primary productivity as well as low content of OM in the source areas of terrestrial materials.

Excluding zones of ice rafted debris, the stable isotopic compositions of OC and nitrogen of sedimentary OM recovered at this site for the glacial core section are depleted relative to the Holocene core section by about 2‰. The difference in the isotopic compositions between the two periods may be partly attributed to low primary productivity during the last glacial maximum, enhanced input of terrestrial material during glacial period by ice bergs, turbidity current channelled through the NAMOC or changes in species assemblages. The isotopic fractionation of carbon and nitrogen is high when the rate of utilization of nutrients and CO_2 is low (Altabet and Francois, 1994a,b; Shemesh et al., 1993). Similarly, organic material is enriched in ^{13}C and ^{15}N in areas where nutrient utilization is high (Francois et al., 1992, 1993a,b; Altabet and Francois, 1994a,b; Shemesh et al., 1993). Enrichment in organic ^{13}C and ^{15}N in the Holocene period is an indication of the rate of increase in nutrient utilization, and thus of high primary productivity when compared to glacial period. An increase in primary productivity is supported by high concentrations of both dinocysts and organic lining of benthic foraminifers (Fig. 5.2) and coccoliths (Hillaire-Marcel et al., 1994a). However, estimates of paleoproductivity based on the equation of Sarthein et al (1988) do not indicate significant differences in productivity (Fig. 5.8). This is probably due to poor preservation of Holocene OM or high supplies of reworked marine OM that can not be easily separated from reworked marine OM using the stable isotopes and C/N ratio methods.

The observation of low abundances of dinocysts (Fig. 5.2) as well as coccoliths and dinoflagellates in the study area during glacial periods, (Aksu et al., 1989; Hillaire-Marcel et al., 1994a), may be a further proof of low primary productivity. The inferred low primary productivity might have been caused by harsh climatic conditions which were very cold compared to the present (CLIMAP, 1976). Inferred low primary productivity is most likely to have been associated with low δ -values resulting from fractionation caused by temperature effect, which has been shown from analysis of widely published data to occur below 16°C (Sackett, 1989), high concentrations of CO₂ and incomplete utilization of available nutrients. The change in the isotopic compositions due to temperature effects for certain phytoplanktonic species has been estimated to be 0.14‰ per degree (Wong and Sackett, 1978). The difference of about 2‰ observed in this study would require a decrease in temperature of at least 12°C. Based on the CLIMAP (1976) and de Vernal et al. (1994) temperature estimates for August, the difference was about 6°C, and thus not enough to account for the observed isotopic difference. It has been reported that high concentration of CO₂ and nutrients in conjunction with low primary productivity, is always associated with high isotope fractionation (Hinga et al., 1994; Goericke and Fry, 1994). Recent observations of latitudinal increases in concentration of CO₂ in the surface waters (Rau et al., 1991a) implies that high latitude areas have high concentration of CO₂ in their surface waters, and are associated with a high fractionation of CO₂ during photosynthesis owing to high discrimination between ¹²C and ¹³C by plants cells (O'Leary, 1981, 1988). High fractionation is supported by low values of particulate matter, as well as sedimentary OC and nitrogen, which have been reported from both southern and northern high latitude areas (Rau et al., 1991b; 1993). During glacial periods, large quantity of CO₂ is inferred to have been stored in the ocean, this based on an increase in the rate of dissolution of carbonates, and an increase in alkalinity (Broecker et al., 1990), thus high concentration. Therefore, the difference between the glacial and interglacial organic $\delta^{13}\text{C}$ can be partly attributed to high concentrations of

CO₂ and temperature effects.

As pointed out previously, the isotopic compositions of OC for planktonic material recovered from the Southern Ocean has been found to be less than -27‰ compared to tropical and temperate values of about -20‰ (Sackett et al., 1965; 1974; Fontugne and Duplessy, 1981; Biggs et al., 1988, 1989). This has been partly attributed to changes in species from calcareous to siliceous producing organisms. The study of Wong and Sackett (1978) has indicated that diatoms shows a more pronounced temperature dependence during fractionation than calcareous species. Thus changes from calcareous to diatomaceous species are expected to cause a pronounced isotope fractionation, and hence, a change in the isotopic compositions of resulting OM. The systematic change observed in this study is unlikely to be a result of changes in species assemblages. This is because there is no strong gradient change in species as the one observed in the southern ocean, and no major change in species assemblages has been observed at this site (Rahman and de Vernal, 1994). Although all the above factors are likely to have contributed to the observed δ -values, a terrestrial input of OM is the most major factor that led to the differences in δ -values between the glacial and Holocene periods.

A spike of high OC and nitrogen contents within the glacial periods at approximately 200 cm might represent an increase in primary productivity or a slight improvement in preservation conditions. This event, which is older than the Young Dryas event, having been dated at 13060-12250 BP (Hillaire-Marcel et al., 1994a), is associated with enrichment in both ¹³C and ¹⁵N. This might represent the Bölling-Allerød event that has been inferred from ice core records (Johnsen et al., 1992; Paterson and Hammer, 1987), and which was associated with warming. Based on high content of primary indicators preserved in this section an increase in primary productivity is inferred to have occurred.

Although primary productivity indicators point to an increase in primary productivity since

the last glacial maximum, there is a minor difference between OC and nitrogen accumulation rates during glacial and interglacial periods (Fig. 5.8). This is contrary to what was expected. Relatively constant burial rates (accumulation rate of both OC and nitrogen) can be attributed partly to increases in the rate of OM degradation. Lack of major differences in C/N ratios may be an indication of high rates of OM degradation in the Holocene period. Enhanced preservation of OM in marine sediments is considered to be caused by high primary productivity in the euphotic zone (Pedersen and Calvert, 1990; Pedersen et al., 1992; Calvert et al., 1992b; Calvert, 1987), anoxic conditions (Demaison and Moore, 1980) and/or high sedimentation rate (Canfield, 1994). Hence, poor preservation of OM could have resulted from low sedimentation rates and/or an increase in oxygen content of bottom sediments. During glacial period the Labrador Sea was characterized by a homogeneous water mass, reduction in the formation of NADW, and most likely poor oxygenation (Hillaire-Marcel et al., 1994a; Bilodeau et al., 1994). Initiation of the NABW led to oxygenation of the bottom water and thus increase in the oxygen of bottom water, while a reduced sedimentation rate could have led to the lack of preservation of recent OM, and hence low burial rates.

Work of Hillaire-Marcel et al. (1994b) has shown major differences in burial rate of inorganic carbon between glacial and interglacial periods. A minor difference in burial rate and paleoproductivity of organic carbon observed at many sites suggest that the organic carbon in the subarctic environment has not been a major sink of atmospheric CO₂. Owing to high differences in burial rate of inorganic carbon between glacial and interglacial periods, possibly inorganic carbon has been a sink of atmospheric CO₂ particularly during glacial period where alkalinity has been inferred to have been high (Broecker and Peng, 1989). This is likely because production of one mole of inorganic carbon is associated with production of one mole of CO₂ ($\text{Ca}^{2+} + \text{HCO}_3^- \rightleftharpoons \text{CaCO}_3 + \text{H}_2\text{O} + \text{CO}_2$), while dissolution of CaCO₃ is accompanied with increase in alkalinity, thus a sink in atmospheric CO₂.

Relatively low $\delta^{13}\text{C}$ and $\delta^{15}\text{N}$ values of OM around 8.4 ka (120-135 cm) can be an indication of massive input of freshwater or re-initiation of the WBUC. The slightly low $\delta^{18}\text{O}$ values around 8.4 ka may indicate an input of fresh meltwater resulting from the final stages of retreat of the Greenland and Laurentide ice sheets. This inference is supported by observation that at around 8,000 BP there was a massive input of meltwater to the Labrador Sea channelled through Hudson Strait, and by 7,000 BP only small remnants of the Laurentide ice sheet remained (Dawson, 1992; Vilks et al., 1989).

A record centred at 179 cm and dated ≤ 11000 BP can be inferred to be a Young Dryas event, and has been previously reported as event H0 by Hillaire-Marcel et al. (1994a). This event is characterized by low isotopic compositions of OC and nitrogen ($\delta^{13}\text{C}$ and $\delta^{15}\text{N}$), low contents of OC and nitrogen, high CaCO_3 contents, high content of >150 microns particle size, as well as low abundance of planktonic foraminifers. Thus during this event there was a massive input of clastic material, and reduction in primary productivity because burial rates were similarly low.

5.3.2. HU-90-013-13 PC

Since various components of plant material such as lignin, lipids, protein, and carbohydrates have different isotopic compositions, the $\delta^{13}\text{C}$ of OM is an average of these components. The carbohydrates and proteins are enriched in ^{13}C in comparison to lipids (Degens, 1969), and they are easily degraded by micro-organisms (Spiker and Hatcher 1984). Preferential removal of ^{13}C -enriched compounds during early diagenesis may lead to the OM that is depleted in ^{13}C . Downcore decreases in $\delta^{13}\text{C}$ values of up to 4‰ observed in various work have been partly attributed to selective preservation of isotopically light material (Spiker and Hatcher, 1984; Hatcher et al., 1983; McArthur et al., 1992). However, the effect of diagenesis on the isotopic signature of OM is controversial. Meyers et al. (1994), Rau et al. (1987) and Dean et al. (1986) have indicated that there is little

alteration of the isotopic signature of sedimentary OM. Nonetheless, very low nitrogen content as well as OC contents, also can indicate a high degree of diagenesis. Thus, the observed downcore decrease in the isotopic compositions of OC in the upper 200 cm, could partly be an effect of diagenetic changes, although other possible factors that may have led to such trend would include changes (i) in the isotopic compositions of the carbon used in the synthesis of OM, (ii) in primary productivity and/or (iii) in the influx of isotopically light material especially terrestrial material.

The isotopic compositions of OM can vary because of differences in the concentration of aqueous CO₂, growth rate, cell size, rate of primary productivity and changes in species assemblage. Because of the differences in the concentration of dissolved CO₂ in oceans, the isotopic compositions of suspended particulate OM has been found to be negatively correlated with concentration of dissolved CO₂ (Rau et al., 1989; 1991a; Francois et al., 1993b). This results from a discrimination of ¹²C over ¹³C by plants cells is high when concentration of CO₂ is high (O'Leary, 1981,1988). In the World's oceans, differences in CO₂ concentrations in the surface layer are caused by differences in temperature, where low temperatures enhance dissolution of atmospheric CO₂. Although there are no data on the variation in the concentration of CO₂ in the Labrador Sea for the past 8,000 B.P., it can be concluded that the concentration of dissolved CO₂ caused by variations in temperatures has not been of the magnitude of that observed between tropical and high latitude areas. This is exemplified by the concentration of CO₂ in the Greenland ice record which is less variable and averages about 270 ppm for the Holocene period (Paterson and Hammer, 1987). Hence, changes in the concentration of aqueous CO₂ had little effect on the observed trend. This trend could have resulted from increases in primary productivity owing to increases in the rate of utilization of available CO₂. This inference is in accordance with the increase in the concentration of primary productivity indicators of coccoliths, diatoms, dinocysts, benthic foraminifers as well as estimated OC fluxes (Hillaire-Marcel et al., 1994a, b).

The stable isotopic compositions of OM for core 11 BC located 50 km upslope of site 13 PC has $\delta^{13}\text{C}$ values which average -21.6‰ for the Holocene period. Although core 13 PC has thick Holocene sediments, the $\delta^{13}\text{C}$ values of greater than -22‰ are confined in the upper 40 cm, with most of the $\delta^{13}\text{C}$ values for glacial and transition periods being less than -23.5‰ . Furthermore, the estimated paleoproductivity is higher at site 13 PC than at site 11 BC (Hillaire-Marcel et al., 1994b). Thus, the systematic decrease in $\delta^{13}\text{C}$ values is not solely due to changes in primary productivity.

Variations in the input of isotopically light material from the surrounding land masses might be the major factor governing the distribution of the $\delta^{13}\text{C}$ values at this site and at all three sites located on the west Greenland Margin, where short cores were collected. Downcore decreases in ^{13}C most likely indicate a systematic increase in the terrestrial input to the area. The source of terrestrial material is most probably from the glacial flour reworked from shelf and slope areas, then transported downslope by slumping processes. The thin cover of Holocene sediments observed at site HU-013-12 PC (Hillaire-Marcel et al., 1994a) as well as at sites 11 BC, 38 TWC and 40 LHC, may be due to erosion by WBUC and scouring icebergs that caused deposition of part of the eroded material downslope. This implies that as deglaciation continued, the rate of erosion decreased, hence a decrease in the dilution of marine OM. It could also be due to a decrease in the rate of erosion by the WBUC.

The result of this work shows that the glacial and transition periods contain OM that are depleted in ^{13}C compared to the Holocene period. Various processes can be invoked to explain low OC stable isotope values observed during glacial period and transition periods. These processes include high fractionation due to low primary productivity, incomplete utilization of CO_2 , changes in species assemblages, terrestrial inputs of OM and temperature effects. As Macko (1989) pointed out, most probably all these processes contributed to the observed low $\delta^{13}\text{C}$ values. Low values of the stable isotopic compositions of sedimentary OC may indicate high fractionation during the

formation of OM and/or measurable inputs of terrestrial OM during glacial period as well as during transition from glacial to interglacial periods. As pointed out previously, high concentrations of CO₂ along with low primary productivity, have been found to be associated with high fractionation (Francois et al., 1993a,b). Since dissolution of CO₂ increases with decreasing temperature, glacial as well as transition periods might have been associated with high fractionation owing to high concentrations of CO₂ in surface waters associated with low primary productivity. However, inputs of terrestrial OM is the major factor that caused low $\delta^{13}\text{C}$ values during glacial and transition periods. Because Greenland was covered by ice almost year-round during glacial periods, primary productivity on land was most probably reduced or halted. Thus, the inferred high input of terrestrial OM is most probably reworked Cretaceous sediments that outcrop in many parts of coastal Greenland. The eroded sedimentary material were transported by icebergs and meltwater plumes. Sediment transport by icebergs is supported by high concentrations of the coarse sediment fraction (>125 microns), which primarily reflects ice-rafting deposition during glacial periods (Hillaire-Marcel et al., 1994a) and increases in the magnetic grain size (Stoner et al., 1994, 1995).

Low δ -values of both OC and nitrogen at around 8,400 B.P. which correspond to high concentrations of magnetic minerals (especially magnetite) and high magnetic grain sizes (Stoner et al., 1994, 1995), most likely indicates high fluxes of terrestrial OM to the area. The terrestrial material input could have been a result of turbidity deposition triggered by abrupt input of meltwater, or a settling of fine suspended matter brought up by meltwater. Although this time interval (about 8.4 ka) is associated with a decrease in $\delta^{18}\text{O}$ values in the Labrador Sea (at sites 13 PC and 94 PC), most likely an indication of significant increase in meltwater flux to the area, the period post-date inferred time of intense melting of the Greenland ice margin toward the modern coast limits of 10 ka (Hillaire-Marcel et al., 1994a). However, isotopically light material from land could have been derived from eastern Canada when glacial lake Ojibway and Agassiz introduced

large quantities of meltwater to the Atlantic Ocean through the Hudson Strait at about 8,000 B.P. (Dawson, 1992). The estimated input of water to the ocean during this period ranged between 70,000 and 150,000 km³ of water (Dawson, 1992). It is probable that such an event led to the transport of terrestrial material to the area through meltwater plumes (Andrews et al., 1994). Although distribution of benthic foraminifers has indicated two distinct zones in the upper 300 cm that have been attributed to changes in the bottom water circulation (Bilodeau et al., 1994), bottom water circulation is unlikely to have produced such low $\delta^{13}\text{C}$ values.

The terrestrial end member for the nitrogen stable isotopic compositions of OM that have been used to estimate various relative contribution of terrestrial OM to the marine environment range from 0 to 3‰ (Macko, 1983; Peters et al., 1978). The $\delta^{15}\text{N}$ values in all zones inferred to have measurable terrestrial OM are characterized by $\delta^{15}\text{N}$ values that are higher than 5‰. Thus, high terrestrial values might be an indication of the effect of diagenesis on the nitrogen stable isotopic compositions. Similar high and homogeneous values were reported by Macko (1989) for the nearby site 646. This is most probably due to the high refractory nature of the material. Although it is considered that diagenetic changes do not alter considerably the isotopic composition of sedimentary material (Rau et al., 1987), sediments with low nitrogen contents and with homogeneous nitrogen isotope values can be attributed to alteration of reworked older sediments, most probably of Cretaceous age. Generally, nitrogen stable isotopes were not a useful tool in delineating sources of OM in the present study area.

The stable isotopic composition of OC indicates slightly low values during the Younger Dryas as well as at about 9,000 B.P. These low values might indicate periods of enhanced input of terrestrial material to the area. Enhanced input of terrestrial material could have been a result of discharge from ice bergs, as well as meltwater to the ocean, which would have formed sediment plumes.

Only Heinrich event H2 can be clearly identified at this site using stable isotopic compositions of both OC and nitrogen. The isotopic compositions of both OC and nitrogen for H1 are not very much different from those of glacial periods. Differences in the isotopic compositions between the two events can be attributed to different sources of allochthonous material. This inference is further supported by the content of detrital carbonate. The detrital carbonate content is not high during Heinrich event 1, an indication that the source of material during this event is not the same as that of H2.

There is a clear difference in the estimated paleoproductivity, burial rate and flux of OC and nitrogen between glacial and present interglacial periods. This can be attributed to increases in primary productivity owing to improvement in the surface water condition. This is in agreement with the abundance of primary productivity indicators, coccoliths, dinocysts, diatoms and benthic foraminifers, as indicators of fluxes of OM at water/sediment interface (Hillaire-Marcel et al., 1994a,b).

5.3.3. HU-90-31-44 PC

Abrupt changes in the stable isotopic compositions of OC and nitrogen that occurs between 160 and 180 cm may represent (i) termination of the Younger Dryas, (ii) reduction in meltwater flux to the area, and (iii) an increase in primary productivity and establishment of the modern marine conditions. Various workers have indicated that prior to 12,000 B.P., meltwater from a disintegrating Laurentide Ice sheet was channelled through the Gulf of Mexico (Spero and Williams, 1990; Dyke and Prest, 1987; Teller, 1990). According to Teller (1990), inflow to the Atlantic Ocean through the Gulf of St Lawrence and Hudson strait was established at around 11,000 B.P. The influx of meltwater to the Atlantic Ocean through the St. Lawrence river valley is inferred to have increased between 11,000 and 10,000 B.P. (Younger Dryas period) by two fold to more than 1700 km³. This

was caused by retreating ice that allowed the glacial Lake Agassiz to drain eastward into the Great Lakes (Teller, 1990). The flux of the freshwater input to the areas resulted in the lowering of salinity, and it has been estimated that salinity was lowered to about 25-27‰ (de Vernal et al., 1993). At about 10,000 B.P., eastward overflow from the western interior of north America was blocked by advancing ice forcing overflow to the Gulf of Mexico and possibly to the northwest into the Arctic Ocean (Teller, 1990). By 9,600, the amount of meltwater flowing to the Atlantic Ocean through the Gulf of St. Lawrence was reduced and much of the flow was routed through the Hudson Strait (Dawson, 1992). A decline in the input of meltwater and establishment of the modern marine conditions is further supported by a sharp transition marked by the occurrence of abundant dinocysts of the species *Gonyaulacales* observed at about 10,000 B.P. at the Cabot Strait (de Vernal et al., 1993), as well as a significant reduction in the sedimentation rate.

The geochemical results for core 44 PC have indicated that there are enrichments in sedimentary organic ^{13}C and ^{15}N in the Holocene section over that of the late Pleistocene. As pointed out previously, this can be partly attributed to differences in the isotopic compositions of carbon used during the formation of OM. As mentioned before, the Gulf of St. Lawrence received enormous amounts of meltwater from the retreating Laurentide ice sheet during the late Pleistocene, and the Scotia shelf was undoubtedly the main route of freshwater discharge to the Atlantic Ocean. Inputs of fresh meltwater may have introduced bicarbonate that was depleted in ^{13}C . Thus when utilized by phytoplankton, the resulting material was depleted in ^{13}C compared to that formed during normal marine conditions. Low inorganic $\delta^{13}\text{C}$ between 13.5 and 12 Ka (Fig. 5.4) might be an indication of this process. Meltwater input to the area might have introduced more nutrients to the euphotic zone. Owing to low rates of nutrient utilization, the resulting OM was depleted in ^{15}N . Therefore, low values of the stable isotopic compositions of OC and nitrogen during the late Pleistocene may partly indicate the effect of high concentrations of nutrients in association with low rates of nutrient utilization resulting from low primary productivity.

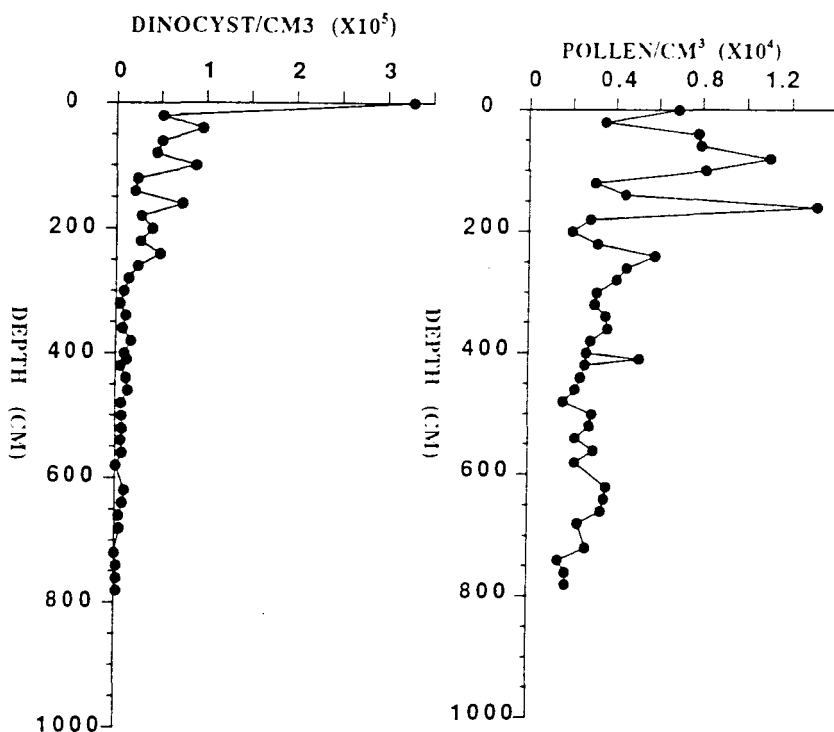


Fig. 5.12. Downcore variation in pollen and dinocysts at Site HU-90-031-44 PC (Source: GEOTOP Data Bank, unpublished data).

It has been shown elsewhere that increases in nutrient utilization owing to increases in the rate of primary productivity is associated with OM that is enriched in ^{15}N (Montoya, 1994). High $\delta^{15}\text{N}$ and $\delta^{13}\text{C}$ values during the Holocene period are an indication of increases in the primary productivity as indicated by sudden increases in the concentration of the dinocysts (Fig. 5.12). This inference is further supported by an increase in the amount of OC, CaCO_3 and nitrogen preserved in the sediments (Fig. 5.4). This is because preservation of OM is controlled by both primary productivity in the euphotic zone and sedimentation rates (Pedersen and Calvert, 1990; Calvert and Pedersen, 1992; Canfield, 1994; Calvert, 1987; Calvert et al., 1992b). Increases in the primary productivity may likely be the result of an improvement in climatic conditions and reduction in the input of meltwater to the area through the Gulf of St. Lawrence.

Apart from primary productivity, another mechanism which might have caused the observed high $\delta^{15}\text{N}$ values during the Holocene is denitrification process. Denitrification can result in a large fractionation of nitrogen stable isotopes (Montoya, 1994; Rau et al., 1987; Table 1.1). Denitrification in marine environments occurs in sub-oxic waters including the mid-water oxygen minimum zone. This process produces nitrogen molecules that are depleted in ^{15}N , leaving the remaining nitrate reservoir enriched in ^{15}N . When this heavier nitrate is used by phytoplankton, the resulting organic material is enriched in ^{15}N . Such a process was invoked as the cause of high $\delta^{15}\text{N}$ values observed in the Quaternary sediments recovered in the Arabian Sea (Muzuka et al., 1991). Continental margins are the depocenters of OM, the denitrification process is a likely explanation for enriched values observed here. This could have been a result of high fluxes of labile OM reaching the sea floor resulting from an increase in primary productivity. Abrupt changes in $\delta^{15}\text{N}$ likely reflect changes in the rate of nitrogen cycling. However, relative contribution of processes like denitrification in relation to the rate of nutrient utilization cannot be evaluated at present.

The major factor that caused differences between the late Pleistocene and Holocene periods is variation in the proportions of OM from terrestrial and marine sources. A decline in the supply of terrestrial material to the area owing to (i) reduction in the amount of water flowing to the Gulf of St. Lawrence, (ii) entrapment of terrestrial OM by the estuarine of the Gulf of St. Lawrence and/or (iii) re-routing of meltwater to the Hudson Strait after 10 ka (Dawson, 1992) may have caused the area's major sources of material to be dominated by marine productivity. This observation is suggested by the downcore variation of the C/N ratios (Fig. 5.4). The C/N ratios have been used as source indicators under the assumption that terrestrial OM has C/N ratios greater than 12, whereas marine OM has C/N ratios less than 10. Downcore increases in C/N ratios may be a further indication of the increase in the input of terrestrial material. Although Meyers (1994) has argued that the C/N signature is not altered by diagenetic changes, care must be taken in interpreting

C/N data because diagenetic changes potentially can alter the original values. It is probable that slightly high C/N ratios (values of greater than 10) in the Holocene section are due to diagenetic changes.

A large proportion of terrestrial OM as indicated by results of the stable isotope compositions of OC and nitrogen as well as the C/N ratios, occurred between 12400 and 13500 years. High inputs of terrestrial OM indicate that there was probably a period of massive meltwater input to the area resulting from the retreat of the Laurentide ice sheet. A freshwater input is partly supported by light values of both inorganic $\delta^{13}\text{C}$ and $\delta^{18}\text{O}$ (Fig. 5.4). This inference is in agreement with the observation that the net retreat of the Laurentide ice sheet between 13 and 12 Ka was more rapid than previous periods (Dyke and Prest, 1987). This period was associated with fast sediment deposition by ice meltwater in the Gulf of St Lawrence (Loring and Nota, 1973) as well as on the Scotia slope.

It can be concluded that the results of the stable isotopic compositions of OC and nitrogen indicate measurable terrestrial inputs between 12 and 13.5 Ka. Because of low $\delta^{13}\text{C}$ and $\delta^{15}\text{N}$ values associated with high contents of CaCO_3 at about 800 cm, the highest input of terrestrial material occurred at this time.

A lack of major influxes of terrestrial OM after 12 Ka can also be explained by the efficiency of the estuary in trapping continentally derived material. All box cores analyzed (Chapter 4) and other previous work have indicated that the OM in the Gulf of St. Lawrence is of marine origin. Most of the allochthonous material transported by the river of St. Lawrence is trapped in the estuarine sediments (Lucotte et al., 1991; Tan and Strain, 1983). Apart from the estuarine, the Champlain Sea might have acted as another sink for terrestrial material during deglaciation. Thus, intermediate values of $\delta^{15}\text{N}$ and $\delta^{13}\text{C}$ values between 12400 and 10,000 years may be representative of a large portion of marine OM.

Low δ -values might have resulted from both low primary productivity and temperature effects. During the glacial period and the transition period, ice coverage per year at the Cabot Strait, a site that is close to the site 44 PC, has been estimated to be 8 months. Low temperature and ice coverage might have led to low primary productivity. As indicated before, low primary productivity is associated with high isotopic fractionation. Thus, increases in the isotopic compositions of OC and nitrogen upcore can be attributed to decreases in the amount of terrestrial material introduced to the area, and decreases in the degree of fractionation owing to slight increases in primary productivity. An increase in the primary productivity with time is supported by increases upcore of both OC and nitrogen content at this site.

5.4.0. CONCLUSION

1. All the Heinrich events are characterized by very low δ -values of OC and nitrogen, as well as low OC and nitrogen contents.
2. There is enhanced accumulation of OC and nitrogen in the Labrador Sea at greater depths (sites 13 PC and 94 PC) caused by sediment focusing, where eroded material from the continental shelf and slope owing to strong WBUC are deposited downslope.
3. Significant difference in the primary productivity in the Labrador Sea between the late Pleistocene and the Holocene occurs after 8 ka. This indicates that modern conditions were established at this time.
4. There are minor differences in the estimated burial rates and primary productivity between the Holocene and the last glacial periods. This can be attributed to deposition of reworked marine OM that cannot be separated from the unworked fraction using stable isotopes and C/N ratios. However, based on the abundance of various primary productivity indicators, primary productivity was diminished during glacial periods and was also considerably reduced during episodes of

deposition of ice rafted debris. The result of this work indicates that burial of organic carbon is not a major remover of CO₂ from the atmosphere.

5. The Gulf of St. Lawrence-Scotia slope has a high burial rate, paleoproductivity, and flux of nitrogen and OC compared to the Labrador Sea. This was caused by high sedimentation rates as well as shallower depths.

6. Climatic conditions improved between 12000 and 1300 BP as indicated by the high contents of primary productivity indicators. This period was associated with high inputs of terrestrial OM on the Scotia slope.

7. The Younger Dryas was characterized by low δ -values of OC and nitrogen, as well as low contents of OC and nitrogen, an indication that primary productivity was reduced and most of the material was derived from the surrounding land masses.

8. At about 8000 BP the Labrador Sea experienced inputs of OM which was depleted in ¹³C and ¹⁵N, possibly caused by inputs of fresh meltwater resulting from the final retreat of the Laurentide and Greenland ice sheets.

9. There is a measurable input of terrestrial OM during glacial-transition periods in the Labrador Sea and on the Scotia slope.

CHAPTER 6

6.0.0. DIAGENETIC CHANGES

6.1.0. GEOCHEMICAL RESULTS OF THE AMINO ACIDS DISTRIBUTION IN SEDIMENTS

6.1.1. HU-90-031-43 PC

Amino acid analysis was performed for the upper 38 cm of the core (Appendix 9.4.0, Table 6.1). The standard used in the analysis of the amino acids did not allow for the detection of basic amino acids (histidine, lysine arginine), and non-protein amino acids. Glycine, aspartic acid and glutamic acid are the most abundant amino acid residues in the whole core followed by alanine and valine (Fig. 6.1; Appendix 9.4.0., Table 6.1). Other amino acids that have slightly higher concentrations include leucine, serine, isoleucine and threonine (Fig. 6.1). The concentrations of methionine, allo-isoleucine, tyrosine and phenylalanine are very low. Glycine, aspartic acid and glutamic acid constitute more than 50% of the total hydrolysable amino acids (THAA). The observed distribution of individual amino acids corresponds well to the THAA spectra of comparable surface sediments reported by Rosenfield (1979), Henrichs et al. (1984), Whelan and Emeis (1992), Burdige and Martens (1988) and Seifert et al. (1990). The downcore concentrations of the THAA generally decrease with depth (Fig. 6.2), and reflects the downcore distribution of OC and total nitrogen (TN) (Fig. 4.27). This general decrease in the concentration of various amino acids downcore is in agreement with the observations by Aizenshtat et al. (1973), Kvenvolden (1975 and references therein), Seifert et al. (1990), Hare (1973, 1969), Burdige and Martens (1988), Henrichs and Farrington (1987), Haugen and Lichtentaler (1991) and Henrichs et al. (1984). The highest concentration of THAA occurs at about 3 cm (Fig. 6.2), possibly resulting from bioturbation, a processes that cause transport of labile OM downward from the sediment-water interface. The

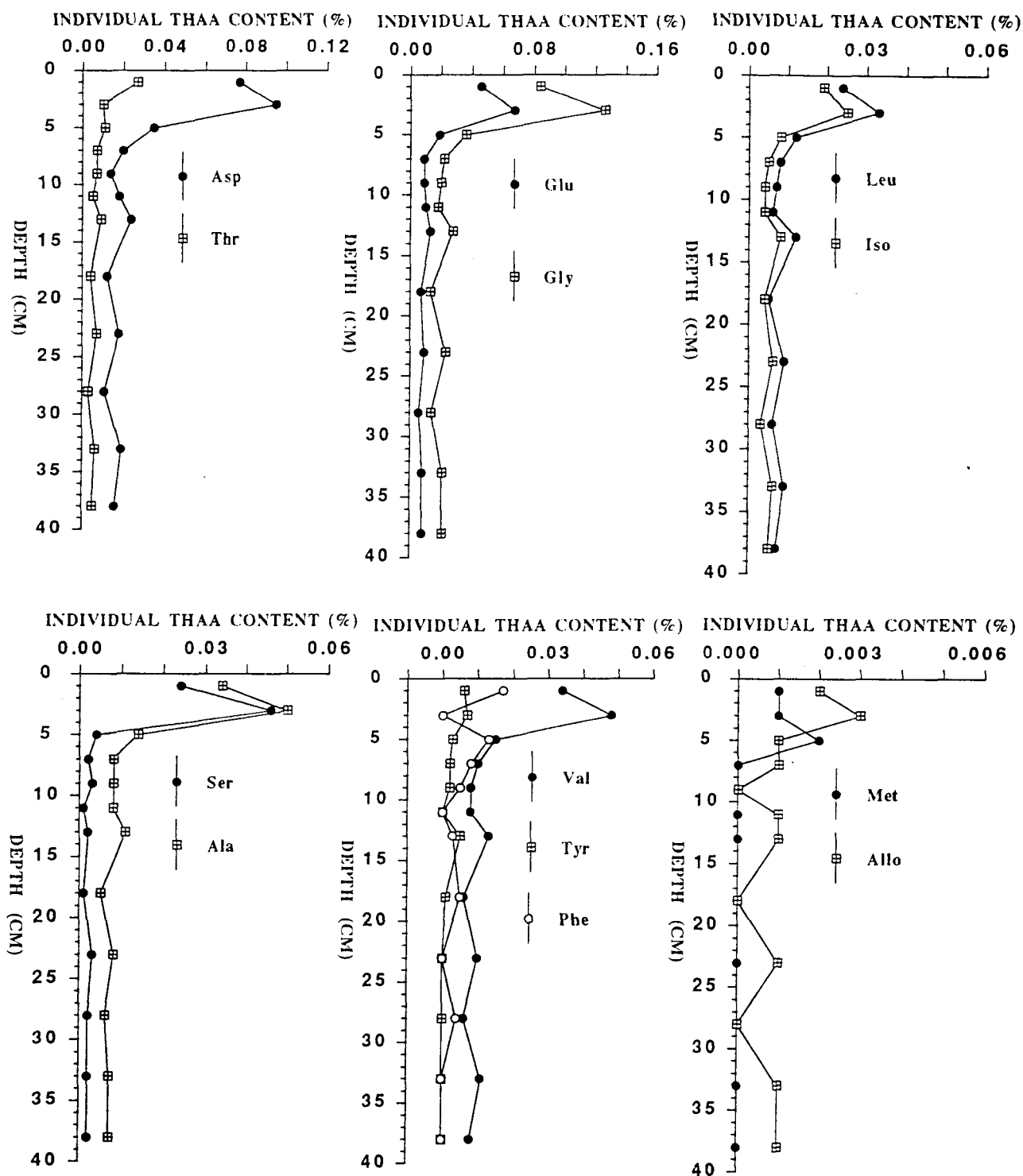


Fig. 6.1. Downcore variations of individual amino acids for core HU-90-031-43 PC (Glu= glutamic acid; Gly = glycine; Ile = Isoleucine; Asp = Aspartic acid; Thr = Threonine; Ser = Serine; Met = Methionine; Alle = Allo-Isoleucine; Tyr = Tyrosine; Val = Valine; Phe = Phenylalanine; Ala = Alanine; Leu = Leucine).

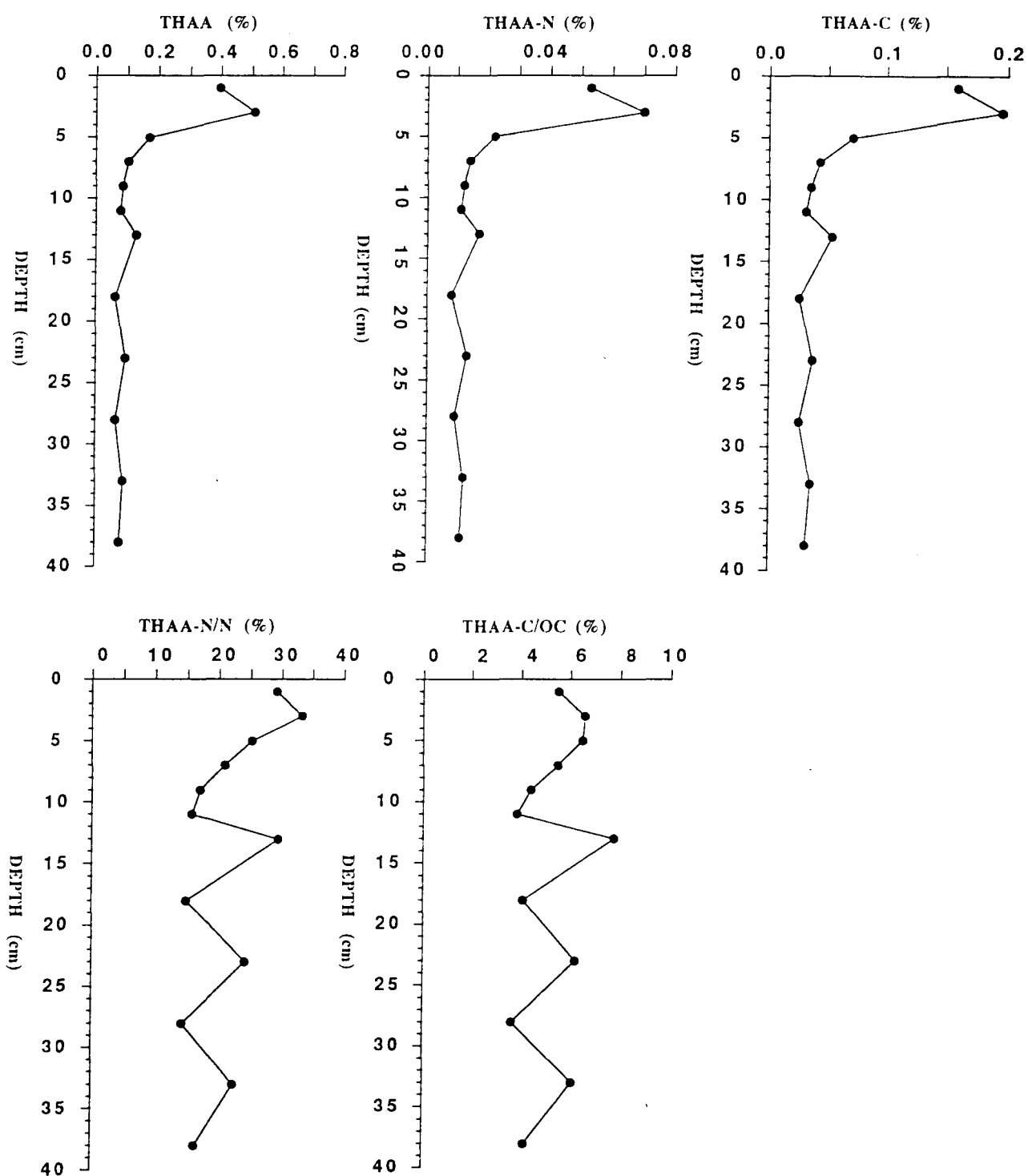


Fig. 6.2. Downcore variations of THAA (%), THAA-C (%), THAA-N (%), THAA-N/TN (%) and THAA-C/OC for core HU-90-031-43 PC.

percentages of total hydrolysable amino acid nitrogen (THAA-N) and total hydrolysable amino acid carbon (THAA-C) show a tendency to decrease downcore (Fig. 6.2). The percentages of nitrogen contributed by THAA to the total nitrogen (THAA-N/TN) ranges from 14.3% to 33.4%, and shows a downcore decrease to about 11 cm, followed by a highly variable values (Fig. 6.2). In contrast, the percentage of carbon contributed by the THAA to the total OC (THAA-C/OC), which range from 3.6 to 7.8%, is relatively uniform down to the base of the core (Fig. 6.2). The percentage of THAA-N has a significant positive linear correlation with the total nitrogen content at the 95% confidence level ($r = 0.99$).

6.1.2. HU-90-031-29 BC

Analysis of the amino acids was performed for the upper 27 cm of the core (Appendix 9.4.0, Table 6.2). Glycine, aspartic acid and glutamic acid are the most abundant amino acid residues in the core, followed by alanine and valine (Fig. 6.3). Other amino acids that have higher concentrations include threonine, leucine, serine isoleucine and phenylalanine (Fig. 6.3). Glycine, aspartic acid and glutamic acid constitute at least 50% of the THAA. The concentrations of methionine, allo-isoleucine and tyrosine are very low. The concentration of THAA shows a slight downcore decrease in the upper 9 cm, followed by more variable values that show a slight downcore increase to the base of the core (Fig. 6.4). A similar downcore distribution of THAA was observed in the Peru upwelling region for short cores covering the upper 10 cm (Henrichs et al., 1984). The percentages of THAA-N and that of THAA-C show a similar downcore decrease to 9 cm followed by a slight increase to the base of the core (Fig. 6.4). The percentage of THAA-N/TN which ranges from 20.4% to 58.2%, decreases slightly downcore in the upper 9 cm, followed by a slight increase to the base of the core (Fig. 6.4). The percentages of THAA-C/OC show a similar downcore trend as that of THAA-N/TN (Fig. 6.4).

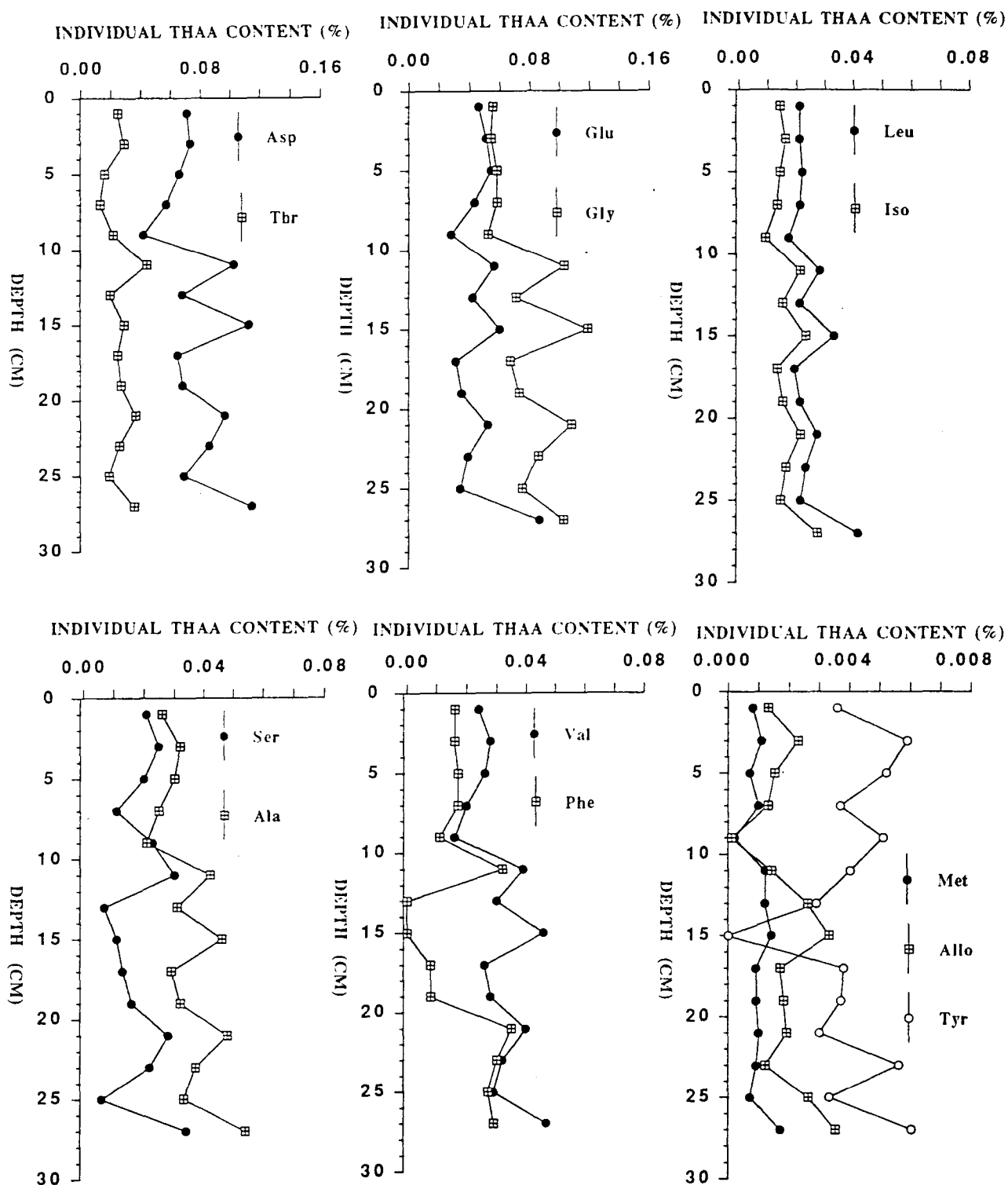


Fig. 6.3. Downcore variations of individual amino acids for core HU-90-031-29 BC (Glu= glutamic acid; Gly = glycine; Ile = Isoleucine; Asp = Aspartic acid; Thr = Threonine; Ser =Serine; Met = Methionine; Aile = Allo-Isoleucine; Tyr = Tyrosine; Val = Valine; Phe = Phenylalanine; Ala = Alanine; Leu = Leucine).

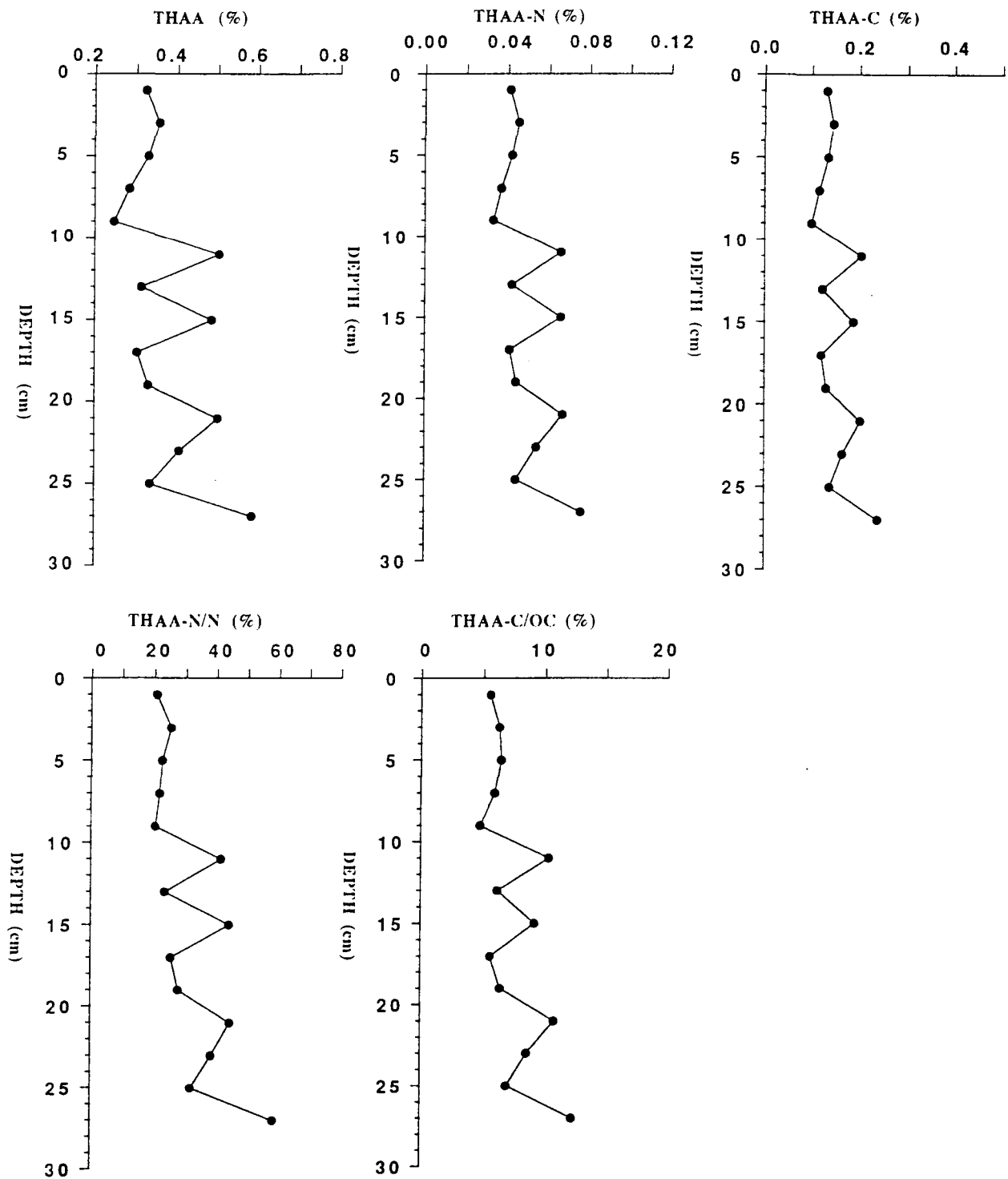


Fig. 6.4. Downcore variations of THAA (%), THAA-C (%), THAA-N (%), THAA-N/TN (%) and THAA-C/OC for core HU-90-031-29 BC.

6.1.3. HU-90-031-45 BC

The result of the amino acid analysis, and the fraction of nitrogen as well as carbon represented by amino acids (THAA-N and THAA-C) is given in appendix 9.4.0., Table 6.3. The THAA content in the sediments range from 0.76% to 0.29% and averages $0.47 \pm 0.13\%$. With the exception of the uppermost (surface) data point which indicate a low concentration, downcore distribution of the THAA, THAA-N, THAA-C, THAA-N/TN and THAA-C/OC shows a general decrease to ~5 cm followed by a slight increase to the base of the core (Fig. 6.5). A section of the core between 4 and 15 cm has the lowest values of the THAA-N/TN percentage, and corresponds to relatively high Eh values (Fig. 3.4). The percentages of THAA-N/TN are on average greater than 20% but less than 38%, an indication of only slight diagenetic alteration. The downcore distributions of individual amino acids (Fig. 6.6) shows a lower value at the surface. There is a general decrease for most of the amino acids downcore to about 10 cm, followed by a slight increase to the base of the core (Fig. 6.6).

The most abundant amino acids, glycine, aspartic acid and glutamic acid, comprise more than 50% of the THAA in the sediments. Methionine and allo-isoleucine have the lowest concentrations. Other amino acids have intermediate concentrations between the two groups. Aspartic acid, isoleucine and threonine show a slight downcore increase to about 5 cm followed by a slight decrease down to the base of the core. Downcore distributions of glycine, alanine, serine, glutamic acid, tyrosine, phenylalanine and leucine show nearly constant concentrations downcore to the base of the core (Fig. 6.6).

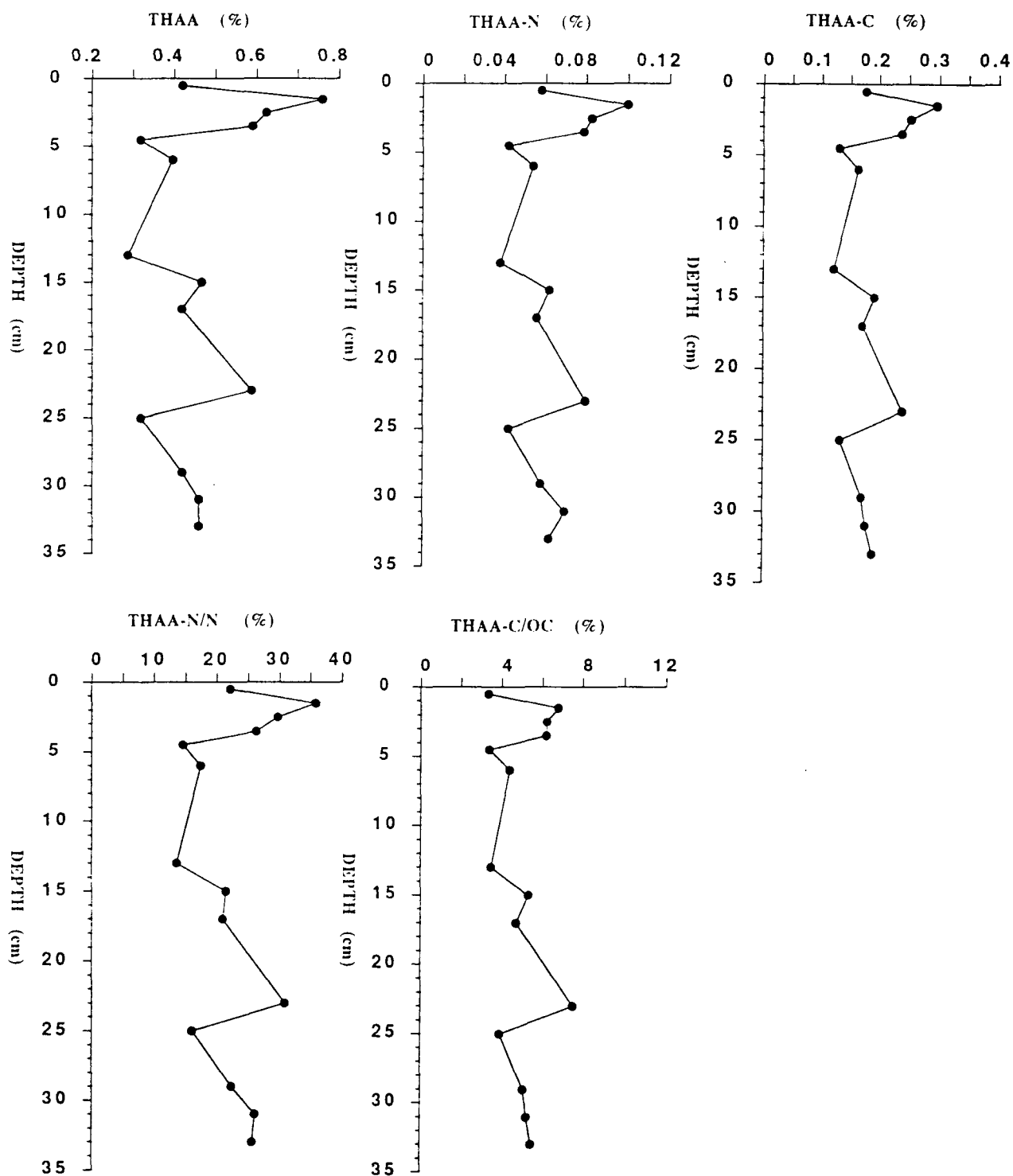


Fig. 6.5. Downcore variations of THAA (%), THAA-C (%), THAA-N (%), THAA-N/TN (%) and THAA-C/OC for core HU-90-031-45 BC.

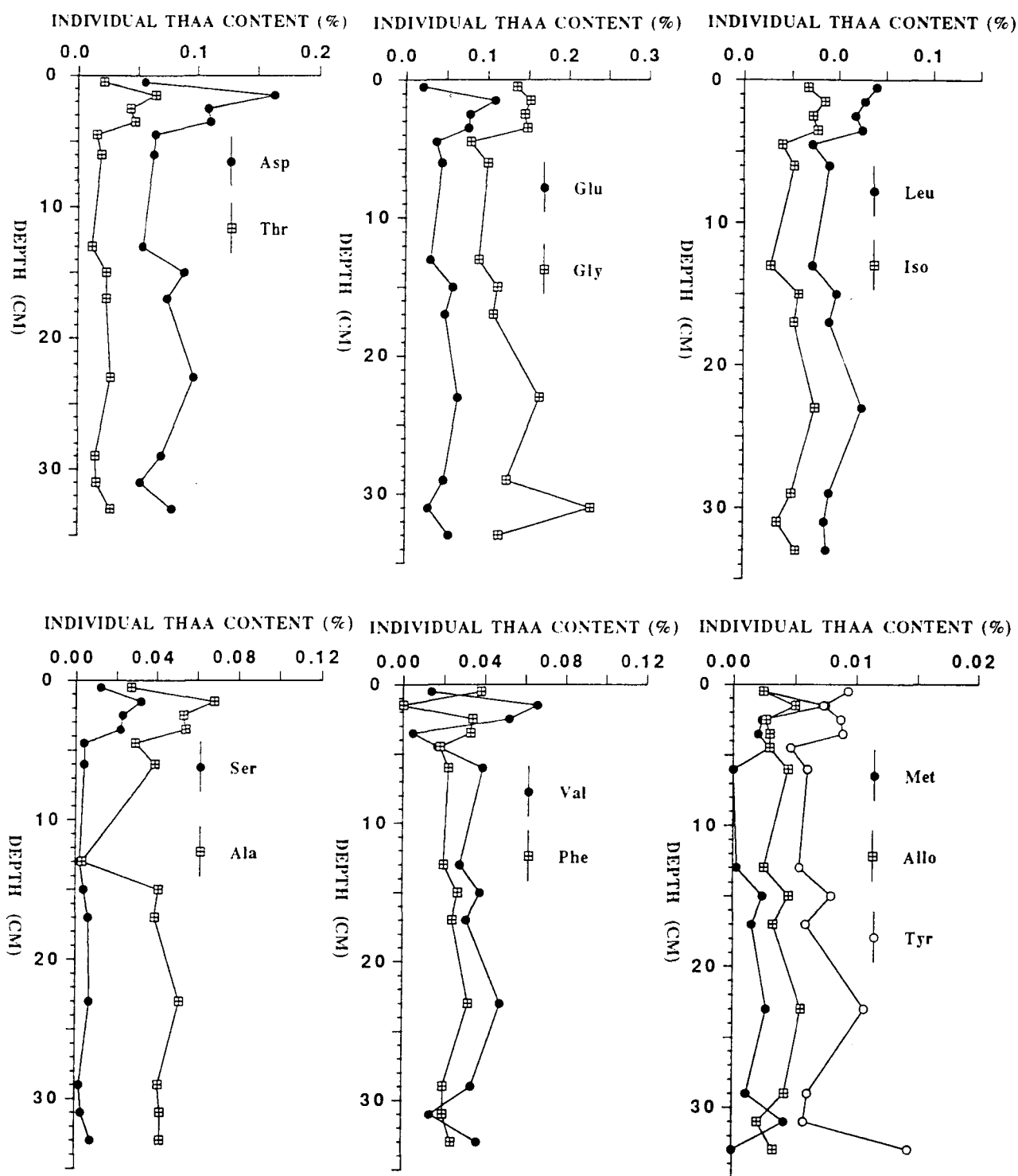


Fig. 6.6. Downcore variations of individual amino acids for core HU-90-031-45 BC (Glu= glutamic acid; Gly = glycine; Ile = Isoleucine; Asp = Aspartic acid; Thr = Threonine; Ser =Serine; Met = Methionine; Allo = Allo-Isoleucine; Tyr = Tyrosine; Val = Valine; Phe = Phenylalanine; Ala = Alanine; Leu = Leucine).

6.1.4. HU-90-031-17 BC

The results of amino acid analysis for this core are presented in appendix 9.4.0., Table 6.4. The most abundant amino acids are aspartic acid, glycine threonine and glutamic acid. These four amino acids constitute more than 55% of the THAA. Allo-isoleucine, methionine, tyrosine and phenylalanine have the lowest concentration, while the remaining amino acids have intermediate concentrations (Fig. 6.7). The downcore distributions of individual amino acids show relatively constant concentrations with a slight downcore decreases that extend to the base of the core (Fig. 6.7). The distributions of THAA, THAA-N, THAA-C, THAA-N/TN and THAA-C/OC shows a general downcore decrease (Fig. 6.8). Downcore distributions of the THAA is in agreement with that of OC and TN content. The THAA-N/TN is less than 30%. Low concentrations of tyrosine and phenylalanine at all four sites can be attributed to a chemically reactive phenolic group present in the structure of these amino acids, which make them to be among the least stable amino acids (Erdman et al., 1956). Similarly, the concentration of allo-isoleucine is expected to be low because this amino acid results from racemization of isoleucine during diagenesis.

6.2.0. RESULTS OF DIAGENETIC MODELLING

6.2.1. Organic Carbon and Nitrogen

As pointed out in section 3.5.0., a multi G-model of Berner (1980) and Westrich and Berner (1984) was adopted to obtain information about the rate of OM decomposition. Sedimentation rate is one of the major limitations of this model. Owing to uncertainty in values of sedimentation rates for the Gulf of St. Lawrence, the model values of first order rate constants (k) of OM decomposition are first order estimates. Since sedimentation rates and porosity were not assumed during curve fitting, the values for labile OM and percentages of remineralized OM presented in Table 6.5 are reasonably accurate. The results of curve fitting (reactivity constants, metabolizable fractions and

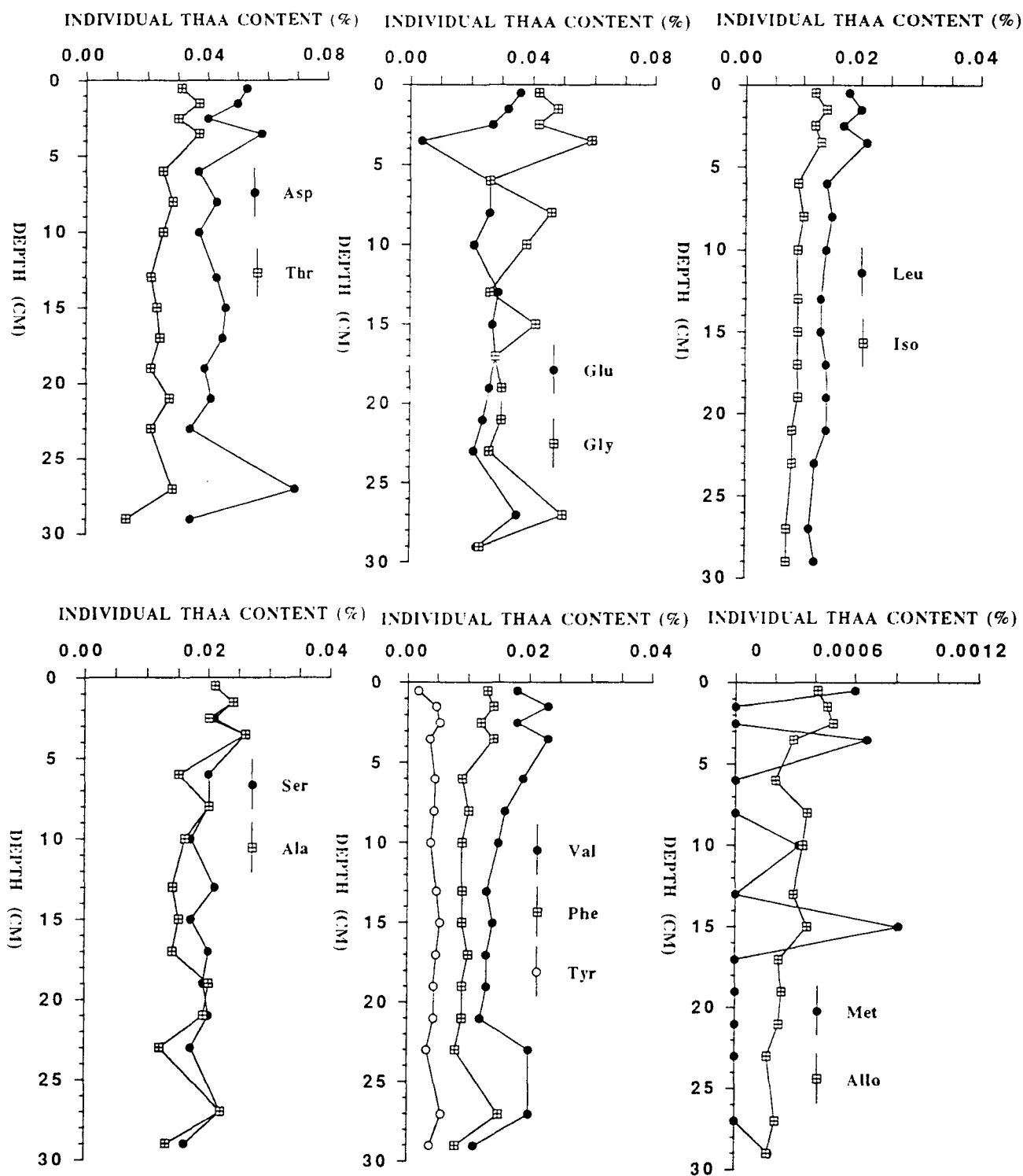


Fig. 6.7. Downcore variations of individual amino acids for core HU-90-031-17 BC (Glu= glutamic acid; Gly = glycine; Ile = Isoleucine; Asp = Aspartic acid; Thr = Threonine; Ser =Serine; Met = Methionine; Alle = Allo-Isoleucine; Tyr = Tyrosine; Val = Valine; Phe = Phenylalanine; Ala = Alanine; Leu = Leucine).

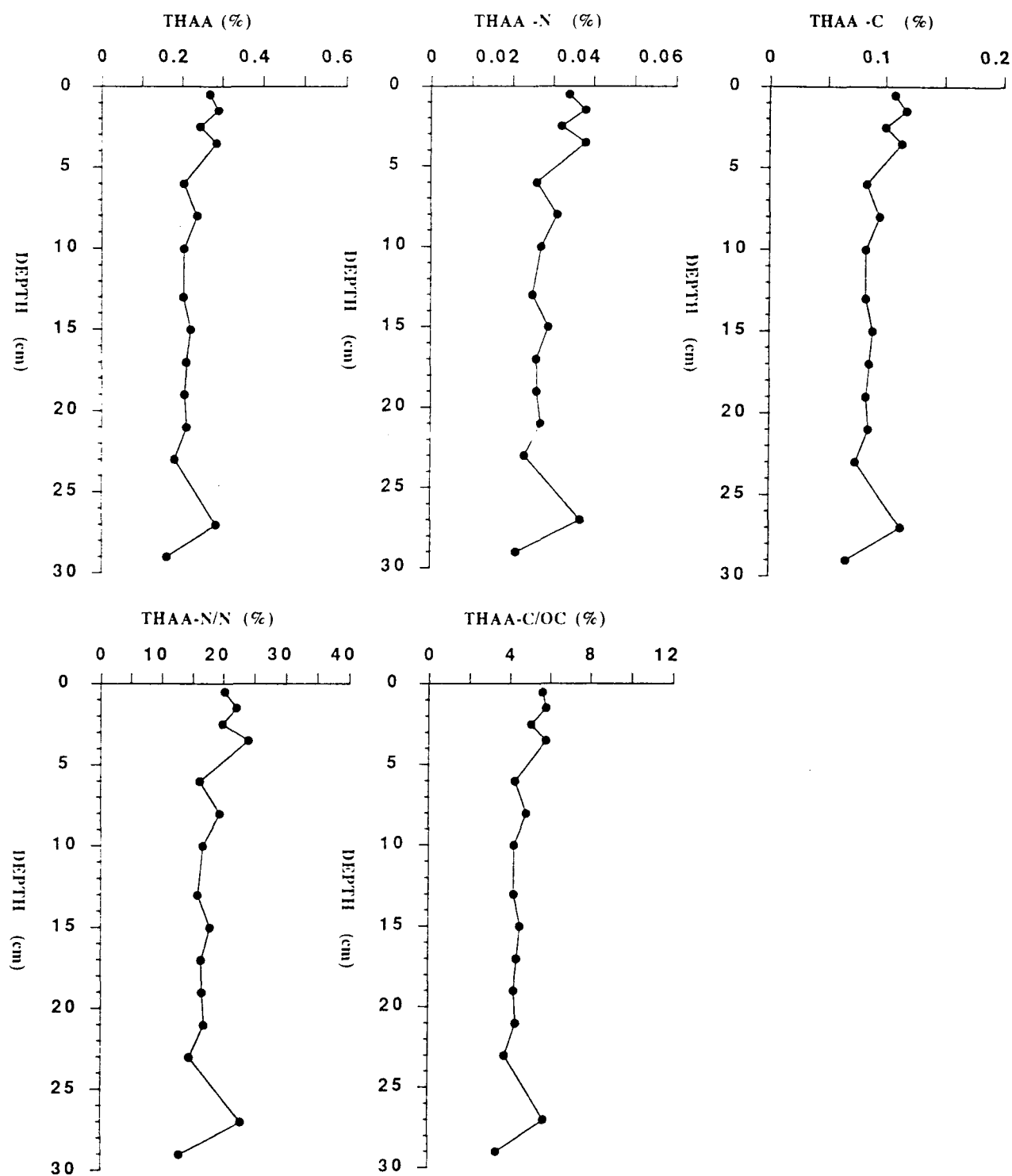


Fig. 6.8. Downcore variations of THAA (%), THAA-C (%), THAA-N (%), THAA-N/TN (%) and THAA-C/OC for core HU-90-031-17 BC.

percentages of remineralized organic carbon and nitrogen) are given in Table 6.5. Because values of B3 for OC are far less than that of B1 and B2 for the cores 17 BC, 41 BC and 45 BC, the exponential factor can be assumed to be equal to 1, and the constant (G3) can be taken as a representative of the refractory material. Similarly, the second exponential factor for both nitrogen and/or organic carbon at sites 17 BC, 29 BC, 41 BC, 43 PC, 45 BC and 44 PC, can be assumed to be equal to 1, and the constant (G2) can be taken as representative of the refractory fraction. These results indicate that the high decomposition rate constants (k) for the metabolizable fraction of OC, increases with sedimentation rates as well as accumulation rates. This trend can be attributed to sedimentation of readily metabolizable compounds, which are destroyed at the sediment-water interface at lower rates of sediment accumulation, and thus do not contribute to k values of sediment OC and nitrogen (Berner, 1980). The results of this work fall within the range of values observed by various workers (Billen, 1982a,b; Henrichs, 1992; Grundmanis and Murray, 1982; Martens and Klump, 1984; Klump and Martens, 1987; Tromp et al., 1995). The results of the curve fitting for carbon and nitrogen are given in Figs. 6.9 and 6.10. The fraction of mineralized OC ranges from 15% to 83%, whereas that of nitrogen ranges from 15% to 77% (Table 6.5). High and rapid mineralization of OC and nitrogen occurs at sites 43 PC and 44 PC. A low fraction of mineralized OC and nitrogen occur at all sites that have high sedimentation rates (17 BC, 29 BC, 41 BC, and 45 BC). This might be an indication of the influence of sedimentation rate on the preservation of organic matter. The results indicate a slight preferential loss of nitrogen over carbon at Site 29 BC, whereas at Site 17 BC PC there is a slight preferential loss of carbon over nitrogen. A preferential loss of nitrogen over that of OC at site 29 BC is in agreement with the observed downcore increase in C/N ratios (Fig. 4.17).

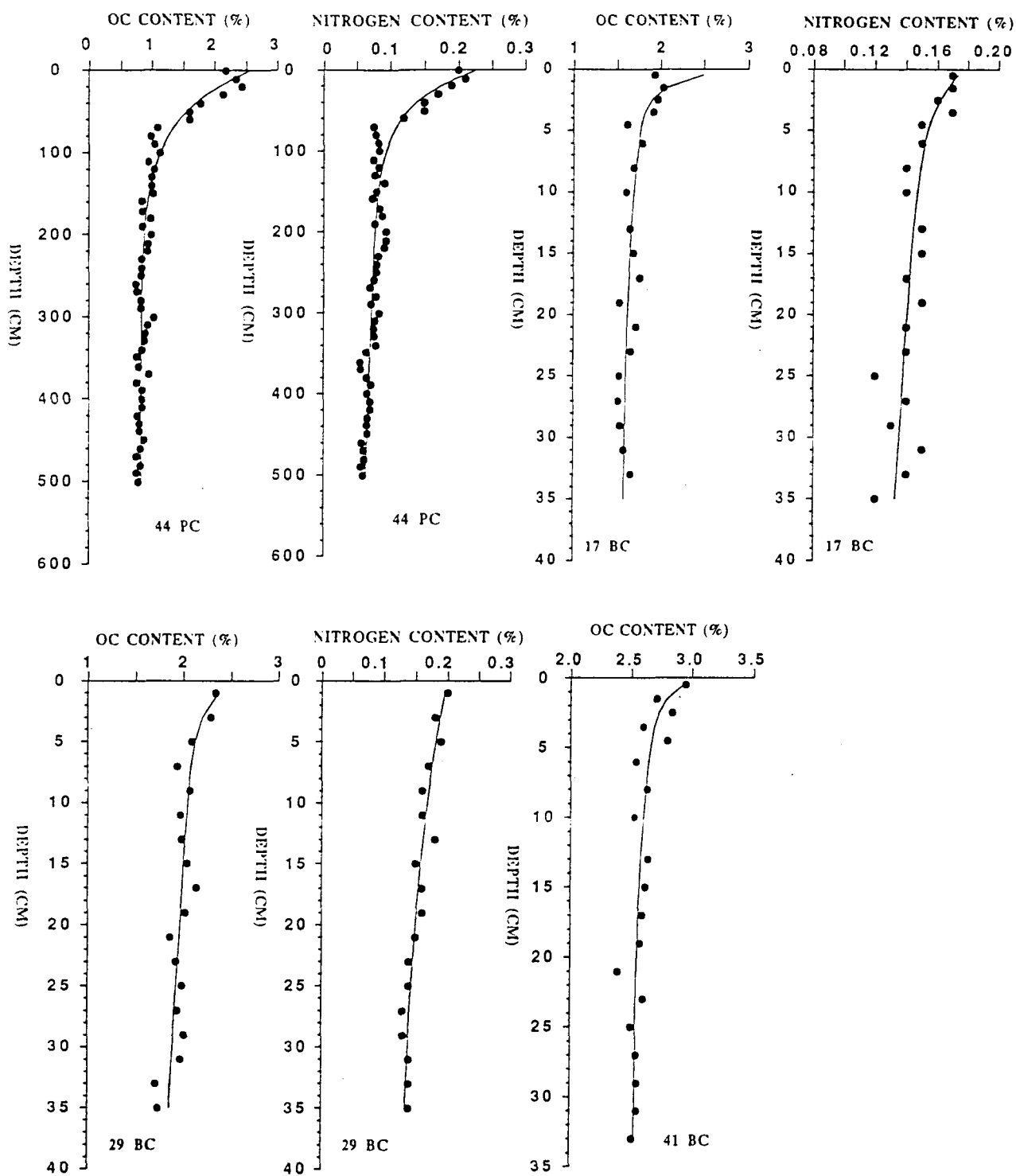


Fig. 6.9. Plots showing curve fitting results of organic carbon and/or total nitrogen for cores HU-90-031-44 PC, HU-90-031-17 BC, HU-90-031-29 BC and HU-90-031-41 BC.

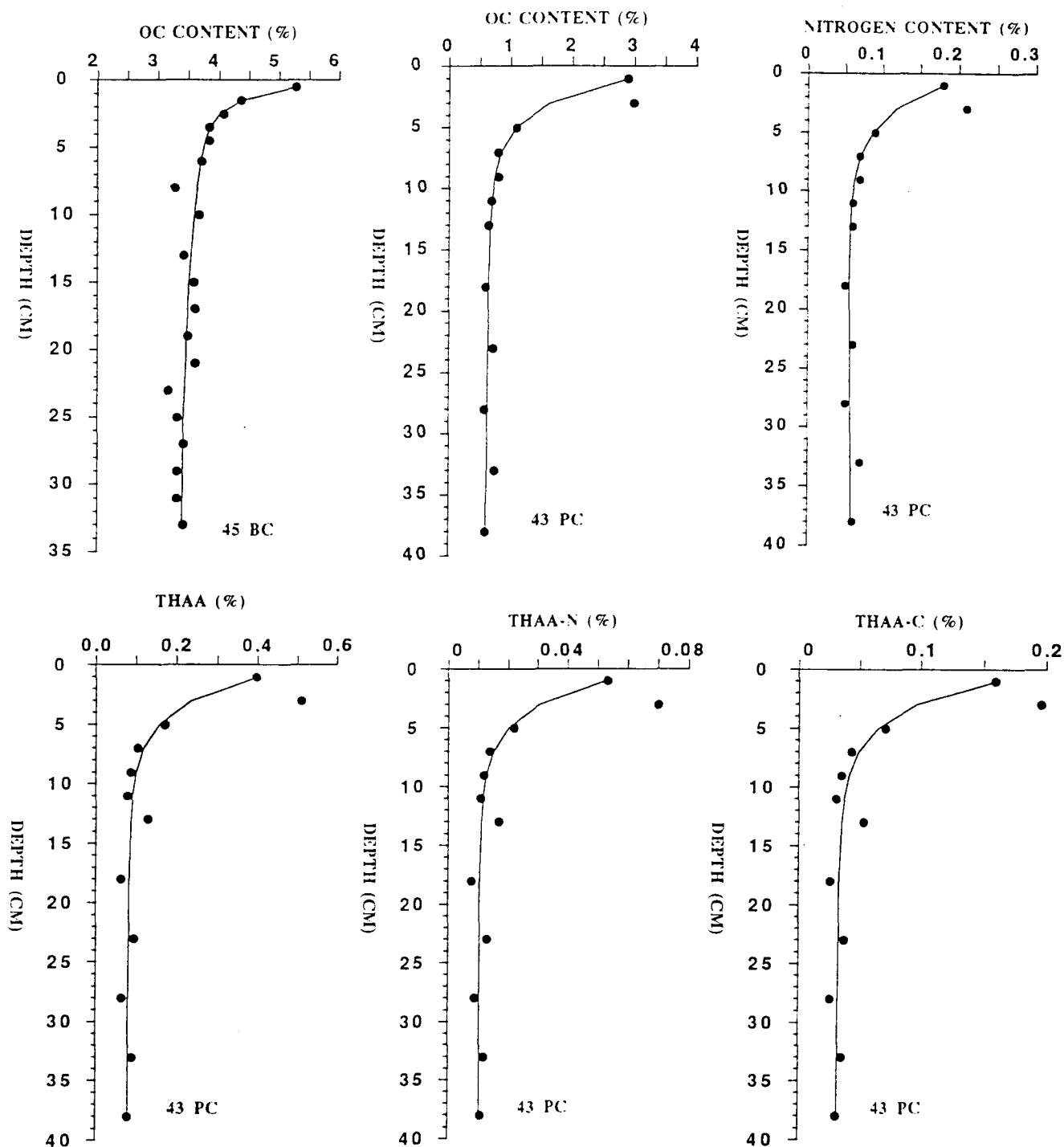


Fig. 6.10. Plots showing curve fitting results of organic carbon and/or total nitrogen for cores HU-90-031-45 BC and HU-90-031-43 PC BC, total hydrolysable amino acids (THAA), total hydrolysable amino acids carbon (THAA-C) and total hydrolysable amino acids nitrogen (THAA-N) for core HU-90-031-43 PC.

Table 6.5. Results of curve fitting (Model)

ORGANIC CARBON												
CORE	SR	B1	B2	B3	G1	G2	G3	G0	%REMI	k1	k2	k3
17 BC	0.130	1.000	9.96×10^{-2}	3.91×10^{-4}	1.03	0.28	1.59	2.90	45	1.30×10^{-1}	1.29×10^{-2}	5.08×10^{-5}
29 BC	0.150	0.456	3.90×10^{-3}		0.40	2.12		2.52	16	6.84×10^{-2}	5.84×10^{-4}	
41 BC	0.440	1.000	9.98×10^{-2}	-1.95×10^{-4}	0.31	0.25	2.50	3.07	18	4.40×10^{-1}	4.39×10^{-2}	-8.6×10^{-5}
43 PC	0.016	0.422	3.13×10^{-3}		3.38	0.68		4.05	83	6.75×10^{-3}	5.00×10^{-5}	
45 BC	0.016	0.983	8.29×10^{-2}	1.93×10^{-4}	2.27	0.59	3.34	6.20	46	1.57×10^{-2}	1.33×10^{-3}	3.09×10^{-6}
44 PC	0.016	0.017	-3.4×10^{-5}		1.78	0.81		2.58	69	2.67×10^{-4}	-5.5×10^{-7}	
NITROGEN												
CORE	SR	B1	B2	B3	G1	G2	G3	G0	%REMI	k1	k2	k3
17 BC	0.130	0.307	3.72×10^{-3}		0.026	0.151		0.178	15	3.99×10^{-2}	4.84×10^{-4}	
29 BC	0.150	0.053	7.80×10^{-4}		0.073	0.126		0.199	37	7.97×10^{-3}	1.17×10^{-4}	
43 PC	0.016	0.336	-3.02×10^{-3}		0.179	0.052		0.231	77	5.38×10^{-3}	-4.8×10^{-5}	
44 PC	0.016	0.024	5.90×10^{-4}		0.143	0.086		0.229	63	3.80×10^{-4}	9.39×10^{-6}	
TOTAL HYDROLYZABLE AMINO ACIDS FOR CORE 43 PC												
TYPE	SR	B1	B2	B3	G1	G2	G3	G0	%REMI	k1	k2	k3
THAA	0.016	0.036	1.12×10^{-3}		4515000	833600		5348600	84	5.80×10^{-4}	1.80×10^{-5}	
THAA-N	0.016	0.371	3.40×10^{-4}		603300	110700		714000	84	5.93×10^{-3}	5.45×10^{-6}	
THAA-C	0.016	0.350	2.00×10^{-3}		1780000	339600		2119600	84	5.59×10^{-3}	3.20×10^{-5}	

6.2.2. Amino Acids

A similar curve fitting was done for the THAA, THAA-N and THAA-C for core 43 PC. The results of this curve fitting are given in Table 6.5. About 80% of the amino acids reaching the sea floor are mineralized in the upper 40 cm of the sediment column. The highest rate of mineralization occur in the upper 10 cm of the sediment. The OC and total nitrogen contents as well as THAA have similar rate constants resulting from similar rates of decomposition. The result of this work is similar to that of Henrichs and Farrington (1987), and Haugen and Lichtentaler (1991).

6.3.0. DISCUSSION

6.3.1. HU-90-031-43 PC and HU-90-031-17 BC

Cowie and Hedges (1992) reported that the percentage of total nitrogen represented by amino acids (%THAA-N) in all species other than woody vascular plant tissues is >38% and can be as high as 84% for unaltered organic material. This parameter is diagenetically sensitive and has generally been found to decrease as degradation progresses (Whelan 1977; Henrichs et al., 1984; Burdige and Martens 1988, Cowie et al., 1992, Cowie and Hedges, 1992, 1994). The values of THAA-N which fall significantly below 38% therefore indicate diagenetic alteration. Values of THAA-N/TN which are less than 38%, and which decrease downcore, have been used to indicate preferential mineralization of THAA over other nitrogen-containing OM preserved in the sediments (Henrichs et al., 1984; Cowie and Hedges, 1994). Furthermore, using this parameter, OM at depth greater than 10 cm have been found to be highly degraded (Henrichs et al., 1984; Cowie and Hedges, 1994). Thus, lower THAA-N/TN percentages ratios observed at sites 17 BC and 43 PC which decrease downcore (Figs. 6.2 and 6.8), may be attributed to enhanced breakdown of amino acids during early diagenesis by high populations of microorganisms owing to lower sedimentation rates (16 cm/ka at nearby site 44 PC). A rapid decline in the THAA, THAA-N and THAA-C in the

upper 10 cm at site 43 PC may be indication of high degradation by microorganisms. These lower values give an indication that OM at these sites has been diagenetically degraded.

Lower values of THAA-N/TN are unlikely to be a result of inputs of terrestrial OM. The stable isotope compositions of organic carbon and nitrogen at this location have suggested little contribution of terrestrial OM. The result of diagenetic modelling indicate that the contents of nitrogen, OC and THAA at site 43 PC have similar reactivities, and that the fraction of mineralizable OC and nitrogen is high. This indicates that there is high degradation and that the remaining material is refractory. This inference is supported by C/N ratio values which are higher than 10 at both sites. A downcore decrease in the C/N ratios observed at site 43 PC (Fig. 4.27) can be attributed to preferential losses of OC over nitrogen during early diagenesis, as indicated by the low rate of change of nitrogen compared to that of OC. A downcore decrease in C/N ratios at site 43 PC could also be explained by (i) the high proportion of inorganic nitrogen (adsorbed NH_4^+ by clay minerals) as indicated by a positive intercept of 0.07% on the nitrogen axis for the scatter plot of nitrogen versus OC (Fig. 4.27), (ii) the variation in the type of OM supplied to the area in the past (i.e. it might have been enriched in nitrogen relative to carbon).

However, other reactions which may convert THAA to other forms of total nitrogen and produce low THAA-N/TN (such as the formation of humic compounds) are possible, especially below 3 cm. But a highly significant linear correlation between THAA and total nitrogen content in the sediments excludes this possibility of conversion of the THAA to other forms of total nitrogen especially during formation of humic compounds. The observed downcore decrease in the concentration of THAA at sites 43 PC and 17 BC can be assumed to be an indication of utilization of labile amino acids as carbon substrate in microbial mediated reactions such as decarboxylation, oxidation, fermentation, sulphate reduction and methanogenesis.

6.3.2. HU-90-031-29 BC and HU-90-31-45 BC

Because the pH of sedimentary environments is generally near neutrality, most amino acids exist as dipolar ions (zwitter ions), with a positive charge associated with the amino group, and a negative charge associated with the carboxyl group. However, basic amino acids behave as cations because of their extra amino group, and acidic amino acids behave as anions because of the extra carboxyl group. Therefore the three groups of free amino acids as well as individual amino acids should have different adsorption properties. Laboratory experiments have shown that amino acid adsorption on sediments is an important process that can rapidly remove dissolved amino acids from the pore water. Higher concentrations of amino acids have been found to be strongly adsorbed in carbonate rich sediments (Rosenfield, 1979). Furthermore, amino acids contents for organic matter associated with fine grained carbonates consists primarily of aspartic acid and glutamic acid, whereas non-carbonate sediments consist primarily of glycine and alanine (Carter and Mitterer, 1978). Higher concentrations of aspartic acid and glutamic acid in carbonate rich sediments can be attributed to a high content of these amino acids in carbonate-bearing organisms. However, as the carbonate content at these two sites is low, the concentrations of the amino acids at these sites might not be explained simply by the preferential adsorption or association of amino acids by carbonate. Higher concentrations of glycine may be partially be due to poor carbonate contents of the sediments.

A slight downcore increase in the content of the THAA below 9 cm at these two sites (Figs. 6.5 and 6.6) may reflect variations in the input of OM with time. This inference is supported by an increase in the sedimentation rate observed at site 29 BC below 15 cm (Jennane, 1992), and is in agreement with the observations of subsurface maxima in THAA contents in sediments for both anoxic and oxic conditions, that has been attributed to changes in the OM input (Balzer et al., 1987; Haugen and Lichtentaler, 1991). Slightly lower values of THAA at the surface for cores 29 BC, 45 BC as well as core 43 PC correspond to low THAA-N/TN ratios, and may be attributed to an

enhanced breakdown of amino acids caused by high populations of microorganisms.

An increase in the C/N ratio to the base of the core at site 29 BC may suggest the preferential breakdown of organic nitrogen compounds. This inference is in agreement with the modelling results which indicate that the mineralized fraction of nitrogen is about twice that of carbon. However, this process is not reflected by the downcore distribution of THAA-N, possibly due to variations in the contribution of organic matter to the sea floor over time. An increase in the content of THAA-N at these two sites is contrary to the downcore distribution of total nitrogen and OC contents which decrease downcore to the base of the core. An increase in the THAA-N/TN downcore implies that some sediments that are buried to a greater depth are not as highly degraded when compared to the near surface sediments. This can be attributed to variations in the content of THAA-N supplied in the past, as well as higher sedimentation rates that remove more labile material from the zone of high OM degradation. This inference is supported by high reactivity constants of organic matter observed at these two sites. Earlier deposited sediments were probably enriched in THAA-N.

Abundances of acidic amino acids have been previously used as source indicators of OM as they are assumed to have originated from land-derived humic compounds. Although the abundances of acidic amino acids (glycine, aspartic acid and glutamic acid) are high, a terrestrial source is unlikely. The isotopic compositions of organic carbon and nitrogen, indicate a marine origin of OM. Amino acids may be less reliable as indicators of OM sources as previously concluded by Cowie and Hedges (1992), and should not be used by themselves.

As indicated in Chapter 4, the nitrogen content at site 45 BC increases slightly in the upper 6 cm of the core, followed by a decrease to the base of the core. In contrast, a downcore distributions of THAA-OC and THAA-N at site 45 BC is inversely related to that of total nitrogen, which may indicate that there is no preferential loss of nitrogen or carbon compounds at this site.

Equal rates of loss of carbon and nitrogen are supported by the modelling results. The downcore decrease in the C/N ratios observed in the upper 8 cm can be explained by variations in input of OM enriched in nitrogen over time, with equal rates of loss of carbon and nitrogen. A slight increase in the C/N below 8 cm to the base of the core at this site is associated with increases in both THAA-C and THAA-N, and may indicate variations in the inputs of nitrogen containing material. Carbon contents remained constant, but with equal rates of loss of nitrogen and carbon during early diagenesis.

Lower concentrations of THAA at the surface of each core can be attributed to sediment loss of labile OM during retrieval of the core. Surficial sediment loss during core retrieval has been observed in the abyssal plain (Macko, personal communication).

6.4.0. CONCLUSION

1. The most abundant amino acids in the Gulf of the St. Lawrence are glycine, aspartic acid and glutamic acid. High concentrations of these three amino acids are not simply due to high contribution of carbonate-bearing organisms because the CaCO_3 content in the Gulf of St. Lawrence is low. Similarly high concentrations of these amino acids are not due to elevated inputs of terrestrial OM, because the stable isotopes of organic carbon and total nitrogen as well as the C/N ratios have suggested little input of this source. As the work of Cowie and Hedges (1992) has recently showed a similar concentrations of amino acids in various land and marine organisms, high concentration of these three amino acids originated from any marine organisms. Therefore, the amino acids alone are not good indicators of sources of OM.
2. Owing to the downcore increase in the concentrations of the THAA, the downcore distribution of THAA indicate enhanced preservation of OM at depths greater than 10 cm at sites 29 BC and 45 BC most likely caused by an increase in the sedimentation rate, where labile OM is rapidly

removed from the zone of intense degradation (upper 10 cm).

3. The downcore distribution of THAA-N/TN is a good indicator of altered OM. Based on this parameter, the OM at sites 17 BC and 43 PC has been considerably diagenetically altered compared to that of sites 29 BC and 45 BC. High alteration of OM at site 43 PC can be attributed to low sedimentation rates. The OM below 10 cm at sites 29 BC and 45 BC has not been highly degraded.
4. The diagenetic modelling presented here reproduces fairly the downcore variation of the OC and total nitrogen. The high decomposition rate constants (k) for the metabolizable fraction of organic carbon increases with the rates of sedimentation and accumulation. Furthermore, based on the result of the diagenetic modelling, a high fraction of mineralized OM occurs at sites 44 PC and 43PC, where the mineralized fractions of organic carbon, total nitrogen and amino acids are as high as 84%. However, because of uncertainty in the values of sedimentation rates, the decomposition rate constants presented here are first order estimates.

CHAPTER 7

7.0.0. GENERAL CONCLUSIONS

7.1.0. METHODOLOGICAL ASPECTS

The stable isotopes of organic carbon and nitrogen have been used widely to document the relative proportions of marine and terrestrial organic matter (OM) in an environment (e.g. Peters et al., 1978; Macko, 1983). In this study, these stable isotopes are used in conjunction with the C/N ratios as indicators of variations in the sources of OM. However, the isotopic composition of nitrogen is relatively high (5‰) even in sections of low $\delta^{13}\text{C}$ values (-25 to -26‰), suggesting that this parameter is either not a good indicator of sources of OM or that the terrestrial end member values for these high latitude areas are higher than previously assumed, (i.e. from 0‰ to 3‰; e.g. Peters et al., 1978; Macko, 1983).

In the Labrador Sea, enrichment in ^{13}C and ^{15}N associated with high abundance of various primary productivity indicators during the Holocene demonstrate the utility of these isotopes as a supplementary tool to infer changes in primary productivity. Their utility stems from the fact that phytoplankton preferentially utilize light stable isotopes of organic carbon (^{12}C) and nitrogen (^{14}N) during photosynthesis (Francois et al., 1992; Montoya, 1994; Altabert and Francois, 1994a).

In this study, the amino acids, which make up a large fraction in living organisms, are a powerful tool in the assessment of the degree of alteration of sedimentary OM. One of the parameters which indicates the degree of alteration is the percentage of nitrogen represented by the total hydrolysable amino acids (THAA-N/TN). However, the concentration of acidic total hydrolysable amino acids (THAA) remains a poor source-indicator of OM in the marine environment, as previously concluded (Burdigen and Martens, 1988; Cowie and Hedges, 1992).

The distribution of organic carbon and nitrogen in the marine sediments have been shown

to be highly correlated with rate of primary productivity (e.g Berger and Herguera, 1992). However, owing to diagenetic alteration of OM, and higher variations in the sedimentation rates in these study areas, a simple assessment of the organic carbon preserved in these sediments cannot be used for paleoproductivity reconstruction. It has been shown (Hillaire-Marcel et al. 1994a) that variations in inorganic carbon are high between glacial and interglacial periods, with lower burial rates during glacial periods. Because burial rates of organic carbon are observed to have small variations, inorganic input may exert more control of atmospheric CO₂.

A downcore decrease in $\delta^{13}\text{C}$ and $\delta^{15}\text{N}$ values observed at several sites, may be partly attributed to diagenetic alteration. Although it is difficult to quantify the effect of diagenesis, the stable isotopic compositions of sedimentary OM from the Labrador Sea, where oxygen penetration depth is high, probably indicate that these parameters may be diagenetically altered.

7.2.0. REGIONAL TRENDS IN OM FLUXES

7.2.1. Labrador Sea

In the Labrador Sea, thin Holocene sediments (5-10 cm) are found at water depths between 1300 and 3000 m. This can be attributed to non-deposition and/or erosion of sediments owing to the strong WBUC. Sediments eroded from the continental slope are deposited in the Labrador basin, as indicated by sedimentation rates about one order of magnitude higher at sites located at greater water depths (Hillaire-Marcel et al., 1994a). Compared to the Labrador Sea slope areas, the Laurentian Channel has a thicker Holocene sediment layer.

The organic materials that were deposited in the Labrador Sea during the Holocene period are enriched in ^{13}C and ^{15}N relative to that of glacial period. Lower isotopic compositions of nitrogen and carbon during glacial periods can be attributed to (i) a low rate of nutrient utilization, and (ii) high relative proportion of terrestrial OM. Owing to high C/N ratios for glacial sedimentary OM, the dominant factor appears to be the latter.

At many sites, downcore distribution of stable isotopes of organic carbon and nitrogen are characterized by a significant downcore decrease. Such downcore trends can be attributed to (i) a diagenetic alteration of labile OM, (ii) changes in the relative proportions of terrestrial versus marine organic material, and (iii) changes in the rates of nutrient utilization (primary productivity). Owing to increases in the C/N ratios associated with downcore decreases in isotope values, probably the major factor is the variation in the proportion of allochthonous organic material. As pointed out previously, the effect of diagenesis cannot be quantified based on these data alone.

On the continental rise (HU-90-013 PC and HU-91-045-94 PC), the $\delta^{13}\text{C}$ values show that at about 8 ka BP, the Labrador Sea experienced fluxes of OM that was depleted in ^{13}C . This can be attributed either to increase in input of terrestrial OM or reduction (collapse) in primary productivity while the level of input of terrestrial OM remained constant.

Apart from the coarse fraction greater than 150 microns, contents of CaCO_3 , and magnetic properties, the sediment layers deposited under rapid sedimentation rates (including the Heinrich events layers) can be identified using stable isotopes, particularly organic carbon. These events are characterized by low δ -values of organic carbon and nitrogen, low contents of organic carbon and nitrogen, suggesting that a large component of the material was derived from the continent.

7.2.2. Gulf of St. Lawrence

Although the St. Lawrence river is one of major rivers in the world that has a potential of transporting large quantities of allochthonous OM, there is no large component of terrestrial OM in the Laurentian Channel (Gulf of St. Lawrence). This can be attributed either to a significant dilution by high fluxes of marine OM, caused by high primary productivity or deposition/trapping of riverine load in the estuary. Furthermore, it has been shown by ^{13}C and ^{15}N values at a few sites that macrophytes could be one of the sources that may contribute a significant amount of OM to the area.

On the Scotian slope (site HU-90-031-44 PC), sediments deposited during glacial-deglacial

periods are depleted in ^{13}C and ^{15}N compared to those of the Holocene period. Although several factors such as differences in primary productivity can be invoked as the possible cause, an enhanced input of terrestrial OM seems the major factor, as indicated by high C/N ratios during the deglacial period. The highest input of OM that was depleted in both ^{13}C and ^{15}N occurred between 12 and 13 ka. This time interval (12-13 ka) corresponds to a warm Bölling-Allerød event.

Contrary to the observations of sediments from the Labrador Sea, the 8 ka event is not recorded on the Scotian slope, probably because most of meltwater were not channelled through the river of St. Lawrence during this interval, but through the Hudson Strait, as pointed out by Dawson (1992).

7.2.3. Lateral Trends

In the Labrador Sea, the stable isotope values of organic carbon decrease with increasing water depth. This is contrary to other observations in which offshore values increase in ^{13}C (Sackett and Thompson, 1963; Schultz and Calder, 1976; Botello et al., 1980; Macko, 1983; Lucotte et al., 1991). The offshore decrease in $\delta^{13}\text{C}$ values can be attributed either to decrease in the rate of nutrient utilization (low primary productivity) or increase in the proportion of terrestrial material reworked from the continental shelf and slope by near bottom currents such as WBUC.

The $\delta^{15}\text{N}$ values for sediments recovered from the Gulf of St. Lawrence are higher (greater than 8‰) compared to those of Labrador Sea (less than 8‰) owing to a higher rate of nutrient utilization in the Gulf of St. Lawrence. In contrast, the CaCO_3 content and C/N ratios are lower in the Gulf of St. Lawrence than in the Labrador Sea. Higher C/N ratios in the Labrador Sea may indicate influence of diagenetic alteration and/or slightly higher input of terrestrial OM.

The contents of organic carbon (>1%) and total nitrogen (>0.1%) in the sediments from the Gulf of St. Lawrence are higher than those of the Labrador Sea (less than 0.6% and 0.1% respectively). This can be attributed to high flux of OM (high rate of nutrient utilization owing to

high primary productivity), higher sedimentation rates and preservation of OM. As mentioned previously, the oxygen penetration depth is high in the Labrador sea relative to that of Gulf of St. Lawrence (see Figs. 3.3 and 3.4). Because the degradation of OM is thought to be enhanced in oxic environments, the observed differences may be attributed to diagenetic alteration of OM as well as to relatively lower primary productivity in the Labrador Sea.

Estimates of burial rate and paleoproductivity in the Labrador Sea for the Holocene period are higher at sites located at greater depth. This can be attributed to sediment focusing, with sediments eroded from the continental shelf and slope re-deposition at deeper sites. In contrast, burial rate and productivity in the Gulf of St. Lawrence decrease with increasing water depth.

There are significant differences in OM burial rates between the Labrador Sea and Gulf of St. Lawrence. Higher OM burial rates in the Gulf of St. Lawrence likely indicate a higher primary productivity.

7.3.0. GLACIAL/INTERGLACIAL

In general, there is a small differences in burial rate and paleoproductivity between glacial and interglacial periods with exception of site HU-90-013-13 PC on the Greenland rise. Most of the sites have lower sedimentation rates during the Holocene than during the glacial-deglacial periods (Hillaire-Marcel et al., 1994a). Because lower sedimentation rates are associated with higher rates of OM degradation, the fraction of OM preserved during the Holocene is likely limited to only the most refractory material.

Reworking of sediments from the continental shelf and slope and its subsequent deposition in the deep Labrador basin has resulted into elevated burial rates of organic carbon and nitrogen. The WBUC is responsible for reworking of sediments. It is difficult to delineate reworked marine OM from unreworke component. As a result, the burial rates estimated for the Labrador Sea and north Atlantic by many workers (e.g. Manighetti and McCave, 1995; Paetsch et al., 1992; Stein, 1991)

may have yielded overestimations of the actual amount of autochthonous OM preserved in the marine sediments.

Through the use of a mixing equation, and the assumption that the end member values for marine and terrestrial OM are -21‰ and -26‰, respectively, the fraction of marine organic carbon obtained for sediments accumulating in a high depositional rate is very low. Such layers, particularly those associated with Heinrich events had low burial rates of marine organic carbon and nitrogen. This indicates that primary productivity during these events was considerably reduced. This conclusion is in agreement with the observed reduction in the concentration of various primary indicators during this time interval (Broecker et al., 1992)

7.4.0. AMINO ACIDS: AN INSIGHT INTO DIAGENETIC EFFECTS?

In the Gulf of St. Lawrence, the most abundant amino acids are glycine, aspartic acid and glutamic acid. These three amino acids contribute about 50% of the total hydrolysable amino acids (THAA) in these sediments. Although high concentrations of these amino acids in marine sediments have been assumed to originate either from carbonate bearing organisms or land-derived humic compounds (Degens and Mopper, 1976; Carter and Mitterer, 1978; Haugen and Lichtentaler, 1991), these amino acids in the Gulf of St. Lawrence cannot be used as indicators for these sources of OM. This is because (i) the results of stable isotopes of organic carbon and nitrogen, and C/N ratios have indicated little influence of terrestrial OM in the area, (ii) of low content of CaCO_3 in the Gulf of St. Lawrence, and (iii) of a recent findings by Cowie and Hedges (1992) that have shown occurrence of high concentration of these amino acids in terrestrial as well as marine organisms (see Fig. 1.12).

Amino acids in marine sediments are important recorders of diagenetic changes. One of the parameters which has shown to be a good measure of the degree of alteration of OM is the percentage of the nitrogen contributed by total hydrolysable amino acids to the total nitrogen (THAA-

N/TN). The percentage of THAA-N/TN for all cores is generally less than 38%, indicating some diagenetic alteration.

7.5.0. PROBLEMS OF INTERPRETATION

In areas with low sedimentation rates, stable isotope compositions of organic carbon and nitrogen can be potentially altered. This could lead to misinterpretation of the actual record. For example, in the Labrador Sea where the oxygen penetration depth is high relative to that of the Gulf of St. Lawrence, part of the downcore decreases in isotope compositions observed in many of the cores can be attributed to diagenetic alteration. But it is difficult to quantify such isotope effects. In the Gulf of St. Lawrence, there is a small downcore change in the isotopic composition of organic carbon suggesting that this parameter is a conservative tracer in environments where the flux of OM is high.

Accurate determination of sedimentation rates are vital in estimating burial rates and primary productivity. Owing to uncertainties, particularly in the Gulf of St. Lawrence, the estimated burial rates and paleoproductivities are first order estimates. Although time control for most of the piston cores was good, estimation of sedimentation rates for the fast deposited layers (Heinrich events and turbidite) is also difficult, thus their burial rates and paleoproductivities may be, at best, only poor estimates.

Assumptions of distinct isotopic compositions from various sources in the marine environments is also not easily met. The horizontal deposition of reworked marine OM from the continental shelf and slope areas through turbidity currents, erosion by WBUC and slumping cannot be clearly identified using stable isotopes or other means. Thus the estimated accumulation of marine OM is at best only of first order estimation of local fluxes.

There is uncertainty in the quantity of reworked marine OM that is transported horizontally

by near bottom currents. A poor discrimination between autochthonous and reworked marine OM presents ambiguous estimates of paleoproductivity, based on the content of organic carbon and nitrogen in the sediments. Manighetti and McCave (1995) also observed lack of differences in primary productivity between glacial and interglacial period and attributed it to errors in the equation of Sarnthein (1992). Although primary productivity indicators may point to higher rates of production, buried OM may not indicate such records, owing to diagenetic alteration and/or deposition of reworked marine OM.

7.7.0. SCIENTIFIC CONTRIBUTIONS

The present study has demonstrated that the horizontal transport of reworked sedimentary OM from shelf and continental slope areas in the Labrador Sea is a dominant process. On the contrary, although large rivers are suspected to transport riverine load to greater distances offshore, in the Gulf of St. Lawrence, most of the organic material is likely deposited within the estuary.

In the Gulf of St. Lawrence, information on the stable isotopes of nitrogen for sedimentary OM was previously non-existent. The present study has provided the first data set that covers large part of the Gulf. The stable isotopic compositions of nitrogen are generally higher than 8‰. Similarly, the previously available data for stable isotopes of organic carbon was mainly for particulate OM and surficial sedimentary OM. Analysis of several box cores and piston cores now provide a more detailed temporal account on the distribution of stable OM isotopes.

Few studies have documented the distribution (spatial and temporal) of the stable isotopic compositions of organic carbon and nitrogen in the Labrador Sea (Macko, 1989; Rogers et al., 1972). These studies utilized samples from Ocean Drilling Program and Deep Sea Drilling Program that were sampled at a low resolution. The present study provides a higher resolution information on spatial and temporal variation in the isotopic compositions of sedimentary OM and covers a much

larger area.

The distribution of amino acids in marine sediments has provided information on the diagenetic alteration of OM. However few studies have been conducted to document diagenetic changes in Gulf of St. Lawrence, an area influenced by high flux of labile OM, using either amino acids or other methods. Therefore, the present study has also provided the first data set on the distribution of amino acids in the Laurentian Channel. The most abundant amino acids are glycine, aspartic acid and glutamic acid. Globally, there are a few amino acid data for coastal environments. Thus, this study has further contributed more information on the compositions of amino acids in marine environments.

In the Gulf of St. Lawrence, there is sufficient information on the present day primary productivity. However, both spatial and temporal quantitative estimates of paleoproductivity are lacking. The present study has provided an insight into variations in primary productivity through time based on preserved organic carbon.

In the northern Atlantic Ocean, rapidly deposited layers (cf. Heinrich layers) have been documented using grain size distribution (> 150 microns), abundance of microfossils and magnetic properties. The stable isotopes of organic carbon and nitrogen can be used as a potential supplementary tool to identify these layers. As pointed out above, the layers are characterized by low stable isotopes values of organic carbon and nitrogen, preserving source signature.

The present study has shown significant differences in the storage of carbon in marginal basins as well as differences in the isotopic compositions of organic carbon and nitrogen of between the Labrador Sea and Gulf of St. Lawrence. Higher burial rates of carbon occurs in the Gulf of St. Lawrence. Such information was previously lacking.

8.0. REFERENCES

- Aizenshtat, Z., Baedeker, M. J., and Kaplan, I. R., 1973. Distribution and diagenesis of organic compounds in JEODES sediments from Gulf of Mexico and western Atlantic. **Geochim. Cosmochim. Acta** **37**, 1881-1898.
- Aksu, A. E., Mudie, P. J., Macko, S. A., and de Vernal, A., 1988. Upper Cenozoic history of the Labrador Sea, Baffin Bay, and the Arctic Ocean. A paleoclimatic and paleoceanographic summary. **Paleoceanography** **3**, 519-538.
- Aksu, A. E. and Hillaire-Marcel, C., 1989. Upper Miocene to Holocene oxygen and carbon isotope stratigraphy of Sites 646 and 647, Labrador Sea. In: Srivastava, S. P., Arthur, M., et al., (eds) *Proceedings, ODP Scientific Results, Vol. 105*. College Station Texas, p. 689-704.
- Aksu, A. E., de Vernal, A. and Mudie, P. J., 1989. High resolution foraminifer, palynologic, and stable isotopic records of upper Pleistocene sediments from the Labrador Sea: Paleoclimatic and paleoceanographic trends. In: Srivastava, S. P., Arthur, M., et al., (eds) *Proceedings, ODP Scientific Results, Vol. 105*. College Station Texas, p. 617-652.
- Aksu, A. E., Mudie, P. J., de Vernal, A. and Gillespie, H., 1992. Ocean-atmosphere responses to climatic change in the Labrador Sea: Pleistocene plankton and pollen records. **Palaogeogr. Palaeoclimatol. Palaeoecol.** **92**, 121-137.
- Altabet, M. A., 1988. Variations in nitrogen isotopic composition between sinking and suspended particles: Implications for nitrogen cycling and particle transformation in open ocean. **Deep Sea Research** **35**, 535-554.
- Altabet, M. A., and McCarthy, J. J., 1985. Temporal and spatial variations in the natural abundance of ^{15}N in POM from a warm-core ring. **Deep Sea Research** **32**, 755-772.
- Altabet, M. A., and McCarthy, J. J., 1986. Vertical patterns in ^{15}N natural abundance in POM from the surface waters of warm-core rings. **Journal of Marine Research** **44**, 185-201.
- Altabet, M. A., and Francois, R., 1994a. The use of nitrogen isotopic ratio for reconstruction of past changes in surface ocean nutrient utilization. In: *Carbon Cycling in Glacial Ocean: Constraints on the Ocean's Role in Global Change*. Eds.: R. Zahn, M. Kaminski, L. D. Labeyrie, and T. F. Pedersen. Springer, Heidelberg, p. 281-306.
- Altabet, M. A., and Francois, R., 1994b. Sedimentary nitrogen isotopic ratio as a recorder for surface ocean nitrate utilization. **Global Biogeochemical Cycles** **8**, 103-116.
- Altabet, M. A., Deuser, W. G., Honjo, S., and Steinen, C., 1991. Seasonal and depth-related changes in the source of sinking particles in the north Atlantic. **Nature** **354**, 136-139.

Anderson, T. F., and Arthur, M. A., 1983. Stable isotopes of oxygen and carbon and their application to sedimentological and paleoenvironmental problems. In: Arthur, M. A., Anderson, T. F., Kaplan, I. R., Viezer, J., and Land, L. S. (eds) *Stable Isotopes in Sedimentary Geology. SEPM Short Course No. 10*, Dallas p. 1-1-1-151.

Anderson, B., Scalan, R. S., Behrens, E. Wm., and Parker, P. L., 1992. Stable carbon isotope variations in sediment from Baffin Bay, Texas, U.S.A.: Evidence for cyclic changes in organic matter source. **Chemical Geology** **101**, 223-233.

Anderson, T. W., and Lewis, C. F., 1992. Climatic influences of deglacial drainage changes in southern Canada at 10 to 8 Ka suggested by pollen evidence. **Géographie Physique et Quaternaire**, **46**, 255-272.

Andrews, J. T., Erlenkeuser, H., Tedesco, K., Aksu, A. E. and Jull, A. J. T., 1994. Late Quaternary (Stage 2 and 3) meltwater and Heinrich Events, Northwest Labrador Sea. **Quaternary Research** **41**, 26-34.

Arthur, M. A., Schlanger, S. O., and Jenkyns, H. C. 1987. The Cenomanian-Turonian oceanic anoxic event, II. Paleoceanographic controls on organic matter production and preservation. In: Brooks, J. and Fleet, A. J. (eds) *Marine Petroleum Source Rocks*. Geological Society Special Publication No. 26 pp. 401-420.

Balsam, W., and Heusser, L. E., 1976. Direct correlation of sea surface paleotemperature, deep circulation, and terrestrial paleoclimates: Foraminiferal and palynological evidence from two cores off Chesapeake Bay. **Marine Geology** **21**, 121-145.

Balzer, W., Erlenkeuser, H., Hartmann, M., Muller, P. J., and Pollehne, F., 1987. Diagenesis and exchange processes at the benthic boundary. In: *Lecture Notes on Coastal and Estuarine Studies No. 13: B: Seawater-Sediment Interactions in Coastal Waters* (eds. J. Ruhmor et al.), pp. 111-161. Springer Edition.

Bard, E., Arnold, M., Maurice, P., Duprat, J., Moyes, J., and Duplessy, J-C., 1987. Retreat velocity of the north Atlantic polar front during the last deglaciation determined by ^{14}C accelerator mass spectrometry. **Nature** **328**, 791-794.

Bard, E., Arnold, M., Fairbanks, R. G., and Hamelin, B., 1993. ^{230}Th , ^{234}U and ^{14}C ages obtained by mass spectrometry on corals. **Radiocarbon** **35**, 191-199.

Behrens, E. W., and Frishman, S. A., 1971. Stable carbon isotopes in blue-green algal mats. **Journal of Geology** **79**, 85-100.

Bender, M. M., 1971. Variations in the $^{13}\text{C}/^{12}\text{C}$ ratios of plants in relation to the pathway of photosynthetic carbon dioxide fixation. **Phytochemistry** **10**, 1239-1244.

Benner, R., Fogel, M. L., Sprague, E. K., and Hodson, R. E., 1987. Depletion of ^{13}C in lignin and its implications for stable carbon isotope studies. **Nature** **329**, 708-710.

Berger, W. H., and Herguera, J. C., 1992. Reading the sedimentary record of the oceans productivity. In: *Primary Productivity and Biogeochemical Cycles in the Sea*. Edited by P. G. Falkowski and A. D. Woodhead, Plenum Press, New York. pp 455-486.

Berner, R. A., 1980. *Early Diagenesis*. A theoretical approach. Princeton University Press, Princeton, N.J. 241pp.

Betzer, P. R., Showers, W. J., Laws, E. A., Winn, C. D., Ditullio, G. R., and Kroopnick, P. M., 1984. Primary productivity and particle flux on a transect of the equator at 153°W in the Pacific Ocean. *Deep Sea Research* **31**, 1-11.

Biggs, D. C., Berkowitz, S. P., Altabet, M. A., Bidigare, R. R., DeMaster, D. J., Macko, S. A., Ondrusek, M. E. and Il Noh, 1989. Cooperative study of upper ocean particulate fluxes. In: Barron, J., Larsen, B., et al., 1989. *Proc. ODP, Init. Repts., 119*: College Station, TX (Ocean Drilling Program), p. 109-120.

Biggs, D. C., Berkowitz, S. P., Altabet, M. A., Bidigare, R. R., DeMaster, D. J., Dunbar, R. B., Leventer, A., Macko, S. A., Nittrouer, C. A. and Ondrusek, M. E. 1988. Cooperative study of upper ocean particulate fluxes in Weddell Sea. In: Barker, P. F., Kennett, J. P., et al., 1988. *Proc. ODP, Init. Repts., 113*: College Station, TX (Ocean Drilling Program), p. 77-86.

Billen, G., 1982a. An idealized model of nitrogen cycling in marine sediments. *Am. J. Sci.* **282**, 512-541.

Billen, G., 1982b. Modelling the processes of organic matter degradation and nutrient recycling in sedimentary systems. In: Nedwell, D. B., and Brown, C. M. (eds), *Sediment Microbiology*, pp. 15-52. Academic Press, London.

Bilodeau, G., de Vernal, A. and Hillaire-Marcel, C., 1994. Benthic foraminifer assemblages in deep Labrador Sea sediments: Relation with deep water mass changes since the deglaciation. *Can. J. Earth Sci.* **31**, 128-138.

Bond, G., Broecker, W., Johnsen, S., McManus, J., Labeyrie, L., Jouzel, J., and Bonani, G., 1993. Correlations between climate records from north Atlantic sediments and Greenland ice. *Nature* **365**, 143-147.

Bond, G., Heinrich, H., Broecker, W., Labeyrie, L., McManus, J., Andrews, J., Huon, S., Jantschik, R., Clasen, S., Simet, C., Tedesco, K., Klas, M., Bonani, G. and Ivy, S., 1992. Evidence of massive discharges of icebergs into the North Atlantic Ocean during the last glacial period. *Nature* **360**, 245-249.

Bonifay, D. and Giresse, P., 1992. Middle to late Quaternary sediment flux and post-depositional processes between the continental slope off Gabon and the Mid-Guinean margin. *Marine Geology*, **106**, 107-129.

Botello, A. V., Mandelli, E. F., Macko, S., and Parker, P. L., 1980. Organic carbon isotope ratios of recent sediments from coastal lagoons of the Gulf of Mexico, Mexico. *Geochim. Cosmochim. Acta* **44**, 557-559.

Broecker, W. S., Andree, M., Wolfli, W., Oeschger, H., Bonani, G. Kennett, J., and Peteet, D., 1988. The chronology of the last deglaciation: Implications to the cause of the Younger Dryas event. **Paleoceanography** 3, 1-19.

Broecker, W. S., Bond, G., McManus, J., Klas, M., and Clark, E., 1992. Origin of the northern Atlantic's Heinrich events. **Climatic Dynamics** 6, 265-273.

Broecker, W. S., Bond, G., Klas, M., Bonani, G., and Wolfli, W., 1990. A salt oscillator in the glacial northern Atlantic I, The concept. **Paleoceanography** 5, 469-477.

Burdige, D. J., and Martens, C. S., 1988. Biogeochemical cycling in an organic-rich coastal marine basin: 10. The role of amino acids in sedimentary carbon and nitrogen cycling. **Geochim. Cosmochim. Acta** 52, 1571-1584.

Calder, J. A., and Parker, P. L., 1973. Geochemical implications of induced changes in ^{13}C fractionation by blue green algae. **Geochim. Cosmochim. Acta** 37, 133-140.

Calvert, S. E., 1987. Oceanographic controls on the accumulation of organic matter in marine sediments. In: Brooks, J., and Fleet, A. J., *Marine Petroleum Source Rocks*. Geological Society of London Special Publication 26, p. 137-151.

Calvert, S. E., and Pedersen, T. F., 1992. Organic carbon accumulation and preservation in marine sediments: How important is anoxia?. In: Whelan, J. K., and Farrington, J. W. (eds) *Organic matter: Productivity, Accumulation, and Preservation in Recent and Ancient Sediments*. Columbia University Press New York, p. 231-263.

Calvert, S. E., Nielsen, B., and Fontugne, M. R., 1992a. Evidence from nitrogen isotope ratios for enhanced productivity during formation of eastern Mediterranean sapropel. **Nature** 359, 223-225.

Calvert S. E., Bustin, R. M., and Pedersen, T. F., 1992b. Lack of evidence for enhanced preservation of sedimentary organic matter in the oxygen minimum of the Gulf of California. **Geology** 20, 757-760.

Canfield, D., 1994. Factors influencing organic carbon preservation in marine sediments. **Chemical Geology** 114, 315-329.

Canfield, D., 1989. Sulphate reduction and oxic respiration in marine sediments: Implications for organic preservation in euxinic environments. **Deep Sea Research**, 36, 121-138.

Carter, P. W. and Mitterer, R. M., 1978. Amino acid composition of organic matter associated with carbonate and non-carbonate sediments. **Geochimica et Cosmochimica Acta** 42, 1231-1238.

Carter, L., Schafer, C. T. and Rashid, M. A., 1979. Observations on depositional environments and benthos of the continental slope and rise, east of Newfoundland. **Can. J. Earth Sci.** 16, 831-846.

Chough, S. K. and Hesse, R., 1985. Contourites from Eirik ridge, south of Greenland. **Sedimentary Geology** 41, 185-199.

Cifuentes, L. A., Sharp, J. H. and Fogel, M. L., 1988. Stable carbon and nitrogen isotope biogeochemistry in Dalware estuary. **Limnology Oceanography** **33**, 1102-1115.

CLIMAP Project Members (1976). The surface of the ice-age earth. **Science** **191**, 1131-1137.

Coote, A. R. and Yeats, P. A., 1979. Distribution of nutrients in the Gulf of St. Lawrence. **J. Fish. Res. Board Can.** **36**, 122-131.

Coppedge, M. L., and Balsam, W. L., 1992. Organic distribution in the north Atlantic Ocean during the last glacial maximum. **Marine Geology** **105**, 37-50.

Cowie, G. L., and Hedges, J. I., 1994. Biochemical indicators of diagenetic alteration in natural organic matter mixtures. **Nature** **369**, 304-307.

Cowie, G. L., and Hedges, J. I., 1992. Sources and reactivities of amino acids in a coastal marine environment. **Limnol. Oceanogr.** **37**, 703-724.

Cowie, G. L., Hedges, J. I., and Calvert, S. E., 1992. Sources and relative reactivities of amino acids, neutral sugars, and lignin in an intermittently anoxic marine environment. **Geochimica et Cosmochimica Acta** **56**, 1963-1978.

Cremer, M., Grousset, F., Faugères, J. C. and Gonthier, E., 1992. Sediment flux patterns in the northeastern Atlantic: Variability since the last interglacial. **Marine Geology**, **104**, 31-53.

d'Anglejan, B. F. and Smith, E. C., 1973. Distribution, transport, and composition of suspended matter in the St. Lawrence Estuary. **Can. J. Earth Sci.**, **10**, 1380-1396.

Dawson, A. G., 1992. *Ice Age Earth: Late Quaternary Geology and Climate*, Chapter 5. Routledge, London.

Dean, W. E., Gardner, J. V., and Anderson, R. Y., 1994. Geochemical evidence for enhanced preservation of organic matter in oxygen minimum zone of the continental margin of northern California during the late Pleistocene. **Paleoceanography** **9**, 47-61.

Dean, W. E., Arthur, M. A., and Claypool, G. E., 1986. Depletion of ^{13}C in Cretaceous marine organic matter: Source, diagenetic, or environmental signal?. **Marine Geology** **70**, 119-157.

Degens, E. T., 1967. Diagenesis of organic matter. In: Larsen, G., and Chilingar, G. V., (eds), *Development in Sedimentology* **8**. Elsevier Publishing Company, New York, p. 343-390

Degens, E. T., 1969. Biogeochemistry of stable carbon isotopes. In: Englington, G. and Murphy, M. T. J. (eds) *Organic Geochemistry*. Springer Verlag, New York, p. 304-329.

Degens, E. T. and Mopper, K., 1976. Factors controlling the distribution and early diagenesis of organic material in marine sediments. In: Riley, J. P. and Chester, R. (eds) *Chemical Oceanography*, Vol. 6, 2nd edition, Academic Press London, p. 59-113.

Deines, E. T. (1980). The isotopic composition of reduced organic carbon. In: Fritz, P. and Fontes, J. Ch., (eds). *Handbook of Environmental Isotope Geochemistry* Vol. 1A. Elsevier, New York. p. 329-406.

Demaison, G. J., and Moore, G. T., 1980. Anoxic environments and oil source bed genesis. **Organic Geochemistry** 2, 9-31.

de Vernal, A., and Hillaire-Marcel, C., 1987. Paleoenvironments along the eastern Laurentide ice sheet margin and timing of the last ice maximum and retreat. **Géographie Physique et Quaternaire** 41, 265-277.

de Vernal, A., and Mudie, P. J., 1989a. Late Pliocene to Holocene palynostratigraphy at ODP site 645, Baffin Bay. In: Srivastava, S. P., Arthur, M., Clement, B. et al., (eds) *Proceedings of the Ocean Drilling Program, Scientific Results, Vol. 105*. College Station Texas, p. 387-399.

de Vernal, A., and Mudie, P. J., 1989b. Pliocene and Pleistocene palynostratigraphy at ODP sites 646 and 647 eastern and southern Labrador Sea. In: Srivastava, S. P., Arthur, M., Clement, B. et al., (eds) *Proceedings of the Ocean Drilling Program, Scientific Results, Vol. 105*. College Station Texas, p. 401-422.

de Vernal, A., and Giroux, L., 1991. Distribution of organic walled microfossils in recent sediments from the estuary and Gulf of St. Lawrence: Some aspects of the organic matter fluxes. In: J.-C. Therriault (ed.) *The Gulf of St. Lawrence: Small Ocean or Big Estuary?*. **Canadian Special Publication of Fisheries and Aquatic Sciences** 113, 189-199.

de Vernal, A., Guiot, J., and Turon, J.-L., 1993. Late and postglacial paleoenvironments of the Gulf of St. Lawrence: marine and terrestrial palynological evidence. **Géographie Physique et Quaternaire** 47, 167-180.

de Vernal, A., Turon, J.-L. and Guiot, J., 1994. Dinoflagellate cyst distribution in high latitude marine environments in relation with sea-surface conditions: Through transfer functions for the reconstructions of temperature, salinity and seasonality. **Can. J. of Earth Sci.** 31, 48-62.

Dowdeswell, J. A., Maslin, M. A., Andrews, J. T. and McCave, I. N., 1995. Iceberg production, debris rafting and the extent and thickness of Heinrich layers (h-1, H-2) in North Atlantic sediments. **Geology** 23, 301-304.

Dyke, S. A., and Prest, V. K., 1987. Late Wisconsinan and Holocene history of the Laurentide Ice sheet. **Géographie Physique et Quaternaire** 41, 237-263.

El-Sabh, M. I., 1976. Surface circulation pattern in the Gulf of St. Lawrence. **J. Fish. Res. Board Can.**, 33, 124-138.

El-Sabh, M. I., 1979. The lower St. Lawrence estuary as a physical oceanographic system. **Naturaliste Can.** 106, 55-73.

Emerson, S., and Hedges, J. I., 1988. Processes controlling the organic carbon content of the open ocean sediments. **Paleoceanography**, 3, 621-634.

Erdman, J. G., Marlett, E. M., and Hanson W. E., 1956. Survival of amino acids in marine sediments. *Science* **124**, 1026.

Fairbanks, R. G., 1989. A 17,000-year glacio-eustatic sea level record: Influence of glacial melting rates on the Younger Dryas event and deep-ocean circulation. *Nature* **342**, 637-642.

Faure, G., 1986. *Principle of Isotope Geochemistry* 2nd Edition. John Willy & sons, New York. 589pp.

Fillon, R. H., 1976. Hamilton Bank, Labrador shelf: Postglacial sediment dynamics and paleoceanography. *Marine geology* **20**, 7-25.

Fillon, R. H. and Duplessy, J. C., 1980. Labrador Sea bio-, terphro- oxygen isotopic stratigraphy and late Quaternary paleoceanography trends. *Can. J. Earth Sci.* **17**, 831-854.

Fogel, M. L., and Cifuentes, L. A., 1993. Isotope fractionation during primary production. In: Engel, M. H., and Macko, S. A., (eds) *Organic Geochemistry*. Plenum Press, New York. p. 73-98.

Fontugne, M. R., and Duplessy, J. C., 1978. Carbon isotope ratio of marine plankton related to surface water masses. *Earth and Planetary Science Letters* **41**, 365-371.

Fontugne, M. R., and Duplessy, J. C., 1981. Organic carbon isotopic fractionation by marine plankton in the temperature range -1 to 31°C. *Oceanologica Acta* **4**, 85-90.

Fontugne, M. R., and Duplessy, J. C., 1986. Variation of monsoon regime during the upper Quaternary: Evidence from carbon isotopic record of organic matter in north Indian Ocean sediment cores. *Paleoceanogr. Paleoclimatol. Paleoecol.*, **56**, 69-88.

Francois, R., and Bacon, M., 1994. Heinrich events in the north Atlantic: radiochemical evidence. *Deep Sea Research* **41**, 315-334.

Francois, R., Altabet, M. A., and Burckle, L. H. 1992. Glacial to interglacial changes in surface nitrate utilization in the Indian sector of the southern ocean as recorded by sediment $\delta^{15}\text{N}$. *Paleoceanography* **7**, 589-606.

Francois, R., Bacon, M. P. Altabet, M. A., and Labeyrie, L. D., 1993a. Glacial to interglacial changes in sediment rain rate in the SW Indian sector of subantarctic waters as recorded by ^{230}Th , ^{231}Pa , U, and $\delta^{15}\text{N}$. *Paleoceanography* **8**, 611-629.

Francois, R., Altabet, M. A., Georicke, R., McCorkle, D. C., Brunet, C. and Poisson, A., 1993b. Changes in the $\delta^{13}\text{C}$ of surface water particulate organic matter across the subtropical convergence in the SW Indian Ocean. *Global Biogeochemical Cycles* **7**, 627-644.

Froelich, P. N., Klinkhammer, G. P., Bender, M. L., Luedtke, N. A., Heath, G. R., Cullen, D., Dauphin, P., Hammond, D., and Hartman, B., 1979. Early oxidation of organic matter in pelagic sediments of the eastern equatorial Atlantic: suboxic diagenesis. *Geochimica et Cosmochimica Acta* **43**, 1075-1090.

Fry, B., and Sherr, E. B., 1984. $\delta^{13}\text{C}$ measurements as indicators of carbon flow in marine and freshwater ecosystems. *Contributions to marine Science* **27**, 13-47.

- Fulton, R. J. and Prest, V. K., 1987. The Laurentide ice sheet and its significance. *Géographie Physique et Quaternaire* **41**, 181-186.
- Funder, S. and Larsen, H. C., 1989. Quaternary geology of the shelves adjacent to Greenland; In Chapter 13 of Quaternary Geology of Canada and Greenland, R. J. Fulton (ed). *Geological Survey of Canada, Geology of Canada No. 1* (Also Geological Society of America, The Geology of North America, V. K-1), p. 769-772.
- Gariépy, C., Ghaleb, B., Hillaire-Marcel, C., Mucci, A., and Vallières, S., 1994. Early diagenetic processes in Labrador sea sediments: Uranium isotope geochemistry. *Can. J. Earth Sci.* **31**, 28-37.
- Gearing, J. N., 1988. The use of stable isotope ratios for tracing the nearshore-offshore exchange of organic matter. In: *Lecture Notes on Coastal-Offshore Ecosystem Studies*, Vol. 22, Jansson, B. O. (ed), Coastal-Offshore Ecosystem Interactions, Springer-Verlag, Berlin, p. 69-101.
- Gearing, J. N., Gearing, P. J., Rudnick, D. T., Requejo, S. G., and Hutchins, M. J., 1984. Isotopic variability of organic carbon in a phytoplankton-based temperate estuary. *Geochim. Cosmochim. Acta*, **48**, 1089-1098.
- Glenn, C. R. and Arthur, M. A., 1985. Sedimentary and geochemical indicators of productivity and oxygen contents in modern and ancient basins: The Holocene Black Sea as the "Type " Anoxic Basin. *Chemical Geology* **48**, 325-354.
- Goericke, R. and Fry, B., 1994. Variations of marine plankton $\delta^{13}\text{C}$ with latitude, temperature, and dissolved CO_2 in the world ocean. *Global Biogeochemical Cycles* **8**, 85-90.
- Grant, A. C., 1972. The continental margin off Labrador and eastern Newfoundland-Morphology and geology. *Can. J. Earth Sci.*, **9**, 1394-1430.
- Grousset, F. E., Labeyrie, L., Sinko, J. A., Cremer, M., Bond, G., Duprat, J., Cortijo, E. and Huon, S., 1993. Patterns of ice-rafted detritus in the glacial North Atlantic (40-55°N). *Paleoceanography* **8**, 175-192.
- Grundmanis, V., and Murray, J. W., 1982. Aerobic respiration in pelagic marine sediments. *Geochim. Cosmochim. Acta* **46**, 1101-1120.
- Hall, F. R., Bloemendal, J., King, J. W., Arthur, M. A. and Aksu, A., 1989. Middle to Late Quaternary sediment fluxes in the Labrador Sea, ODP Leg 105, Site 646: A synthesis of rock-magnetic, oxygen-isotopic, carbonate, and planktonic foraminiferal data. In: Srivastava, S. P., Arthur, M., et al., (eds) *Proceedings, ODP Scientific Results*, Vol. 105. College Station Texas, p. 653-688.
- Hare, P. E., 1973. Amino acids, amino sugars, and ammonia in sediments from the Cariaco trench. In: Kaneps (ed.) *Initial Reports of the Deep Sea Drilling Project* Vol. 20. p. 941-942.
- Hare, P. E., 1969. Geochemistry of proteins, peptide, and amino acids. In: Eglinton, G. and Murphy, M. T. J., (eds) *Organic Geochemistry Methods and Results*. Springer-Verlag, New York, p. 438-463.

- Hare, P. E., and Estep, M., 1983. Carbon and nitrogen isotopic composition of amino acids in modern and fossil collagens. *Carnegie Institution Geophysical Laboratory Yearbook*, Washington, p. 410-414.
- Hatcher, P. G., Spiker, E. C., Szeverenyi, N. M., and Maciel, G. E., 1983. Selective preservation and origin of petroleum-forming aquatic kerogen. *Nature* **305**, 498-501.
- Haugen, J.-E., and Lichtentaler, R., 1991. Amino acids diagenesis, organic carbon and nitrogen mineralization in surface sediments from the inner Oslofjord, Norway. *Geochim. Cosmochim. Acta* **55**, 1649-1661.
- Hay, W. W., 1993. The role of polar deep water formation in global climate change. *Annu. Rev. Earth Planet. Sci.* **21**, 227-254.
- Hedges, J. I., Clark, W., and Cowie, G. L., 1988. Organic matter sources to the water column and surficial sediments of marine bay. *Limnol. Oceanogr.* **33**, 1116-1136.
- Heezen, B. C. and Hollister, C. D., 1971. *The Face of the Deep*. Oxford University Press, New York, 659pp.
- Heezen, R., Hollister, C. D. and Ruddiman, W. F., 1966. Shaping of the continental rise by deep geostrophic contour currents. *Science* **152**, 502-508.
- Henderson, G., Schiener, J. B., Croxton, C. A. and Andersen, B. B., 1981. The west Greenland Basin. In: Kerr, J. W. M., Fergusson, A. J. and Machan, L. C. (eds). *Geology of the North Atlantic Borderlands*. Can. Soc. Petrol. Geol., Memoir 7, Calgary, p. 399-428.
- Heinrich, H., 1988. Origin and consequences of cyclic ice rafting in the northeast Atlantic Ocean during the past 130,000 years. *Quaternary Research* **29**, 142-152.
- Henrich, R., Wagner, T., Goldschmidt, P., and Michels, K., 1995. Depositional regimes in the Norwegian-Greenland Sea: the last two glacial to interglacial transitions. *Geol. Rundsch* **84**, 28-48.
- Henrichs, S. M., 1992. Early diagenesis of organic matter in marine sediments: progress and perplexity. *Marine Chemistry* **39**, 119-149.
- Henrichs, S. M., and Farrington, J. W., 1987. Early diagenesis of amino acids and organic matter in two coastal marine sediments. *Geochim. Cosmochim. Acta* **51**, 1-15.
- Henrichs, S. M., Farrington, J. W., and Lee, C., 1984. Peru upwelling region sediments near 15°S. Dissolved free and total hydrolysable amino acids. *Limnol. Oceanogr.* **29**, 20-34.
- Hesse, R., 1992. Continental slope sedimentation adjacent to an ice margin. I. Seismic facies of Labrador slope. *Geo-Marine Letters* **12**, 189-199.
- Hesse, R., Chough, S. K. and Rakofsky, A., 1987. The northwest Atlantic mid-Ocean channel of the Labrador Sea. V. Sedimentology of a giant deep-sea channel. *Can. J. Earth Sci.* **24**, 1595-1624.

Hesse, R., Rakofsky, A., and Chough, S. K., 1990. The central Labrador Sea: Facies and dispersal patterns of clastic sediments in a small ocean basin. **Marine and Petroleum Geology** 7, 13-28.

Hillaire-Marcel, C., de Vernal, A., Aksu, A. and Macko, S., 1989. High-resolution isotopic and micropaleontological studies of upper Pleistocene sediments at ODP site 645, Baffin Bay. In: Srivastava, S. P., Arthur, M., Clement, B. et al., (eds) *Proceedings of the Ocean Drilling Program, Scientific Results, Vol. 105*. College Station Texas, p. 599-616.

Hillaire-Marcel, C., Aksu, A., Causse, C., de Vernal, A. and Ghaleb, B., 1990. Response of Th/U in deep Labrador Sea sediments (ODP Site 646) to changes in sedimentation rates and paleoproductivities. **Geology** 18, 162-165.

Hillaire-Marcel, C. and de Vernal, A., 1989. Isotopic and palynological records of the late Pleistocene in eastern Canada and adjacent Ocean basins. **Géographie Physique et Quaternaire** 43, 263-290.

Hillaire-Marcel, C., and Rochon, A., 1990. Cruise report and on board studies CSS HUDSON 90-13 Leg 1: The Labrador Sea. Geological Survey of Canada, open file report.

Hillaire-Marcel, C., Vallières, S., and onboard participants 1991. Report of cruise HU-90-045 in Labrador Sea, Greenland Sea and northwest Atlantic. Geological Survey of Canada, open file report.

Hillaire-Marcel, C., de Vernal, A., Bilodeau, G., and Wu, G., 1994a. Isotope stratigraphy, sedimentation rates, deep circulation and carbonate events in the Labrador Sea during the last 200 ka. **Can. J. Earth Sci.** 31, 63-89.

Hillaire-Marcel, C., de Vernal, A., Lucotte, M., Mucci, A., Bilodeau, G., Rochon, A., Vallières, S., and Wu, G., 1994b. Productivité et flux de carbone dans la mer du Labrador au cours des derniers 40 000 ans. **Can. J. Earth Sci.** 31, 139-157.

Hinga, K. R., Arthur, M. A., Pilson, M. E. Q., and Whitaker, D., 1994. Carbon isotope fractionation by marine phytoplankton in culture: The effects of CO₂ concentration, pH, temperature, and species. **Global Biogeochemical Cycles** 8, 91-102.

Hoefs, J., 1987. *Stable Isotope Geochemistry*. 3rd edition. Springer-Verlag, Berlin. 241p.

Hoefs, J., 1982. Isotope geochemistry of carbon. In: Schmidt, H.-L., Förstel, H., and Heinzinger, K. (eds) *Analytical Chemistry Symposia Series-Vol. 11: Stable Isotopes*. Elsevier Scientific Publishing Company, Amsterdam, p. 103-113.

Howell, M. W. and Thunell, R. C., 1992. Organic carbon accumulation in Bannock Basin: Evaluating the role of productivity in the formation of eastern Mediterranean sapropel. **Marine Geology** 103, 461-471.

Hubner, H., 1986. Isotope effect of nitrogen in the soil and biosphere. In: Fritz, P. and Fontes, J. Ch. *Handbook of Environmental Isotope Geochemistry, Vol. 2. The Terrestrial Environment*, B. Elsevier, New York, p. 361-425.

Ibach, L. E. J., 1982. Relationship between sedimentation rate and total organic carbon content in ancient marine sediments. *Am. Assoc. Petrol. Geol. Bull.* **66**, 170-188.

Ichiye, T., 1966. Labrador Sea. In: Fairbridge, R. W. (ed) *The Encyclopedia of Oceanography. Encyclopedia of Earth Sciences Series*, Vol. 1. Reinhold Publishing Corporation, New York. p. 439-441.

Isemer, H.-J., and Hasse, L., 1985. *The Bunker Climate Atlas of the North Atlantic Ocean. Vol. 1. Observations*. Springer-Verlag, Berlin, --pp.

Jansen, E., and Veum, T., 1990. Evidence for two-step deglaciation and its impact on North Atlantic deep-water circulation. *Nature* **344**, 612-616.

Jasper, J. P., and Gagosian, R. B., 1989. Glacial-interglacial climatically forced $\delta^{13}\text{C}$ variations in sedimentary organic matter. *Nature* **342**, 60-62.

Jasper, J. P., and Gagosian, R. B., 1990. The sources and deposition of organic matter in the Late Quaternary Pigmy Basin. *Geochim. Cosmochim. Acta* **54**, 1117-1132.

Jennane, A., 1992. Application de la Méthode du Plombe-210 dans L'estuaire Maritime et le Golfe de Saint-Laurent. Taux de Sédimentation, Flux et Modes D'ablation. M.Sc. Thesis, Université du Québec a Montréal, 79pp.

JGOFs-Canada, 1989. Canadian national programme for the joint global ocean flux study. (unpublished).

Johnsen, S. J., Clausen, H. B., Dansgaard, W., Gundestrup, N. S., Hansson, M., Jonsson, P., Steffensen, J. P. and Sveinbjørnsdottir, A. E., 1992. A "deep" ice core from east Greenland. *Meddelelser om Grønland, Geoscience* **29**, 1-22.

Johnson, C., Henshaw, J., and McInnes, G., 1992. Impact of air craft and surface emission of nitrogen oxides on tropospheric ozone and global warming. *Nature* **355**, 69-71.

Jones, G., A., and Keigwin, L. D., 1988. Evidence from Fram Strait (78°N) for early deglaciation. *Nature* **336**, 56-59.

Josenhans, H. W., Zevenhuizen, J. and Klassen, R. A., 1986. The Quaternary geology of the Labrador shelf. *Can. J. Earth Sci.* **23**, 1190-1213.

Josenhans, H., Johnston, L., Jarrett, K., Smith, D., and Zevenhuizen, J., 1990. Surfical geological investigations of the Gulf of St. Lawrence. Cruise report HUDSON 90-028. Geological Survey of Canada, open file report.

Kaplan, I. R., 1983. Stable isotopes of sulfur, nitrogen and deuterium in recent marine sediments. In: Arthur, M. A., Anderson, T. F., Kaplan, I. R., Viezer, J. and Land, L. S. (eds) *Stable Isotopes in Sedimentary Geology*. SEPM Short Course No. 10, Dallas, p. 2-1-2-108.

Karamanos, R. E., and Rennie, D. A., 1978. Nitrogen isotope fractionation during ammonium exchange reactions with soil clays. *Can. J. Soil Sci.* **58**, 53-60.

Keen, C., Blanchard, J. E. and Keen, M. J., 1966. Gulf of St. Lawrence. In: Fairbridge, R. W. (ed) *The Encyclopedia of Oceanography. Encyclopedia of Earth Sciences Series*, Vol. 1. Reinhold Publishing Corporation, New York. p. 331-335.

Keigwin, L. D., and Jones, G. A., 1990. Deglacial climatic oscillations in the Gulf of California. *Paleoceanography*, **5**, 1009-1023.

Keigwin, L. D., Jones, G. A., and Lehman, S. J., 1991. Deglacial meltwater discharge, North Atlantic deep circulation, and abrupt climate change. *Journal of Geophysical Research*, **96**, 16811-16826.

Kelly, M., 1985. A review of the Quaternary geology of western Greenland. In: Andrews, J. T. (ed.) *Quaternary Environments Eastern Canadian Arctic, Baffin Bay and Western Greenland*. Allen & Unwin, Boston, p. 461-501.

Kerr, R. A., 1980. A new kind of storm beneath the sea. *Science* **208**, 484-486.

Klump, J. V., and Martens, C. S., 1987. Biogeochemical cycling in an organic-rich coastal marine basin. 5. Sedimentary nitrogen and phosphorus budgets based upon kinetic models, mass balances, and the stoichiometry of nutrient regeneration. *Geochim. Cosmochim. Acta* **51**, 1161-1173.

Kvenvolden, K. A., 1975. Advances in the geochemistry of amino acids. *Annual Review of Earth and Planetary Sciences* **3**, 183-212.

Lee, C., 1992. Controls on organic carbon preservation: The use of stratified water bodies to compare intrinsic rates of deposition in oxic and anoxic systems. *Geochim. Cosmochim. Acta* **56**, 3323-3335.

Lee, C. J., and Cronin, C., 1982. The vertical flux of particulate organic nitrogen in the sea. Decomposition of amino acids in Peru upwelling area and the equatorial Atlantic. *J. Mar. Res.* **40**, 227-251.

Létolle, R., 1980. Nitrogen-15 in natural environment. In: Fritz, P. and Fontes, J. (eds) *Handbook of Environmental Geochemistry*, Vol. 1. Elsevier Sci. Publ., New York p. 407-433.

Libes, S. M., and Deuser, W. G., 1988. The isotope geochemistry of particulate nitrogen in the Peru upwelling area and the Gulf of Maine. *Deep Sea Research* **35**, 517-533.

Littke, R., Rullkötter, J. and Schaefer, G., 1991. Organic and carbonate accumulation on Broken Ridge and Nintyeast Ridge, Central Indian Ocean. In: Weissel, J., Peirce, J., Taylor, E., Alt, J. et al., *Proceedings, ODP Scientific Results, Vol. 121*. College Station, Texas, p. 467-487.

Loring, D. H., 1971. Marine geology of the Gulf of St. Lawrence. Earth Science Symposium on Offshore Eastern Canada, Geol. Surv. Can., Paper 71-23, 1973, p. 305-324.

Loring, D. H., 1975. Surficial geology of the Gulf of St. Lawrence. In: Offshore Geology of Eastern Canada. Geol. Sur. Can., Paper 74-30, Vol. 2., p. 11-34.

Loring, D. H. and Nota, D. J. G., 1973. Morphology and sediments of the Gulf of St. Lawrence. **Fish. Res. Board Can. Bull.** **182**, 147p.

Lucotte, M., 1989. Organic carbon isotope ratios and implications for the maximum turbidity zone of the St. Lawrence upper Estuary. **Estuarine, Coastal and Shelf Science** **29**, 293-304.

Lucotte, M., and d'Anglejan, B., 1988. Seasonal changes in the phosphorous-iron geochemistry of the St. Lawrence Estuary. **Journal of Coastal Research** **4**, 339-349.

Lucotte, M., and Hillaire-Marcel, C., 1994. Identification et distribution des grades masses d'eau dans les mer du Labrador et d'Irminger. **Can. J. Earth Sci.** **31**, 5-13.

Lucotte, M., Hillaire-Marcel, C. and Louchouart, P., 1991. First-order organic carbon budget in the St. Lawrence lower Estuary from ^{13}C data. **Estuarine, Coastal and Shelf Science** **32**, 297-312.

Lucotte, M., Mucci, A., Hillaire-Marcel, C., and Tran, S., 1994. Early diagenetic processes in deep Labrador Sea sediments: Reactive and non-reactive iron and phosphorous. **Can. J. Earth Sci.** **31**, 14-27.

Lyle, M., Zahn, R., Prahl, F., Dymond, J., Collier, R., Pisias, N. and Suess, E., 1992. Paleoproductivity and carbon burial across the California Current: The multi-tracers transect, 42°N. **Paleoceanography** **7**, 251-272.

Macko, S. A., 1981. Stable nitrogen isotope ratios as tracer of organic geochemical processes. (Ph.D. dissert.). University of Texas, Austin. 181pp.

Macko, S. A., 1983. Source of organic nitrogen in mid-Atlantic coastal Bays and continental shelf sediments of the United States: Isotopic evidence. Carnegie Institution Geophysical Laboratory Yearbook, Washington, 390-394.

Macko, S. A., 1989. Stable isotope organic geochemistry of sediments from the Labrador Sea (Sites 646 and 647) and Baffin Bay (Site 645), ODP Leg 105. In: Srivastava, S. P., Arthur, M., et al., (eds) *Proceedings, ODP Scientific Results, Vol. 105*. College Station Texas, p. 209-231.

Macko, S. A., and Estep, M. L. F., 1984. Microbial alteration of stable nitrogen and carbon isotopic compositions of organic matter. **Organic Geochemistry** **6**, 787-790.

Macko, S. A., Engel, M. H., and Quian, Y., 1994. Early diagenesis and organic matter preservation - a molecular stable carbon isotope perspective. **Chemical Geology** **114**, 365-379.

Macko, S. A., Engel, M. H. and Parker, P. L., 1993. Early diagenesis of organic matter in sediments. Assesment of mechanisms and preservation by the use of isotopic approaches. In: Engel, M. H., and Macko, S. A., (eds) *Organic Geochemistry*. Plenum Press, New York. p. 211-224.

Macko, S. A., Estep, M. L. F., Hare, P. E., and Hoering, T. C., 1983. Stable nitrogen and carbon isotopic composition of individual amino acids isolated from cultured microorganisms. Carnegie Institution Geophysical Laboratory Yearbook, Washington, 404-410.

Martens, C. S. and Klump, J. V., 1984. Biogeochemical cycling in an organic-rich coastal marine basin. 4. An organic carbon budget for sediments dominated by sulfate reduction and methanogenesis. *Geochim. Cosmochim. Acta* **48**, 1987-2004.

Mayewski, P. A., Meeker, L. D., Whitlow, S., Twickler, M. S., Morrison, M. C., Bloomfield, P., Bond, G. C., Alley, R. B., Gow, A. J., Grootes, P. M., Meese, D. A., Ram, M., Taylor, K. C. and Wumkes, W., 1994. Changes in atmospheric circulation and ocean ice cover over the north Atlantic during the last 41,000 years. *Science* **263**, 1747-1751.

McArthur, J. M., Tyson, R. V., Thompson, J., and Matthey, D., 1992. Early diagenesis of marine organic matter: Alteration of the carbon isotopic composition. *Marine Geology* **105**, 51-61.

McCartney, M. S., 1992. Recirculating components to the deep boundary current of the northern north Atlantic. *Prog. Oceanog.* **29**, 283-383.

McMillan, N. J., 1971. Surficial geology of Labrador and Baffin Island shelves. Earth Science Symposium on Offshore Eastern Canada, Geol. Surv. Can., Paper 71-23; 1973, p. 451-468.

Meyers, P. A., 1994. Preservation of elemental and isotopic source identification of sedimentary organic matter. *Chemical Geology* **114**, 289-302.

Meyers, P. A. 1992. Organic matter variations in sediments from DSDP sites 362 and 532: Evidence of changes in the Benguela Current upwelling system. In: Summerhayes, C. P., Prell, W. L., and Emeis, K. C., (eds). *Upwelling Systems: Evolution Since the Early Miocene*. Geological Society Special Publication No. 64, p. 323-329.

Montoya, J. P., 1994. Nitrogen isotope fractionation in the modern ocean: Implications for the sedimentary record. In: Zahn, R., Kaminski, M., Labeyrie, L. D., and Pedersen T. F. (eds). *Carbon Cycling in the Glacial Ocean: Constraints on the Ocean's Role in Global Change*. Springer, Heldeiberg. p. 259-279.

Montoya, J. P., Wiebe, P. H., and McCarthy, J. J., 1992. Natural abundance of ^{15}N in particulate nitrogen and zooplankton in the Gulf stream region and warm-core ring 86A. *Deep Sea Research* **39 Suppl.1**, s363-s392.

Müller, P. J., 1977. C/N ratios in Pacific deep-sea sediments. Effect of inorganic ammonium and organic nitrogen compounds sorbed by clays. *Geochim. Cosmochim. Acta* **41**, 765-776.

Müller, P. J., and Suess, E., 1979. Productivity, sedimentation rate, and sedimentary organic matter in the oceans-1. Organic carbon preservation. *Deep Sea Res.* **26**, 1347-1362.

Muzuka, A. N. N., 1990. Late Pliocene-Quaternary history of the northwestern Indian Ocean: An organic geochemistry perspective. M.Sc. Thesis, Memorial University, 164p.

Muzuka, A. N. N., Macko, S. A., and Pedersen, T. F., 1991. Stable carbon and nitrogen isotope compositions of organic matter from Sites 724 and 725, Oman Margin. In: Prell, W. L., Niitsuma, N. et al., (eds) *Proceedings of the Ocean Drilling Program, Scientific Results*, Vol. 117, p. 571-586.

- Myers, R. A. and Piper, D. J., 1988. Seismic stratigraphy of late Cenozoic in the norther Labrador Sea: A history of bottom circulation and glaciation. **Can. J. Earth Sci.** **25**, 2059-2074.
- O'Leary, M. H., 1981. Carbon isotope fractionation in plants. **Phytochemistry** **20**, 553-567.
- O'Leary, M. H., 1988. Carbon isotopes in photosynthesis. **Bioscience** **38**, 328-336.
- Olson, J. S., Garrels, R. M., Berner, R. A., Armentano, T. V., Dyer, M. I., and Yaalon, D. H., 1985. The nature of carbon cycle. In: Trabalka, J. R. (ed.) *Atmospheric Carbon Dioxide and the Global Cycle*. U.S. Department of Energy, Washington, D.C. p. 176-213.
- Ostrom, N. E. and Macko, S. A., 1992. Sources, cycling, and distribution of water column particulate and sedimentary organic matter in northern Newfoundland Fjords and bays: A stable isotope study. In: Whelan, J. K. and Farrington, J. W. *Organic Matter: Productivity, Accumulation and Preservation in Recent and Ancient Sediments*. Columbia University Press, New York. p. 55-81.
- Paetsch, H., Botz, R., Scholten, J. C. and Stoffers, P., 1992. Accumulation rates of surface sediments in the Norwegian-Greenland Sea. **Marine Geology** **104**, 19-30.
- Paterson, W. S. B. and Hammer, C. U., 1987. Ice core and other glaciological data. In: Ruddiman, W. F., and Wright, H. E., Jr., eds., *North America and Adjacent Oceans During the Last Deglaciation: Boulder, Colorado*, Geological Society of America, The Geology of North America, V. K-3, p. 91-109.
- Pedersen, T. F., 1983. Increased productivity in the eastern equatorial Pacific during the last glacial maximum (19,000 to 14,000 yr B.P.). **Geology** **11**, 16-19.
- Pedersen, T. F. and Calvert, S. E. 1990. Anoxia vs Productivity: What controls the formation of organic-carbon-rich sediments and sedimentary rocks?. **Am. Assoc. Petrol. Geol. Bull.** **74**, 454-466.
- Pedersen, T. F., Shimmield, G. B., and Price, N. B., 1992. Lack of enhanced preservation of organic matter in sediments under the oxygen minimum on the Oman Margin. **Geochim. Cosmochim. Acta** **56**, 545-551.
- Pedersen, T. F., Nielsen, B., and Pickering, M., 1991. Timing of late Quaternary productivity pulses in the Panama basin and implications for atmospheric CO₂. **Paleoceanography** **6**, 657-677.
- Peters, K. E., Sweeney, R. E., and Kaplan, I. R., 1978. Correlation of carbon and nitrogen stable isotope ratios in sedimentary organic matter. **Limnol. Oceanogr.** **23**, 598-604.
- Peters, K. E., Rohrback, B. G., and Kaplan, I. R., 1981. Carbon and hydrogen stable isotope variations in kerogen during laboratory simulated thermal maturation. **Am. Assoc. Petrol. Geol. Bull.** **65**, 501-508.
- Peterson, B. J., and Fry, B., 1987. Stable isotopes in ecosystem studies. **Ann. Rev. Ecol. Syst** **18**, 293-320.
- Piper, D. J. W., Mudie, P. J., Fader, G. B., Josenhans, H. W., MacLean, B., and Vilks, G., 1990. Quaternary geology. In: Keen, M. J., and Williams, G. L., (eds.) *Geology of the Continental Margin of Eastern Canada*. Geological Survey of Canada, Geology of Canada, no.2, p. 475-607 (also Geological Society of America, The Geology of North America, V. I-1).

- Plutchak, N. B., 1966. Labrador current. In: Fairbridge, R. W. (ed) *The Encyclopedia of Oceanography. Encyclopedia of Earth Sciences Series*, Vol. 1. Reinhold Publishing Corporation, New York. p. 438-439.
- Pocklington, R., 1976. Terrigenous organic matter in surface sediments from the Gulf of St. Lawrence. **J. Fish. Res. Board Can.** **33**, 93-97.
- Pocklington, R., 1988. Organic matter in the Gulf of St. Lawrence. In: Strain, P. M. (ed) *Chemical Oceanography in the Gulf of St. Lawrence*. **Can. Bull. Fish. Aquat. Sci.** **220**, 49-58.
- Pocklington, R. and Tan, F., 1987. Seasonal and annual variations in the organic matter contributed by the St. Lawrence River to the Gulf of St. Lawrence. **Geochim. Cosmochim. Acta** **51**, 2579-2586.
- Qian, Y., Engel, M. H. and Macko, S. A., 1992. Stable isotope fractionation of biomonomers during protokerogen formation. **Chemical Geology** **101**, 201-210.
- Rahman, A., and de Vernal, A., 1994. Surface oceanographic changes in the eastern Labrador Sea: nanofossil record of the last 31 thousand years. **Marine Geology** **121**, 247-263.
- Rahman, A. (accepted). Reworked nanofossils in the north Atlantic and subpolar basins: Implications for Heinrich events and ocean circulation. *Geology*.
- Ramanathan, V., Cicerone, R. J., Singh, H. B., and Kiehl, J. T., 1985. Trace gas trends and their potential role in climate change. **J. Geophys. Res.** **90**, 5547-5566.
- Rau, G. H., Arthur, M. A., Dean, W. E., 1987. $^{15}\text{N}/^{14}\text{N}$ variations in Cretaceous Atlantic sedimentary sequences: implication for past changes in marine nitrogen biogeochemistry. **Earth and Planetary Science Letters** **82**, 269-279.
- Rau, G. H., Takahashi, T., and Des Marais, D. J., 1989. Latitudinal variations in plankton $\delta^{13}\text{C}$: Implications for CO_2 and productivity in past ocean. **Nature** **341**, 516-518.
- Rau, G. H., Froelich, N., Takahashi, T., and Des Marais, D. J., 1991a. Does sedimentary organic $\delta^{13}\text{C}$ record variations in Quaternary ocean $[\text{CO}_2]$? **Paleoceanography** **6**, 335-347.
- Rau, G. H., Sullivan, C. W., and Gordon, L. I., 1991b. $\delta^{13}\text{C}$ and $\delta^{15}\text{N}$ variations in Weddell Sea particulate organic matter. **Marine Chemistry** **35**, 355-369.
- Rau, G. H., Takahashi, T., Des Maris, D. J., and Sullivan, C. W., 1991c. Particulate organic matter $\delta^{13}\text{C}$ variations across the Drake Passage. **J. Geophys. Res.** **96**, 15131-15135.
- Rau, G. H., Takahashi, T., Des Maris, D. J., Repeta, D. J., and Martin, J. H., 1992. The relationship between $\delta^{13}\text{C}$ of organic matter and $[\text{CO}_2(\text{aq})]$ in ocean surface water: Data from JGOFS site in the northeast Atlantic Ocean and a model. **Geochim Cosmochim. Acta** **56**, 1413-1419.
- Reimers, C. E., Jahnke, R. A., and McCorkle, D. C., 1992. Carbon fluxes and burial rates over the continental slope and rise off central California with implications for the global carbon cycle. **Global Biogeochemical Cycles** **6**, 199-224.

Rittenberg, S. C., Emery, K. O., Hülsemann, J., Degens, E. T., Fay, R. C., Reuter, J. H., Grady, J. R., Richardson, S. H., and Bray, E. E., 1963. Biogeochemistry of sediments in the experimental Mohole. **Journal of Sedimentary Petrology** 33, 140-172.

Rochon, A., and de Vernal, A., 1994. Palynomorph distribution in recent sediments from the Labrador Sea. **Can. J. Earth Sci.** 31, 115-127.

Rodrigues, C. G., Ceman, J. A., and Vilks, G., 1993. Late Quaternary paleoceanography of deep and intermediate water masses off Gaspé Peninsula, Gulf of St. Lawrence: foraminiferal evidence. **Can. J. Earth Sci.** 30, 1390-1403.

Rogers, M. A., van Hinte, J. E. and Sugden, J. G., 1972. Organic carbon ^{13}C values from Cretaceous, Tertiary and Quaternary marine sequences in the north Atlantic. In: Laughton, A. S., Berggren, W. A. et al., 1972, *Initial Reports of the Deep Sea Drilling Project Vol. XII*, Washington (U.S. Government Printing Office), p. 1115-1126.

Romankevich, E. A., 1984. *Geochemistry of Organic Matter in the Ocean*. Springer-Verlag, New York. 343pp.

Rosenfield, J. K., 1979. Amino acid diagenesis and adsorption in nearshore anoxic sediments. **Limnol. Oceanogr.** 24, 1014-1021.

Rosswall, T., 1981. The biogeochemical nitrogen cycle. In: Linkens, G. E. *Some Perspective of the Major Biogeochemical Cycles*. John Wiley & Sons, Chichester. SCOPE 17, p. 25-49.

Ruddiman, W. F., 1977. Late Quaternary deposition of ice-rafted sand in the subpolar north Atlantic (lat 40° to 65°N). **Geol. Soc. Am. Bull.** 88, 1813-1827.

Sackett, W. M., 1986. $\delta^{13}\text{C}$ signature of organic carbon in southern high latitude deep sea sediments; paleotemperature implications. **Organic Geochemistry** 9, 63-68.

Sackett, W. M., 1989. Stable carbon isotope studies on organic matter in marine environment. In: Fritz, P., and Fontes, J. Ch., *Handbook of Environmental Isotope Geochemistry*. Elsevier, New York, p. 139-169.

Sackett, W. M. and Thompson, R. R., 1963. Isotopic organic carbon composition of recent continental derived clastic sediments of eastern Gulf Coast, Gulf of Mexico. **Bull. Am. Assoc. Petrol. Geol.** 47, 525-528.

Sackett, W. M., Eckelmann, W. R., Bender, M. L., and Be', A. W. H., 1965. Temperature dependence of carbon isotope composition in marine Plankton and sediments. **Science** 130, 235-237.

Sackett, W. M., Eadie, B., and Exner, M., E. 1974. Stable isotopic composition of organic carbon in recent Antarctic sediments. In: Tisot, B. and Biennet, F. (eds) *Advances in Organic Geochemistry*. p. 661-671.

Saino, T. and Hattori, A., 1980. ^{15}N natural abundance in oceanic suspended particulate matter. **Nature** 283, 752-754.

Saino, T., and Hattori, A., 1985. Variation of ^{15}N natural abundance of suspended organic matter in shallow oceanic waters. In: Sigleo, A. C., and Hattori, A. (eds.) *Marine and Estuarine Geochemistry*. Lewis Publishers, Chelsea. p. 1-13.

Saino, T. and Hattori, A., 1987. Geographic distribution of suspended particulate organic nitrogen and its ^{15}N natural abundance in the Pacific and its marginal seas. **Deep Sea Research** **34**, 807-827.

Sancetta, C., 1992. Primary production in the glacial north Atlantic and north Pacific Oceans. **Nature** **360**, 249-250.

Sarthein, M., Pflaumann, U., Ross, R., Tiedemann, R., and Winn, K., 1992. Transfer functions to reconstruct ocean palaeoproductivity: a comparison. In: Summerhayes, C. P., Prell, W. L., and Emeis, K. C., (eds). *Upwelling Systems: Evolution Since the Early Miocene*. Geological Society Special Publication No. 64, pp. 411-427.

Sarthein, M., Winn, K., Duplessy, J. C., and Fontugne, M. R., 1988. Global variation of surface ocean productivity in low and mid latitudes: Influence of CO_2 reservoirs of the deep ocean and atmosphere during the last 21,000 years. **Paleoceanography** **3**, 361-399.

Sarthein, M., Winn, K., and Zahn, R., 1987. Paleoproductivity of oceanic upwelling and the effect on atmospheric CO_2 and climatic change during deglaciation times. In: Berger, W. H. and Labeyrie (eds), *Abrupt Climatic Change*, D. Reidel Publishing Company, Dordrecht. p. 311-337

Schafer, C. T., Tan, F. C., Williams, D. F. and Smith, J. N., 1985. Late glacial to Recent stratigraphy, paleontology, and sedimentary processes: Newfoundland continental slope and rise. **Can. J. Earth Sci.** **22**, 266-282.

Schneider, E. D., Fox, P. J., Hollister, C. D., Needham, H. D. and Heezen, B. C., 1967. Further evidence of contour currents in the western north Atlantic. **Earth and Planetary Science Letters** **2**, 351-359.

Schroeder, R. A., and Bada, J. L., 1976. A review of the geochemical applications of the amino acid racemization reaction. **Earth Sci. Rev.** **12**, 347-391.

Schultz, D. J. and Calder, J. A., 1976. Organic carbon $^{13}\text{C}/^{12}\text{C}$ variation in estuarine environment. **Geochim. Cosmochim. Acta** **40**, 381-385.

Scott, D. B., Mudie, P. J., de Vernal, A., Hillaire-Marcel, C., Baki, V., MacKinnon, K. D., Medioli, F. S. and Mayer, L., 1989. Lithostratigraphy, biostratigraphy, and stable isotope stratigraphy of cores from ODP Leg 105 site survey, Labrador Sea and Baffin Bay. In: Srivastava, S. P., Arthur, M., et al., (eds) *Proceedings, ODP Scientific Results*, Vol. 105. College Station Texas, p. 561-582.

Seifert, R., Emeis, K.-C., Michaelis, W., and Degens, E. T., 1990. Amino acids and carbohydrates in sediments and interstitial waters from Site 681 Leg. 112, Peru continental margin. In: Suess, E., von Huene, R. et al., (eds) *Proceedings of the Ocean Drilling Program Scientific Results, Vol. 112*, College Station Texas, p. 555-566.

Shemesh, A., Macko, S. A., Charles, C. D., and Rau, G. H., 1993. Isotopic evidence for reduced productivity in the glacial southern ocean. **Science** **262**, 407-410.

Shine, K. P., Derwent, R. G., Wuebbles, D. J., and Morcrette, J. J., 1990. Radiative forcing climate. In: Houghton, J. T., Jenkins, G. J. and Ephraums, J. J. (eds) *Climate Change-The IPCC Scientific Assessment*. Cambridge University Press, Cambridge, p. 41-68.

Silfert, J. A., Engel, M. H., and Macko, S. A., 1992. Kinetic fractionation of stable carbon and nitrogen isotopes during peptide bond hydrolysis: Experimental evidence and geochemical implications. **Chemical Geology** **101**, 211-221.

Silverberg, N., Edenborn, H. M. and Belzile, N., 1985. Sediment response to seasonal variations in organic matter input. In: Sigleo, A. C. and Hattori (eds) *Marine and Estuarine Geochemistry*. Lewis Publishers, Inc., Michigan, p. 69-80.

Silverberg, N., Nguyen, H. V., Delibrias, G., Koide, M., Sundby, B., Yokoyama, Y. and Chesselet, R., 1986. Radionuclide profiles, sedimentation rate, bioturbation in marine sediments of the Laurentian Trough, Gulf of St. Lawrence. **Oceanologica Acta** **9**, 285-290.

Silverberg, N., Bakker, J., Edenborn, H. M. and Sundby, B., 1987. Oxygen profiles and organic carbon fluxes in Laurentian Trough sediments. **The Netherlands J. Sea Res.**, **21**, 95-105.

Sinclair, M., El-Sabh, M. and Brindle, J., 1976. Seaward nutrient transport in the lower St. Lawrence Estuary. **J. Fish. Res. Board Can.** **33**, 1271-1277.

Singer, A., J., and Shemesh, A., 1995. Climatically linked carbon isotope variation during the past 430,000 years in southern ocean sediments. **Paleoceanography** **10**, 171-177.

Smith, B. M., and Epstein, S. 1971. Two categories of $^{13}\text{C}/^{12}\text{C}$ ratios for higher plants. **Plant Physiol.** **47**, 380-383.

Spero, H. J., Williams, D. F., 1990. Evidence for seasonal low salinity surface waters in the Gulf of Mexico over the last 16,000 years. **Paleoceanography** **5**, 965-975.

Spiker, E. C., and Hatcher, P. C., 1984. Carbon isotope fractionation of sapropelic organic matter during early diagenesis. **Organic Geochemistry** **6**, 283-290.

Spiker, E. C., and Hatcher, P. C., 1987. The effects of early diagenesis on the chemical and stable carbon isotopic composition of wood. **Geochim. Cosmochim. Acta** **51**, 1385-1391.

Srivastava, S. P., Falconer, R. K. H. and MacLean, B., 1981. Labrador Sea, Davis strait, Baffin Bay: Geology and geophysics-A review. In: Kerr, J. Wm., Fergusson, A. J. and Machan, L. C. (eds). *Geology of the North Atlantic Borderlands*. Can. Soc. Petrol. Geol., Memoir 7, Calgary, p. 333-398.

Stein, R., 1991. Organic carbon accumulation in Baffin Bay and paleoenvironment in high northern latitudes during the past 20 m.y. **Geology** **19**, 356-359.

Stein, R., 1986a. Organic carbon and sedimentation rate-Further evidence for anoxic deep-water conditions in the Cenomanian/Turonian Ocean. **Marine Geology** **72**, 199-209.

Stein, R., 1986b. Surface-water paleoproductivity as inferred from sediments deposited in oxic and anoxic deep-water environments of the mesozoic Atlantic Ocean. In Degens, E. T., et al. (eds) *Biogeochemistry of Black Shales*. Mitt. Geol. Palaont. Inst. Univ. Hamburg, 60, 55-70.

Stein, R., Rullkötter, J., and Welte, D. H., 1986. Accumulation of organic carbon rich sediments in the late Jurassic and Cretaceous Atlantic Ocean. A synthesis. **Chem. Geol.** **56**, 1-32.

Stein, R., Littke, R., Stax, R., and Welte, D. H., 1989a. Quantity, provenance and maturity of organic matter at ODP Sites 645, 646, and 647: Implications for reconstruction of paleoenvironment in Baffin Bay and Labrador Sea during Tertiary and Quaternary time. In: Srivastava, S. P., Arthur, M., et al., (eds) *Proceedings, ODP Scientific Results, Vol. 105*. College Station Texas, p. 185-208.

Stein, R., ten Haven, H. L., Littke, R., Rullkötter, J., and Welte, D. H., 1989b. Accumulation of marine and terrigenous organic carbon at upwelling Site 658 and nonupwelling Sites 657 and 659: Implications for the reconstruction of paleoenvironments in the eastern subtropical Atlantic through late Cenozoic times. In: Ruddiman, W., Sarnthein, M., et al., *Proceedings, ODP Scientific Results, Vol. 108*. College Station, Tx, p. 361-385.

Stephenson, R. L., Tan, F. C., and Mann, K. H., 1984. Isotopic variability in marine macrophytes and its implications to food web studies. **Marine Biology** **81**, 223-230.

Steven, D. M., 1975. Biological production in the Gulf of St. Lawrence. In: Cameron, T. W. M. and Billingsley, L. W. (eds). *Energy Flow-Its Biological Dimension*. Royal Society of Canada, Ottawa, p. 229-248.

Stevenson, F. J., and Cheng, C. N., 1972. Organic geochemistry of the Argentine Basin sediments: Carbon-nitrogen relationships and Quaternary correlations. **Geochim. Cosmochim. Acta**, **36** 653-671.

- Stoner, J. S., Channell, J. E. T., Hillaire-Marcel, C. and Mareschal, J.-C., 1994. High resolution rock magnetic study of a late Pleistocene core from the Labrador Sea. **Can. J. Earth Sci.** **31**, 104-114.
- Stoner, J. S., Channell, J. E. T., Hillaire-Marcel, C., 1995. Magnetic properties of deep-sea sediments off southwest Greenland. Evidence for major differences between the last deglaciations. **Geology** **23**, 241-244.
- Strain, P. M., 1988. Chemical Oceanography in the Gulf of St. Lawrence: Geographic, physical oceanography, and geologic setting. In: Strain, P. M. (ed) Chemical Oceanography in the Gulf of St. Lawrence. **Can. Bull. Fish. Aquat. Sci.** **220**, 1-14.
- Stuiver, M., Braziunas, T., Becker, B., and Kromer, B., 1991. Climatic, solar, oceanic, and geomagnetic influences on late glacial and Holocene atmospheric $^{14}\text{C}/^{12}\text{C}$ change. **Quaternary Research** **35**, 1-24.
- Suess, E., 1980. Particulate organic carbon flux in the oceans-surface productivity and oxygen utilization. **Nature** **288**, 260-263.
- Suess, E., and Müller, P. J., 1980. Productivity, sedimentation rate and sedimentary organic matter in the oceans II. Elemental fractionation. In: *Biogéochimie de la Matière Organique à l'interface eau-sédiment Marin*, CNRS, Paris. p. 17-26.
- Sunby, B., 1974. Distribution and transport of suspended particulate matter in the Gulf of St. Lawrence. **Can. J. Earth Sci.** **11**, 1517-1533.
- Sutcliffe, W. H., Loucks, R. H., Drinkwater, K. F. and Coote, A. R., 1983. Nutrient flux onto the Labrador Shelf from Hudson Strait and its biological consequences. **Can. J. Fish. Aquat. Sci.** **40**, 1692-1701.
- Sweeney, R. E. and Kaplan, I. R., 1980. Natural abundances of ^{15}N as a source indicator for near-shore marine sedimentary and dissolved nitrogen. **Marine Chemistry** **9**, 81-94.
- Sweeney, R. E., Khalil, E. K., and Kaplan, I. R., 1980. Characterization of domestic and industrial sewage in southern California coastal sediments using nitrogen, carbon, sulfur and uranium traces. **Marine and Environmental Res.** **3**, 225-243.
- Syvitski, P. M. and Praeg, D. B., 1989. Quaternary sedimentation in the St. Lawrence estuary and adjoining areas, eastern Canada: An overview based on high resolution seismo-stratigraphy. **Géographie physique et Quaternaire** **43**, 291-210.
- Tan, F. C. and Strain, P. M., 1979a. Organic carbon isotope ratios in recent sediments in the St. Lawrence Estuary and the Gulf of St. Lawrence. **Estuarine and Coastal Marine Science** **8**, 213-225.

Tan, F. C. and Strain, P. M., 1979b. Carbon isotope ratios of particulate organic matter in the Gulf of St. Lawrence. **J. Fish. Res. Board Can.** **36**, 678-682.

Tan, F. C. and Strain, P. M., 1983. Sources, sinks and distribution of organic carbon in the St. Lawrence Estuary, Canada. **Geochim. Cosmochim. Acta** **47**, 125-132.

Tan, F. C. and Strain, P. M., 1988. Stable isotope studies in the Gulf of St. Lawrence. In: Strain, P. M. (ed) Chemical Oceanography in the Gulf of St. Lawrence. **Can. Bull. Fish. Aquat. Sci.** **220**, 59-77.

Tan, F. C., 1989. Stable carbon isotopes in dissolved inorganic carbon in marine and estuarine environments. In: Fritz, P. and Fontes, J. Ch., *Handbook of Environmental Isotope Geochemistry* Vol. 3. Elsevier, New York, p. 171-190.

Tang, C. L., 1980. Mixing and circulation in the northwestern Gulf of St. Lawrence: A study of a buoyancy-driven current system. **Jour. Geophys. Res.** **85**, 2787-2796.

Taylor, G. T. and Karl, D. M., 1992. Vertical fluxes of biogenic particles and associated biota in the eastern north Pacific: Implications for biogeochemical cycling and productivity. **Global Biogeochemical Cycles** **5**, 289-303.

Teller, J. T., 1990. Volume and routing of late-glacial runoff from the southern Laurentide ice sheet. **Quaternary Research** **34**, 12-23.

Therriault, J. and Lacroix, G., 1976. Nutrients, chlorophyll, and internal tides in the St. Lawrence Estuary. **J. Fish. Res. Board Can.** **36**, 678-682.

Thibaut, S., and Currie, R., 1990. Cruise report CSS HUDSON 90-31. Geological Survey of Canada, Open File.

Thornton, S. F., and McManus, J., 1994. Application of organic carbon and nitrogen stable isotope and C/N ratios as source indicators of organic matter provenance in estuarine systems: Evidence from Tay Estuary, Scotland. **Estuarine, Coastal and Shelf Science** **38**, 219-233.

Tissot, B. P., 1984. *Petroleum Formation and Occurrence: A New Approach to Oil and Gas Exploration* 2nd edition. Springer-Verlag, Berlin. 588pp.

Tromp, T. K., Van Cappellen, P. and Key, R. M., 1995. A global model for the early diagenesis of organic carbon and organic phosphorus in marine sediments. **Geochim. Cosmochim. Acta** **59**, 1259-1284.

Umpleby, D. C., 1979. Geology of the Labrador shelf. Geol. Sur. Can. Paper 79-13, 34p.

Van der Weijden, C. H., 1992. Early Diagenesis and marine pore water. In: Wolf, K. H., and Chilingarian, G. V. (eds). *Developments in Sedimentology 47: Diagenesis, III*. Elsevier, Amsterdam. p. 13-135.

Velinsky, D. J., Burdige, D. J. and Fogel, M. L., 1991. Nitrogen diagenesis in anoxic marine sediments: Isotope effects. *Geophysical Laboratory, Carnegie Institution Year Book 1990/91*, 154-162.

Vilks, G., Rashid, M. A. and Van der Linden, W. J. M., 1974. Methane in Recent sediments of the Labrador shelf. *Can. J. Earth Sci.* **11**, 1427-1434.

Vilks, G., 1980. Postglacial basin sedimentation on Labrador shelf. *Geol. Sur. Can. Paper* 78-28.

Vilks, G., MacLean, B., Deonaraine, B., Currie, C. G. and Moran, K., 1989. Late Quaternary paleoceanography and sedimentary environments in Hudson Strait. *Géographie Physique et Quaternaire* **43**, 161-178.

Volk, T., and Liu, Z., 1988. Controls of CO₂ sources and sinks in the earth scale surface ocean: Temperature and nutrients. *Global Biogeochemical Cycles* **2**, 73-89.

Wada, E., 1980. Nitrogen isotope fractionation and its significance in biogeochemical processes occurring in marine environments. In: E. D. Goldberg, Y. Horibe, and K. Saruhashi (eds.) *Isotope Marine Chemistry*. Uchida Rukakuho, Tokyo. p. 375-398.

Wada, E., and Hattori, A., 1991. *Nitrogen in the Sea: Forms, Abundances, and Rate Processes*. CRC Press Boston, 208pp.

Walsh, J. J., 1991. Importance of continental margins in the marine biogeochemical cycling of carbon and nitrogen. *Nature* **350**, 53-55.

Walsh, J. J., 1989. Arctic carbon sinks: Present and future. *Global Biogeochemical Cycles* **3**, 393-411.

Walsh, J. J., Rowe, G. T., Iverson, R. L., and McRoy, P., 1981. Biological carbon export of shelf carbon is a sink of the global CO₂ cycle. *Nature* **291**, 196-201.

Watson, R. T., Rodhe, H., Oescheger, H. and Seigenthaler, U., 1990. Greenhouse gases and aerosols. In: Houghton, J. T., Jenkins, G. J. and Ephraums, J. J. (eds) *Climate Change-The IPCC Scientific Assessment*. Cambridge University Press, Cambridge, p. 1-40.

Westrich, J. T., and Berner, R. A., 1984. The role of sedimentary organic matter in bacterial sulfate reduction: The G model tested. *Limnol. Oceanogr.* **29**, 236-249.

Whelan, J. K., 1977. Amino acids in a surface sediment core of the Atlantic abyssal plain. **Geochim. Cosmochim. Acta** **41**, 803-810.

Whelan, J. K., and Emeis, K.-C., 1992. Sedimentation and preservation of amino compounds and carbohydrates in marine sediments. In: Whelan, J. K., and Farrington, J. W. (eds) *Organic matter: Productivity, Accumulation, and Preservation in Recent and Ancient Sediments*. Columbia University Press New York, p. 178-200.

Wong, W. W., and Sackett, W. M., 1978. Fractionation of stable carbon isotopes by marine phytoplankton. **Geochim. Cosmochim. Acta** **42**, 1809-1815.

Wu, G., and Hillaire-Marcel, C., 1994. Accelerator mass spectrometry radiocarbon stratigraphies in deep Labrador Sea cores: paleoceanographic implications. **Can. J. Earth Sci.** **31**, 38-47.

Yeats, P. A., 1988. Nutrients. In: Strain, P. M. (ed) *Chemical Oceanography in the Gulf of St. Lawrence*. **Can. Bull. Fish. Aquat. Sci.** **220**, 29-48.

9.0.0. APPENDIX

9.1.0. TABLES FOR CHAPTER 3

Table 3.2. Colour, sediment types and number of samples analyzed for various cores used in this study.	213
Table 3.3. Various constants used to express relationships between fluxes of OM and primary productivity.	216

Table 3.2. Colour, sediment types and number of samples analyzed for various cores used in this study.

CORE	INTERVAL (CM)	COLOUR AND SEDIMENT TYPE	C/L	No.
HU-91-045-05 BC ¹	0-2	dark olive grey sandy silty mud	16	16
	2-30	dark grey silty mud heavily bioturbated		
HU-91-045-14 BC ¹	0-12	olive grey muddy sand with high abundance of gravel between 7-9 cm. Macrofauna (worms, sponges, echinoderms) in surface sediments	12	11
HU-91-045-16 BC ¹	0-5	dark greyish brown sandy mud	25	19
	5-9	dark grey sandy mud intercalated with clayey clasts		
	9-22	grey sandy clay mixed with gravel and clayey clasts		
	22-30	grey clayey mud mixed with gravel		
HU-91-045-18 BC ¹	0-7	dark greyish brown sandy mud	28	14
	7-15	greyish brown sand-silt mud rich in foraminifers		
	15-23	dark greyish brown sandy mud with abundant foraminifers; bioturbated		
	23-31	brown silt mud intercalated with sandy and clasts; bioturbated		
HU-91-045-23 BC ¹	31-40	dark greyish brown clayey mud	26	14
	0-3	dark greyish brown muddy sand intercalated with pebbles, algae and macrofauna		
	3-19	greyish brown sandy mud		
	19-31	greyish brown clayey mud intercalated with sand and gravels		
HU-91-045-28 BC ¹	0-6	greyish brown mud rich in foraminifers and intercalated with gravels	30	15
	6-28	greyish brown to dark greyish brown mud heavily bioturbated		
	28-33	grey mud		
HU-91-045-93 BC ¹	0-5	olive brown mud	25	25
	5-11	brown to dark brown mud; bioturbated		
	11-42	grey mud		

HU-91-045-94 PC ¹	0-173	grey to dark grey mud	641	68
	173-217	greyish brown mud		
	228-248	dark greyish brown to greyish brown mud		
	248-312	dark grey to very greyish brown mud		
	338-365	dark grey mud		
	365-381	greyish brown silty mud		
	381-401	dark grey to very dark greyish brown clayey mud		
	401-463	dark grey mud		
	463-560	grey to dark grey silty mud grading to mud		
	560-589	greyish brown silty mud		
	589-691	dark grey to very grey mud		
HU-91-013-11 BC ²	upper part	fine sand	35	17
	lower part	clayey silt intercalated with coarse sands and pebbles		
HU-91-013-13 PC ²	0-470	finely laminated silty clays that contains small sand lenses	620	63
	470-950	dark green to brown loose clayey silts with abundant silty, sandy nodules and disseminated gravels		
HU-91-045-38 TWC ¹	20-30	Mn and Fe enriched horizon	18	7
	0-8	brown muddy sand with abundant foraminifers		
	8-20	dark greyish brown to very dark greyish brown sandy mud grading to silty mud		
HU-91-045-40 LHC ¹	0-1	brownish sandy-silty mud intercalated with gravels	12	5
HU-90-031-13 BC ³	0-1	brown silty mud with few tube worms	37	20
	1-37	grey silty mud		

HU-90-031-17 BC ³	0-1	brown silty mud with few tube worms	36	20
	1-36	grey silty mud		
HU-90-031-29 BC ³	0-37	grey silty mud	36	18
HU-90-031-34 BC ³	surface	brown silty mud with abundant macrophytes(?), juvenile echinoderms and	36	20
		few tube worms		
HU-90-031-41 BC ³	0-2	brown silty clay	34	19
	2-36	greyish mud		
HU-90-028-06 BC ⁴		brown silty clay	22	13
		grey clay rich in benthic fauna		
HU-90-031-43 PC ³	0-2	brownish silty mud	38	12
	2-57	dark grey mud; barely visible laminations between 2 and 19 cm		
HU-90-031-45 BC ³	0-1	brownish mud	34	19
		greyish mud		
HU-90-031-59 BC ³	surface (few cm)	brownish mud	34	19
	below	greyish mud		
HU-90-031-44 PC ³	0-36	olive grey	941	94
	36-344	dark grey mud with barely visible bioturbation		
	344-514	dark grey clayey mud		
	514-601	dark greenish grey clayey mud		
	601-624	dark grey clayey mud with black clots		
	624-941	dark grey clayey mud with scattered granules and black dots		

NOTE: BC = BOX CORE, PC = PISTON CORE, TWC = TRIGGER WEIGHT CORE, LHC = LE HIGH CORE, C/L = core length analyzed (cm), No. = numbers of samples analyzed

Superscript numbers indicate source of information: 1 Hillaire-Marcel et al., 1991; 2 Hillaire-Marcel and Rochon, 1990; 3 Thibaudau and Curie, 1990; 4 Josenhans et al., 1990.

Table 3.3. Various constants used to express relationships between fluxes of OM and primary productivity

ELEMENT	K	a	b	d	SOURCE
Nitrogen	0.00206	2.5690	-0.1618	-	Taylor and Karl, 1992
Carbon	0.65160	1.9130	-0.5900	-	Taylor and Karl, 1992
Carbon	0.41000	1.4100	-0.6300	-	Suess, 1980
Carbon	0.09000	1.5000	-0.5000	1.08	Sarnthein et al., 1987
Carbon	0.38300	1.3296	-0.5537	1.166	Sarnthein et al., 1988
Carbon	-	-	-	1.523	Muller and Suess, 1979
Carbon	5.90000	1.0000	-0.6160	-	Suess and Muller, 1980

9.2.0. TABLES FOR CHAPTER 4

Table 4.1. Geochemical results for cores:

HU-91-045-05 BC	218
HU-91-045-14 BC	219
HU-91-045-16 BC	220
HU-91-045-18 BC	221
HU-91-045-23 BC	222
HU-91-045-28 BC	223
HU-91-045-93 BC	224
HU-91-045-38 TWC	225
HU-91-045-40 LHC	225
HU-90-013-11 BC	226

Table 4.2. Geochemical Results for Cores:

HU-90-031-13 BC	227
HU-90-031-17 BC	228
HU-90-031-29 BC	229
HU-90-031-34 BC	230
HU-90-031-41 BC	231
HU-90-031-43 PC	232
HU-90-028-06 BC	233
HU-90-031-45 BC	234
HU-90-031-59 BC	235

Table 4.1. Core HU-91-045-05 BC

DEPTH	$\delta^{15}\text{N}$	$\delta^{13}\text{C}$	N	OC	CaCO_3	C/N
0.5	8.12	-21.47	0.17	1.59	7.32	10.91
1.5	7.98	-21.36	0.16	1.97	4.21	14.36
2.5	8.41	-21.36	0.16	1.64	6.18	11.96
3.5	8.53	-21.36	0.17	1.83	5.68	12.56
4.5	7.31	-21.51	0.17	1.76	6.54	12.08
5.5	7.01	-21.47	0.18	1.81	5.56	11.73
6.5	7.52	-21.15	0.17	1.82	5.20	12.49
7.5	7.84	-21.54	0.18	2.01	4.63	13.03
8.5	7.56	-21.55	0.16	1.75	6.15	12.76
9.5	7.14	-21.49	0.17	1.58	7.99	10.84
10.5	7.21	-21.45	0.16	1.87	4.92	13.64
11.5	7.44	-21.54	0.17	1.98	4.73	13.59
12.5	8.32	-21.36	0.16	2.02	4.15	14.73
13.5	8.01	-21.55	0.16	1.89	4.77	13.78
14.5	7.85	-21.53	0.16	1.59	7.13	11.59
15.5	7.42	-21.43	0.15	1.60	6.95	12.44
MEAN	7.73	-21.44	0.17	1.79	5.76	12.66
STD	0.46	0.10	0.01	0.15	1.15	1.11
MIN	7.01	-21.55	0.15	1.58	4.15	10.84
MAX	8.53	-21.15	0.18	2.02	7.99	14.73
RANGE	1.52	0.40	0.03	0.44	3.84	3.89

Table 4.1. Core HU-91-045-14 BC

DEPTH	$\delta^{15}\text{N}$	$\delta^{13}\text{C}$	N	OC	CaCO_3	C/N
0.5	7.33	-22.04	0.026	0.26	5.37	11.47
1.5	7.26	-21.63	0.032	0.29	4.70	10.43
3.5	7.69	-21.85	0.015	0.15	4.22	11.92
5.5	7.92	-21.42	0.041	0.33	3.17	9.37
6.5	8.07	-21.78	0.029	0.18	3.47	7.38
7.5	8.15	-21.62	0.013	0.16	2.96	14.81
8.5	8.29	-21.62	0.018	0.18	4.23	11.80
9.5	7.30	-22.30	0.008	0.14	3.37	19.73
10.5	8.78	-21.95	0.011	0.17	3.13	18.50
11.5	8.40	-21.57	0.026	0.31	4.97	14.08
MEAN	7.92	-21.78	0.022	0.22	3.96	12.95
STD	0.49	0.25	0.010	0.07	0.81	3.69
MIN	7.26	-22.30	0.008	0.14	2.96	7.38
MAX	8.78	-21.42	0.041	0.33	5.37	19.73
RANGE	1.52	0.88	0.033	0.19	2.41	12.35

Table 4.1. Core HU-91-045-16 BC

DEPTH	$\delta^{15}\text{N}$	$\delta^{13}\text{C}$	N	OC	CaCO_3	C/N
1.5	9.04	-21.42	0.035	0.34	15.37	11.34
2.5	8.72	-21.72	0.028	0.28	14.21	11.67
3.5	7.90	-21.70	0.037	0.39	13.95	12.30
4.5	8.05	-22.02	0.031	0.27	14.80	10.16
5.5	7.86	-21.60	0.033	0.48	12.66	16.97
6.5	8.06	-21.75	0.033	0.27	15.80	9.55
7.5	7.58	-22.14	0.026	0.26	13.30	11.67
8.5	8.09	-22.25	0.022	0.21	12.48	11.14
9.5	7.85	-22.29	0.024	0.22	13.96	10.70
10.5	6.78	-23.24	0.023	0.26	19.92	13.19
11.5	7.41	-23.20	0.025	0.33	19.33	15.40
12.5	8.11	-24.01	0.021	0.22	23.93	12.23
13.5	7.57	-24.20	0.018	0.26	25.31	16.86
14.5	7.39	-24.55	0.021	0.43	25.69	23.90
15.5	5.30	-24.18	0.023	0.29	28.82	14.71
18.0	7.31	-23.51	0.021	0.35	21.86	19.45
20.0	3.25	-23.95	0.019	0.35	32.01	21.50
22.0	6.45	-24.36	0.018	0.28	33.58	18.15
24.0	6.84	-24.82	0.019	0.34	44.73	20.88
MEAN	7.34	-22.99	0.025	0.31	21.14	14.83
STD	1.26	1.14	0.006	0.07	8.59	4.19
MIN	3.25	-24.82	0.018	0.21	12.48	9.55
MAX	9.04	-21.42	0.037	0.48	44.73	23.90
RANGE	5.79	3.39	0.019	0.27	32.25	14.35

Table 4.1. Core HU-91-045-18 BC

DEPTH	$\delta^{15}\text{N}$	$\delta^{13}\text{C}$	N	OC	CaCO_3	C/N
1.0	7.72	-22.03	0.017	0.12	26.06	8.24
3.0	8.65	-22.37	0.015	0.20	29.76	15.56
5.0	8.45	-22.57	0.015	0.24	25.50	18.67
7.0	7.13	-23.88	0.012	0.14	36.46	13.62
9.0	7.50	-24.30	0.009	0.13	31.59	16.86
11.0	8.32	-24.83	0.008	0.12	29.92	17.51
13.0	7.94	-24.92	0.007	0.08	25.47	13.34
15.0	8.73	-24.99	0.008	0.11	24.94	16.05
17.0	8.47	-24.48	0.008	0.10	30.42	14.59
19.0	6.63	-24.92	0.007	0.08	24.48	13.34
21.0	7.83	-24.48	0.007	0.11	22.05	18.34
23.0	7.38	-24.29	0.010	0.13	21.46	15.17
25.0	7.64	-24.17	0.008	0.11	22.15	16.05
27.0	7.18	-25.73	0.009	0.13	31.64	16.86
MEAN	7.82	-24.14	0.010	0.13	27.28	15.30
STD	0.61	1.05	0.003	0.04	4.26	2.57
MIN	6.63	-25.73	0.007	0.08	21.46	8.24
MAX	8.73	-22.03	0.017	0.24	36.46	18.67
RANGE	4.07	3.69	0.010	0.16	15.00	10.43

Table 4.1. Core HU-91-023 BC

DEPTH	$\delta^{15}\text{N}$	$\delta^{13}\text{C}$	N	OC	CaCO_3	C/N
1.0	6.88	-22.42	0.017	0.24	16.04	16.13
3.0	7.45	-21.70	0.026	0.33	20.02	14.72
5.0	5.42	-22.40	0.014	0.16	18.05	13.66
7.0	6.96	-23.88	0.009	0.18	20.20	22.76
13.0	5.85	-25.06	0.011	0.16	37.90	17.12
14.5	7.23	-25.27	0.013	0.19	33.87	16.62
15.5	6.39	-25.47	0.013	0.23	32.88	21.08
16.5	6.23	-25.30	0.013	0.29	34.26	25.96
17.5	5.49	-25.09	0.016	0.32	35.39	23.56
19.0	6.95	-25.11	0.019	0.35	41.75	21.46
22.5	5.42	-25.64	0.019	0.36	48.36	21.88
23.5	5.90	-25.91	0.015	0.36	50.62	27.65
24.5	3.18	-26.04	0.018	0.33	51.99	21.47
25.5	5.55	-25.91	0.017	0.36	50.04	25.03
MEAN	6.06	-24.66	0.016	0.28	35.10	20.65
STD	1.05	1.40	0.004	0.08	12.21	4.19
MIN	3.18	-26.04	0.009	0.16	16.04	13.66
MAX	7.45	-21.70	0.026	0.36	51.99	27.65
RANGE	4.27	4.34	0.017	0.20	35.95	13.99

Table 4.1. Core HU-91-045-28 BC

DEPTH	$\delta^{15}\text{N}$	$\delta^{13}\text{C}$	N	OC	CaCO_3	C/N
1	7.31	-21.65	0.037	0.41	43.26	12.88
3	8.57	-21.54	0.033	0.33	41.00	11.68
5	7.80	-21.33	0.030	0.31	41.29	11.87
7	7.36	-21.68	0.028	0.33	33.83	13.79
9	7.77	-21.73	0.028	0.31	33.91	12.94
11	7.75	-21.62	0.026	0.29	36.54	12.81
13	8.63	-21.67	0.029	0.31	34.95	12.30
15	7.49	-21.57	0.027	0.30	34.06	13.11
17	8.20	-21.94	0.024	0.28	29.11	13.44
19	8.27	-22.02	0.021	0.25	27.98	14.00
21	8.14	-22.30	0.018	0.25	24.34	16.18
23	8.07	-22.31	0.020	0.25	27.38	14.83
25	6.58	-23.57	0.012	0.24	12.11	23.07
27	8.00	-23.09	0.017	0.23	21.43	15.64
29	7.95	-22.91	0.017	0.25	21.49	17.24
MEAN	7.86	-22.06	0.024	0.29	30.84	14.39
STD	0.51	0.63	0.007	0.05	8.31	2.79
MIN	6.58	-23.57	0.012	0.23	12.11	11.68
MAX	8.63	-21.33	0.037	0.41	43.26	23.07
RANGE	2.05	2.24	0.025	0.18	31.16	11.39

Table 4.1. Core HU-91-045-93 BC

DEPTH	$\delta^{15}\text{N}$	$\delta^{13}\text{C}$	N	OC	CaCO_3	C/N
0.50	7.88	-21.62	0.074	1.28	38.63	20.19
1.50	9.52	-21.65	0.077	1.03	38.89	15.61
2.50	8.36	-21.65	0.079	0.92	43.18	13.59
3.50	8.08	-21.63	0.084	0.90	47.62	12.50
4.50	8.33	-21.63	0.077	0.75	47.12	11.37
5.50	8.42	-21.56	0.080	0.83	48.53	12.11
6.50	3.60	-21.54	0.087	0.74	51.67	9.93
7.50	8.77	-21.55	0.083	0.65	51.78	9.14
8.50	7.85	-21.51	0.075	0.79	48.45	12.29
9.50	8.50	-21.72	0.063	0.84	42.86	15.56
10.50	8.54	-21.88	0.068	0.97	41.65	16.65
11.50	7.95	-21.68	0.064	0.94	41.60	17.14
12.50	7.33	-21.68	0.069	0.86	42.41	14.55
13.50	8.63	-21.65	0.061	0.99	40.66	18.94
14.50	9.38	-21.59	0.057	0.67	41.82	13.72
15.50	8.55	-21.57	0.056	0.79	40.76	16.46
16.50	7.34	-21.61	0.058	0.79	42.33	15.90
17.50	8.56	-21.64	0.057	0.95	40.28	19.45
18.50	7.43	-21.74	0.058	0.84	41.30	16.90
19.50	7.98	-21.71	0.056	0.84	40.88	17.51
20.50	8.63	-21.67	0.059	0.97	39.72	19.19
21.50	7.57	-21.87	0.049	0.83	39.19	19.77
22.50	8.20	-21.75	0.048	0.71	39.17	17.26
23.50	7.66	-21.84	0.047	0.79	38.63	19.62
24.50	8.57	-21.82	0.046	0.84	37.57	21.31
MEAN	8.06	-21.67	0.065	0.86	42.67	15.87
STD	1.06	0.10	0.012	0.13	4.02	3.29
MIN	3.60	-21.88	0.046	0.65	37.57	9.14
MAX	9.52	-21.51	0.087	1.28	51.78	21.31
RANGE	5.91	0.374	0.041	0.63	14.21	12.17

Table 4.1. Core HU-91-045-38 TWC

DEPTH	$\delta^{15}\text{N}$	$\delta^{13}\text{C}$	N	OC	CaCO_3	C/N
4.0	6.93	-21.79	0.014	0.16	30.48	13.33
6.0	6.89	-22.31	0.010	0.10	28.27	11.67
8.0	7.82	-23.37	0.012	0.12	29.50	11.67
9.5	7.05	-23.66	0.008	0.13	10.92	18.96
13.0	8.05	-23.17	0.008	0.17	4.06	24.79
15.0	6.87	-23.70	0.006	0.12	4.65	23.33
17.0	6.07	-23.82	0.008	0.17	3.09	24.79
MEAN	7.10	-23.12	0.009	0.14	15.85	18.36
STD	0.61	0.72	0.003	0.03	11.99	5.64
MIN	6.07	-23.82	0.006	0.10	3.09	11.67
MAX	8.05	-21.79	0.014	0.17	30.48	24.79
RANGE	1.99	2.02	0.008	0.07	27.39	13.13

Table 4.1. Core HU-91-045-40 LHC

DEPTH	$\delta^{15}\text{N}$	$\delta^{13}\text{C}$	N	OC	CaCO_3	C/N
3	7.31	-22.21	0.006	0.15	10.84	29.17
5	6.59	-22.89	0.004	0.17	2.97	49.58
7	5.06	-23.13	0.005	0.13	2.48	30.33
9	5.33	-23.19	0.006	0.13	2.52	25.28
11	6.98	-23.53	0.005	0.13	2.33	30.33
MEAN	6.25	-22.99	0.005	0.14	4.23	32.94
STD	0.90	0.44	0.001	0.02	3.31	8.53
MIN	5.06	-23.53	0.004	0.13	2.33	25.28
MAX	7.31	-22.21	0.01	0.17	10.84	49.58
RANGE	2.25	1.32	0.002	0.04	8.51	24.31

Table 4.1. Core HU-90-013-11 BC

DEPTH	*age	$\delta^{15}\text{N}$	$\delta^{13}\text{C}$	N	OC	CaCO_3	C/N
1	4150	7.52	-21.62	0.032	0.33	32.41	12.08
3	4200	7.08	-21.64	0.027	0.29	32.93	12.46
5	4390	7.56	-21.95	0.022	0.27	33.39	14.48
7	4920	7.92	-21.31	0.019	0.23	31.62	13.86
9	5990	7.87	-21.25	0.014	0.24	28.64	20.22
11	6795	7.66	-22.25	0.012	0.20	21.11	19.18
13	7600	8.52	-22.70	0.008	0.20	14.70	28.61
15	8760	8.10	-23.16	0.011	0.16	13.79	16.46
18	10120	7.91	-23.11	0.012	0.38	5.43	36.78
20	10550	8.38	-22.60	0.014	0.43	4.76	35.72
22	11585	7.35	-23.57	0.013	0.31	5.31	28.04
24	11673	7.01	-23.02	0.016	0.40	3.11	28.97
26	11760	7.21	-23.10	0.015	0.53	2.53	40.94
28	12040	6.79	-22.97	0.016	0.40	3.62	28.81
30	12320	6.59	-23.13	0.017	0.38	4.74	26.15
32	12110	7.08	-23.05	0.016	0.34	4.21	25.15
34		6.99	-23.05	0.016	0.45	3.12	32.50
MEAN		7.50	-22.56	0.016	0.33	14.44	24.73
STD		0.54	0.71	0.006	0.10	12.22	8.76
MIN		6.59	-23.57	0.008	0.16	2.53	12.08
MAX		8.52	-21.25	0.032	0.53	33.39	40.94
RANGE		1.93	2.32	0.024	0.37	30.86	28.86

Table 4.2. Core HU-90-031-13 BC

DEPTH	$\delta^{15}\text{N}$	$\delta^{13}\text{C}$	N	OC	CaCO_3	C/N
0.5	9.07	-22.05	0.087	1.57	2.21	21.11
1.5	9.15	-22.03	0.080	1.73	1.07	25.25
3.5	8.91	-22.08	0.043	1.82	0.10	49.33
4.5	8.76	-22.10	0.044	1.77	0.00	46.98
6.0	7.78	-22.22	0.086	1.52	2.11	20.58
8.0	8.21	-22.30	0.117	1.55	2.31	15.49
10.0	8.84	-22.22	0.082	1.64	1.65	23.37
13.0	8.49	-22.28	0.052	1.44	2.09	32.29
15.0	8.40	-22.22	0.050	1.71	0.00	39.82
17.0	8.86	-22.19	0.046	1.48	0.95	37.43
19.0	8.77	-22.17	0.110	1.17	4.45	12.36
21.0	8.25	-22.18	0.118	1.33	2.92	13.15
23.0	8.22	-22.36	0.122	1.52	1.05	14.57
25.0	8.07	-22.16	0.121	1.48	1.05	14.31
27.0	8.34	-22.30	0.105	1.59	0.00	17.62
29.0	7.55	-22.16	0.114	1.60	0.00	16.34
31.0	8.00	-22.24	0.093	1.45	0.00	18.14
33.0	7.95	-22.19	0.104	1.45	0.00	16.27
35.0	8.23	-22.24	0.101	1.45	0.00	16.73
36.5	8.02	-22.15	0.119	1.30	2.44	12.72
MEAN	8.39	-22.19	0.09	1.53	1.22	23.19
STD	0.44	0.08	0.03	0.16	1.24	11.31
MIN	7.55	-22.36	0.04	1.17	0.00	12.36
MAX	9.15	-22.03	0.12	1.82	4.45	49.33
RANGE	1.60	0.33	0.08	0.65	4.45	36.97

Table 4.2 Core HU-90-031-17 BC

DEPTH	$\delta^{15}\text{N}$	$\delta^{13}\text{C}$	N	OC	CaCO_3	C/N
0.5	8.36	-22.07	0.17	1.93	14.58	13.25
1.5	9.18	-22.05	0.17	2.03	12.50	13.93
2.5	8.08	-22.16	0.16	1.97	12.62	14.34
3.5	8.13	-22.18	0.17	1.92	12.76	13.17
4.5	8.91	-22.20	0.15	1.62	14.44	12.58
6.0	8.08	-22.21	0.15	1.79	13.60	13.91
8.0	8.00	-22.11	0.14	1.69	12.20	14.05
10.0	8.48	-22.15	0.14	1.61	13.71	13.38
13.0	9.41	-22.10	0.15	1.65	14.09	12.83
15.0	8.27	-22.06	0.15	1.69	13.23	13.16
17.0	8.26	-22.07	0.14	1.76	12.73	14.69
19.0	8.27	-22.09	0.15	1.53	15.10	11.89
21.0	8.30	-22.13	0.14	1.72	13.69	14.31
23.0	9.73	-22.23	0.14	1.66	12.87	13.80
25.0	8.03	-22.21	0.12	1.53	14.30	14.91
27.0	8.36	-22.21	0.14	1.52	14.99	12.68
29.0	8.07	-22.23	0.13	1.54	15.11	13.79
31.0	8.18	-22.26	0.15	1.58	15.29	12.26
33.0	8.05	-22.25	0.14	1.66	12.36	13.80
35.0	8.05	-22.34	0.12	0.94	20.24	9.15
MEAN	8.42	-22.17	0.15	1.67	14.02	13.29
STD	0.48	0.08	0.01	0.22	1.73	1.23
MIN	8.00	-22.34	0.12	0.94	12.20	9.15
MAX	9.73	-22.05	0.17	2.03	20.24	14.91
RANGE	1.73	0.29	0.05	1.09	8.04	5.76

Table 4.2. Core HU-90-031-29 BC

DEPTH	$\delta^{15}\text{N}$	$\delta^{13}\text{C}$	N	OC	CaCO_3	C/N
1	8.71	-21.94	0.20	2.34	1.45	13.62
3	8.69	-21.93	0.18	2.29	1.45	14.82
5	8.73	-21.88	0.19	2.09	2.74	12.84
7	8.78	-21.88	0.17	1.94	4.41	13.32
9	8.77	-21.84	0.16	2.07	3.35	15.08
11	8.84	-21.94	0.16	1.97	3.51	14.35
13	8.76	-21.90	0.18	1.98	4.12	12.80
15	8.45	-21.83	0.15	2.04	2.02	15.85
17	8.45	-21.91	0.16	2.14	1.83	15.60
19	8.44	-21.82	0.16	2.02	2.82	14.74
21	8.94	-21.86	0.15	1.86	4.38	14.50
23	8.85	-21.87	0.14	1.92	3.40	16.02
25	8.44	-21.97	0.14	1.99	3.73	16.61
27	8.68	-21.95	0.13	1.94	3.20	17.37
29	8.71	-21.89	0.13	2.01	3.02	18.02
31	8.70	-21.91	0.14	1.97	3.72	16.45
33	8.80	-21.89	0.14	1.71	9.30	14.29
35	8.21	-21.96	0.14	1.74	4.52	14.48
MEAN	8.66	-21.90	0.16	2.00	3.50	15.04
STD	0.18	0.04	0.02	0.15	1.69	1.44
MIN	8.21	-21.97	0.13	1.71	1.45	12.80
MAX	8.94	-21.82	0.20	2.34	9.30	18.02
RANGE	0.73	0.15	0.07	0.62	7.85	5.21

Table 4.2. Core HU-90-031-34 BC

DEPTH	$\delta^{15}\text{N}$	$\delta^{13}\text{C}$	N	OC	CaCO_3	C/N
0.5	6.70	-22.33	0.21	1.95	3.71	10.81
1.5	6.68	-22.42	0.21	2.07	2.84	11.50
2.5	6.46	-22.31	0.21	2.04	3.34	11.33
3.5	6.67	-22.44	0.24	1.69	8.37	8.20
4.5	4.25	-22.59	0.18	1.59	7.30	10.33
6.0	6.28	-22.43	0.22	1.52	8.12	8.04
8.0	5.52	-22.38	0.19	1.84	3.87	11.27
11.0	5.79	-22.60	0.16	1.83	3.86	13.32
13.0	5.01	-22.52	0.18	1.47	6.42	9.52
15.0	5.61	-22.52	0.17	1.58	4.25	10.84
17.0	6.59	-22.40	0.15	1.25	6.00	9.72
19.0	5.31	-22.47	0.17	1.63	3.10	11.17
21.0	5.75	-22.48	0.16	1.13	6.95	8.21
23.0	5.64	-22.44	0.14	1.14	5.93	9.49
25.0	5.50	-22.38	0.14	1.41	3.13	11.79
27.0	6.17	-22.46	0.11	0.92	4.08	9.77
29.0	5.36	-22.43	0.12	1.00	4.29	9.68
31.0	6.03	-22.45	0.09	0.79	3.58	10.25
33.0	5.13	-22.36	0.07	0.67	2.39	11.23
35.0	5.94	-22.30	0.10	0.87	3.51	10.13
MEAN	5.82	-22.44	0.16	1.42	4.75	10.33
STD	0.63	0.08	0.05	0.42	1.80	1.29
MIN	4.25	-22.60	0.07	0.67	2.39	8.04
MMAX	6.70	-22.30	0.24	2.07	8.37	13.32
RANGE	2.45	0.30	0.17	1.40	5.98	5.28

Table 4.2. Core HU-90-031-41 BC

DEPT	$\delta^{15}\text{N}$	$\delta^{13}\text{C}$	N	OC	CaCO_3	C/N
H						
0.5	8.84	-21.74	0.22	2.95	0.00	15.65
1.5	8.71	-21.80	0.24	2.71	0.00	13.17
2.5	8.79	-21.76	0.25	2.84	0.88	13.28
3.5	8.88	-21.77	0.23	2.60	1.60	13.18
4.5	8.53	-21.81	0.23	2.80	0.00	14.18
6.0	8.90	-21.76	0.23	2.54	1.59	12.88
8.0	9.16	-21.71	0.23	2.63	1.50	13.34
10.0	8.99	-21.76	0.20	2.53	0.53	14.74
13.0	8.85	-21.70	0.23	2.64	0.86	13.38
15.0	8.67	-21.61	0.23	2.62	1.82	13.30
17.0	9.11	-21.62	0.24	2.59	2.25	12.59
19.0	8.87	-21.65	0.23	2.57	1.17	13.03
21.0	9.04	-21.60	0.23	2.39	3.47	12.14
23.0	9.06	-21.65	0.22	2.60	1.50	13.79
25.0	9.07	-21.63	0.22	2.50	2.22	13.27
27.0	8.81	-21.67	0.22	2.54	1.49	13.48
29.0	8.97	-21.66	0.22	2.55	0.95	13.50
31.0	9.01	-21.67	0.22	2.55	2.02	13.51
33.0	9.19	-21.72	0.22	2.51	1.69	13.29
MEAN	8.92	-21.70	0.23	2.61	1.34	13.46
STD	0.17	0.06	0.01	0.13	0.85	0.74
MIN	8.53	-21.81	0.20	2.39	0.00	12.14
MAX	9.19	-21.60	0.25	2.95	3.47	15.65
RANGE	0.66	0.22	0.05	0.56	3.47	3.51

Table 4.2. Core HU-90-031-43 PC

DEPTH	$\delta^{15}\text{N}$	$\delta^{13}\text{C}$	N	OC	CaCO_3	C/N
1	8.57	-21.20	0.180	2.89	16.65	18.73
3	9.24	-21.34	0.210	2.98	22.38	16.56
5	9.75	-21.70	0.088	1.09	16.56	14.45
7	9.24	-21.30	0.065	0.79	9.54	14.18
9	9.14	-21.32	0.068	0.80	8.93	13.73
11	7.91	-21.75	0.058	0.68	9.20	13.68
13	8.15	-21.73	0.055	0.64	8.03	13.58
18	7.70	-21.68	0.054	0.60	7.87	12.96
23	7.73	-21.60	0.060	0.72	6.91	14.00
28	8.21	-21.67	0.054	0.58	9.16	12.53
33	7.87	-21.61	0.067	0.74	8.74	12.89
38	7.77	-21.68	0.059	0.60	9.17	11.86
MEAN	8.44	-21.55	0.085	1.09	11.10	14.10
STD	0.69	0.19	0.050	0.83	4.56	1.79
MIN	7.70	-21.75	0.054	0.58	6.91	11.86
MAX	9.75	-21.20	0.210	2.98	22.38	18.73
RANGE	2.05	0.55	0.156	2.40	15.47	6.87

Table 4.2. Core HU-90-028-06 BC

DEPTH	$\delta^{15}\text{N}$	$\delta^{13}\text{C}$	N	OC	CaCO_3	C/N
0.5	8.03	-21.65	0.17	1.79	8.47	12.31
1.5	8.42	-21.70	0.15	1.65	5.66	12.84
2.5	8.54	-21.64	0.15	1.60	5.92	12.44
3.5	8.64	-21.69	0.14	1.59	6.50	13.25
4.5	8.72	-21.64	0.14	1.61	6.23	13.44
7.0	8.59	-21.63	0.16	1.65	7.53	12.00
9.0	8.64	-21.61	0.15	1.69	7.07	13.15
11.0	8.42	-21.60	0.15	1.55	8.74	12.07
13.0	8.58	-21.62	0.16	1.71	6.39	12.49
15.0	8.65	-21.68	0.16	1.65	7.24	12.04
17.0	7.78	-21.72	0.14	1.53	10.80	12.79
19.0	8.70	-21.68	0.15	1.67	7.95	12.96
21.0	8.41	-21.70	0.15	1.70	8.38	13.25
MEAN	8.47	-21.66	0.15	1.65	7.45	12.69
STD	0.27	0.04	0.01	0.07	1.37	0.48
MIN	7.78	-21.72	0.14	1.53	5.66	12.00
MAX	8.72	-21.60	0.17	1.79	10.80	13.44
RANGE	0.94	0.12	0.03	0.26	5.14	1.44

Table 4.2. Core HU-90-031-45 BC

DEPTH	$\delta^{15}\text{N}$	$\delta^{13}\text{C}$	N	OC	CaCO_3	C/N
0.5	6.97	-21.75	0.26	5.28	0.00	23.70
1.5	8.11	-21.71	0.28	4.37	0.00	18.20
2.5	7.97	-21.72	0.28	4.08	0.02	16.98
3.5	7.46	-21.72	0.30	3.84	0.05	14.94
4.5	7.27	-21.75	0.29	3.84	0.04	15.45
6.0	7.81	-21.79	0.31	3.72	0.06	14.01
8.0	8.18	-21.62	0.28	3.28	0.09	13.66
10.0	8.00	-21.66	0.29	3.68	0.07	14.80
13.0	6.72	-21.79	0.28	3.43	0.09	14.28
15.0	6.76	-21.78	0.29	3.60	0.08	14.47
17.0	7.76	-21.66	0.27	3.61	0.08	15.62
19.0	7.17	-21.70	0.29	3.49	0.09	14.05
21.0	7.08	-21.72	0.25	3.61	0.07	16.85
23.0	7.49	-21.65	0.26	3.18	0.11	14.27
25.0	8.07	-21.59	0.26	3.33	0.10	14.96
27.0	7.92	-21.57	0.25	3.42	0.10	15.97
29.0	7.23	-21.66	0.26	3.32	0.10	14.89
31.0	6.46	-21.68	0.27	3.32	0.10	14.33
33.0	7.38	-21.66	0.24	3.42	0.09	16.63
MEAN	7.46	-21.69	0.27	3.67	0.07	15.69
STD	0.51	0.06	0.02	0.48	0.03	2.22
MIN	6.46	-21.79	0.24	3.18	0.00	13.66
MAX	8.18	-21.57	0.31	5.28	0.11	23.70
RANGE	1.72	0.23	0.07	2.10	0.11	10.04

Table 4.2. Core HU-90-031-59 BC

DEPTH	$\delta^{15}\text{N}$	$\delta^{13}\text{C}$	N	OC	CaCO ₃	C/N
0.5	8.37	-22.08	0.20	1.91	6.33	11.15
1.5	8.00	-22.08	0.20	2.14	3.37	12.46
2.5	7.77	-22.06	0.20	1.97	4.83	11.49
3.5	7.79	-22.13	0.23	2.21	5.91	11.22
4.5	7.56	-22.10	0.21	2.34	2.71	12.97
6.0	7.71	-22.09	0.22	2.37	3.56	12.58
9.0	8.27	-22.00	0.20	2.06	3.44	12.00
11.0	8.21	-22.03	0.21	1.86	6.09	10.33
13.0	8.31	-21.95	0.21	2.68	0.00	14.90
15.0	8.67	-22.04	0.16	1.59	4.55	11.62
17.0	8.54	-22.31	0.20	2.31	2.07	13.48
19.0	8.32	-21.95	0.15	1.66	2.82	12.93
21.0	8.65	-21.94	0.16	1.38	4.74	10.07
23.0	8.23	-21.94	0.14	1.50	2.20	12.47
25.0	8.41	-21.97	0.13	1.73	0.78	15.49
27.0	8.67	-22.12	0.14	1.53	3.65	12.77
29.0	8.22	-22.10	0.15	1.35	5.49	10.51
31.0	8.21	-22.14	0.14	1.19	5.59	9.91
33.0	8.68	-22.22	0.16	1.14	7.81	8.34
MEAN	8.24	-22.07	0.18	1.84	4.00	11.93
STD	0.33	0.10	0.03	0.42	1.94	1.69
MIN	7.56	-22.31	0.13	1.14	0.00	8.34
MAX	8.68	-21.94	0.23	2.68	7.81	15.49
RANGE	1.12	0.37	0.10	1.54	7.81	7.16

9.3.0. TABLES FOR CHAPTER 5

Table 5.1. Geochemical Results for core HU-91-045-94 PC	237
Table 5.2. Geochemical Results for core HU-90-013-13 PC	239
Table 5.3. Geochemical Results for core HU-90-031-44 PC	241
Table 5.4. Estimated accumulation rate of OC (AR_{OC} , $gC/m^2/yr$), and nitrogen (AR_N , $gN/m^2/yr$), new paleoproductivity (PP_N , $gC/m^2/yr$), total paleoproductivity (PP_T , $gC/m^2/yr$), and fluxes ($gC/m^2/yr$) of OC at various sites.	244
Table 5.5. Estimated accumulation rate of total OC (AR_{OC} , $mgC/m^2/yr$), nitrogen (AR_N , $mgN/m^2/yr$) and marine OC (AR_{MOC} , $mgC/m^2/yr$), new paleoproductivity (PP_N , $gC/m^2/yr$), total paleoproductivity (PP_T , $gC/m^2/yr$), and fluxes ($gC/m^2/yr$) of OC for core HU-90-013-11 BC.	245
Table 5.6. Estimated accumulation rate of total OC (AR_{OC} , $mgC/m^2/yr$), nitrogen (AR_N , $mgN/m^2/yr$) and marine OC (AR_{MOC} , $mgC/m^2/yr$), new paleoproductivity (PP_N , $gC/m^2/yr$), total paleoproductivity (PP_T , $gC/m^2/yr$), and fluxes ($gC/m^2/yr$) of OC for core HU-91-045-94 PC.	246
Table 5.7. Estimated accumulation rate of total OC (AR_{OC} , $mgC/m^2/yr$), nitrogen (AR_N , $mgN/m^2/yr$) and marine OC (AR_{MOC} , $mgC/m^2/yr$), new paleoproductivity (PP_N , $gC/m^2/yr$), total paleoproductivity (PP_T , $gC/m^2/yr$), and fluxes ($gC/m^2/yr$) of OC for core HU-90-013-13 PC.	248
Table 5.8. Estimated accumulation rate of total OC (AR_{OC} , $gC/m^2/yr$), nitrogen (AR_N , $gN/m^2/yr$) and marine OC (AR_{MOC} , $gC/m^2/yr$), new paleoproductivity (PP_N , $gC/m^2/yr$), total paleoproductivity (PP_T , $gC/m^2/yr$), and fluxes ($gC/m^2/yr$) of OC for core HU-90-031-44 PC.	250

Table 5.1. Geochemical results for core HU-91-045-94 PC

DEPTH	$\delta^{15}\text{N}$	$\delta^{13}\text{C}$	N	OC	CaCO_3	C/N	$\delta^{13}\text{C}_{\text{in}}$	$\delta^{18}\text{O}$
1.0	7.26	-22.20	0.041	0.52	38.26	14.76	0.73	2.50
5.5	8.26	-22.10	0.047	0.42	39.91	10.44	0.66	2.41
15.5	7.13	-21.99	0.041	0.43	37.28	12.14	0.81	2.61
25.0	7.03	-22.37	0.041	0.39	38.82	11.14	0.78	2.65
34.5	8.26	-22.51	0.035	0.42	37.54	14.16	0.73	2.47
43.0	7.92	-22.76	0.038	0.37	33.48	11.44	0.59	2.51
52.0	8.10	-22.82	0.027	0.32	37.95	13.68	0.63	2.21
61.0	7.74	-23.00	0.033	0.44	38.21	15.73	0.57	2.52
70.5	7.71	-23.17	0.035	0.37	36.87	12.21	0.66	2.07
79.0	7.88	-23.04	0.032	0.34	35.98	12.98	0.64	2.29
88.5	8.37	-23.26	0.027	0.32	35.10	13.75	0.48	2.14
97.5	7.88	-23.48	0.026	0.28	31.58	12.59	0.50	2.18
106.5	7.07	-23.93	0.039	0.52	27.93	15.53	0.46	2.18
115.5	7.24	-23.94	0.031	0.36	36.10	13.47	0.49	2.16
124.5	7.27	-24.25	0.028	0.39	37.79	16.08	0.45	2.22
133.5	7.33	-24.13	0.033	0.36	36.75	12.75	0.52	2.23
143.0	7.79	-23.87	0.025	0.32	29.18	14.88	0.48	2.22
152.0	7.51	-23.64	0.023	0.33	19.93	16.66	0.53	2.49
161.0	7.58	-23.20	0.025	0.33	22.02	15.29	0.42	2.48
170.0	7.81	-23.39	0.018	0.20	26.34	12.89	0.31	2.55
179.0	6.66	-24.83	0.019	0.14	43.66	8.65	0.32	2.75
193.0	6.33	-23.72	0.022	0.21	19.08	11.16	0.37	2.62
202.5	7.40	-22.99	0.030	0.43	19.90	16.83	0.19	3.14
212.0	6.41	-23.71	0.023	0.20	20.34	10.10	0.23	3.41
228.5	5.65	-24.96	0.016	0.20	20.09	14.57	-0.05	2.46
238.0	5.14	-26.14	0.013	0.19	41.56	17.31	-0.11	3.16
246.5	5.06	-26.45	0.013	0.17	49.74	15.34	-0.09	2.61
255.5	7.12	-23.51	0.028	0.33	6.35	13.66	-0.03	3.04
265.0	6.49	-23.40	0.022	0.37	3.79	19.39	0.00	3.26
274.0	6.11	-23.57	0.029	0.35	7.75	14.11	0.03	3.47
276.0	6.21	-23.48	0.034	0.46	5.47	15.90	0.10	4.04
283.0	6.39	-23.77	0.027	0.34	6.79	14.91	0.14	4.33
292.0	5.86	-23.68	0.031	0.57	7.47	21.60	0.17	4.61
301.5	6.21	-23.52	0.026	0.31	4.80	14.10	0.12	4.58
311.0	5.66	-23.93	0.022	0.35	5.59	18.53	0.25	3.77
320.0	6.28	-23.46	0.031	0.38	5.60	14.21	0.25	4.56
344.0	6.07	-23.69	0.034	0.39	5.35	13.32	0.38	4.63

351.0	5.64	-24.48	0.037	0.56	3.68	17.62	0.23	4.55
360.0	6.24	-23.17	0.046	0.76	5.18	19.24	0.08	4.47
369.0	6.37	-24.69	0.017	0.14	30.85	9.49	0.01	4.41
378.0	5.01	-26.24	0.013	0.16	41.35	14.22	-0.03	4.38
387.5	6.59	-23.71	0.026	0.29	7.36	12.89	-0.05	4.37
397.0	5.90	-23.64	0.044	0.63	6.44	16.63	-0.07	4.35
404.0	7.19	-23.57	0.028	0.37	4.31	15.55	0.14	4.45
413.0	6.28	-23.60	0.029	0.33	5.84	13.26	0.40	3.92
422.5	6.60	-23.28	0.022	0.34	8.43	17.97	0.26	4.01
431.5	6.96	-23.10	0.021	0.32	9.61	17.58	0.34	4.19
441.0	6.23	-23.72	0.032	0.41	5.80	15.12	0.05	4.00
450.5	6.71	-23.44	0.021	0.34	9.29	19.15	0.18	3.95
459.5	6.28	-23.96	0.018	0.26	17.45	16.59	0.05	3.25
469.0	6.47	-24.98	0.015	0.19	25.79	14.43	0.03	3.12
489.0	6.59	-22.83	0.024	0.29	11.05	14.27	0.35	3.89
501.0	6.47	-23.27	0.023	0.38	7.59	19.22	0.39	3.92
510.5	6.68	-22.39	0.027	0.31	10.64	13.52	0.42	3.94
520.0	7.28	-22.93	0.016	0.31	13.75	22.65	0.39	4.15
529.0	6.43	-22.11	0.039	0.56	9.93	16.71	0.30	3.92
538.5	6.77	-22.84	0.025	0.33	8.51	15.38	0.23	3.78
548.0	6.38	-22.19	0.037	0.54	15.23	17.11	0.29	3.80
557.0	6.27	-22.99	0.024	0.38	20.83	18.48	0.34	3.82
566.0	6.64	-25.77	0.010	0.15	32.09	17.44	0.28	3.86
575.5	6.04	-26.39	0.010	0.18	35.75	20.99	0.24	3.87
585.0	6.89	-26.08	0.012	0.17	31.66	16.62	0.21	3.89
594.0	6.91	-22.66	0.016	0.31	10.39	22.88	0.43	4.02
603.0	5.95	-21.57	0.044	0.58	12.71	15.51	0.31	4.12
612.0	7.70	-22.48	0.026	0.26	16.25	11.65	0.51	4.04
621.5	7.48	-22.51	0.029	0.35	12.33	14.11	0.34	3.88
631.0	7.61	-22.94	0.027	0.33	12.82	14.32	0.51	3.99
640.5	6.58	-22.38	0.038	0.53	17.08	16.30		
MEAN	6.78	-23.56	0.027	0.35	20.74	15.19	0.31	3.40
STD	0.78	1.08	0.009	0.12	13.41	2.93	0.23	0.83
MIN	5.01	-26.45	0.010	0.14	3.68	8.65	-0.11	2.07
MAX	8.37	-21.57	0.047	0.76	49.74	22.88	0.81	4.63
RANGE	3.36	4.88	0.037	0.62	46.06	14.23	0.92	2.56

Table 5.2. Geochemical results for core HU-90-013-13 PC.

DEPTH	*age	$\delta^{15}\text{N}$	$\delta^{13}\text{C}$	N	OC	CaCO_3	C/N	$\delta^{13}\text{C}_{\text{in}}$	$\delta^{18}\text{O}$
4	910	7.24	-21.18	0.045	0.57	36.18	14.73	0.85	2.39
9		6.92	-21.34	0.046	0.49	38.39	12.50	0.73	2.47
19	1620	6.91	-21.40	0.042	0.48	35.52	13.26	0.71	2.55
29	1840	6.55	-21.82	0.035	0.43	39.33	14.36	0.73	2.54
39		6.69	-21.98	0.039	0.44	38.30	13.29	0.73	2.52
49		6.66	-22.24	0.035	0.46	34.54	15.50	0.95	2.79
59		6.82	-22.33	0.037	0.54	31.13	17.16	0.85	2.61
69		6.31	-22.50	0.040	0.59	29.48	17.28	0.76	2.60
79		7.40	-22.33	0.035	0.61	26.68	20.29	0.69	2.59
89		6.56	-22.72	0.033	0.53	27.86	18.62	0.79	2.59
99	3980	5.89	-23.06	0.042	0.59	26.90	16.45	0.99	2.42
109		6.22	-22.80	0.043	0.64	25.13	17.47	0.76	2.54
119		7.27	-23.16	0.042	0.57	28.57	15.88	0.78	2.52
129		7.10	-22.90	0.040	0.56	26.51	16.29	0.80	2.54
139		7.30	-22.89	0.040	0.56	28.07	16.37	0.80	2.43
149		7.02	-22.83	0.034	0.56	25.71	19.38	0.70	2.42
159		7.21	-23.10	0.037	0.56	22.89	17.75	0.67	2.44
169		7.06	-23.18	0.034	0.56	21.90	19.30	0.83	2.51
179		6.93	-23.52	0.038	0.53	21.54	16.14	0.75	2.36
189	6810	7.60	-23.68	0.035	0.54	19.59	17.96	0.65	2.46
199		7.10	-23.75	0.035	0.59	18.17	19.64	0.66	2.57
209	7580	7.34	-24.05	0.045	0.64	16.47	16.68	0.63	2.38
219		7.10	-24.03	0.034	0.57	10.56	19.65	0.69	2.31
229		7.64	-24.04	0.047	0.65	19.39	16.21	0.61	2.61
239	7790	7.59	-24.64	0.056	0.73	20.49	15.24	0.49	2.61
249		7.78	-24.75	0.030	0.48	14.51	18.62	0.64	2.55
259		7.39	-24.91	0.041	0.51	16.68	14.47	0.65	2.72
269		7.48	-25.45	0.037	0.54	12.30	17.15	0.63	2.72
279		6.89	-25.68	0.043	0.63	11.07	17.14	0.60	2.66
289		6.67	-24.56	0.035	0.52	8.84	17.33	0.57	2.60
299		6.68	-23.85	0.029	0.52	4.28	20.80	0.45	2.65
309		6.53	-23.73	0.013	0.26	3.67	23.35	0.46	2.61
319		6.66	-23.68	0.022	0.50	4.53	26.33	0.64	2.59
329		6.17	-23.74	0.016	0.33	4.03	23.80	0.49	2.78
339	8830	7.05	-23.84	0.024	0.44	5.55	21.59	0.49	2.65
349		7.29	-23.77	0.019	0.34	3.69	20.70	0.40	2.72
359	9230	7.33	-23.46	0.031	0.54	5.60	20.26	0.34	2.76

369	10040	7.06	-23.19	0.036	0.55	6.31	17.92	0.35	3.31
379		6.76	-23.32	0.028	0.49	8.02	20.32	0.48	2.97
389	10430	6.36	-23.46	0.041	0.68	9.24	19.37	0.45	3.35
399	10720	7.26	-23.16	0.029	0.46	8.43	18.42	0.41	3.55
409		7.08	-23.26	0.023	0.64	7.96	32.22	0.47	3.64
419	11990	6.25	-23.63	0.022	0.42	10.06	22.42	0.42	3.43
429	12450	6.80	-23.80	0.021	0.43	11.02	23.73	0.36	3.54
439	12560	6.33	-23.72	0.033	0.63	10.72	22.42	0.09	3.41
449	14150	6.93	-23.52	0.021	0.45	10.43	24.89	0.11	3.89
460		6.71	-23.47	0.017	0.41	6.57	28.22	0.14	4.58
469		6.04	-23.55	0.010	0.25	4.60	28.95	0.16	4.65
479	16990	7.95	-23.36	0.010	0.38	3.36	43.98	0.27	4.55
489		6.16	-23.78	0.020	0.42	5.63	24.78	0.17	4.60
499		6.61	-23.87	0.017	0.44	6.16	30.28	0.21	4.65
509	20950	3.69	-25.55	0.011	0.22	34.10	23.07	0.13	4.13
519		7.43	-22.92	0.020	0.34	5.93	19.76	0.26	4.43
529	22190	7.61	-22.77	0.022	0.35	6.71	18.31	0.26	4.29
539		6.16	-23.30	0.020	0.32	4.37	18.41	0.23	4.05
549		7.18	-22.91	0.024	0.35	4.21	17.23	0.52	4.33
559		6.62	-22.40	0.025	0.40	3.36	18.49	0.60	4.13
569		6.61	-22.75	0.019	0.33	3.52	20.15	0.51	3.97
579		6.88	-22.51	0.021	0.32	1.80	18.01	0.53	4.06
589		7.24	-22.36	0.022	0.36	1.55	19.32	0.41	4.02
599		6.49	-22.65	0.020	0.39	0.43	22.66	0.29	3.97
609		6.89	-23.09	0.027	0.45	4.16	19.47	0.54	4.35
619		6.51	-22.36	0.027	0.45	3.30	19.64	0.40	4.01
MEAN		6.86	-23.29	0.030	0.48	15.02	19.86	0.54	3.15
STD		0.61	0.92	0.010	0.11	11.47	5.04	0.22	0.77
MIN		3.69	-25.68	0.010	0.22	0.43	12.50	0.09	2.31
MAX		7.95	-21.18	0.056	0.73	39.33	43.98	0.99	4.65
RANGE		4.26	4.50	0.046	0.51	38.90	31.48	0.90	2.34

Table 5.3. Geochemical results for core HU-90-031-44 PC

DEPTH	AGE	$\delta^{15}\text{N}$	$\delta^{13}\text{C}_{\text{or}}$	$\delta^{13}\text{C}_{\text{in}}$	$\delta^{18}\text{O}$	N	OC	CaCO_3	C/N
1		7.53	-21.26	0.93	2.55	0.200	2.18	30.88	12.74
11		8.55	-21.25	1.00	2.45	0.210	2.35	32.51	13.05
20	2210	8.02	-21.10	1.06	2.42	0.190	2.44	29.81	15.00
30		8.08	-21.41	0.94	2.05	0.170	2.14	30.90	14.71
41	3830	7.52	-21.61	0.80	1.94	0.150	1.78	28.15	13.86
51		7.92	-21.59	0.57	1.61	0.150	1.61	26.40	12.54
60		8.20	-21.79	0.73	1.90	0.120	1.61	22.05	15.69
70		8.08	-22.02	0.59	1.90	0.076	1.10	18.59	12.83
80		7.91	-21.61	0.45	2.06	0.079	0.99	18.07	11.57
90		8.44	-21.95	0.57	2.22	0.083	1.05	17.04	12.20
100		8.29	-21.70	0.54	2.05	0.084	1.13	14.81	13.22
111		8.47	-21.89	0.49	2.07	0.075	0.95	15.92	11.09
120		8.17	-21.56	0.39	2.55	0.083	1.04	12.67	12.13
130		8.45	-21.71	0.46	2.50	0.078	1.00	12.25	11.67
140	9640	8.18	-21.43	0.44	2.65	0.092	1.00	13.00	12.69
150		8.10	-21.58	0.37	2.23	0.080	1.02	12.27	14.85
159		6.52	-21.60	0.40	2.62	0.074	0.84	12.95	13.18
171		7.16	-21.58	0.26	2.42	0.085	0.85	14.08	11.68
180	10100	7.01	-22.03	0.09	2.99	0.089	0.98	8.60	12.82
190		6.23	-22.05	-0.04	2.93	0.078	0.85	9.86	12.68
200		7.27	-21.71	0.24	3.17	0.094	0.99	9.91	12.30
211		6.67	-21.25	0.05	2.81	0.094	0.94	13.84	11.66
220	10440	6.07	-21.45	0.01	2.81	0.092	0.93	12.43	11.77
230		6.91	-21.51	-0.14	2.70	0.083	0.84	12.96	11.87
241		6.85	-21.61	-0.14	2.87	0.081	0.84	11.95	12.05
250		7.02	-21.63	-0.14	2.77	0.080	0.83	11.84	12.09
260		6.12	-21.73	-0.07	2.87	0.076	0.74	13.09	11.34
269		4.59	-21.81	-0.17	2.75	0.071	0.76	11.76	12.47
280		7.10	-21.66	0.14	3.28	0.079	0.83	10.29	12.19
289		6.33	-22.07	0.17	3.16	0.072	0.83	8.02	13.42
301	11390	6.74	-21.89	0.17	3.25	0.084	1.03	9.39	14.35
310		6.71	-22.17	0.15	3.40	0.078	0.93	8.56	13.95
320		6.25	-22.03	0.12	3.53	0.076	0.89	7.70	13.61
329		5.96	-22.08	0.07	3.48	0.077	0.88	7.87	13.26
340		6.56	-22.29	0.07	3.41	0.079	0.84	8.21	12.47
349		6.46	-22.51	0.03	3.54	0.065	0.76	7.87	13.56
361		6.36	-22.52	0.05	3.56	0.056	0.79	7.44	16.39
370		6.48	-22.37	0.04	3.48	0.057	0.96	6.56	19.70

380		5.46	-22.29	-0.05	3.28	0.066	0.76	8.06	13.49
389		6.02	-22.42	-0.04	3.51	0.072	0.85	9.03	13.71
400		6.46	-22.56	0.20	3.60	0.067	0.84	7.84	14.61
410	12490	6.43	-22.52	-0.03	3.94	0.071	0.84	7.94	13.77
420		6.22	-22.66	-0.17	4.06	0.071	0.77	6.98	12.69
430		6.38	-22.92	-0.13	3.69	0.067	0.80	7.09	13.92
439		6.31	-22.72	-0.12	3.96	0.066	0.80	7.18	14.11
449		5.77	-22.83	-0.32	3.66	0.067	0.87	6.96	15.23
460		3.32	-23.43	-0.32	3.93	0.058	0.82	6.56	16.54
470		5.98	-23.03	-0.34	3.75	0.061	0.75	7.77	14.29
481		6.06	-23.10	-0.25	3.94	0.062	0.82	6.83	15.43
490		6.18	-22.98	-0.54	3.55	0.057	0.75	7.60	15.32
501		5.70	-22.81	-0.28	3.65	0.060	0.78	6.63	15.25
511		5.95	-23.00	-0.43	3.33	0.058	0.79	5.73	15.93
520		5.80	-23.12	-0.29	3.63	0.053	0.61	6.70	13.35
531		5.24	-23.10	-0.56	3.13	0.053	0.62	6.80	13.75
540		5.15	-23.24	-0.79	3.34	0.048	0.61	6.61	14.76
549	12550	5.78	-23.19	-0.64	3.06	0.043	0.57	7.29	15.35
560		6.01	-23.84	-0.69	3.21	0.049	0.54	8.54	12.74
569		6.07	-22.94	-0.71	2.70	0.054	0.51	8.13	11.12
581		5.84	-23.16	-0.73	3.03	0.049	0.80	4.57	19.09
590		5.87	-23.85	-0.75	2.63	0.045	0.58	6.24	15.08
600		5.53	-23.18	-0.60	2.60	0.043	0.50	7.42	13.57
610		5.84	-23.06	-0.66	2.77	0.047	0.60	8.46	14.77
620		3.71	-22.98	-0.53	3.18	0.050	0.63	7.86	14.62
630		5.63	-23.23	-0.50	2.83	0.049	0.61	6.61	14.46
641		5.08	-23.35	-0.54	3.02	0.048	0.63	6.00	15.31
650		5.61	-23.65	-0.63	2.79	0.034	0.62	5.37	21.11
660		4.23	-23.65	-0.62	2.95	0.034	0.58	6.59	19.88
671		3.67	-23.56	-0.68	2.66	0.038	0.58	6.94	17.72
680		5.97	-23.45	-0.59	2.84	0.036	0.51	7.69	16.46
690		5.36	-23.62	-0.65	2.58	0.032	0.54	5.95	19.55
701		5.23	-23.91	-0.68	2.67	0.029	0.54	5.60	21.65
710		4.70	-23.79	-0.71	2.48	0.030	0.56	5.17	21.76
720		3.73	-23.97	-0.72	2.94	0.033	0.58	5.71	20.67
731		5.50	-24.12	-0.70	2.52	0.032	0.53	4.28	19.20
739		5.67	-24.25	-0.49	2.82	0.030	0.57	4.91	22.19
751		4.49	-23.98	-0.52	2.58	0.029	0.58	5.27	23.25
761		4.24	-24.20	-0.56	2.44	0.026	0.55	5.17	24.69
770		5.36	-24.65	-0.19	2.92	0.037	0.48	5.31	15.23
781		3.56	-24.23	-0.69	2.61	0.041	0.57	7.20	16.11

791	4.74	-24.26	-0.58	2.64	0.035	0.62	15.99	20.73
800	5.12	-25.01	-0.45	2.49	0.017	0.43	29.24	29.63
810	5.52	-24.09	-0.44	2.99	0.030	0.54	14.42	20.97
822	4.77	-23.80	-0.48	3.17	0.045	0.61	5.28	15.72
841	5.73	-23.56	-0.56	3.02	0.038	0.67	4.78	20.47
850	6.20	-23.31	-0.34	3.17	0.037	0.61	5.46	19.38
860	4.92	-23.26	-0.54	2.91	0.039	0.61	7.05	18.36
881	5.01	-23.37	-0.37	3.38	0.039	0.55	6.84	16.45
891	5.03	-23.16	-0.40	2.62	0.034	0.51	7.86	17.39
900	5.96	-23.01	-0.37	3.56	0.049	0.62	7.24	14.80
910	5.26	-23.02	-0.36	3.78	0.052	0.58	6.41	13.02
920	5.31	-23.13	-0.47	3.46	0.043	0.58	5.89	15.84
930	5.82	-23.26	-0.23	3.52	0.040	0.46	8.61	13.33
940	3.76	-23.00	-0.16	3.75	0.041	0.49	7.15	14.01
MEAN	6.10	-22.72	-0.14	2.97	0.07	0.83	10.40	15.27
STD	1.24	0.93	0.47	0.54	0.04	0.39	6.52	3.43
MIN	3.32	-25.01	-0.79	1.61	0.02	0.43	4.28	11.09
MAX	8.55	-21.10	1.06	4.06	0.21	2.44	32.51	29.63
RANGE	5.23	3.91	1.85	2.45	0.19	2.01	28.23	18.54

Table 5.4. Estimated accumulation rates of OC (AR_{OC} , $mgC/m^2/yr$) and nitrogen (AR_N , $mgN/m^2/yr$), new paleoproductivity (PP_N , $gC/m^2/yr$) and total paleoproductivity (PP_T , $gC/m^2/yr$), and fluxes ($gC/m^2/yr$) of OC at various sites.

CORE	SR	OC	N	AR_{OC}	AR_N	w/d (m)	PP_N	PP_T	Flux
11 BC	2.3	0.298	0.027	12.69	1.15	2805	6.12	49.5	0.85
23 BC	2.8	0.242	0.019	12.57	0.99	1984	4.54	42.6	0.84
28 BC	3.5	0.348	0.033	22.52	2.14	3992	11.74	68.5	1.07
94 PC	18.0	0.420	0.039	139.81	12.98	3448	32.29	113.7	2.28
13 PC	28.0	0.480	0.086	188.16	33.71	3380	39.18	125.2	2.62
44 PC	13.0	2.090	0.180	498.91	42.97	1380	34.68	117.8	3.97
13 BC	17.0	1.530	0.090	480.78	28.28	322	10.04	63.4	3.90
17 BC	13.0	1.670	0.150	400.32	35.96	372	10.14	63.7	3.62
29 BC	11.0	2.000	0.160	405.60	32.45	408	11.09	66.6	3.65
41 BC	13.0	2.600	0.230	621.50	54.98	448	15.73	79.3	4.37

Table 5.5. Estimated accumulation rate of total OC (AR_{OC} , $mgC/m^2/yr$), nitrogen (AR_N , $mgN/m^2/yr$) and marine OC (AR_{MOC} , $mgC/m^2/yr$), new paleoproductivity (PP_N , $gC/m^2/yr$), total paleoproductivity (PP_T , $gC/m^2/yr$), and fluxes ($gC/m^2/yr$) of OC for core HU-90-013-11 BC.

DEPTH	*age	MOC	TOC	AR_{OC}	AR_N	AR_{MOC}	PP_N	PP_T	Flux
1	4150	0.29	0.04	10.2	0.99	8.9	5.1	45.0	0.74
3	4200	0.25	0.04	8.9	0.83	7.7	4.6	42.9	0.70
5	4390	0.22	0.05	8.3	0.68	6.8	4.2	41.1	0.66
7	4920	0.21	0.01	7.1	0.59	6.5	4.1	40.5	0.65
9	5990	0.23	0.01	7.4	0.43	7.1	4.4	41.7	0.67
11	6795	0.15	0.05	6.2	0.37	4.6	3.3	36.4	0.56
13	7600	0.13	0.07	6.2	0.25	4.0	3.0	34.7	0.53
15	8760	0.09	0.07	5.0	0.34	2.8	2.4	30.9	0.45
18	10120	0.22	0.16	11.8	0.37	6.8	4.2	41.2	0.66
20	10550	0.29	0.14	13.3	0.43	8.9	5.1	45.0	0.74
22	11585	0.15	0.16	9.6	0.40	4.7	3.3	36.4	0.56
24	11673	0.24	0.16	12.4	0.50	7.5	4.5	42.4	0.69
26	11760	0.31	0.22	16.3	0.46	9.6	5.3	45.9	0.77
28	12040	0.24	0.16	12.4	0.50	7.5	4.5	42.4	0.69
30	12320	0.22	0.16	11.8	0.53	6.8	4.2	41.2	0.66
32	12110	0.20	0.14	10.6	0.50	6.2	4.0	40.0	0.64
34		0.26	0.18	14.0	0.50	8.1	4.7	43.5	0.71
MEAN		0.22	0.11	10.1	0.51	6.7	4.2	40.7	0.65
STD		0.06	0.06	3.1	0.18	1.8	0.7	3.9	0.08
MIN		0.09	0.01	5.0	0.25	2.8	2.4	30.9	0.45
MAX		0.31	0.22	16.3	0.99	9.6	5.3	45.9	0.77
RANGE		0.22	0.21	11.4	0.74	6.8	2.9	15.0	0.31

Table 5.6. Estimated accumulation rate of total OC (AR_{OC} , $mgC/m^2/yr$), nitrogen (AR_N , $mgN/m^2/yr$) and marine OC (AR_{MOC} , $mgC/m^2/yr$), new paleoproductivity (PP_N , $gC/m^2/yr$), total paleoproductivity (PP_T , $gC/m^2/yr$), and fluxes ($gC/m^2/yr$) of OC for core HU-91-045-94 PC.

DEPTH	MOC	TOC	AR_{OC}	AR_N	AR_{MOC}	PP_N	PP_T	Flux
1.0	0.39	0.12	139.4	11.0	104.5	27.7	105.2	2.06
5.5	0.33	0.09	112.6	12.6	88.4	24.8	99.7	1.91
15.5	0.34	0.08	115.2	11.0	91.1	25.3	100.7	1.94
25.0	0.28	0.11	104.5	11.0	75.0	22.4	94.6	1.78
34.5	0.30	0.13	112.6	9.4	80.4	23.4	96.7	1.84
43.0	0.24	0.13	99.2	10.2	64.3	20.2	90.0	1.67
52.0	0.20	0.11	85.8	7.2	53.6	18.0	84.9	1.54
61.0	0.27	0.18	117.9	8.8	72.4	21.8	93.5	1.76
70.5	0.21	0.16	99.2	9.4	56.3	18.6	86.2	1.58
79.0	0.20	0.14	91.7	8.6	53.6	18.0	84.9	1.54
88.5	0.17	0.14	85.8	7.2	45.6	16.2	80.5	1.44
97.5	0.14	0.14	75.0	7.0	37.5	14.3	75.7	1.33
106.5	0.22	0.30	139.4	10.5	59.0	19.1	87.5	1.61
115.5	0.15	0.21	96.5	8.3	40.2	15.0	77.4	1.37
124.5	0.14	0.25	104.5	7.5	37.5	14.3	75.7	1.33
133.5	0.13	0.23	96.5	8.8	34.8	13.6	73.9	1.28
143.0	0.14	0.18	85.8	6.7	37.5	14.3	75.7	1.33
152.0	0.16	0.17	88.4	6.2	42.9	15.6	79.0	1.40
161.0	0.18	0.14	88.4	6.7	48.2	16.8	82.0	1.48
170.0	0.10	0.09	53.6	4.8	26.8	11.5	67.9	1.15
179.0	0.03	0.11	37.5	5.1	8.0	5.3	46.1	0.69
193.0	0.10	0.11	56.3	5.9	26.8	11.5	67.9	1.15
202.5	0.26	0.17	115.2	8.0	69.7	21.3	92.3	1.73
212.0	0.09	0.11	53.6	6.2	24.1	10.8	65.6	1.10
228.5	0.04	0.16	53.6	4.3	10.7	6.4	50.6	0.78
238.0	0.00	0.19	50.9	3.5	0.0	0.0	0.0	0.00
246.5	0.00	0.17	45.6	3.5	0.0	0.0	0.0	0.00
255.5	0.16	0.16	89.1	7.6	43.2	15.7	79.1	1.41
265.0	0.19	0.18	99.9	5.9	51.3	17.5	83.6	1.52
274.0	0.17	0.18	93.8	7.8	45.6	16.2	80.5	1.44
276.0	0.23	0.23	123.3	9.1	61.6	19.7	88.8	1.64
283.0	0.15	0.19	91.8	7.3	40.5	15.0	77.5	1.37
292.0	0.27	0.31	152.8	8.3	72.4	21.8	93.5	1.76
301.5	0.16	0.16	83.7	7.0	43.2	15.7	79.1	1.41
311.0	0.14	0.20	94.5	5.9	37.8	14.4	75.8	1.33
320.0	0.19	0.19	102.6	8.4	51.3	17.5	83.6	1.52
344.0	0.18	0.21	105.3	9.2	48.6	16.9	82.2	1.48

351.0	0.17	0.39	150.1	9.9	45.6	16.2	80.5	1.44
360.0	0.43	0.33	203.7	12.3	115.2	29.5	108.6	2.14
369.0	0.04	0.10	37.5	4.6	10.7	6.4	50.6	0.78
378.0	0.00	0.16	42.9	3.5	0.0	0.0	0.0	0.00
387.5	0.13	0.16	78.3	7.0	35.1	13.7	74.0	1.29
397.0	0.30	0.33	168.8	11.8	80.4	23.4	96.7	1.84
404.0	0.18	0.19	99.9	7.6	48.6	16.9	82.2	1.48
413.0	0.16	0.17	89.1	7.8	43.2	15.7	79.1	1.41
422.5	0.18	0.15	91.1	5.9	48.2	16.8	82.0	1.48
431.5	0.18	0.13	85.8	5.6	48.2	16.8	82.0	1.48
441.0	0.19	0.23	109.9	8.6	50.9	17.4	83.5	1.51
450.5	0.18	0.17	91.1	5.6	48.2	16.8	82.0	1.48
459.5	0.10	0.15	69.7	4.8	26.8	11.5	67.9	1.15
469.0	0.04	0.15	50.9	4.0	10.7	6.4	50.6	0.78
489.0	0.19	0.11	77.7	6.4	50.9	17.4	83.5	1.51
501.0	0.21	0.17	101.8	6.2	56.3	18.6	86.2	1.58
510.5	0.23	0.09	83.1	7.2	61.6	19.7	88.8	1.64
520.0	0.19	0.12	83.1	4.3	50.9	17.4	83.5	1.51
529.0	0.43	0.12	150.1	10.5	115.2	29.5	108.6	2.14
538.5	0.21	0.12	88.4	6.7	56.3	18.6	86.2	1.58
548.0	0.41	0.13	144.7	9.9	109.9	28.6	106.9	2.10
557.0	0.23	0.15	101.8	6.4	61.6	19.7	88.8	1.64
566.0	0.01	0.14	40.2	2.7	2.7	2.6	32.4	0.43
575.5	0.00	0.18	48.2	2.7	0.0	0.0	0.0	0.00
585.0	0.00	0.17	45.6	3.2	0.0	0.0	0.0	0.00
594.0	0.21	0.10	83.1	4.3	56.3	18.6	86.2	1.58
603.0	0.52	0.07	155.4	11.8	139.4	33.3	115.4	2.33
612.0	0.18	0.08	69.7	7.0	48.2	16.8	82.0	1.48
621.5	0.24	0.11	93.8	7.8	64.3	20.2	90.0	1.67
631.0	0.20	0.13	88.4	7.2	53.6	18.0	84.9	1.54
640.5	0.38	0.15	142.0	10.2	101.8	27.2	104.3	2.03
MEAN	0.19	0.16	94.22	7.343	50.38	16.3	76.5	1.39
STD	0.11	0.06	33.38	2.421	29.41	7.3	25.9	0.52
MIN	0.00	0.07	37.52	2.680	0.00	0.0	0.0	0.00
MAX	0.52	0.39	203.68	12.596	139.36	33.3	115.4	2.33
RANGE	0.52	0.32	166.16	9.916	139.36	33.3	115.4	2.33

Table 5.7. Estimated accumulation rate of total OC (AR_{OC} , $mgC/m^2/yr$), nitrogen (AR_N , $mgN/m^2/yr$) and marine OC (AR_{MOC} , $mg/m^2/yr$), new paleoproductivity (PP_N , $gC/m^2/yr$), total paleoproductivity (PP_T $gC/m^2/yr$), and fluxes ($gC/m^2/yr$) of OC for core HU-90-013-13 PC.

DEPTH	MOC	TOC	AR_{OC}	AC_N	AC_{MOC}	PP_N	PP_T	Flux
4	0.55	0.02	255.4	20.2	246.4	46.5	136.3	2.93
9	0.46	0.03	221.1	20.8	207.6	41.6	128.9	2.72
19	0.44	0.04	213.5	18.7	195.7	40.1	126.6	2.66
29	0.36	0.07	196.8	16.0	164.7	35.8	119.6	2.47
39	0.36	0.09	198.5	17.6	162.4	35.5	119.2	2.45
49	0.35	0.12	207.6	15.8	157.9	34.9	118.1	2.42
59	0.40	0.15	241.9	16.6	179.2	37.8	123.0	2.56
69	0.41	0.18	260.5	17.7	181.1	38.2	123.5	2.57
79	0.45	0.16	267.4	15.3	197.3	40.4	127.0	2.67
89	0.35	0.18	239.1	14.9	157.9	34.9	118.1	2.42
99	0.35	0.24	260.5	18.5	154.6	34.5	117.4	2.40
109	0.41	0.23	282.6	19.0	181.1	38.2	123.5	2.57
119	0.32	0.25	255.4	18.8	143.4	32.8	114.5	2.33
129	0.35	0.21	268.8	19.2	168.0	36.0	120.1	2.48
139	0.35	0.21	259.8	18.6	162.4	35.4	119.0	2.45
149	0.36	0.21	250.9	15.2	161.3	35.4	118.9	2.45
159	0.33	0.24	250.9	16.6	147.8	33.4	115.6	2.36
169	0.32	0.24	252.7	15.3	144.4	32.9	114.7	2.33
179	0.26	0.26	235.7	16.9	115.6	28.6	106.9	2.12
189	0.25	0.29	241.9	15.7	112.0	28.0	105.8	2.09
199	0.27	0.32	262.4	15.6	120.1	29.3	108.2	2.16
209	0.25	0.39	329.7	23.2	128.8	30.1	109.8	2.20
219	0.23	0.35	249.9	14.9	100.8	26.2	102.4	2.00
229	0.26	0.40	282.9	20.5	113.2	28.2	106.3	2.11
239	0.20	0.53	566.1	43.4	155.1	34.0	116.6	2.38
249	0.12	0.36	359.0	22.4	89.8	24.0	98.0	1.89
259	0.11	0.40	415.1	33.4	89.5	23.7	97.5	1.88
269	0.06	0.48	415.8	28.5	46.2	15.6	79.0	1.42
279	0.04	0.59	512.8	35.0	32.6	12.4	70.4	1.22
289	0.15	0.37	406.1	27.3	117.2	28.4	106.5	2.11
299	0.22	0.29	403.3	22.5	170.6	36.1	120.2	2.48
309	0.12	0.14	230.2	11.5	106.3	26.3	102.5	2.01
319	0.23	0.27	415.3	18.3	191.0	38.6	124.2	2.59
329	0.15	0.18	285.0	13.8	129.5	29.9	109.4	2.19
339	0.19	0.25	358.2	19.5	154.7	33.7	116.2	2.37
349	0.15	0.19	321.6	18.0	141.9	31.4	112.1	2.26
359	0.27	0.27	424.7	24.4	212.4	41.5	128.9	2.72

369	0.31	0.24	196.7	12.9	110.9	27.8	105.4	2.08
379	0.26	0.23	168.2	9.6	89.2	24.3	98.5	1.91
389	0.35	0.33	231.7	14.0	119.3	29.3	108.2	2.16
399	0.26	0.20	154.6	9.7	87.4	24.0	98.0	1.89
409	0.35	0.29	221.2	7.9	121.0	29.5	108.6	2.17
419	0.20	0.22	146.2	7.7	69.6	20.7	90.9	1.71
429	0.19	0.24	149.6	7.3	66.1	20.0	89.4	1.67
439	0.29	0.34	85.1	4.5	39.2	14.6	76.3	1.36
449	0.22	0.23	59.1	2.8	28.9	12.0	69.3	1.19
460	0.21	0.20	52.0	2.2	26.6	11.5	67.7	1.16
469	0.12	0.13	34.2	1.4	16.4	8.3	57.7	0.93
479	0.20	0.18	51.0	1.3	26.8	11.4	67.6	1.15
489	0.19	0.24	55.2	2.6	25.0	10.9	66.2	1.12
499	0.19	0.25	58.6	2.3	25.3	11.0	66.4	1.13
509	0.02	0.20	55.1	2.8	5.0	3.8	38.8	0.55
519	0.21	0.13	69.5	4.1	42.9	15.3	78.3	1.40
529	0.22	0.12	72.5	4.6	45.6	15.9	79.8	1.44
539	0.17	0.15	65.0	4.1	34.5	13.3	73.0	1.28
549	0.22	0.14	70.6	4.8	44.4	15.7	79.2	1.43
559	0.29	0.11	80.6	5.0	58.5	18.7	86.6	1.60
569	0.21	0.11	65.1	3.8	41.5	15.0	77.6	1.39
579	0.23	0.10	63.6	4.2	45.7	16.0	80.0	1.45
589	0.27	0.10	70.1	4.3	52.5	17.6	83.8	1.54
599	0.26	0.13	76.4	3.9	51.0	17.2	82.9	1.52
609	0.26	0.19	88.2	5.3	51.0	17.2	82.9	1.52
619	0.33	0.12	90.1	5.4	66.1	20.3	90.1	1.69
MEAN	0.26	0.22	216.3	13.9	108.4	26.21	100.13	1.97
STD	0.10	0.11	125.5	8.9	60.0	10.14	21.39	0.54
MIN	0.02	0.02	34.2	1.3	5.0	3.77	38.84	0.55
MAX	0.55	0.59	566.1	43.4	246.4	46.45	136.31	2.93
RANGE	0.53	0.57	531.9	42.1	241.4	42.68	97.48	2.38

Table 5.8. Estimated accumulation rate of total OC (AR_{OC} , $gC/m^2/yr$), nitrogen (AR_N $gN/m^2/yr$) and marine OC (AR_{MOC} $gC/m^2/yr$), new paleoproductivity (PP_N , $gC/m^2/yr$), total paleoproductivity (PP_T , $gC/m^2/yr$), and fluxes ($gC/m^2/yr$) of OC for core HU-90-031-44 PC.

DEPTH	AGE		INTERPORATED		SR		MOC	AR_{OC}	AR_N	AR_{MOC}	PP_N	PP_T	FLUX
	^{14}C	TRUE	^{14}C	TRUE	TRUE	^{14}C							
1					13.05	18.07	2.07	0.65	0.060	0.62	39	125	4.28
11					13.05	18.07	2.23	0.73	0.065	0.69	42	129	4.48
20	2210	2352	2211	2353	13.05	18.07	2.39	0.77	0.060	0.75	44	132	4.64
30			2764	3119	9.50	9.94	1.96	0.46	0.037	0.42	31	111	3.66
41	3830	4239	3870	4277	10.60	11.32	1.56	0.40	0.034	0.35	27	105	3.39
51			4754	5221	11.70	12.71	1.42	0.38	0.036	0.34	27	103	3.34
60			5462	5990	12.91	14.27	1.36	0.42	0.032	0.36	28	105	3.41
70			6162	6764	14.32	16.11	0.88	0.29	0.020	0.23	21	91	2.83
80			6783	7463	15.87	18.18	0.87	0.28	0.022	0.24	22	93	2.91
90			7333	8093	17.58	20.49	0.85	0.33	0.026	0.27	23	96	3.03
100			7821	8662	19.55	23.21	0.97	0.40	0.030	0.35	27	104	3.37
111			8295	9225	21.63	26.11	0.78	0.36	0.028	0.30	24	99	3.15
120			8640	9641	23.78	29.17	0.92	0.44	0.035	0.39	29	108	3.55
130			8983	10061	26.27	32.73	0.86	0.47	0.036	0.40	30	109	3.57
140	9640	10690	9288	10442	28.98	36.68	0.91	0.52	0.047	0.47	33	114	3.82
150			9561	10787	31.79	40.82	0.90	0.58	0.046	0.51	34	117	3.96
159			9781	11070	35.16	45.84	0.74	0.51	0.044	0.44	32	112	3.73
171			10043	11411	38.86	51.39	0.75	0.56	0.056	0.50	34	116	3.91
180	10100	11684	10218	11643	42.48	56.86	0.78	0.74	0.067	0.59	37	122	4.17
190			10394	11878	46.59	63.11	0.67	0.68	0.062	0.53	35	119	4.01
200			10552	12093	51.24	70.21	0.85	0.90	0.085	0.77	44	133	4.67

211			10709	12308	56.02	77.53	0.89	0.92	0.092	0.88	48	139	4.93
220	10440	12106	10825	12468	60.86	84.92	0.85	0.99	0.098	0.90	49	140	4.99
230			10943	12633	66.57	93.62	0.75	0.96	0.094	0.86	47	138	4.88
241			11060	12798	72.36	102.40	0.74	1.04	0.100	0.91	49	140	5.01
250			11148	12922	78.16	111.11	0.73	1.10	0.106	0.96	51	143	5.12
260			11238	13050	84.26	120.19	0.63	1.04	0.106	0.88	48	139	4.94
269			11313	13157	90.96	130.02	0.64	1.15	0.108	0.97	51	143	5.12
280			11398	13278	97.98	140.15	0.72	1.38	0.132	1.20	58	153	5.60
289			11462	13370	105.59	150.92	0.65	1.49	0.129	1.17	57	151	5.54
301	11390	13284	11542	13483	113.50	161.84	0.85	2.09	0.171	1.72	73	171	6.50
310			11597	13563	120.81	171.68	0.71	1.97	0.165	1.51	67	164	6.14
320			11655	13645	128.26	181.45	0.71	1.97	0.169	1.57	69	166	6.25
329			11705	13716	136.19	191.52	0.69	2.06	0.180	1.62	70	167	6.32
340			11762	13796	144.21	201.38	0.62	2.07	0.195	1.54	68	164	6.18
349			11807	13859	152.60	211.32	0.53	1.94	0.166	1.35	62	158	5.86
361			11864	13937	160.99	220.87	0.55	2.14	0.151	1.49	66	163	6.09
370			11905	13993	168.46	229.04	0.70	2.85	0.169	2.07	81	180	6.99
380			11948	14053	175.82	236.77	0.56	2.23	0.194	1.66	71	168	6.37
389			11986	14104	183.36	244.37	0.61	2.67	0.226	1.91	77	176	6.76
400			12031	14164	191.05	251.78	0.58	2.74	0.219	1.89	77	175	6.72
410	12490	14648	12071	14216	198.10	258.26	0.58	2.85	0.241	1.98	79	178	6.86
420			12110	14267	204.86	264.19	0.51	2.65	0.244	1.77	73	171	6.54
430			12148	14315	210.98	269.32	0.49	2.85	0.239	1.76	73	171	6.51
439			12181	14358	216.78	273.96	0.52	2.93	0.242	1.92	77	176	6.77
449			12218	14404	222.82	278.56	0.55	3.33	0.257	2.11	82	181	7.03
460			12257	14454	228.47	282.64	0.42	3.18	0.225	1.64	70	167	6.31

470			12292	14497	233.70	286.22	0.45	2.93	0.238	1.74	72	170	6.48
481			12331	14544	238.32	289.21	0.48	3.32	0.251	1.93	77	176	6.76
490			12362	14582	242.56	291.80	0.45	3.04	0.231	1.84	75	173	6.62
501			12400	14628	246.65	294.15	0.50	3.23	0.249	2.06	81	180	6.96
511			12434	14668	250.02	295.97	0.47	3.32	0.244	1.99	79	178	6.85
520			12464	14704	253.24	297.59	0.35	2.49	0.216	1.43	64	160	5.97
531			12501	14748	256.15	298.96	0.36	2.56	0.219	1.48	65	162	6.06
540			12531	14783	258.52	299.97	0.34	2.54	0.200	1.40	63	159	5.91
549	12550	14722	12561	14817	260.88	300.90	0.32	2.36	0.178	1.33	61	156	5.78
560			12598	14860	262.99	301.63	0.23	2.24	0.204	0.97	50	141	5.05
569			12628	14894	264.92	302.21	0.31	2.11	0.223	1.29	60	155	5.72
581			12667	14939	266.62	302.62	0.45	3.60	0.221	2.05	80	179	6.93
590			12697	14973	267.95	302.87	0.25	2.47	0.192	1.06	53	145	5.25
600			12730	15010	269.17	303.00	0.28	2.10	0.181	1.18	57	151	5.51
610			12763	15047	270.21	303.03	0.35	2.59	0.203	1.53	67	163	6.13
620			12796	15084	271.09	302.97	0.38	2.77	0.220	1.67	71	168	6.37
630			12829	15121	271.85	302.81	0.34	2.67	0.214	1.48	65	162	6.04
641			12865	15162	272.44	302.58	0.33	2.78	0.212	1.47	65	161	6.03
650			12895	15195	272.88	302.31	0.29	2.72	0.149	1.28	59	154	5.68
660			12928	15231	273.26	301.94	0.27	2.52	0.148	1.18	57	151	5.50
671			12965	15272	273.52	301.55	0.28	2.52	0.165	1.23	58	152	5.59
680			12994	15305	273.68	301.13	0.26	2.18	0.154	1.11	54	148	5.36
690			13028	15341	273.77	300.63	0.26	2.34	0.138	1.11	54	148	5.36
701			13064	15381	273.78	300.12	0.23	2.34	0.125	0.98	50	142	5.07
710			13094	15414	273.73	299.60	0.25	2.42	0.130	1.07	53	146	5.27
720			13128	15451	273.61	299.01	0.24	2.52	0.144	1.02	52	144	5.17

731			13164	15491	273.45	298.45	0.20	2.28	0.137	0.86	46	136	4.79
739			13191	15520	273.23	297.84	0.20	2.48	0.130	0.87	46	136	4.81
751			13232	15564	272.95	297.16	0.23	2.52	0.126	1.02	51	143	5.15
761			13265	15601	272.67	296.55	0.20	2.37	0.112	0.85	46	135	4.78
770			13296	15634	272.33	295.90	0.13	2.03	0.156	0.55	35	118	3.96
781			13333	15674	271.95	295.21	0.20	2.46	0.177	0.87	47	136	4.83
791			13367	15711	271.58	294.57	0.22	2.71	0.153	0.94	49	140	4.99
800			13397	15744	271.19	293.92	0.09	1.78	0.071	0.35	26	102	3.29
810			13431	15781	270.71	293.17	0.21	2.31	0.128	0.88	47	137	4.85
822			13472	15825	269.99	292.10	0.27	2.65	0.196	1.17	56	150	5.46
841			13537	15896	269.31	291.12	0.33	2.94	0.167	1.44	64	160	5.96
850	13500	15900	13568	15929	268.84	290.46	0.33	2.64	0.160	1.42	64	160	5.94
860			13602	15966	268.04	289.36	0.33	2.63	0.168	1.44	64	160	5.98
881			13675	16045	267.22	288.27	0.29	2.32	0.165	1.22	58	152	5.58
891			13710	16082	266.70	287.60	0.29	2.12	0.141	1.21	57	152	5.55
900			13741	16116	266.18	286.92	0.37	2.66	0.210	1.59	68	165	6.23
910			13776	16153	265.63	286.21	0.35	2.45	0.220	1.46	65	161	6.02
920			13811	16191	265.07	285.50	0.33	2.44	0.181	1.40	63	159	5.92
930			13846	16229	264.50	284.79	0.25	1.87	0.163	1.03	52	144	5.19
940			13881	16266	264.50	284.79	0.29	2.01	0.168	1.21	57	152	5.56
MEAN							0.60	1.93	0.15	1.14	54	146	5.30
STD							0.44	0.93	0.07	0.51	16	23	1.11
MIN							0.23	0.28	0.02	0.23	21	91	2.83
MAX							2.39	3.60	0.26	2.11	82	181	7.03
RANGE							2.17	3.33	0.24	1.89	61	90	4.20

9.4.0. TABLES FOR CHAPTER 6.

Table 6.1 Geochemical results of total hydrolyzable amino acids (THAA) for core HU-90-031-43 PC	255
Table 6.2. Geochemical results of total hydrolyzable amino acids (THAA) for core HU-90-031-29 BC	257
Table 6.3. Geochemical results of total amino acids (THAA) for core HU-90-031- 45 BC	259
Table 6.4. Geochemical results of total hydrolyzable amino acids (THAA) for core HU-90-031-17 BC	261

Table 6.1. Geochemical results of total hydrolyzable amino acids (THAA) for core HU-90-031-43 PC

Percentage of THAA for core HU-90-31-43 PC													
DEPTH	Asp	Thr	Ser	Glu	Gly	Ala	Val	Met	Allo	Iso	Leu	Tyr	Phe
1.0	0.077	0.027	0.024	0.046	0.084	0.034	0.034	0.00079	0.0021	0.0188	0.024	0.006	0.017
3.0	0.095	0.010	0.046	0.067	0.126	0.050	0.048	0.00063	0.0029	0.0247	0.033	0.007	0.000
5.0	0.035	0.011	0.004	0.019	0.036	0.014	0.015	0.00151	0.0010	0.0079	0.012	0.003	0.013
7.0	0.020	0.007	0.002	0.009	0.022	0.008	0.010	0.00021	0.0005	0.0050	0.008	0.002	0.008
9.0	0.014	0.007	0.003	0.009	0.020	0.008	0.008	0.00000	0.0004	0.0042	0.007	0.002	0.005
11.0	0.018	0.005	0.001	0.010	0.018	0.008	0.008	0.00016	0.0007	0.0043	0.006	0.000	0.000
13.0	0.024	0.009	0.002	0.013	0.028	0.011	0.013	0.00000	0.0013	0.0077	0.012	0.005	0.003
18.0	0.012	0.004	0.001	0.007	0.013	0.005	0.006	0.00013	0.0004	0.0035	0.005	0.001	0.005
23.0	0.018	0.007	0.003	0.009	0.023	0.008	0.010	0.00000	0.0008	0.0061	0.009	0.000	0.000
28.0	0.011	0.003	0.002	0.006	0.014	0.006	0.006	0.00015	0.0003	0.0034	0.006	0.000	0.004
33.0	0.019	0.006	0.002	0.008	0.021	0.007	0.011	0.00000	0.0011	0.0058	0.009	0.000	0.000
38.0	0.016	0.005	0.002	0.008	0.021	0.007	0.008	0.00000	0.0007	0.0045	0.007	0.000	0.000

Percentage of each amino acid relative to total amino acids for core HU-90-031-43 PC													
DEPTH	Asp	Thr	Ser	Glu	Gly	Ala	Val	Met	Allo	Iso	Leu	Tyr	Phe
1.0	19.42	6.88	6.05	11.59	21.24	8.67	8.49	0.20	0.53	4.75	6.14	1.63	4.39
3.0	18.63	1.88	9.02	13.22	24.68	9.77	9.42	0.12	0.57	4.85	6.56	1.29	0.00
5.0	20.34	6.53	2.36	11.17	20.85	7.95	8.57	0.88	0.57	4.62	6.99	1.78	7.39
7.0	19.00	6.80	1.89	9.11	21.61	8.16	9.93	0.20	0.48	4.83	7.75	2.10	8.14
9.0	16.34	7.70	2.93	10.17	23.48	8.99	9.36	0.00	0.50	4.85	7.65	2.63	5.40
11.0	22.51	6.11	1.74	12.11	22.80	9.77	10.50	0.20	0.83	5.40	8.03	0.00	0.00
13.0	18.35	6.81	1.83	10.07	22.01	8.37	10.42	0.00	0.99	5.95	9.03	3.89	2.29
18.0	19.56	6.13	1.83	10.58	20.62	7.77	9.78	0.20	0.69	5.61	8.09	1.53	7.63
23.0	19.35	7.30	3.20	9.25	24.73	8.90	10.99	0.00	0.85	6.38	9.05	0.00	0.00
28.0	17.66	4.89	3.64	10.06	22.26	10.10	9.67	0.24	0.53	5.25	8.64	0.53	6.53
33.0	21.44	6.51	2.67	8.80	23.06	8.13	11.91	0.00	1.29	6.54	9.64	0.00	0.00
38.0	20.36	6.08	1.98	9.62	26.54	9.33	10.12	0.00	0.83	5.75	9.41	0.00	0.00

Percentage of THAA, THAA-N, THAA-C, THAA-N/N and
THAA-C/OC for core HU-90-031-43 PC

DEPTH	THAA	THAA-N	THAA-C	THAA-N/TN	THAA-C/OC
1.0	0.397	0.053	0.159	29.21	5.50
3.0	0.509	0.070	0.196	33.35	6.57
5.0	0.171	0.022	0.071	25.30	6.49
7.0	0.104	0.014	0.043	20.92	5.48
9.0	0.086	0.012	0.035	16.92	4.39
11.0	0.079	0.011	0.031	15.69	3.84
13.0	0.129	0.017	0.053	29.43	7.75
18.0	0.063	0.008	0.026	14.88	4.10
23.0	0.095	0.013	0.037	24.16	6.20
28.0	0.064	0.009	0.026	14.29	3.63
33.0	0.089	0.012	0.035	22.35	6.07
38.0	0.079	0.011	0.031	16.26	4.15

Table 6.2. Geochemical results of total hydrolyzable amino acids (THAA) for core HU-90-031-29 BC

THAA for core HU-90-31-29 BC (%)													
DEPTH	Asp	Thr	Ser	Glu	Gly	Ala	Val	Met	Allo	Iso	Leu	Tyr	Phe
1.0	0.071	0.025	0.021	0.046	0.055	0.026	0.024	0.0008	0.0013	0.014	0.021	0.004	0.016
3.0	0.073	0.029	0.025	0.051	0.054	0.032	0.028	0.0011	0.0023	0.016	0.021	0.006	0.016
5.0	0.066	0.016	0.020	0.054	0.058	0.030	0.026	0.0007	0.0015	0.014	0.022	0.005	0.017
7.0	0.057	0.013	0.011	0.043	0.058	0.025	0.020	0.0010	0.0013	0.013	0.021	0.004	0.017
9.0	0.042	0.022	0.023	0.028	0.052	0.021	0.016	0.0002	0.0001	0.009	0.017	0.005	0.011
11.0	0.103	0.044	0.030	0.056	0.103	0.042	0.039	0.0012	0.0014	0.021	0.028	0.004	0.032
13.0	0.068	0.020	0.007	0.042	0.071	0.031	0.030	0.0012	0.0026	0.015	0.021	0.003	0.000
15.0	0.113	0.029	0.011	0.060	0.119	0.046	0.046	0.0014	0.0033	0.023	0.033	0.000	0.000
17.0	0.065	0.025	0.013	0.031	0.067	0.029	0.026	0.0009	0.0017	0.013	0.019	0.004	0.008
19.0	0.068	0.027	0.016	0.035	0.073	0.032	0.028	0.0009	0.0018	0.015	0.021	0.004	0.008
21.0	0.097	0.037	0.028	0.052	0.108	0.048	0.040	0.0010	0.0019	0.021	0.027	0.003	0.035
23.0	0.086	0.026	0.022	0.039	0.086	0.037	0.032	0.0009	0.0012	0.016	0.023	0.006	0.030
25.0	0.069	0.019	0.006	0.034	0.075	0.033	0.029	0.0007	0.0026	0.014	0.021	0.003	0.027
27.0	0.115	0.036	0.034	0.087	0.103	0.054	0.047	0.0017	0.0035	0.027	0.041	0.006	0.029

Percentage of each amino acid relative to total amino acids for core HU-90-031-29 BC													
DEPTH	Asp	Thr	Ser	Glu	Gly	Ala	Val	Met	Allo	Iso	Leu	Tyr	Phe
1.0	21.94	7.88	6.44	14.10	17.09	8.08	7.34	0.25	0.41	4.20	6.36	1.13	4.80
3.0	20.49	8.29	7.06	14.40	15.22	8.88	7.81	0.31	0.65	4.56	6.05	1.66	4.63
5.0	20.06	4.79	6.06	16.23	17.50	8.98	7.87	0.21	0.44	4.29	6.73	1.57	5.26
7.0	20.07	4.57	4.01	15.05	20.46	8.94	6.96	0.35	0.44	4.49	7.29	1.32	6.04
9.0	16.97	9.07	9.43	11.31	21.03	8.54	6.39	0.07	0.02	3.48	6.97	2.07	4.66
11.0	20.38	8.66	5.90	11.10	20.42	8.29	7.85	0.23	0.29	4.11	5.58	0.79	6.41
13.0	21.80	6.43	2.24	13.45	22.82	9.93	9.66	0.39	0.82	4.70	6.85	0.92	0.00
15.0	23.21	6.03	2.32	12.46	24.61	9.44	9.41	0.29	0.68	4.75	6.78	0.00	0.00
17.0	21.45	8.25	4.30	10.37	22.08	9.52	8.63	0.28	0.55	4.23	6.40	1.26	2.69
19.0	20.74	8.26	4.74	10.54	22.26	9.67	8.62	0.26	0.54	4.59	6.36	1.12	2.30
21.0	19.37	7.45	5.66	10.43	21.66	9.63	7.98	0.19	0.38	4.14	5.48	0.60	7.03
23.0	21.29	6.33	5.33	9.62	21.23	9.24	8.01	0.22	0.29	4.04	5.63	1.38	7.39
25.0	20.60	5.78	1.78	10.14	22.44	9.70	8.74	0.20	0.77	4.32	6.37	0.99	8.18
27.0	19.70	6.12	5.77	14.93	17.59	9.19	8.10	0.30	0.61	4.58	7.04	1.03	5.05

Percentage of THAA, THAA-N, THAA-C, THAA-N/N and THAA-C/OC
for core HU-90-031-29 BC

DEPTH	THAA	THAA-N	THAA-C	THAA-N/N	THAA-C/OC
1.0	0.323	0.041	0.130	20.74	5.57
3.0	0.355	0.045	0.144	25.20	6.29
5.0	0.330	0.042	0.134	22.34	6.40
7.0	0.284	0.037	0.115	21.74	5.95
9.0	0.246	0.033	0.098	20.35	4.75
11.0	0.503	0.066	0.203	41.32	10.31
13.0	0.313	0.042	0.122	23.44	6.15
15.0	0.485	0.066	0.187	44.04	9.15
17.0	0.303	0.041	0.119	25.38	5.58
19.0	0.329	0.044	0.129	27.69	6.40
21.0	0.500	0.067	0.201	44.41	10.79
23.0	0.405	0.054	0.164	38.23	8.54
25.0	0.335	0.044	0.137	31.77	6.90
27.0	0.585	0.076	0.237	58.22	12.24

Table 6.3. Geochemical results of total amino acids (THAA) for core HU-90-031-45 BC

THAA for core HU-90-31-45 BC (%)													
DEPTH	Asp	Thr	Ser	Glu	Gly	Ala	Val	Met	Allo	Iso	Leu	Tyr	Phe
0.5	0.056	0.021	0.012	0.021	0.135	0.027	0.014	0.0025	0.0024	0.027	0.056	0.009	0.038
1.5	0.164	0.065	0.032	0.109	0.152	0.068	0.066	0.0075	0.0050	0.034	0.051	0.007	0.000
2.5	0.109	0.043	0.023	0.078	0.145	0.053	0.052	0.0023	0.0026	0.029	0.047	0.009	0.034
3.5	0.111	0.047	0.022	0.076	0.148	0.054	0.005	0.0020	0.0029	0.031	0.050	0.009	0.033
4.5	0.065	0.015	0.004	0.037	0.079	0.029	0.017	0.0029	0.0029	0.016	0.029	0.005	0.018
6.0	0.064	0.019	0.004	0.044	0.100	0.039	0.039	0.0000	0.0044	0.021	0.036	0.006	0.022
13.0	0.054	0.011	0.002	0.030	0.089	0.003	0.028	0.0003	0.0025	0.011	0.029	0.005	0.020
15.0	0.089	0.023	0.004	0.058	0.112	0.041	0.038	0.0024	0.0045	0.023	0.039	0.008	0.027
17.0	0.075	0.023	0.006	0.048	0.107	0.039	0.031	0.0015	0.0032	0.021	0.036	0.006	0.024
23.0	0.097	0.027	0.007	0.064	0.164	0.051	0.048	0.0027	0.0055	0.030	0.050	0.011	0.032
29.0	0.070	0.014	0.002	0.047	0.124	0.041	0.034	0.0011	0.0042	0.020	0.036	0.006	0.020
31.0	0.052	0.015	0.003	0.028	0.228	0.042	0.014	0.0042	0.0020	0.014	0.034	0.006	0.020
33.0	0.079	0.027	0.008	0.053	0.114	0.042	0.037	0.0000	0.0033	0.022	0.035	0.014	0.024
HAA relative to THAA (%)													
DEPTH	Asp	Thr	Ser	Glu	Gly	Ala	Val	Met	Allo	Iso	Leu	Tyr	Phe
0.5	13.34	4.97	2.86	4.92	32.05	6.43	3.42	0.59	0.57	6.36	13.27	2.21	9.01
1.5	21.53	8.60	4.17	14.29	19.99	8.91	8.74	0.99	0.66	4.41	6.73	0.97	0.00
2.5	17.44	6.83	3.69	12.42	23.24	8.42	8.26	0.37	0.41	4.62	7.50	1.40	5.41
3.5	18.77	8.03	3.74	12.81	25.03	9.15	0.82	0.33	0.49	5.19	8.49	1.50	5.64
4.5	20.28	4.78	1.19	11.61	24.80	8.96	5.36	0.90	0.91	4.91	9.19	1.45	5.65
6.0	16.02	4.87	0.97	11.12	25.07	9.81	9.78	0.00	1.11	5.25	8.98	1.51	5.52
13.0	18.84	3.93	0.84	10.39	30.97	1.13	9.74	0.12	0.86	3.99	10.27	1.87	7.05
15.0	18.97	4.82	0.91	12.38	24.08	8.69	8.06	0.52	0.97	4.85	8.34	1.63	5.78
17.0	17.80	5.38	1.55	11.46	25.43	9.19	7.32	0.36	0.77	5.01	8.55	1.42	5.76
23.0	16.51	4.58	1.18	10.81	27.90	8.63	8.20	0.45	0.93	5.11	8.49	1.82	5.37
25.0	15.45	14.16	6.58	9.77	17.52	8.51	7.72	0.00	0.27	5.05	7.39	2.25	5.32
29.0	16.74	3.39	0.58	11.27	29.40	9.87	8.03	0.27	1.00	4.74	8.53	1.46	4.74
31.0	11.26	3.15	0.76	6.17	49.37	9.01	2.97	0.91	0.43	3.00	7.33	1.25	4.40
33.0	17.14	5.90	1.82	11.54	24.87	9.23	8.01	0.00	0.72	4.74	7.69	3.11	5.22

Percentage of THAA, THAA-N, THAA-C, THAA-N/N and THAA-C/OC
for core HU-90-031-45 BC

DEPTH	THAA	THAA-N	THAA-C	THAA-N/N	THAA-C/OC
1	0.421	0.058	0.177	22.16	3.35
2	0.760	0.100	0.296	35.86	6.78
3	0.624	0.083	0.253	29.67	6.21
4	0.591	0.079	0.238	26.25	6.19
5	0.319	0.042	0.130	14.63	3.38
6	0.397	0.054	0.163	17.34	4.38
13	0.287	0.038	0.120	13.62	3.49
15	0.467	0.062	0.191	21.39	5.31
17	0.420	0.056	0.171	20.92	4.73
23	0.589	0.080	0.239	30.85	7.53
25	0.320	0.042	0.131	16.01	3.94
29	0.420	0.058	0.169	22.34	5.09
31	0.461	0.070	0.175	26.06	5.27
33	0.459	0.062	0.187	25.66	5.48

Table 6.4. Geochemical results of total hydrolyzable amino acids (THAA) for core HU-90-031-17 BC

261

THAA for core HU-90-31-17 BC (%)													
DEPTH	Asp	Thr	Ser	Glu	Gly	Ala	Val	Met	Allo	Iso	Leu	Tyr	Phe
0.5	0.053	0.031	0.021	0.036	0.042	0.021	0.018	0.0006	0.0004	0.012	0.018	0.0017	0.013
1.5	0.050	0.037	0.024	0.032	0.048	0.024	0.023	0.0000	0.0005	0.014	0.020	0.0047	0.014
2.5	0.040	0.030	0.021	0.027	0.042	0.020	0.018	0.0000	0.0005	0.012	0.017	0.0053	0.012
3.5	0.058	0.037	0.026	0.004	0.059	0.026	0.023	0.0007	0.0003	0.013	0.021	0.0037	0.014
6.0	0.037	0.025	0.020	0.026	0.026	0.015	0.019	0.0000	0.0002	0.009	0.014	0.0046	0.009
8.0	0.043	0.028	0.020	0.026	0.046	0.020	0.016	0.0000	0.0004	0.010	0.015	0.0044	0.010
10.0	0.037	0.025	0.017	0.021	0.038	0.016	0.015	0.0003	0.0003	0.009	0.014	0.0039	0.009
13.0	0.043	0.021	0.021	0.029	0.026	0.014	0.013	0.0000	0.0003	0.009	0.013	0.0048	0.009
15.0	0.046	0.023	0.017	0.027	0.041	0.015	0.014	0.0008	0.0004	0.009	0.013	0.0054	0.009
17.0	0.045	0.024	0.020	0.028	0.028	0.014	0.013	0.0000	0.0002	0.009	0.014	0.0048	0.010
19.0	0.039	0.021	0.019	0.026	0.030	0.020	0.013	0.0000	0.0002	0.009	0.014	0.0044	0.009
21.0	0.041	0.027	0.020	0.024	0.030	0.019	0.012	0.0000	0.0002	0.008	0.014	0.0044	0.009
23.0	0.034	0.021	0.017	0.021	0.026	0.012	0.020	0.0000	0.0002	0.008	0.012	0.0033	0.008
27.0	0.069	0.028	0.022	0.035	0.050	0.022	0.020	0.0000	0.0002	0.007	0.011	0.0057	0.015
29.0	0.034	0.013	0.016	0.022	0.023	0.013	0.011	0.0002	0.0002	0.007	0.012	0.0038	0.008

Percentage of each amino acid relative to total amino acids for core HU-90-031-17 BC													
DEPTH	Asp	Thr	Ser	Glu	Gly	Ala	Val	Met	Allo	Iso	Leu	Tyr	Phe
0.5	19.84	11.67	7.98	13.58	15.50	7.80	6.77	0.22	0.15	4.37	6.77	0.64	4.71
1.5	17.20	12.70	8.35	10.92	16.63	8.08	8.04	0.00	0.16	4.71	6.85	1.63	4.73
2.5	16.31	12.39	8.75	10.87	17.22	8.07	7.47	0.00	0.20	4.73	7.04	2.16	4.79
3.5	20.39	12.79	9.20	1.37	20.55	9.20	7.91	0.23	0.10	4.66	7.44	1.29	4.87
6.0	17.92	12.19	9.68	12.72	12.51	7.48	9.39	0.00	0.10	4.41	6.81	2.22	4.57
8.0	17.93	11.76	8.25	10.76	19.18	8.23	6.82	0.00	0.15	4.32	6.44	1.86	4.29
10.0	18.16	12.20	8.19	10.12	18.36	7.86	7.42	0.16	0.16	4.44	6.60	1.89	4.43
13.0	20.92	10.08	10.45	14.37	12.74	7.00	6.42	0.00	0.14	4.37	6.56	2.37	4.57
15.0	20.67	10.59	7.72	12.38	18.54	6.66	6.41	0.36	0.16	3.94	5.85	2.46	4.26
17.0	21.56	11.59	9.54	13.35	13.13	6.41	6.30	0.00	0.11	4.35	6.76	2.27	4.64
19.0	19.11	10.08	9.40	12.73	14.54	9.92	6.28	0.00	0.11	4.32	6.75	2.16	4.60
21.0	19.56	13.00	9.69	11.22	14.18	9.23	5.89	0.00	0.10	4.02	6.56	2.08	4.47
23.0	18.70	11.57	9.07	11.32	14.28	6.80	11.01	0.00	0.09	4.14	6.67	1.82	4.52
27.0	24.10	9.92	7.82	12.14	17.47	7.73	7.18	0.00	0.07	2.45	3.89	2.00	5.22
29.0	20.75	7.81	9.84	13.37	14.29	8.24	7.01	0.10	0.10	4.30	7.11	2.30	4.77

Percentages of THAA, THAA-N, THAA-C, THAA-N/N and
THAA-C/OC for core HU-90-031-17 BC

DEPTH	THAA	THAA-N	THAA-C	THAA-N/N	THAA-C/OC
0.5	0.269	0.034	0.108	20.20	5.61
1.5	0.291	0.038	0.118	22.16	5.81
2.5	0.245	0.032	0.100	19.87	5.06
3.5	0.286	0.038	0.114	24.06	5.79
6.0	0.205	0.026	0.084	16.16	4.27
8.0	0.237	0.031	0.095	19.47	4.83
10.0	0.205	0.027	0.083	16.74	4.20
13.0	0.204	0.025	0.083	15.90	4.21
15.0	0.222	0.029	0.089	17.84	4.52
17.0	0.211	0.026	0.086	16.43	4.36
19.0	0.206	0.026	0.083	16.53	4.22
21.0	0.211	0.027	0.085	16.91	4.32
23.0	0.182	0.023	0.074	14.52	3.78
27.0	0.285	0.037	0.113	22.88	5.75
29.0	0.163	0.021	0.066	12.96	3.37